

SEMMELWEIS EGYETEM
DOKTORI ISKOLA

Ph.D. értekezések

2295.

GAMPE NÓRA

A gyógyszerészeti tudományok korszerű kutatási irányai
című program

Programvezető: Dr. Antal István, egyetemi docens

Témavezetők: Dr. Béni Szabolcs, egyetemi docens

Dr. Kursinszki László egyetemi docens

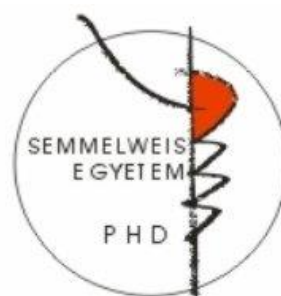
Phytochemical analysis of *Ononis* species

Ph.D. dissertation

Nóra Gampe

Semmelweis University

Doctoral School of Pharmaceutical Sciences



Supervisors: Szabolcs Béni, Ph.D.

László Kursinszki, Ph.D.

Reviewers: Márta Mazákné Kraszni, Ph.D.

Dezső Csupor, Ph.D.

Chair of final examination committee: Imre Klebovich, D.Sc.

Members of final examination committee:

Éva Ledniczkyné Lemberkovics, Ph.D.

Zsuzsanna Hajdú, Ph.D.

László Abrankó, Ph.D.

Budapest

2019

Table of contents

List of abbreviations	5
1. Introduction	7
1.I. Characterization of <i>Ononis</i> species.....	8
1.I.1. Botanical characterization of <i>Ononis spinosa</i> L. and <i>Ononis arvensis</i> L... 8	
1.I.2. Chemical characterization of <i>Ononis</i> species.....	10
1.I.3. Biological activities of <i>Ononis spinosa</i> extracts.....	12
1.I.4. Biological activities of <i>Ononis arvensis</i>	18
1.I.5. Biological activities of other <i>Ononis</i> species	19
1.I.6. Possibilities to produce isoflavonoids by <i>in vitro</i> cultures of <i>Ononis</i> species	19
1.II. Isoflavonoids.....	24
1.II.1. Structural features and occurrence of isoflavonoids.....	24
1.II.2. Biosynthesis of isoflavonoids.....	27
1.II.3. Biological activities of selected isoflavonoids	32
1.II.4. Analytical methods aiming the qualitative and quantitative determination of isoflavonoids.....	43
2. Objectives	58
3. Materials and methods.....	59
3.I. Plant material	59
3.II. Solvents and chemicals	59
3.III. Extraction and sample preparation.....	60
3.III.1. Analytical samples	60
3.III.2. Isolation of aglycones	61
3.III.3. Isolation of licoagroside B	61
3.III.4. Isolation of but-2-enolide aglycones and calycosin D aglycone	62
3.III.5. Isolation of but-2-enolide glycosides and calycosin D glycosides	63

3.III.6.	Isolation of homopipecolic acid isoflavonoid glucoside esters	63
3.IV.	Chromatographic conditions	64
3.IV.1.	HPLC-DAD conditions.....	64
3.IV.2.	HPLC-DAD-ESI-MS/MS conditions	65
3.IV.3.	UHPLC-DAD-ESI-Orbitrap-MS/MS conditions	66
3.V.	Polarimetry and CD conditions.....	66
3.VI.	NMR conditions	66
3.VII.	Method validation	67
4.	Results	68
4.I.	Qualitative phytochemical results.....	68
4.I.1.	Chromatographic results.....	68
4.I.2.	Mass spectrometry results	74
4.I.3.	Detailed structural identification	75
4.II.	Quantitative phytochemical results.....	89
4.II.1.	Sample preparation	89
4.II.2.	Method validation.....	91
4.II.3.	Quantitative results	92
5.	Discussion.....	94
5.I.	Qualitative phytochemical results.....	94
5.I.1.	Structural identification of licoagroside B	94
5.I.2.	Structural identification of but-2-enolides.....	94
5.I.3.	Structural identification of isoflavones	96
5.I.4.	Structural identification of isoflavanones.....	98
5.I.5.	Structural identification of pterocarpan	100
5.I.6.	Structural identification of 2'-methoxy isoflavones.....	101
5.I.7.	Structural identification of nitrogen-containing derivatives.....	104

5.II. Quantitative phytochemical results.....	108
5.II.1. Sample preparation.....	108
5.II.2. Quantitative results.....	109
6. Conclusions.....	113
7. Summary.....	114
8. Összefoglalás.....	115
9. Bibliography.....	116
10. List of own publications.....	137
11. Acknowledgement.....	138

List of abbreviations

2-HIS	2-hydroxy isoflavone synthase
ABTS	2,2'-azino-bis(3-ethylbenzothiazoline-6-sulphonic acid)
AChE	acetylcholinesterase
A β	amyloid beta
BChE	butyrylcholinesterase
BPC	base peak chromatogram
CID	collision induced dissociation
COSY	correlation spectroscopy
CUPRAC	cupric reducing antioxidant capacity
CZE	capillary zone electrophoresis
DAD	diode-array detector
DMID	7,2'-dihydroxy-4'-methoxyisoflavanol dehydratase
DMSO	dimethyl sulfoxide
DPPH	2,2-diphenyl-1-picrylhydrazyl
ED	electrochemical detection
EDTA	Ethylenediaminetetraacetic acid
ER α , β	estrogen receptor α , β
ESI	electrospray ionization
FRAP	ferric reducing antioxidant capacity
HI4'OMT	hydroxy isoflavone 4'- <i>O</i> -methyltransferase
HM3OMT	6a-hydroxymaackiain 3- <i>O</i> -methyltransferase
HMBC	heteronuclear multiple bond correlation
HPLC	high pressure liquid chromatography
HSQC	heteronuclear single quantum coherence
HUVEC	human umbilical vein endothelial cell
I2'H, I3'H	isoflavone 2'/3'-hydroxylase
IC ₅₀	50 % inhibitory concentration
IFR	isoflavone reductase
IOMT	isoflavone- <i>O</i> -methyltransferase
LC	liquid chromatography
LOD	limit of detection

LOQ	limit of quantitation
LPS	lipopolysaccharide
MAO	monoamine oxidase
MEKC	micellar electrokinetic capillary chromatography
MIC	minimal inhibitory concentration
MS	mass spectrometry
MS/MS	tandem mass spectrometry
NADPH	nicotinamide adenine dinucleotide phosphate
NF- κ B	nuclear factor κ B
NMR	nuclear magnetic resonance
NOESY	nuclear Overhauser effect spectroscopy
Ovx	ovariectomized
P2CP, P4CP	pterocarpan C-2/4 prenyltransferase
P6aH	pterocarpan 6a-hydroxylase
PPAR α , γ , δ	peroxisome proliferator-activated receptor α , γ , δ
pRi T-DNA	root infecting plasmid transfer DNA
rDA	retro Diels-Alder
ROESY	rotating frame Overhauser effect spectroscopy
SAM	<i>S</i> -adenosyl-L-methionine
SC ₅₀	50% radical scavenging concentration
SFE	supercritical fluid extraction
SIM	selective ion monitoring
SPE	solid-phase extraction
TIC	total ion-current chromatogram
TOCSY	total correlation spectroscopy
TRAIL	tumor necrosis factor α -related apoptosis inducing ligand
UHPLC	ultrahigh pressure liquid chromatography
VEGF	vascular endothelial growth factor
VR	vestitone reductase

1. Introduction

Natural products and plant derived remedies accompanied us since prehistoric times and they are still a popular choice of self-healing. Although, many herbal extracts are proved to have beneficial health effects, the responsible components are undefined in the majority of cases. With the help of phytochemical and phytoanalytical techniques, the aim of pinpointing the most potent molecules in the herbal drugs can be executed. The results of these studies are not only feeding the intrinsic curiosity – How and why does it work? – but can be the base of the quality control of herbal drugs and preparations. Taking advantage of the capacities of biotechnology, the metabolite profile of the plant can be fine-tuned, resulting in easier accessibility to the beneficial molecules. Furthermore, with the structural knowledge of the effective compounds, new semisynthetic, structurally optimized molecules can be created.

The aim of this work is to reveal the phytochemical and phytomedicinal values of *O. spinosa* and *O. arvensis*, as these plants have been used in ethnomedicine since hundreds of years. The roots of this plants are a typical example of herbal drugs, where the ethnomedicinal use is confirmed by *in vitro* and *in vivo* tests, however, the exact compounds responsible for the effects are unknown.

In the literature overview, the as complete as possible description of the plants, their chemical constituents and their biological effects was carried out. As related species can possess similar phytochemical profile, their most interesting constituents and pharmacological effects are summarized, too. As isoflavonoids seemed to be the most promising compounds, their analytical possibilities are presented, as a base of the experimental work. During our research, we aimed to explore the isoflavonoid profile in details using various analytical techniques, to understand the operation of the plant as a miniature chemical factory. The chemical profile of *O. spinosa* and *arvensis* roots and their *in vitro* hairy root cultures were compared regarding qualitative and quantitative points of view.

1.I. Characterization of *Ononis* species1.I.1. Botanical characterization of *Ononis spinosa* L. and *Ononis arvensis* L.

The members of the *Ononis* genus, which belongs to the family *Leguminosae*, are natively distributed in Europe, Central Asia and North-Africa. *Ononis* genus includes 86 species (see Figure 1) [1].

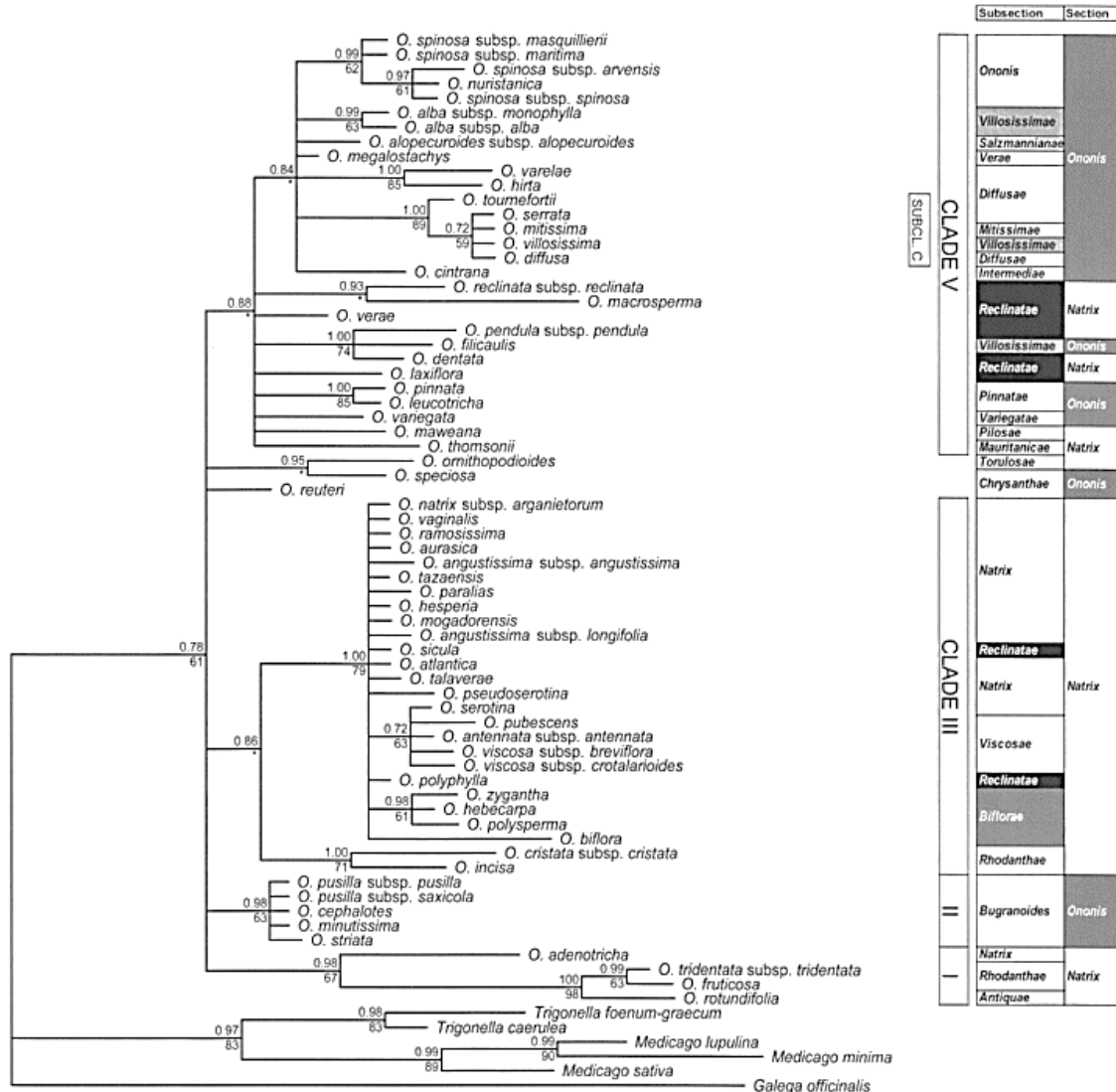


Figure 1: The phylogenetic tree of *Ononis* species (and some other *Leguminosae* species) based on ITS DNA sequences [1].

Ononis spinosa L. (spiny restharrow) is a tall subshrub which grows to a height of 60 cm. It has a short rhizome and a ligneous taproot which can be up to 50 cm long. The upright stems which grow out of this are lignified at the base and slightly hairy. Numerous short shoots have developed into prickly thorns, but thornless varieties also exist. The lower leaflets are trifoliate and pinnate, while the upper ones are small and unifoliate with a

long oval shape and dentate edges. The leaves are covered with very fine glandulous hairs. The striking butterfly-shaped flowers are pink or purplish in color and grow in the upper angles between leaf and stem. The flowers are generally solitary but sometimes also grow in loose clusters (Figure 2). They produce soft-haired pods bearing rounded, lumpy seeds. Spiny restharrow is to be found in dry meadows and pastures, by fields and waysides, but also in peat areas and sand dunes. It favors sunny locations with weak loamy or chalky soils. Fertilizing causes it to disappear [2].

Ononis arvensis L. (field restharrow) is a perennial shrub preferring humid fields and meadows overall in Europe. The 30–80 cm high erect stem is covered by long and thick trichomes, but thornless. The plant has an unpleasant smell due to the excrete of the glandular trichomes. It has alternating stalked leaves; the blade has three elliptic-quite round leaflets with serrated margins. The terminal leaflet is stalked. The large stipules are united with the stalks. The butterfly-like corolla is pinkish and fused at base. The flowers are axillary in pairs. Inflorescence is a leafy terminal raceme or flowers axillary in pairs (Figure 3). The 1-3 seeded opening pod is 6-9 mm. The synonym names are *Ononis hircina* Jacq. and *Ononis spinosa* subsp. *hircina* (Jacq.) Gams. It usually grows in dry places in different kinds of fields like inland meadows, grazing land and banks [3].



Figure 2: *Ononis spinosa* L.



Figure 3: *Ononis arvensis* L.

1.I.2. Chemical characterization of *Ononis* species***Ononis spinosa* L.**

The following chemical constituents were identified in Restharrow root:

Isoflavonoids [4]–[11]:

- formononetin, ononin (formononetin 7-*O*-glucoside), formononetin 7-*O*-glucoside 6''-malonate, rothinidin (pseudobaptigenin 7-*O*-glucoside), genistein, genistin (genistein 7-*O*-glucoside), biochanin A, sissotrin (biochanin A 7-*O*-glucoside), biochanin A 7-*O*-glucoside 6''-malonate, daidzein, daidzin (daidzein 7-*O*-glucoside), calycosin D (3'-methoxy daidzein), tectoridin,
- trifolirhizin (maackiain 3-*O*-glucoside), medicarpin 3-*O*-glucoside
- 2,3-dihydro-ononin, onogenin, onogenin-7-*O*-glucoside, sativanone, and sativanone-7-*O*-glucoside.

Phenolic lactones:

- spinonin [12], and clitorienolactone B [11] were also characterized.

Triterpenes:

- α -onocerin (onocol) [13]
- β -sitosterol, stigmasterol, campesterol, cholesterol, α -spinasterol [7], [14]
- saponin (3-*O*-[α -L-rhamnopyranosyl-(1 \rightarrow 2)- β -D-xylopyranosyl-(1 \rightarrow 2)- β -D-glucuronopyranosyl]-3 β ,22 α -dihydroxyolean-13-en-11) [15]

Phenolic acids:

- p-hydroxybenzoic, vanillic acid, caffeic acid, syringic acid, p-coumaric acid, cinnamic acid, sinapin acid, salicylic acid, gentisic acid [7, 14]

Lectins:

- Lectins Index Nomenclature LECp.Ono.Spi.ro.Hga1 [16]

Essential oil (small amount):

- trans-anethole (major constituent), carvone, menthol, menthone, isomenthone, linalool, estragole, borneol and cis-anethole [17]

***Ononis arvensis* L.**

Isoflavonoids (from roots) [18]–[21]:

- ononin
- onogenin
- maackiain, trifolirhizin

Phenolic acids (from aerial parts):

- hydroxycinnamic acids [22]
- hydroxybenzoic acid, ellagic acid [23]

Flavonoids (from aerial parts) [23]:

- dihydro-querctetin, rutin, quercetin, kaempferol, isorhamnetin
- catechin, epicatechin
- luteolin, apigenin, chrysin, eriodyctiol, naringenin
- phloridzin, phloretin

Stilbenes (from aerial parts):

- piceol, trans-resveratrol [23]

Coumarins (from aerial parts):

- scopoletin, scopolin [24]

Triterpenes (from whole plant) [13]:

- α -onocerin (onocol)
- β -sitosterol, stigmasterol, campesterol, cholesterol, α -spinasterol

Lectins [25]

The representative structures of isoflavonoid derivatives, special phenolics and terpenoids can be seen in Figure 4.

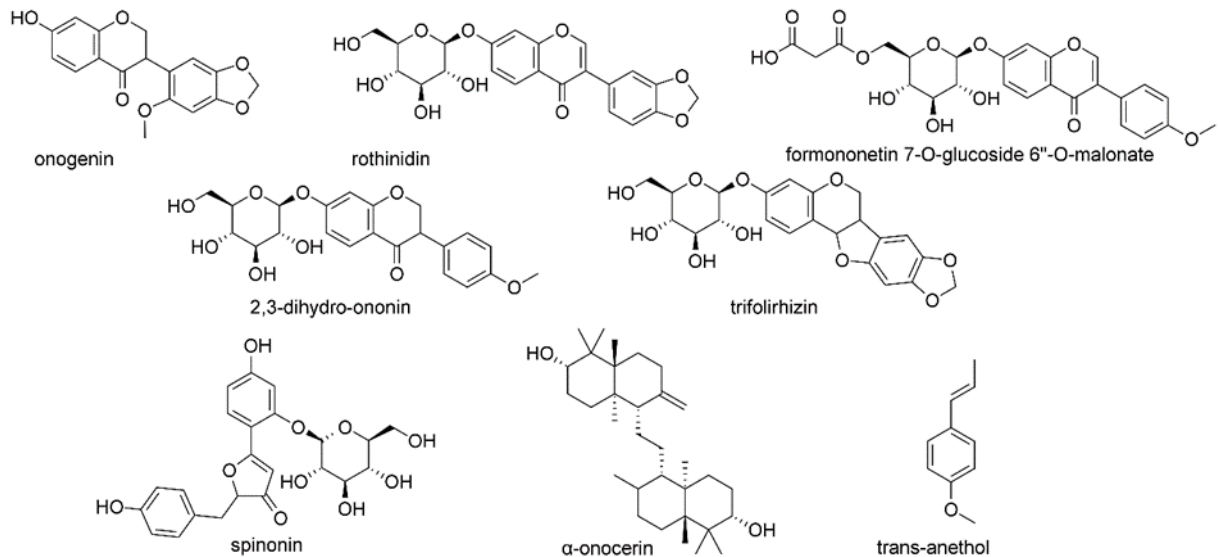


Figure 4: Representative structures of *O. spinosa* and *O. arvensis*

Other *Ononis* species

Isoflavonoids were also described for *O. angustissima* [26], *O. speciosa* [27], *O. natrix* [28], [29], *O. viscosa* [30], *O. vaginalis* [31], [32], *O. serrata* [33], *O. pusilla* [34], while flavonoids were found to be in *O. angustissima* [35], [36], *O. speciosa* [27], *O. natrix* [37], and *O. pusilla* [34]. Special phenolic lactones were isolated from *O. angustissima* [26] and *O. speciosa* [38]. The essential oil of *O. angustissima* [39], [40], *O. reclinata* [34], *O. natrix* [41], *O. viscosa* [42] were studied. Probably the most unique compounds in *Ononis* species are the alkyl derivatives of resorcinol, benzoic acid, isocoumarin and anthranilic acid (see Figure 5), which are present in *O. speciosa* [27], [43], *O. natrix* [28], [37], [44]–[49], *O. viscosa* [50], [51], *O. pubescens* [52] and *O. pusilla* [34].

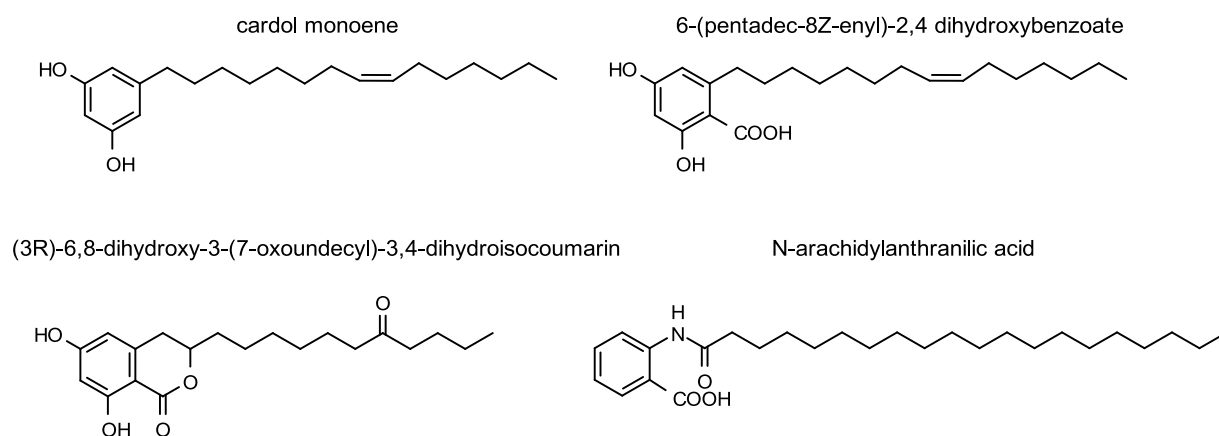


Figure 5: Alkyl derivatives of resorcinol, benzoic acid, isocoumarin and anthranilic acid found in various *Ononis* species

1.I.3. Biological activities of *Ononis spinosa* extracts

Ethnomedicinal use

O. spinosa root has been widely used since ancient times and it is mentioned in many old documents such as Dioskurides (increases diuresis and breaks stones), Plinius (the root expels bladder-stones), Matthiolus (stimulates diuresis, powerfully breaks the stones), Lonicerus (expels the stone and urine) or Schroder (stimulates diuresis and against kidney- and bladder-stones). It has been traditionally used for the treatment of the lower urinary tract disorders in the irrigation therapy as a diuretic medicine for inflammatory conditions of the lower urinary tract and for preventing and treating kidney and bladder disorders, gravel and small stones [53]. *Ononis* species have been used for centuries as

folk remedies in Turkey as diuretic, antiseptic and antimicrobial aids. In their folk medicine, restharrow root is also used for gout and rheumatic complaints and skin disorders [40], [54].

Diuretic effect

In vivo experimental studies on the diuretic effect of *Ononidis radix* were performed and described in a dissertation thesis of Wilhelm Bulow already in 1891 [55]. Fifty years later, Vollmer *et al.* investigated again the diuretic effects of *Ononis* extracts on various species. The *per os* administration of aqueous extract of the roots to rats induced the most pronounced effect, although in a very high dose of 1 g/animal. Infusion of *O. spinosa* root was administrated orally to rabbits and resulted in an elevation of urinary output by 26% [56], [57].

Hilp *et al.* confirmed a diuretic activity with *in vivo* studies. Oral administration of infusions of the *O. spinosa* root caused slight diuresis (average of 12% increase compared to the control) and decoctions an antidiuretic effect of 7-20% in rats. The essential oil extracted with steam distillation showed a diuretic effect as well, however, the aqueous residue of steam distillation exhibited a weak anti-diuretic effect [17].

Rebuelta *et al.* aimed to investigate the diuretic mechanism of *O. spinosa* extracts and investigated the urinary output as well as the alkali ion excretion. In order to specify the compounds responsible for the flushing effect, they tested the dried aqueous and methanol extracts and the ash of the roots on rats in a dose of 0.3 g. Theophylline (5 mg/kg) served as positive control, whereas the control group received distilled water. The urinary volume was registered in every hour (see Figure 6) and the cumulative amount of Na⁺ and K⁺ ions was measured by atom absorption spectrometry (see Figure 7). The results showed that the various extracts and ash of the root were slightly more effective than theophylline. The highest increase in volume was experienced with the aqueous extract and the ash. The Na⁺ and K⁺ excretion was elevated mostly by the administration of ash and dried methanol extract. Rebuelta *et al.* have drawn the conclusion that the diuretic effect is caused mainly by the flavonoid glycosides and the high potassium content of the root [58].

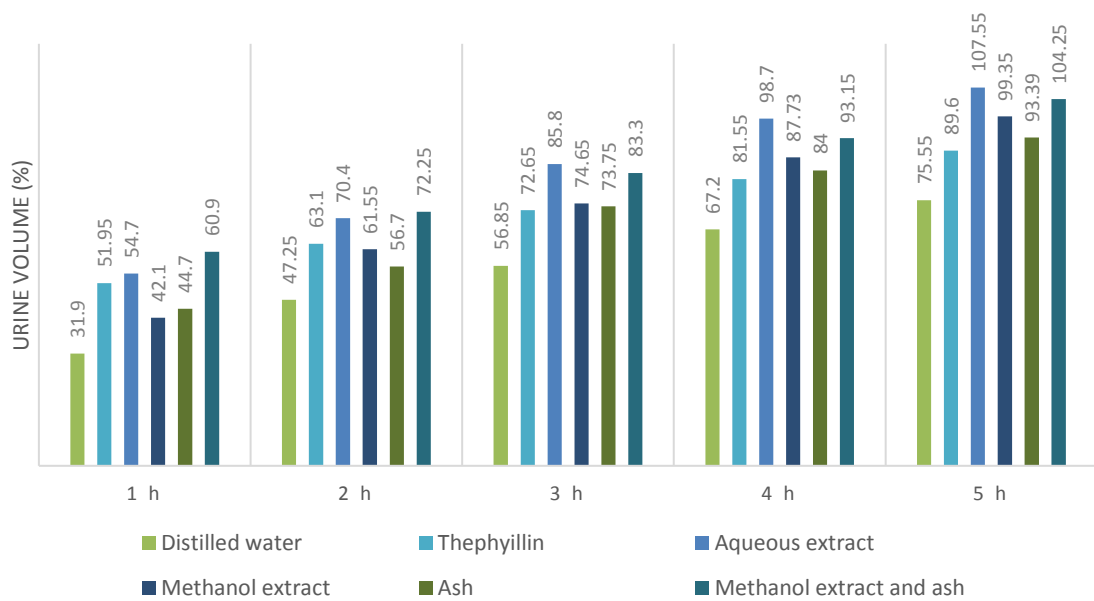


Figure 6: Effects of intragastrical administration of distilled water, theophyllin, dried aqueous and methanol extract and the mix of ash and methanol of *O. spinosa* root [58]

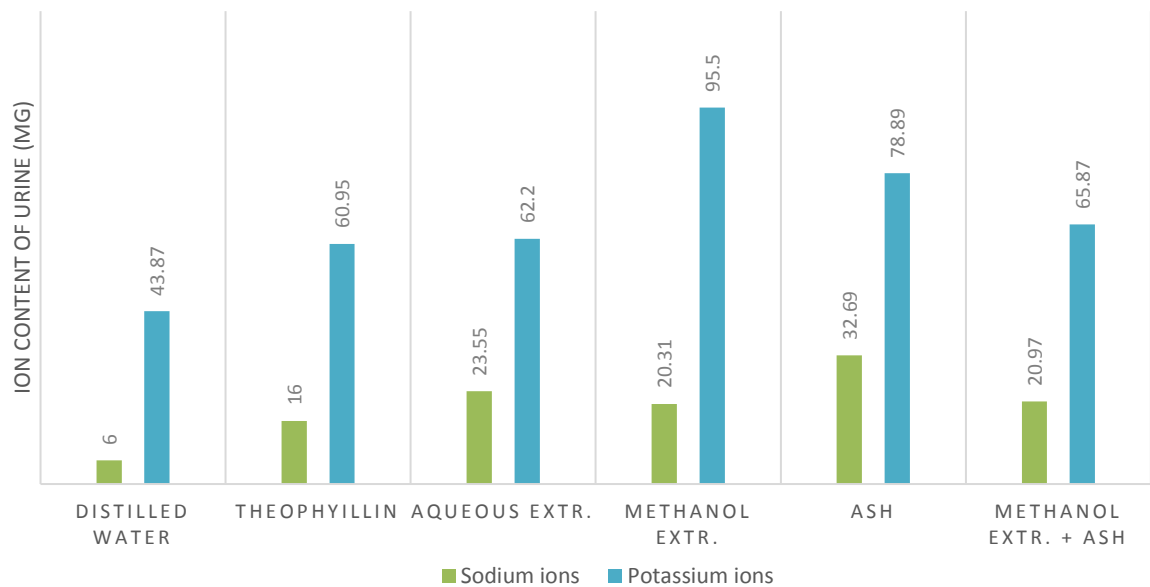


Figure 7: Cumulative sodium- and potassium ion content of urine collected from rats treated with distilled water, theophyllin, dried aqueous and methanol extract of *O. spinosa* root, ash, and mix of dried methanolic extract and ash [58]

Bolle *et al.* administered 2 g/kg *O. spinosa* root extract to rats *per os* and intraperitoneally. As a control, isotonic saline solution was used. After 2 hours the urinary volume increased in the *per os* group with 103%, which means a significant difference. However, according

to their results, the excretion of Na⁺ and K⁺ did not change. Interestingly, in the intraperitoneal group difference in diuresis was not observable [59].

Anti-inflammatory and analgesic effect

Investigating the analgesic activity, nor the *per os* neither the intraperitoneally administered ethanol extract showed effectiveness during the murine hot plate test. The phenylquinone-induced writhing reaction was decreased by 80% if the rats had been pre-treated with 100 or 500 mg/kg dry ethanol extract. Administering 500 mg/kg ethanol extract intraperitoneally to rats decreased the carrageen induced paw edema by 46% after 3 hours and 34% after 5 hours [59].

Yölmaz *et al.* evaluated the analgesic effect of aqueous *O. spinosa* root extract using the murine tail flick test. For positive controls, aspirin (100 mg/kg) and morphine (10 mg/kg) were used. The herbal extract was administered in 25 mg/kg, 50 mg/kg and 100 mg/kg intraperitoneally. Their results showed, that the *O. spinosa* extract significantly alleviated pain after 30, 90 and 150 minutes to administration in 50 mg/kg and 100 mg/kg doses. The most outstanding results emerged in the 50 mg/kg group (see Figure 8) [60].

Öz *et al.* investigated the anti-inflammatory effect of fractions of *O. spinosa* root ethyl acetate extract obtained by column chromatography. In the carrageenan-induced paw edema in mice, the dried extract administered in 100 mg/kg dose showed significant inhibition of swelling thickness, which was similar to the effect of 10 mg/kg indomethacin. However, nor in the 12-*O*-tetradecanoylphorbol-13-acetate-induced ear edema test, neither in the adjuvant-induced chronic arthritis exhibited any extract significant inhibitory effect [61].

The cytosolic phospholipase A2 α is one of the potential targets for anti-inflammatory drugs, since this enzyme plays a key role in the inflammation processes seen in health disorders, like asthma, allergic reactions, arthritis and neuronal diseases. In the study of Wink *et al.*, inhibition of the enzyme by methanol extracts from medicinal plants rich in polyphenols was determined. *O. spinosa* exhibited an IC₅₀ value of 39.4 μ g/mL, resulting one of the most potent tested medicinal plant [62].

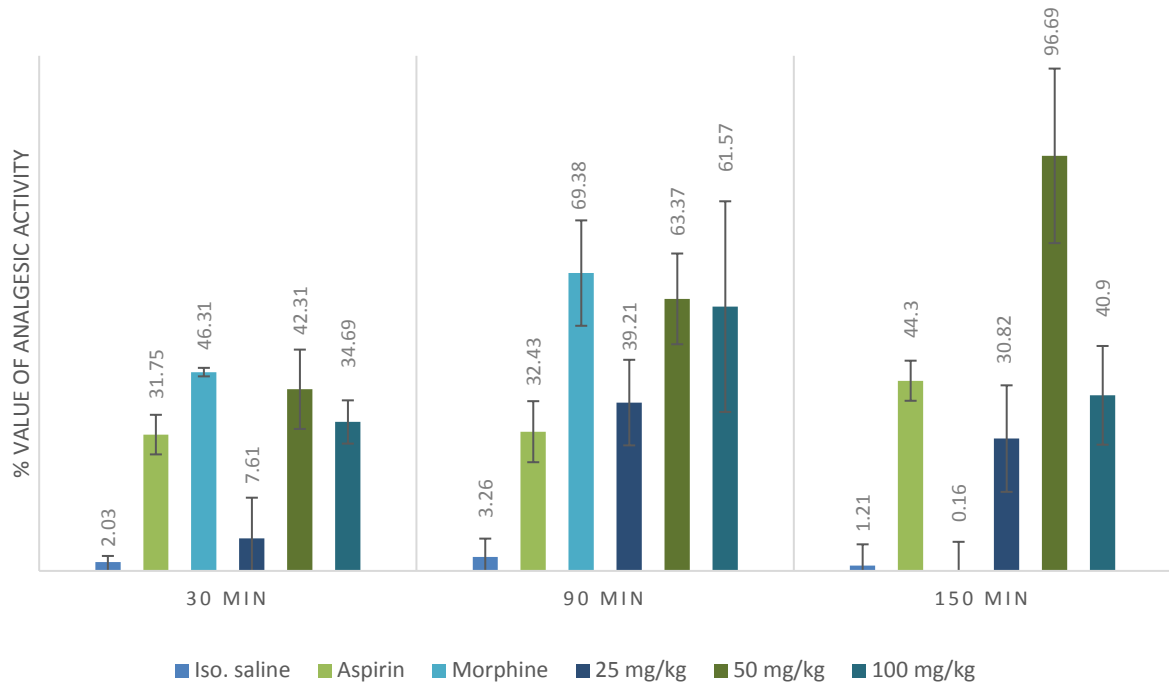


Figure 8: The standardized results of tail flick test using aspirin, morphine and 25, 50 and 100 mg of aqueous extract of *O. spinosa* root [60]

Antibiotic effect

Petroleum ether, ethanol, butanol and aqueous crude extracts of the whole aerial parts of *O. spinosa* were tested against four bacterial and three fungal species by Mahasneh *et al.* Using the disc diffusion method, methanol and hexane extracts did not show any activity and compared with standard antibiotics, the other extracts had low to moderate activity. The butanol extracts at 4 mg/disc had high-moderate antifungal activity against *Aspergillus flavus*, *Fusarium moniliforme* and *Candida albicans* relative to miconazole nitrate at 40 µg/disc [63].

Çitoğlu and Altanlar aimed to evaluate the antibiotic effect of the aerial parts of *O. spinosa* using the same method. The discs were impregnated with *O. spinosa* extract made with 75% aqueous ethanol, ampicillin or fluconazole. The tested microorganisms and the results can be seen in Table 1, which suggest that the extract had a moderate antibiotic and antifungal effect [64]

Table 1: Inhibition zones after the application of *O. spinosa* extract, ethanol, ampicillin or fluconazole

	Inhibition zones (mm)						
	<i>E. Coli</i>	<i>P. Aeruginosa</i>	<i>B. Subtilis</i>	<i>S. Aureus</i>	<i>C. Albicans</i>	<i>C. Glabrata</i>	<i>C. Krusei</i>
<i>O. spinosa</i>	11	11	1	11	16	7	16
Ethanol	-	-	-	-	-	-	-
Ampicillin	12	n.d.	13	15	n.d.	n.d.	n.d.
Fluconazole	n.d.	n.d.	n.d.	n.d.	18	20	20

Antioxidant effect

Çoban *et al.* evaluated ethanol extracts from six species representing six different families, used in traditional medicine in Turkey for their antioxidant activities. *In vitro* tests included superoxide anion radical scavenging activity (determined spectrophotometrically on the basis of inhibition of cytochrome c reduction) and lipid peroxidation (investigated on rat liver homogenate induced with FeCl₂-ascorbic acid). The extract of *O. spinosa* aerial part showed concentration-dependent superoxide anion radical scavenging activity. The results of the superoxide anion formation assay showed that the ethanol extract of *O. spinosa* had moderate scavenging activity (IC₅₀ 1.35 mg/ml) and it had no significant effect on lipid peroxidation [65].

Wound healing effect

In order to establish the ethnopharmacological wound healing use of *Ononis* species, Öz *et al.* investigated the *n*-hexane, ethyl acetate and methanol extracts of *O. spinosa* roots and aerial parts. As the results showed that the most potent was the ethyl acetate extract of the roots [66], they continued the experiments with the silica gel fractions of this extract. The fractions were tested in linear incision and circular excision wound models and hydroxyproline estimation assay on rats. The fifth fraction (Fr5) exhibited remarkable wound healing activity with the 33.4% tensile strength value on the linear incision wound model (madecassol as internal standard 53.8%) and 51.4% reduction of the wound area at the day 12 on the circular excision wound model (madecassol 100%). Hydroxyproline content of the tissue treated by Fr5 was found to be 30.9 ± 0.72 µg/mg (madecassol 47.7 ± 0.57 µg/mg). Trifolirhizin, ononin, medicarpin 3-*O*-glucoside, onogenin 7-*O*-glucoside and sativanone 7-*O*-glucoside were isolated from Fr5 and tested for their wound healing activities by measuring their inhibition of hyaluronidase,

collagenase and elastase enzymes. Ononin and sativanone 7-*O*-glucoside inhibited hyaluronidase and elastase enzymes by 31.66% and 41.75%; 45.58% and 46.88%, respectively, at the dose of 100 µg/mL [61].

Addotey *et al.* executed bioactivity guided isolation from *O. spinosa* root extracts, based on hyaluronidase inhibition activity, too. Hot water and hydroalcoholic extracts showed moderate inhibiting effects (IC₅₀ 1.36 and 0.73 mg/ml) while dichloromethane extract exerted an IC₅₀ of 190 µg/mL. Bioassay guided fractionation of the dichloromethane extract yielded four isoflavonoids with anti-Hyal-1 activity: onogenin, sativanone, medicarpin and calycosin-D with inhibition rates of 25.4, 61.2, 22.4 and 23.0%, respectively, at test concentration level of 250 µM. The IC₅₀ value of sativanone, the most active compound was determined of 151 µM, which was better than that of the positive control glycyrrhizinic acid (177 µM) [11].

1.I.4. Biological activities of *Ononis arvensis*

In ethnomedicine, the aerial part has been applied for typhus and hernia, as aphrodisiac, and for stomach disorders as decoction. It is believed, that the plant maintains the optimal level of living water in the body therefore it can be used against diarrhea. The herb is traditionally applied for liver and stomach disorders as a decoction in the human and veterinary medicine [23].

Dénes *et al.* investigated the antimicrobial activity of different extract of *O. arvensis* aerial parts. Firstly, the methanolic extracts of separated leaves and stems were partitioned with *n*-hexane, chloroform, ethyl acetate and butanol, then these fractions were dried and re-dissolved in DMSO. The activity of the extracts was tested against *Staphylococcus aureus* (ATCC 25923), *Escherichia coli* (ATCC 25922), *Pseudomonas aeruginosa* (ATCC 27853), *Salmonella typhimurium* (ATCC 14028) and *Candida albicans* (ATCC 90028) using tube diluting and microdiluting method. The chloroform extract of the leaves exhibited strong antimicrobial activity against *E. coli* and *C. albicans* (MIC = 51 µg/ml and 12.75 µg/ml), interestingly, the *n*-hexane extract showed only antifungal activity against *C. albicans* (MIC = 8 µg/ml). The ethyl acetate extract of the leaves inhibited the growths of *S. aureus* and *C. albicans*, however, the same extracts of the stems proved to be more effective (MIC = 16 and 8 µg/ml). The chloroform extract of the stems could inhibit only the growth of *P. aeruginosa* (MIC = 43.5 µg/ml) and the butanol extract could

inhibit only *S. typhimurium* (MIC = 46.5 µg/ml). The methanol and aqueous extracts showed no significant antimicrobial effects and no extract could inhibit the growth of *E. coli*.

1.I.5. Biological activities of other *Ononis* species

The results of the most important *in vitro* and *in vivo* tests of various other *Ononis* species are summarized in the Table 2.

1.I.6. Possibilities to produce isoflavonoids by *in vitro* cultures of *Ononis* species

Plant cells are miniature reactors which produce a vast array of natural products. Most of these products are small molecules and are of keen interest, because they have shown potential as food additives, nutraceuticals, pharmaceuticals and cosmetic ingredients. Some metabolites can be accumulated with a higher yield in *in vitro* cultures than those in parent plants, suggesting that the production of plant-specific secondary metabolites by plant *in vitro* cultures instead of whole plant cultivation possesses great potential. Plants can also be genetically engineered to produce commercially interesting proteins including vaccines, antibodies, and other mainly therapeutic proteins [67], [68]. Secondary metabolites, including isoflavonoids, can be produced by using different biotechnological approaches, such as callus cultures, cell suspension cultures and/or organ cultures. Since it was observed that production of secondary metabolites is generally higher in differentiated plant tissues, there were attempts to cultivate whole plant organs, i.e. shoots or roots in *in vitro* conditions. As it was expected, such organ cultures produced similar patterns of secondary metabolites as intact plants.

Table 2: Summary of the biological activities, the type of experiments and used extracts of various *Ononis* species

Species	Investigated effect	Type of substance	of Experiment	Result	Source
<i>O. angustissima</i>	α -amylase and α -glucosidase inhibition	MeOH-H ₂ O extract n-BuOH extract	<i>in vitro</i> enzymatic test	IC ₅₀ = 0.94 mg/ml IC ₅₀ = 0.99 mg/ml	[69]
	antioxidant	isolated trifolirhizin	DPPH, ABTS, reducing power assays	IC ₅₀ = 19.53 μ g/ml IC ₅₀ = 28.29 μ g/ml IC ₅₀ = 38.53 μ g/ml	[26]
	neuroprotective	isolated maackiain and medicarpin (30 / 75 μ M)	protective effect on A β 25–35 peptide induced cytotoxicity in PC12 cells	significant increase in cell viability	
<i>O. macrosperma</i>	wound healing effect	aqueous and EtOH extracts of aerial parts (5 mg extract topically)	<i>in vivo</i> linear incision model	significant increase in tension strength (40.7% and 45.3%)	[54]
	wound healing effect	aqueous extract of aerial parts (5 mg extract topically)	<i>in vivo</i> circular excision model	significant wound contraction after 8, 10 and 12 days	
	anti-inflammatory activity	aqueous (200 mg/kg) and EtOH extracts of aerial parts (100 and 200 mg/kg)	<i>in vivo</i> acetic acid-induced increase in capillary permeability	inhibition of 35.7% and inhibition of 30.3% and 37.6%	

<i>O. vaginalis</i>	anti-inflammatory activity	isolated maackiain (2.8 mg/kg)	<i>in vivo</i> carageenan induced rat paw edema	65.7%	[32]
	hepatoprotective activity	isolated trifolirhizin (7.5 mg/kg)	<i>in vivo</i> CCl ₄ induced liver damage	SGOT 28.79% decrease, SGPT 34.57% decrease, ALP 31.20% decrease, bilirubin 27.48% decrease	
	estrogenic activity	isolated trifolirhizin	<i>in vivo</i> increase in uterine weight	93%	
<i>O. natrix</i>	cholinesterase inhibition	EtAc extract of aerial parts	<i>in vitro</i> enzyme inhibitory assay (Elmann's method)	1.46 mg galanthamine equivalent/g AChE 0.93 mg galanthamine equivalent/g BChE	[29]
	tyrosinase inhibition	aqueous extract of aerial parts	<i>in vitro</i> enzyme inhibitory assay (dopachrome method)	52.81 mg kojic acid equivalent/g	
	α -glucosidase inhibition	MeOH extract of aerial parts	<i>in vitro</i> enzyme inhibitory assay (chromogenic PNPG method)	17.52 mg acarbose equivalent/g	
	DNA protective effect	aqueous extract of aerial parts (5 and 10 mg/ml)	<i>in vitro</i> plasmid stability	70 and 78% inhibition	
	cytotoxicity	EtAc extract of aerial parts	<i>in vitro</i> test on MDA MB-231 cell line	IC ₅₀ = 28.75 μ g/ml	[70]
	anti-inflammatory activity	EtAc extract of aerial parts	<i>in vitro</i> test on LPS induced HeLa cell line	10 μ g/ml 80-100% inhibition of production of TNF α	[71]

The advantage of using organ cultures is that they are relatively more stable in production of secondary metabolites than cultures of undifferentiated cells, such as callus or suspension cultures. For the objective of production of plant secondary products, generally two types of organ cultures are considered, i.e. root cultures and shoot cultures. Root systems of higher plants, however, generally exhibit slower growth than cultures of undifferentiated plant cells and are difficult to harvest. Compared to the cell suspension cultures, organ cultures generally display a lower sensitivity to shear stress, but they show a high degree of spatial heterogeneity in biomass production [72].

Callus culture is the culture of dedifferentiated plant cells induced on media usually containing relatively high auxin concentrations or a combination of auxin and cytokinin in *in vitro* conditions. Fedoreyev *et al.* established callus cultures from *Maackia amurensis* and analyzed them for isoflavonoids. The isoflavones daidzein, retuzin, genistein and formononetin and the pterocarpan maackiain and medicarpin were found to be produced by these cultures in approximately four times higher concentration than the content of the heartwood of *M. amurensis* plants [73]. Moreover, Li *et al.* established six callus cultures of *Genista* species with the objective to produce isoflavones with phytoestrogenic activity. Callus cultures of all species produced more isoflavones than the parent herbs. *In vitro* cultures had lower contents of genistein esters than the herbs [74]. Stable and optimized callus cultures are the first step of preparing the inoculum for liquid suspension cultures. Production of secondary metabolites in cell suspension cultures have been widely published and it was proposed as a technology to overcome problems of variable product quantity and quality from whole plants due to the effects of different environmental factors, such as climate, diseases and pests. The approach of using plant cell suspension cultures for secondary metabolite production is based on the concept of biosynthetic totipotency of plant cells, which means that each cell in the cultures retains the complete genetic information for production of the range of compounds found in the whole plant. The effect of the potential elicitors (killed cells of *P. aeruginosa* and *E. coli*, linoleic acid, arachidonic acid, chitosan, CrCl₃, AgNO₃, CoCl₂, NiCl₂, CdCl₂, CuSO₄, jasmonic acid, salicylic acid, iodoacetic acid and substituted anilides as pyrazine-2-carboxylic acid) on the production of flavonoids in callus culture and cell suspension of *Ononis arvensis* L. was examined by Tůmová and coworkers. All the tested elicitors markedly increased the production of flavonoids in comparison to the

control, however, only spectrophotometric methods were used to characterize the flavonoid content [77–86].

Genetic transformation of plants mediated by root inducing (Ri) plasmid of *Agrobacterium rhizogenes* bacterium occupies a special place in plant cell engineering, since this technique is based on a natural phenomenon that allows cultivation of isolated growing plant roots on hormone-free media. Application of wild-type unmodified agrobacterial strains allows to obtain root cultures capable of long-term growth *in vitro* due to an increased sensitivity of the cells to auxins while other biochemical properties remain unaltered. The *in vitro* cultivated roots could synthesize root-specific metabolites, which makes their application possible for large-scale biotechnological production of ecologically pure crude drugs. A collection of pRi T-DNA transformed roots of certain dicotyledons was made by Kuzovkina *et al*; including *O. arvensis* transformed by R 1601, A4 plasmids and *O. spinosa* transformed by R 1601 plasmid [89]. Although, the qualitative and quantitative relations of isoflavonoid content of these root cultures are unknown.

1.II. Isoflavonoids

1.II.1. Structural features and occurrence of isoflavonoids

The Leguminosae, with 19500 estimated species, is the main source of naturally occurring isoflavonoids. With only a few exceptions, *Leguminosae* isoflavonoids are restricted to the *Papilionoideae*, the largest of the three subfamilies currently recognized by legume taxonomists (Figure 9). For example, no reports of isoflavonoids from either the *Caesalpinioideae* or the *Mimosoideae* appeared [90].

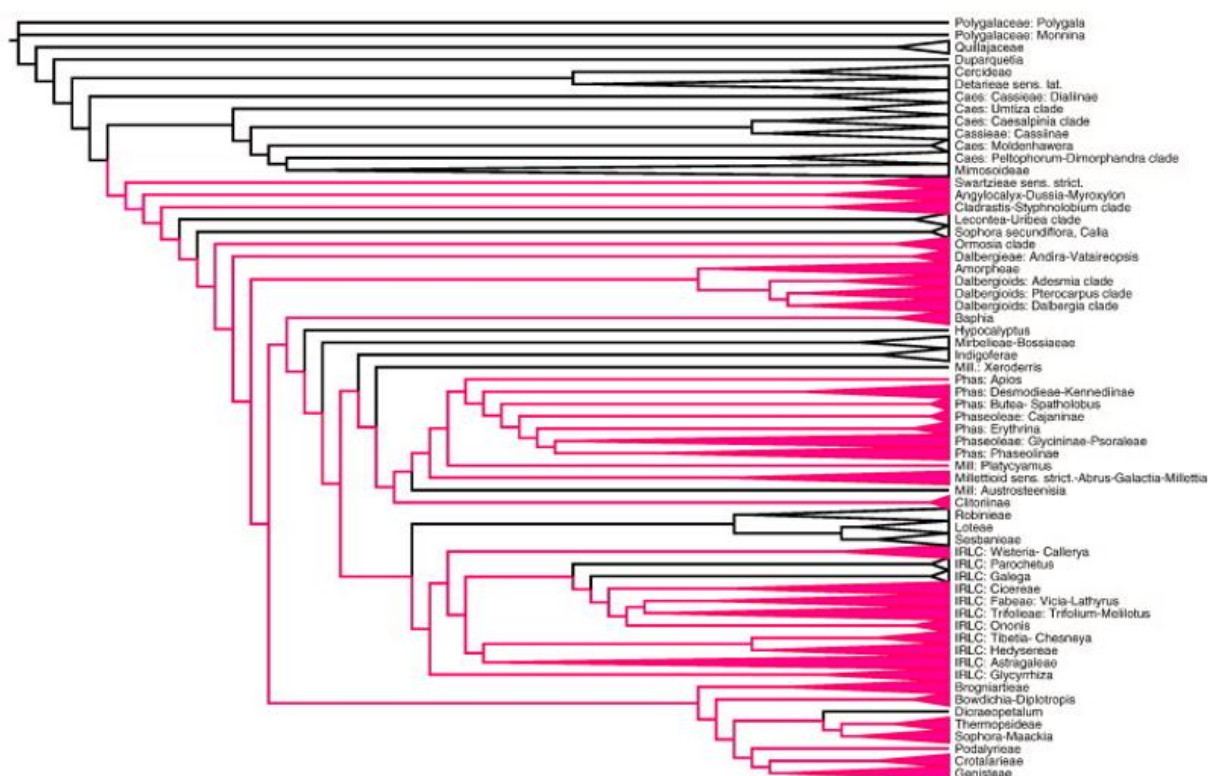


Figure 9: Distribution of isoflavonoids in legumes. Clades that produce isoflavonoids are highlighted with pink [91]

Isoflavones are the most frequently reported of all the isoflavonoid subclasses, whereas isoflavanones are considerably rarer and can be found usually in racemic form (Figure 10). Reduction of isoflavanones leads to isoflavans, many of which act as phytoalexins in legumes. Laevorotatory, dextrorotatory, and racemic isoflavans are known in nature. Pterocarpans contain a tetracyclic ring system derived from the basic isoflavonoid skeleton by an ether linkage between the C-4 and C-2' positions. Pterocarpans act as phytoalexins in leguminous plants and are produced following either fungal infection or

abiotic elicitor treatment. Dextrorotatory, levorotatory and racemic pterocarpan are known in nature with either a 6aR,11aR or 6aS,11aS configuration at the two chiral centers. Coumestans represent the fully oxidized version of pterocarpan. Rotenoids are a class of isoflavonoids characterized by the inclusion of an extra carbon atom into a heterocyclic ring. Almost all the known rotenoids contain an isoprenoid substituent and are noted for their insecticidal, piscicidal and antiviral activities. They can be conveniently subdivided into three major types, rotenoids, 12a-hydroxyrotenoids and dehydro-rotenoids depending on the oxidation level. Some rarities amongst isoflavonoids are coumaronochromones, isoflav-3-enes, isoflav-3-en-2-ones (3-arylcoumarins) and 2-arylbenzofurans (see Figure 10). In contrast to flavonoid oligomers which are a major group of flavonoid derivatives, similar oligomers of isoflavonoids are sporadic in nature [92].

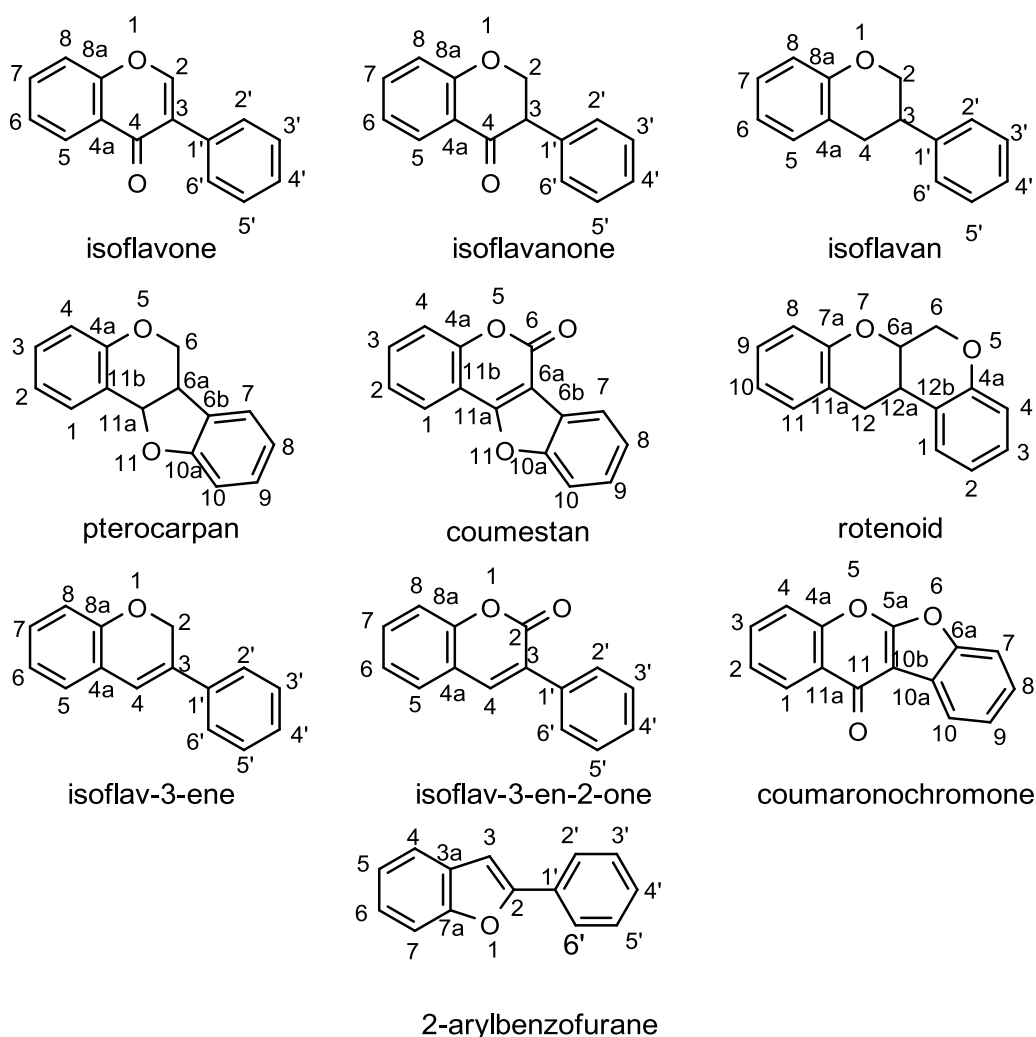


Figure 10: Structure and numbering of isoflavonoid skeletons

The structural diversity of isoflavonoids is a result of the metabolic engineering of the aglycone skeleton and glycosylation. The number and complexity of possible substituents on the basic structural skeleton (hydroxyl, methoxy, methylenedioxy, prenyl or isoprenyl, *etc.*), the different oxidation levels and the frequent presence of extra heterocyclic rings (formed by cyclization between vicinal hydroxy and methoxy or monoprenyl groups) account for the multiplicity of subgroups among isoflavonoids (see Figure 11). Some isoflavonoids are amino-substituted; these are called “isoflavonoid alkaloids”, whereas others may be chlorinated [93]

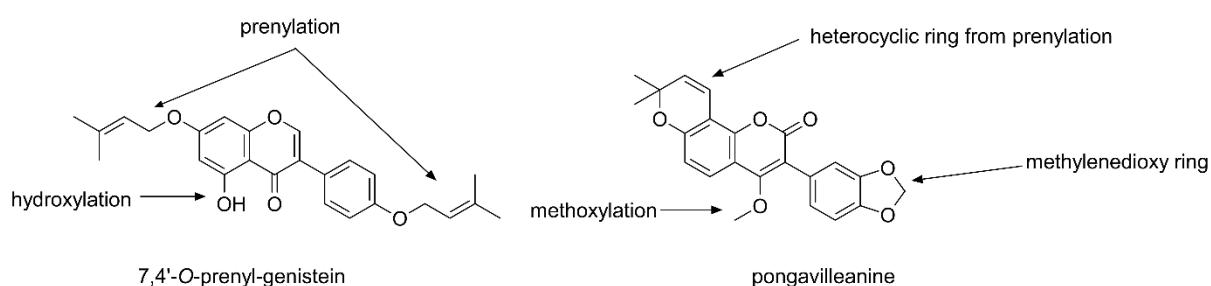


Figure 11: Examples for the structural modification of isoflavonoid skeletons

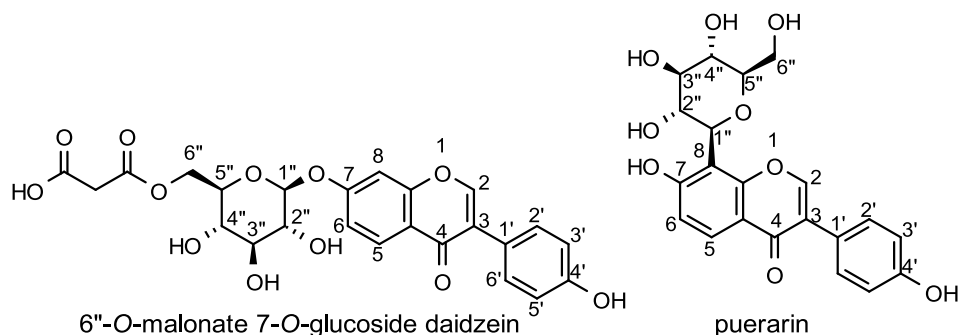


Figure 12: Examples for *O*- and *C*-glycosides

In plants, isoflavonoids may be encountered as aglycones or as glycosides with generally glucose, rhamnose or apiose as the sugar component [93]. The number of known isoflavonoid glycosides is extremely small compared with the vast range of flavonoid glycosides [92]. Although the majority of glycosides are *O*-linked glycosides, several *C*-linked glycosides are also known together with a few compounds characterized by both *C*- and *O*-glycosylation (see Figure 12). One of the most important sources of *C*-linked isoflavones is the genus *Pueraria*. Through an enzymatic step, the 7-*O*-glucosides of

isoflavones and isoflavanones, and the 3-*O*-glucosides of pterocarpans could be malonylated to their 6''-*O*-malonyl derivatives [90].

Although isoflavonoids could be observed with vast majority in *Leguminosae* species, there are some examples in other families, as well. In monocots, few families (only 6 have been reported) seem able to produce isoflavonoids. The *Iridaceae* are the major source of isoflavonoids in this group, with more than 50 different compounds described, mainly in the genus *Iris* where they are present in the rhizomes of approximately 20 species. Among the dicots, five non-leguminous families are particularly outstanding because of their relative abundance in isoflavonoids: the *Asteraceae* (21 molecules), the *Chenopodiaceae* and the *Nyctaginaceae* (19 molecules each), the *Moraceae* (18 molecules), the *Ochnaceae* (17 molecules). However, the presence of isoflavonoids has been reported in only few species among these five families. Isoflavonoids have also been mentioned in various commercial beers, bourbons, teas and coffees but no study has documented their occurrence in the plants themselves [93].

1.II.2. Biosynthesis of isoflavonoids

Both flavonoids and isoflavonoids are synthesized through the central phenyl-propanoid pathway [94]. The factor differentiating isoflavonoids from other flavonoids is the linking of the B-ring to the C-3 rather than the C-2 position of the C-ring. The initial steps of isoflavonoid biosynthesis are now well characterized at the molecular level, but there is limited progress on the later enzymatic steps that produce the wide range of complex derivatives found in different legume species [95].

2-Hydroxyisoflavon synthase

2-HIS is a key cytochrome P450 enzyme that catalyzes the entry-point reaction into isoflavonoid biosynthesis, converting flavanones to isoflavones by an unusual aryl migration reaction (Figure 13). 2-HIS only present in legumes for the synthesis of isoflavonoids. *Arabidopsis* possesses 273 putative P450 genes, but none of them has 2-HIS activity for synthesizing isoflavone. Introducing soybean 2-HIS into *Arabidopsis thaliana* resulted in production of genistein at a high level, indicating its central role in the biosynthesis of isoflavonoids and extremely high substrate specificity [94].

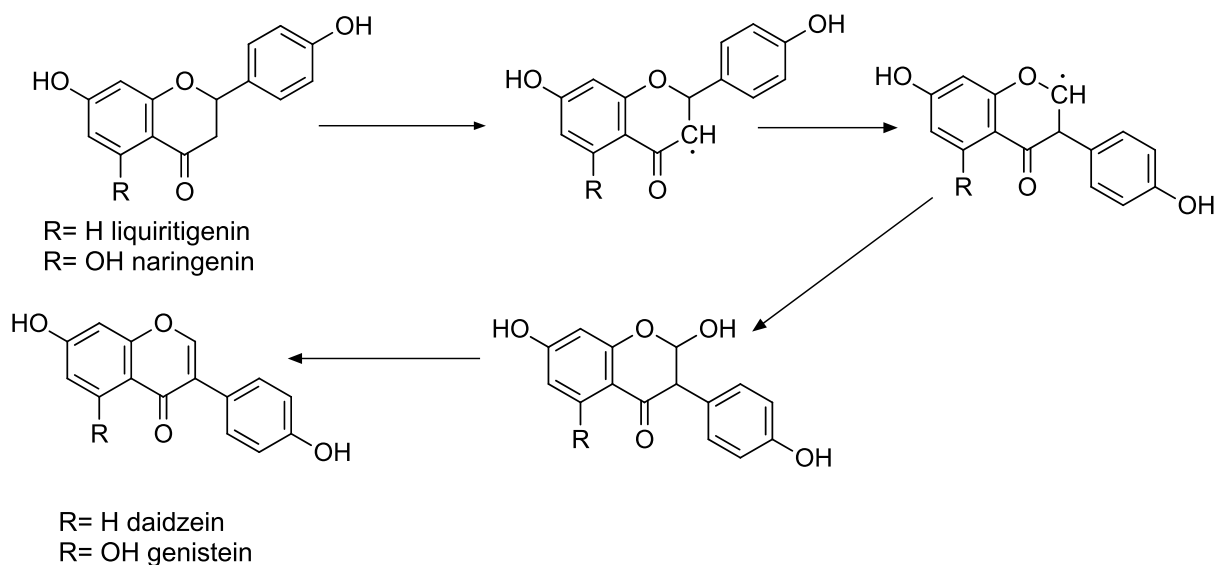


Figure 13: The biosynthesis of isoflavonoids from flavonoids catalyzed by 2-HIS [95]

Methylation

Methylation is one of the key modifications of natural products including (iso)flavonoids to modulate their *in vivo* activity by limiting the number of reactive hydroxyl groups, thus altering their solubility and functions. Isoflavone-*O*-methyltransferase (IOMT) has been identified in various leguminous plants. It is an S-adenosyl-L-methionine (SAM)-dependent methyltransferase transferring a methyl group from SAM to isoflavones yielding the methyl ether derivatives (see Figure 14). 4'-*O*-methyltransferase (HI4'OMT) is a dual function enzyme with both 4'-*O*- and 3'-*O*-methylation activity [94].

Isoflavone 2'- and 3'-hydroxylase

Two P450s of the CYP81E subfamily, isoflavone 2'-hydroxylase (I2'H) and isoflavone 3'-hydroxylase (I3'H), catalyze key steps in the formation of the more complex isoflavonoids. Hydroxylation of formononetin at the C-3' position produces calycosin, a precursor for subsequent methylenedioxy bridge formation (yielding pseudobaptigenin) as part of the branches leading to maackiain- and pisatin-type phytoalexin end products, as well as to the rotenoids and other complex derivatives. Hydroxylation at the C-2' position of daidzein, formononetin, or pseudobaptigenin provides the hydroxyl required for C–O–C bridge formation that defines the pterocarpan (e.g., glycinol) (Figure 14) [96].

Isoflavone reductase

The 2'-hydroxyisoflavones are reduced to the corresponding isoflavanones by a NADPH-dependent isoflavone reductase (IFR). IFR catalyzes enantiospecific conversions with high specificity for isoflavones [94]. The isoflavanones are the final isoflavonoid intermediates of pterocarpin biosynthesis (see Figure 14). Variant IFR activities between species are thought to contribute to the stereochemistry of the pterocarpanes produced, in particular, (+)-maackiain in *Pisum sativum*, (-)-maackiain in *Cicer arietinum*, (-)-3,9-dihydroxypterocarpan in *G. max*, and (-)-medicarpin in *M. sativa* [95].

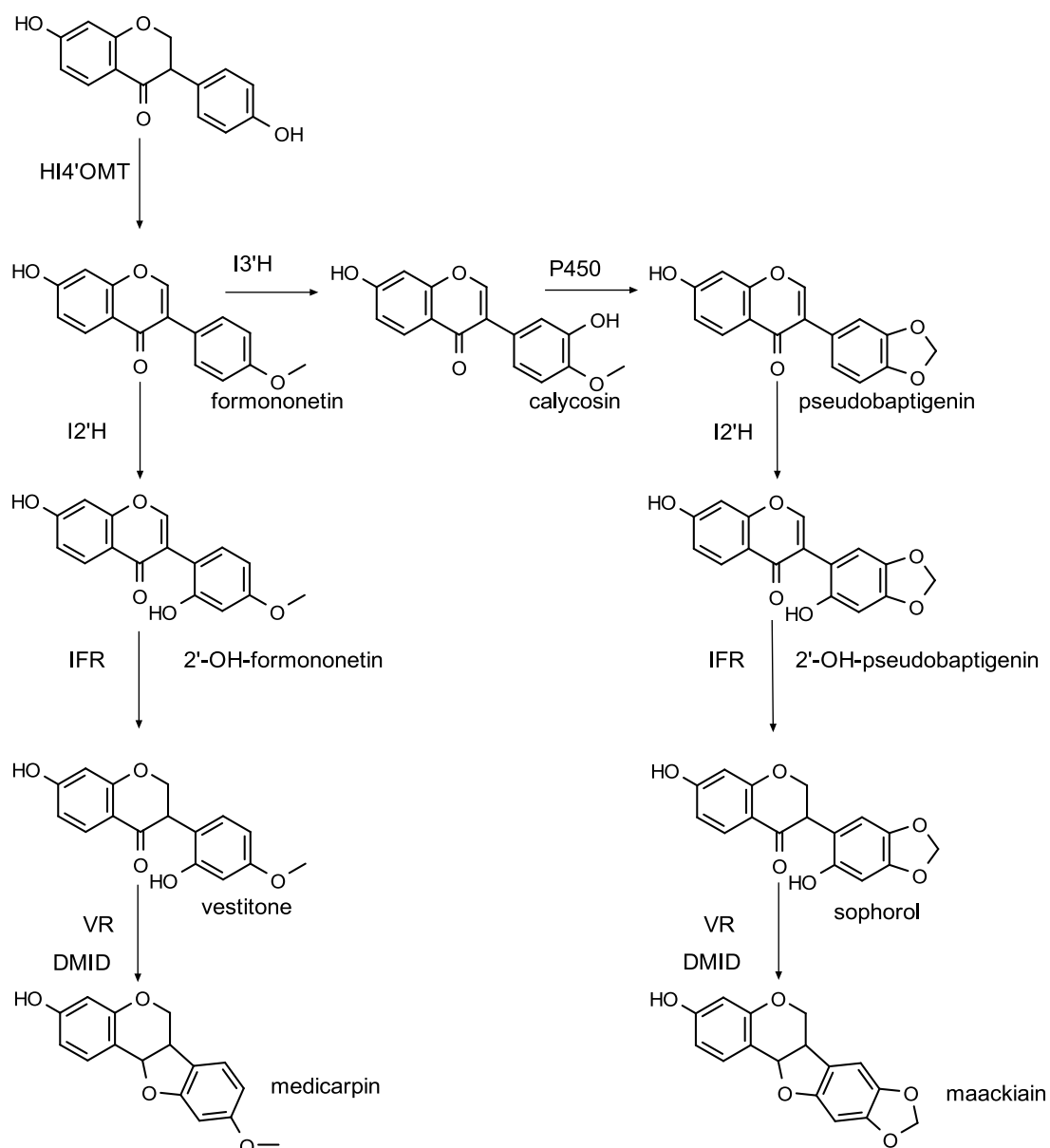


Figure 14: Steps of isoflavonoid biosynthesis resulting pterocarpanes [95]

Vestitone reductase and 7,2'-dihydroxy-4'-methoxyisoflavanol dehydratase

Based on analysis of enzyme preparations, the conversion of isoflavanones to pterocarpan was thought initially to be catalyzed by a single NADPH-dependent enzyme, termed the pterocarpan synthase. However, it was subsequently shown that in *M. sativa* the conversion of vestitone to medicarpin involves two enzymes, vestitone reductase (VR) and 7,2'-dihydroxy-4'-methoxyisoflavanol dehydratase (DMID) (Figure 14). The reaction series from vestitone to the pterocarpan is thought to proceed by the VR-catalyzed reduction of vestitone to DMI, followed by the loss of water and formation of the C–O–C bridge between the heterocycle and the B-ring, catalyzed by DMID. In some species, the products of VR and DMID (maackiain and medicarpin) are the main pterocarpan phytoalexins. They are typically glucosylated and malonylated and stored in the vacuole. In species such as *G. max*, *P. sativum* and *P. vulgaris*, the pterocarpan are further converted by a series of reactions to species-specific compounds. For *G. max* and *P. sativum*, the initial reaction is a hydroxylation catalyzed by pterocarpan 6 α -hydroxylase (P6aH) (Figure 15) [95].

SAM:6 α -hydroxymaackiain 3-O-methyltransferase

Methylation of the 3-hydroxyl of (+)-6 α -hydroxymaackiain by hydroxymaackiain 3-O-methyltransferase (HM3OMT) produces the major phytoalexin of *P. sativum*, (+)-pisatin (Figure 15) [95].

Prenyltransferases

The formation of phytoalexins such as glyceollins and phaseollins requires C-prenylation by a range of pterocarpan prenyltransferase activities, with dimethylallyl pyrophosphate as the prenyl donor. For glyceollins and phaseollins, prenylation occurs at position C-2 (pterocarpan C-2 prenyltransferase, P2CP) or C-4 (pterocarpan C-4 prenyltransferase, P4CP) of glycinol or C-10 of 3,9-dihydroxypterocarpan (Figure 15) [95].

Prenylpterocarpan cyclases

The final step of glyceollin and phaseollin formation is the cyclization of the prenyl residues of glyceollidins and phaseollidins, carried out by P450 prenylcyclases. These activities have been studied in detail for the formation of three glyceollins (I, II, and III) from glyceollidin I and II, and it is thought that specific activities are involved in each reaction (Figure 15) [95].

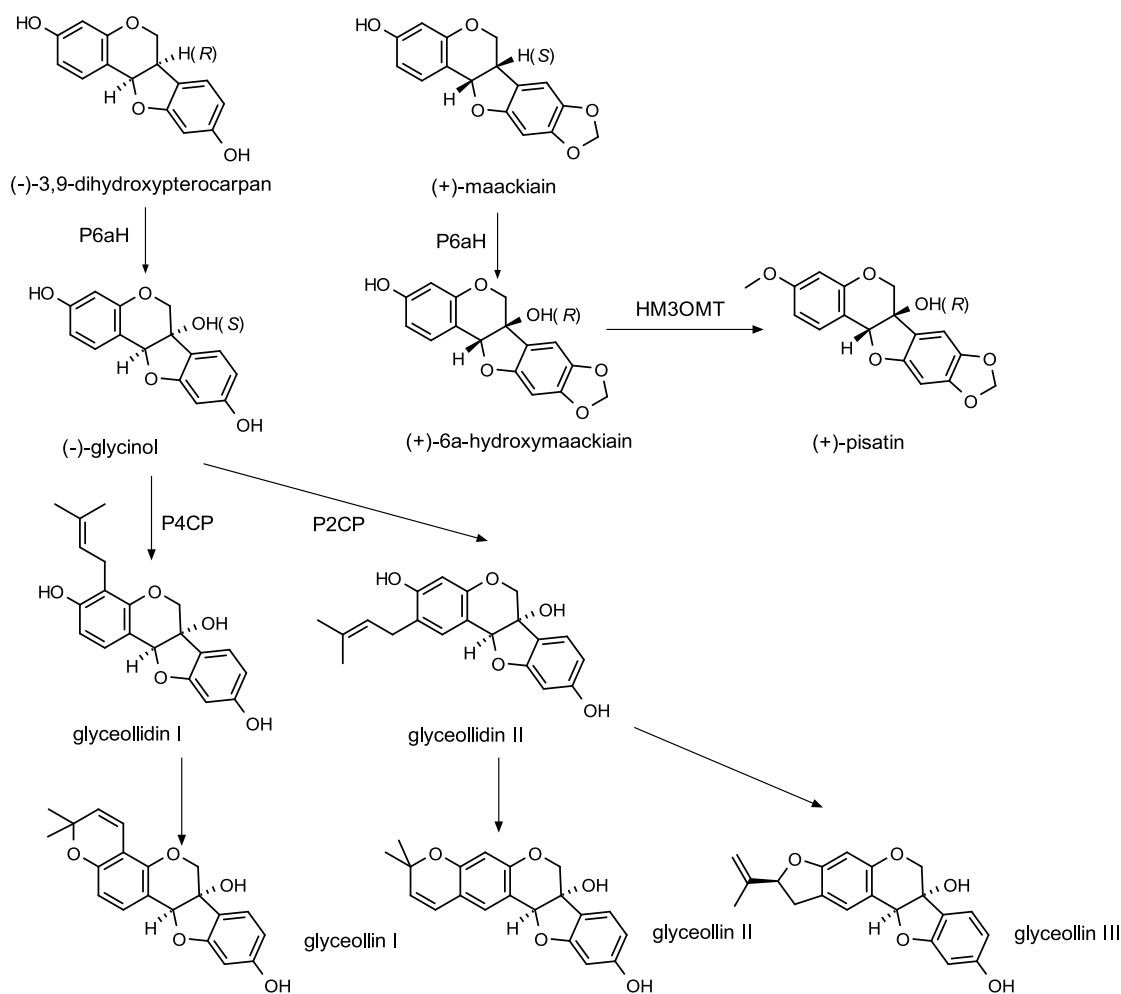


Figure 15: Biosynthesis of pterocarpane based phytoalexins [95]

Isoflavonoid glycosyltransferase and malonyltransferase

Glycosylation is a key modification to decorate plant natural products with various sugars, enhancing their solubility and stability and facilitating their storage and accumulation in plant cells. It is also a major factor in determining the bioactivity and bioavailability of natural products. Uridine diphosphate glycosyltransferases are the central players in glycosylation of plant natural products. Isoflavonoids are often modified by glycosylation, for example, the predominant soy isoflavones are genistein 7-*O*-glucoside and daidzein 7-*O*-glucoside and some malonyl conjugates [94]. In various isoflavonoid *O*-glucoside containing plants the main isoflavone constituents are actually isoflavone 7-*O*-glucoside 6''-*O*-malonates, however, these labile esters could be overlooked due to inadequate sample preparation methods [97].

Flavonoid 6-hydroxylase

The hydroxyl groups at C-5 and C-7 of the A-ring are introduced during the formation of chalcones by chalcone synthase. However, isoflavonoids also occur with C-6 and C-8 hydroxylation. The cDNA of the possible enzyme represented an elicitor induced P450 (CYP71D9) with flavonoid 6-hydroxylase activity, which may be involved in the biosynthesis of isoflavonoids with 6,7-dihydroxylation of the A-ring. The recombinant protein did not act on the isoflavonoids or pterocarpan directly, but rather accepted flavanone and dihydroflavonol substrates, including liquiritigenin, suggesting hydroxylation occurs prior to aryl migration of the B-ring (see Figure 13) [95].

1.II.3. Biological activities of selected isoflavonoids

In the following section, the biological activities of the eight isoflavonoids characterized in this thesis are highlighted in order to emphasize their importance.

Biological activities of formononetin

As formononetin is one of the most basic isoflavonoids regarding their biosynthesis (see page 27), it can be identified in many *Leguminosae* plants (175 hits for “Isolated as Natural Product” in Reaxys database) which possesses beneficial biological activities. As a consequence, there is magnitude orders higher amount of publications investigating the biological effects of formononetin.

- Neuroprotective effect

Amyloid beta ($A\beta$) is the main component of the amyloid plaques that accumulate in the brains of Alzheimer patients. Chen *et al.* reported the protective role of formononetin against $A\beta_{25-35}$ -induced neurotoxicity as formononetin (1-5 μ M) significantly increased the viability of the cells and decreased the cell apoptosis. Formononetin also accelerated the non-amyloidogenic process of amyloid β precursor protein by enhancing α -secretase activity and soluble amyloid β precursor protein α release [98]. The study of Sun *et al.* also shows that formononetin increases soluble amyloid β precursor protein α secretion and thus protects cells from hypoxia-induced apoptosis [99]. In the study of Fei *et al.*, it is established that formononetin in a 15 mg/kg/day dose significantly improved learning and memory ability by suppressing $A\beta$ production from amyloid β precursor protein processing. Moreover, these results did not differ significantly from that of achieved with 1 mg/kg/day donepezil [100].

The work of Li *et al.* concluded that formononetin mediates promising anti-traumatic brain injury effects against neurocytes [101], [102]. In addition, the work of El-Bakoush *et al.* established that formononetin inhibits neuroinflammation by targeting nuclear factor κ B (NF- κ B) [103]. In the study of Jia *et al.*, formononetin reduced H₂O₂-induced apoptosis of retinal ganglion cells in a dose of 0.5-10 μ M [104].

- Angiogenic effect

The study of Huh *et al.* investigated the influence of formononetin on the expression of growth factors contributing to wound healing in human umbilical vein endothelial cells (HUVECs). Formononetin (10 and 50 μ M) in *in vitro* and *ex vivo* tests resulted to be more potent than recombinant vascular endothelial growth factor (VEGF₁₂₅), but in the *in vivo* test of wound closure it did not differ from VEGF₁₂₅ significantly [105]. Based on *in vivo* tests, formononetin promotes early fracture healing through angiogenesis activation in the early stage of fracture repair, and osteogenesis acceleration in the later stages used in a 200 μ g/kg dose [106]. On the contrary to the previous results, Auyeung *et al.* aimed to examine the potential of formononetin in controlling angiogenesis and tumor cell invasiveness in human colon cancer cells and tumor xenografts in mice. The results showed that 200 μ M formononetin downregulated the expression of the key pro-angiogenic factors. The tumor size and the number of proliferating cells were reduced in the tumor tissues obtained from the formononetin-treated group [107]. In the study of Wu *et al.*, formononetin could inhibit the VEGF secretion of human retinal pigment endothelial cells under hypoxia in 0.2-5.0 μ M concentration. Furthermore, formononetin could prevent hypoxia-induced retinal neovascularization *in vivo* (5-10 mg/kg), however, it did not reach the effectiveness of conbercept (1 mg/kg) [108].

- Vasorelaxive activity

Wu *et al.* and Sun *et al.* evaluated the vasorelaxation effects of formononetin, on rat isolated aorta and *in vivo*, the underlying mechanisms involved. Their results suggest that formononetin caused vascular relaxation via endothelium/NO-dependent mechanism and endothelium-independent mechanism which involves the activation of BK_{Ca} and K_{ATP} channels. The antihypertensive mechanism *in vivo* may be associated with the down-regulation of α_1 -adrenoceptors and 5-HT_{2A/1B} receptors, and the up-regulation of endothelial NO synthase expression in arteries [109]–[111]. The NO-dependent mechanism was also supported by the study of Bai *et al.* [112].

- Osteogenic activity

In the study of Ha *et al.*, therapeutic potencies of phytoestrogens were investigated. In ovariectomized (Ovx) rats, formononetin-treated groups given 1 and 10 mg/kg/day displayed increased trabecular bone areas within the tibia [113]. Tyagi *et al.* achieved similar results. Formononetin treatment (10 mg/kg/day for 12 weeks) significantly restored the lost trabecular microarchitecture in the femurs and tibia of osteopenic Ovx rats and promoted new bone formation [114], [115]. Microcomputed tomography analysis showed that formononetin promoted bone healing and this effect observed was equal to parathyroid hormone treatment in many aspects [116]. In the study of Huh *et al.*, formononetin led to a dramatic increase in normal osteoblast progenitor proliferation and differentiation, while decrease in osteoarthritic osteoblasts [117]. According to the results of Gautam *et al.* formononetin maximally stimulated osteoblast differentiation at 100 nM but had no effect on osteoblast proliferation. It neither activated estrogen receptor in osteoblasts nor had any effect on osteoclast differentiation and did not exhibit estrogen agonistic effect *in uteri*. Daily oral administration at 10.0 mg/kg/day dose to recently weaned female Sprague-Dawley rats for 30 consecutive days increased bone mineral density [118].

- Phytoestrogenic activity

To investigate a possible mechanism by which phytoestrogens might influence mammary carcinogenesis, Wang *et al.* examined the capacity of formononetin to stimulate mammary gland proliferation. Among animals treated with formononetin at 40 mg/kg/day for five days, mammary gland proliferation was enhanced 3.3-fold over saline-treated controls and was comparable to that of animals treated with 17 β -estradiol at 1 μ g/kg/day for five days. In subsequent *in vitro* binding studies, formononetin competitively bound murine mammary estrogen receptors, but with a relative binding affinity 15,000 times less potent than that of 17 β -estradiol [119]. Ji *et al.* established a highly sensitive bioassay system by placing estrogen-responsive elements upstream of the luciferase reporter gene and used this assay to determine the estrogenic activity of formononetin. Formononetin activated expression of the estrogen-responsive reporter gene in human breast cell line MCF-7 in a concentration-dependent manner (0.5-500 μ M), and this activation was inhibited by estrogen antagonist (ICI 182780 at 100 nM) [120]. Umehara *et al.* investigated the concentrations, in which isoflavones can show

similar results to 10 and 100 pM 17 β -estradiol. On on T47D cell line 30 nm formononetin had equivalent effect to 10 pm 17 β -estradiol. Formononetin activated expression of the estrogen-responsive reporter gene in cell line MCF-7 and T47D equivalent to 10 pM 17 β -estradiol at 10 nM concentration [121]. Chen *et al.* aimed to further investigate the potential effect of formononetin in promoting cell proliferation in ER-positive cells and used *in vivo* and *in vitro* studies to elucidate the possible mechanism. Compared with the control, low formononetin concentrations (2-6 μ M) stimulated ER α -positive cell proliferation. Additionally, in the *in vivo* studies, uterine weight in Ovx mice treated with formononetin increased significantly (in contrast to page 36) [122]. The growth of uterine tissues was confirmed by other researchers, as well [123], [124].

- Antigiardial activity

Khan *et al.* isolated several isoflavones from *Dalbergia frutescens* and determined their antiprotozoal activities against *Giardia intestinalis*. Among the isolated compounds, formononetin was the most potent anti-giardial agent, with an IC₅₀ value of 0.03 μ g/ml, as compared to the value for metronidazole, the current drug of choice, of 0.1 μ g/ml. The *in vivo* results indicated that, although formononetin is active, relatively large doses are required [125]. According to Lauwaet *et al.* the anti-giardial activity of formononetin is at least partially due to its capacity to rapidly detach trophozoite [126].

- α -glucosidase activity

The heartwoods extract of *Dalbergia odorifera* demonstrated a potent inhibition on yeast α -glucosidase *in vitro*. Thus, bioassay-guided purification of EtAc soluble fraction was conducted to purify the active principles responsible for the inhibition. All active components isolated demonstrated a significant inhibition on yeast α -glucosidase in a dose-dependent manner, but formononetin showed an outstanding activity (IC₅₀ = 0.51 mM) [127]. As the methanol extracts of all the parts of *Dalbergia tonkinensis* were found to be potential sources of α -glucosidase inhibitors, as well (showing more efficient inhibitory activity than that of acarbose), Van Bon *et al.* executed a bioassay-guided fractionation and isolated the most active compounds, sativanone and formononetin. Formononetin showed weak inhibition against rice α -glucosidase, good inhibition against rat α -glucosidase, and a very efficient effect on α -glucosidases from yeast and bacterium (on yeast, its potency was approximately the twice as in the report of Choi *et al.*) (see Figure 16) [128].

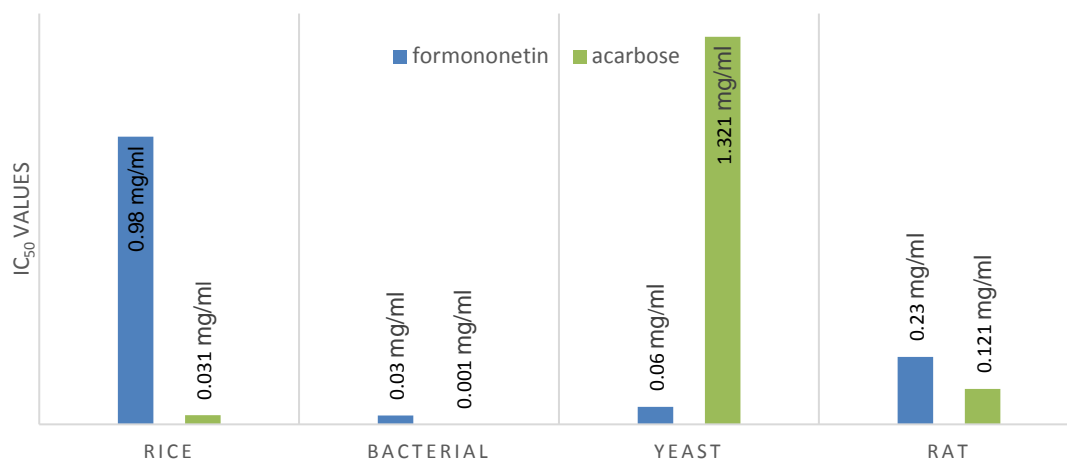


Figure 16: α -glucosidase inhibitory effect of formononetin and acarbose in different enzyme systems [128]

- Pro-apoptotic effect

Many researchers aimed to define the pro-apoptotic characteristics of formononetin, however, no outstanding results have been published yet. On the other hand, these studies are a great help for the understanding of the underlying molecular biological pathways which contribute to the beneficial health effects of formononetin [129]–[144].

Biological activities of pseudobaptigenin

- Peroxisome proliferator-activated receptor agonism

Salam *et al.* executed a structure-based virtual screening of the peroxisome proliferator-activated receptor γ (PPAR γ) ligand binding domain against a natural product library which revealed 29 potential agonists. *In vitro* testing of this list identified six flavonoids to have stimulated PPAR γ transcriptional activity in a transcriptional factor assay. Of these, isoflavonoid pseudobaptigenin was classed as the most potent PPAR γ agonist, possessing low micromolar affinity ($EC_{50} = 2.9 \mu\text{M}$) [145]. Matin *et al.* aimed to develop novel, efficacious, and yet safer pan agonists of PPAR receptors. Based on the aforementioned results of Salam *et al.*, pseudobaptigenin and its derivatives were screened beside numerous other natural product-based derivatives. 3',5'-dimethoxy-7-hydroxyisoflavone, pseudobaptigenin, 4'-fluoro-7-hydroxyisoflavone and 3'-methoxy-7-hydroxyisoflavone exhibited a substantially higher PPAR γ fold activation compared to rosiglitazone at 5 μM and 25 μM . In the PPAR α activity tests they all demonstrated higher

fold activity than the positive control fenofibrate (1.3-fold activation). Pseudobaptigenin exhibited more potent PPAR α activation than PPAR γ activation. These four molecules were therefore identified as the most potent dual PPAR α and γ agonists evaluated. The highest PPAR δ agonist activity in the isoflavone series was observed for the same compounds as mentioned previously. Moreover, these isoflavones proved to be almost twice as potent activators of PPAR δ than bezafibrate. To ensure that these active compounds were nontoxic to HEK 293 cell line, cytotoxicity profiles were investigated. Pseudobaptigenin and the other three compounds exhibited excellent tolerability [149, 150].

Biological activities of calycosin

- Antioxidant activity

Promden *et al.* evaluated the antioxidant activities of 24 isoflavonoids that were previously isolated as pure compounds from *D. parviflora* using three different *in vitro* antioxidant-based assay systems: xanthine/xanthine oxidase, oxygen radical absorbing capacity, and 2,2-diphenyl-1-picrylhydrazyl (DPPH). The subgroup of isoflavones, and particularly calycosin showed the highest activities with 50% radical scavenging concentration (SC₅₀) value of 0.25 μ M. A further SAR analysis revealed that these active isoflavonoids from all three subgroups have the following common substituent pattern: the presence of R7-OH in ring A and the R4'-OMe in ring B with either R3'-OH or R5'-OH. However, the presence of R7-OH and R4'-OMe in the molecule with no other key substituents (i.e., formononetin, SC₅₀ = 117 μ M), showed considerably lower activity, suggesting that these two substituents are not as important. In the other two assays, calycosin displayed only intermediate activity [148].

- NO production inhibition

Morikawa *et al.* isolated constituents from *Erycibe expansa* (*Convolvaceae*) originating from Thailand and examined their inhibitory activities on lipopolysaccharide-activated nitric oxide production in mouse peritoneal macrophages. The most active component was calycosin showing an IC₅₀ value of 13 μ M. This result is nearly equivalent to that of caffeic acid phenethyl ester, an inhibitor of NF- κ B activation (IC₅₀ 15 μ M) [149].

- Alleviating the cellular effects of hypoxia

Fan *et al.* intended to investigate the effect of calycosin on impairment of barrier function induced by hypoxia in HUVECS. The *in vitro* results indicated that calycosin could inhibit hypoxia induced hyperpermeability [150].

- Antiprotozoal activity

Araujo *et al.* isolated calycosin from *Centrolobium sclerophyllum* (*Leguminosae*) and tested its activity against *Leishmania amazonensis* promastigotes. Calycosin showed good antileishmanial activity, with calculated $IC_{50} = 140$ nM [151]. ElSohly *et al.* isolated calycosin, based on bioassay-guided fractionation, as the most active anti-giardial compound of *Machaenum aristulatum*. Calycosin was tested against *G. intestinalis* and the anti-giardial IC_{50} was determined as 1.9 $\mu\text{g/ml}$, which is twice as high as the IC_{50} of metronidazole (1.1 $\mu\text{g/ml}$) and ten times higher than that of formononetin (0.28 $\mu\text{g/ml}$) [152]. The extracts of *Psoralea arborescens*, a desert shrub common in Mojave Desert, exhibited significant activity against *Leishmania donovani* axenic amastigotes and bloodstream form *Trypanosoma brucei brucei*. Bioassay-guided fractionation led to the isolation of calycosin, which showed very weak activity against *L. donovani* axenic amastigotes, but it displayed selective toxicity (about 15-fold) toward *T. b. brucei* bloodstream forms ($IC_{50} = 12.7$ μM) over Vero cells [153].

Biological activities of calycosin D (3'-methoxydaidzein)

- Antiprotozoal activity

Beldjoudi *et al.* isolated 4 new flavonoids along with 13 known compounds from the heartwood of *Dalbergia louvelii* by following their potential to inhibit the growth of *Plasmodium falciparum in vitro*. One of the most active compounds 3'-methoxydaidzein showed antiplasmodial activity with IC_{50} value at 6.8 μM , however, this result is not comparable with the activity of chloroquine ($IC_{50} = 0.13$ μM). Since the antiplasmodial effect of the extracts of the plant and their fractions showed higher activity, than the isolated compounds itself, a synergistic play of the constituents is supposed [154].

Biological activities of onogenin

- Antioxidant activity

Promden *et al.* evaluated the antioxidant activities of 24 isoflavonoids that were previously isolated as pure compounds from *D. parviflora* using three different in vitro antioxidant-based assay systems: xanthine/xanthine oxidase, oxygen radical absorbing capacity and DPPH. Onogenin showed a very weak activity in the xanthine/xanthine oxidase test, and no activity at all in the other two assays [148].

- Estrogenic effect

In the same study (see page 32), Umehara *et al.* investigated the estrogenic effect of isoflavanone onogenin, too. Onogenin stimulated the proliferation of both cells, but its activity was only about the one millionth of the positive control, estradiol, and one thousands of genistein and T47D cells. Interestingly, luciferase induction at low concentrations was only observable on T47D/luc cells, but it still could not approach the activity of genistein [121].

Biological activities of sativanone

- Dermocosmetic use

The study of Ham *et al.* examined the antiwrinkle effects of ethanol extracts of *D. odorifera* in UVB-irradiated human skin cells. Ethanol extracts of *D. odorifera* and their constituents, dalbergin and sativanone, induced expression of collagen type I and transforming growth factor- β 1 in human dermal fibroblasts in a dose-dependent manner [155].

- α -glucosidase inhibitory activity

The other active compound which was responsible for the α -glucosidase inhibitor activity of *Dalbergia tonkinensis* extracts beside formononetin (see page 32), is sativanone. Regarding its enzyme inhibitory activity, it was similarly prominent as the isoflavone formononetin (see Figure 17). Moreover, their maximum inhibition rates were in the same range, and showed no significant difference from acarbose. As both isoflavanone sativanone and isoflavone formononetin differ markedly from the sugar analogue acarbose, the mechanism of enzyme inhibition still needs to be explored [128].

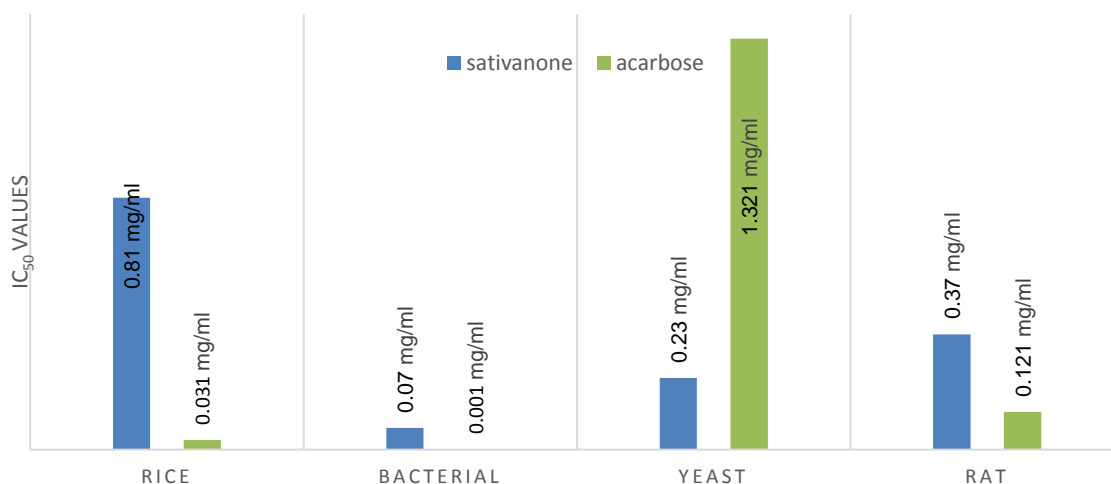


Figure 17: α -glucosidase inhibitory effect of sativanone and acarbose in different enzyme systems [128]

Biological activities of medicarpin

- Anti-allergenic effect

To define the anti-allergenic components from Saiboku-To, a herbal medicine for bronchial asthma, Taniguchi *et al.* examined the effect of 11 compounds found in post-administrative urine of Saiboku-To in *in vitro* and *in vivo* tests. In the *in vitro* test of blastogenesis, medicarpin displayed an IC_{50} value of 3.3 $\mu\text{g/ml}$ (prednisolone 0.08 $\mu\text{g/ml}$). In a 100 mg/kg dose, medicarpin could inhibit ear swelling by 40.1% (prednisolone 5 mg/kg 52.9%) [156]. However, its activity could not be linked to the metabolism of prednisolone, as it does not have a pronounced 11β -hydroxysteroid dehydrogenase activity [157].

- Pro-apoptotic activity

Shosaiko-to is a Kampo medicine used for the treatment of chronic hepatitis in Japan. Lately, over 200 cases of interstitial pneumonia have been reported resulting from Shosaiko-to therapy, and the number of cases increased when patients were administered interferon- α at the same time. In the study of Liu *et al.*, the *in vitro* effects of 7 phenolic compounds which had been detected from human urine after administration of Shosaiko-to were examined by flow cytometry analysis, on inducing apoptosis. In human lung fibroblasts, medicarpin significantly inhibited the growth and reduced the viability of lung fibroblasts. Interferon- α had no apoptosis-inducing effect, and it did not show synergistic

interaction with any of the compounds derived from Shosaiko-to on inducing apoptosis [158]. Tumor necrosis factor α -related apoptosis-inducing ligand (TRAIL) is a promising anticancer agent with cancer cell-selective cell death inducing effect. However, the major limitation in the usage of TRAIL as a chemotherapeutic agent is the development of TRAIL resistance in many cancer types including myeloid leukemia. In the study of Trivedi *et al.*, medicarpin is reported to sensitize myeloid leukemia cells to TRAIL-induced apoptosis for the first time [159]. Gatouillat *et al.* aimed to determine if medicarpin may have pro-apoptotic effects against drug-sensitive (P388) and multidrug resistant P388 leukemia cells (P388/DOX). While 3 μ M doxorubicin alone could not induce cell death in P388/DOX cells, concomitant treatment with doxorubicin and subtoxic concentration of medicarpin restored the pro-apoptotic cascade. Vinblastine cytotoxicity was also enhanced in P388/DOX cells (IC_{50} = 210 nM to 23 nM with medicarpin) [160].

- Osteogenic activity

During the phytochemical investigation of the stem bark of *Butea monosperma*, Maurya *et al.* isolated medicarpin and investigated it using neonatal (1–3 day old) rat calvaria derived primary osteoblast cultures. Medicarpin showed promising osteogenic activity, attributed to increased osteoblast proliferation, differentiation and mineralization. [161]. Bhargavan *et al.* evaluated osteogenic effect of medicarpin, too. According to their results, medicarpin stimulated osteoblast differentiation and mineralization at as low as 0.1 nM. Co-activator interaction studies demonstrated the osteogenic action of medicarpin is ER β -dependent. Medicarpin increased cortical thickness and bone biomechanical strength in rats, too [162]. Moreover, medicarpin at 0.1 nM suppressed osteoclast genesis in bone marrow cells and induced apoptosis of mature osteoclasts isolated from long bones. [163]. Goel *et al.* developed a convenient synthesis of natural and synthetic pterocarpanes and investigated their osteogenic activity. A comparative mechanism study for osteogenic activity of medicarpin (racemic versus enantiomerically pure material) revealed that (+)-(6aS,11aS)-medicarpin significantly increased the bone morphogenetic protein-2 expression and the level of the bone specific transcription factor Runx-2 mRNA, while the effect was opposite for the other enantiomer, (-)-(6aR,11aR)-medicarpin. For the racemate, (\pm)-medicarpin, the combined effect of both the

enantiomers on transcription levels was observed [164]. In conclusion, given its excellent oral bioavailability [162], medicarpin can be potential osteogenic agent.

Biological activities of maackiain

- Phytoalexin activity

Enantiomers of the isoflavonoid phytoalexins maackiain and pisatin were tested for toxicity to 36 fungal isolates by Delserone *et al.* Nine of these species were pathogens of red clover, which synthesizes (-)-maackiain; seven species were reported to be pathogenic on garden pea, which synthesizes predominantly (+)-pisatin and minor amounts of (-)-maackiain. In general, non-host phytoalexins were more potent inhibitors than host phytoalexins to growth of these pathogens. In addition, the opposite enantiomer of the host phytoalexin was often more inhibitory to a pathogenic fungus than the normally-occurring enantiomer [165].

- Anti-allergenic effect

Mizuguchi *et al.* identified (-)-maackiain as the responsible component of the antiallergic effect of *S. flavescens*. Pretreatment with (-)-maackiain alleviated nasal symptoms [166]. In a further study, Nariai *et al.* identified the target protein of (-)-maackiain as Hsp90 [167].

- Neuraminidase inhibiting activity

Ryu *et al.* isolated pterocarpans and flavanones from *S. flavescens* and screened for their ability to inhibit neuraminidase. Maackiain was shown to have an IC₅₀ value of 3.2 μM, whereas its glycoside had an IC₅₀ value of 237.5 μM. The best inhibitor was the 3-*O*-methylated derivative of maackiain with an IC₅₀ value of 1.4 μM. Kinetic analysis disclosed that pterocarpans are noncompetitive [168].

- Monoamine oxidase (MAO) inhibition activity

Of the compounds isolated from the roots of *S. flavescens*, Lee *et al.* found (-)-maackiain to inhibit potently and selectively human MAO-B, with an IC₅₀ of 0.68 μM, and to have a selectivity index of 126.2 for MAO-B. As compared with other herbal natural products, the IC₅₀ value of maackiain for MAO-B is one of the lowest reported to date. In addition, maackiain reversibly and competitively inhibited MAO-B. Molecular docking simulation revealed that the binding affinity of maackiain for MAO-B (-26.6kcal/mol) was greater

than its affinity for MAO-A (-8.3kcal/mol), which was in-line with the inhibitory activity findings [169].

1.II.4. Analytical methods aiming the qualitative and quantitative determination of isoflavonoids

Extraction and purification methods

Although solvent extraction is the simplest and oldest method, it is still the most widely used technique for the analyte isolation in the case of solid samples, mainly because of its ease of use and wide-ranging applicability. Liquid samples can be directly injected into the separation system after filtration or the analytes can be firstly isolated using liquid-liquid extraction or solid-phase extraction. Soxhlet extraction (which has been known since 1879) is used less frequently to isolate isoflavonoids. Concerning solvent- and Soxhlet extraction, aqueous methanol or acetonitrile is used as a solvent, usually favoring more than 50% organic solvent content. Liquid-liquid extraction is usually aiming the extraction of aglycones as they can be extracted from aqueous environments using more apolar solvents e.g. ethyl acetate. If the determination of total isoflavonoid content in the form of aglycones is the purpose, chemical hydrolysis is usually performed with hydrochloric acid or formic acid at elevated temperatures (80-100 °C) [170]. Csupor *et al.* executed investigations to establish an acid hydrolysis method for the quantitative HPLC determination of total isoflavones including daidzein, genistein and glycitein. To optimize the extraction and hydrolysis of isoflavones, the effect of HCl concentration (1.5–6 N), hydrolysis time (25–210 min) and temperature (30–100°C) on total isoflavone aglycone content was studied. By mathematical fitting and optimization methods optimum hydrolysis conditions for maximizing the quantification of isoflavones were determined ($t = 94$ min, $c\text{HCl} = 5.09$ N, $T = 80^\circ\text{C}$) [171]. Enzymatic hydrolysis with β -glucuronidase or β -glucosidase is also used [170]. If the interest is in the intact isoflavonoid-glycosides, harsh extraction conditions and heating should be avoided as glucoside malonates are extremely sensitive to heat [172]. Ultrasound-assisted methods substantially shorten the time needed for liquid extraction. High intensity ultrasound-assisted extraction (sonication) has been used for routine analyses. Longer extraction times, however, lower the recovery [173]. Microwave assisted extraction appears to be a fast and reliable method for soy isoflavones, as recovery of 97–103% was achieved. A

comparative study proved that microwave-assisted and Soxhlet methods were better for isoflavone content quantification, while sonication or stirring was the method of choice for determination of isoflavone composition (aglycones and glucoside conjugates) [173]. Supercritical fluid extraction (SFE) is used both for analytical purposes and in industrial scale for the preparation of functional foods. SFE with continuous on-line modifier addition to the extraction phase was applied to the extraction of isoflavones from red clover yielded extraordinarily high recoveries. According to a comparative study of daidzin and genistein recovery, SFE was slightly more efficient than pressurized solvent extraction and much better than Soxhlet or sonication [174]. Non-selective solid-phase extraction (SPE), typically alkyl-bonded silica or copolymer sorbents, is widely used for analyte extraction and enrichment from aqueous samples and sample extracts - primarily in environmental, pharmaceutical and biomedical analysis. In most cases the sorbent is C18-bonded silica and the sample solution and solvents are usually slightly acidified to prevent ionization of the isoflavonoids, which would reduce their retention. A prominent application could be the determination of isoflavonoids in plasma and other biological samples [170].

Separation techniques

Classical liquid chromatography techniques and several modifications using modern instrumentation are currently the most frequently applied techniques. Separation on reversed phase sorbents C18 (possibly C8) is one of the most preferred. The retention order of individual isoflavones increases in the order β -glucosides, malonyl-, and acetyl- β -glucosides, and free aglycones are the most hydrophobic. Several factors influence the retention times of separated isoflavones, i. e. their affinity to the stationary phase, which can be modified with different functional groups, composition of the mobile phase, application of gradient elution, column temperature, etc. In most cases aglycones and glucosides are separated together with their derivatives in a single run on a reversed phase column. Isocratic elution is usually insufficient; therefore a suitable gradient therefore has to be optimized for gradient elution. It usually starts at ca. 10% v/v of organic modifier (acetonitrile or methanol are the most suitable modifiers), but separation of glucosides improves with gradually increasing modifier content [175]. A mixture of daidzin, glycitin, genistin, ononin, daidzein, glycitein, sissotrin, genistein, formononetin, and biochanin A

was completely separated in 40 min using optimized linear gradient elution with 0.2% formic acid and acetonitrile on a 150 mm x 2.1 mm, 3.0 μm C18 column. Later, complete separation was accomplished in 7 minutes on a 20 mm x 2.1 mm, 3.0 μm C18 column after re-optimization of the gradient-profile [176]. Application of columns of smaller inner diameter and mainly with a smaller stationary phase particle size (size below 2 μm) and application of new technologies in chromatographic instrumentation are preferred in chromatographic separation of isoflavones at present. These techniques allowed reduction of retention times to less than 60 s for complete separation of 10 isoflavones [8]. A mixture of phenolic acids and selected isoflavones was separated with retention times not exceeding 2.0 min on C18, cyanopropyl and phenyl stationary phases using ultrahigh-pressure liquid chromatography (UHPLC) [10]. Also, columns with a monolithic stationary phase have found wide applicability in separation of isoflavones. Using a monolithic silica-based reversed-phase column, isoflavones in soy extracts were separated and quantified with a mobile phase consisting of acetonitrile and acetic acid and separation of 12 isoflavones was complete in ca. 10 min with very good resolution [175].

In the previous decade an enormous increase was observed in the number of papers dealing with the application of electromigration methods to the separation of natural substances, including isoflavonoids. Their ease of coupling to sensitive electrochemical detectors (EDs) is the main advantage of electromigration techniques. Capillary zone electrophoresis (CZE) is the most commonly used electromigration technique. Results obtained with CZE were compared with those obtained by HPLC separation. CZE separation was much faster than HPLC, however, the HPLC separation is more selective for identified isoflavones. This applies mainly to various real samples. Using ED sub- μM concentrations of isoflavones could be detected. The same electrochemical detector was used for micellar electrokinetic capillary chromatography (MEKC) analyzing puerarin and daidzein in plant materials and pharmacological preparation from *Puerariae radix*. A UV detector was used for the analysis of red clover and both methods applied sodium dodecyl sulfate as a surfactant for the pseudo-stationary phase. In contrast to CZE, MEKC also allows effective separation of hydrophobic aglycones that are sparingly soluble in the buffers used in CZE. Capillary electrochromatography is based on separation of analytes in a capillary filled with a sorbent. In contrast to HPLC, the separation is driven

by an electric field. A lauryl acrylate stationary phase polymerized directly inside the capillary was used for separation of a mixture of daidzein, genistein and glycitein and their conjugates in soy-based infant formulas. In addition to UV and ED detectors, electromigration column separations can also be directly coupled to mass-selective detectors and/or fluorescence detectors [175].

Spectrometric methods

UV-Vis detectors, and mainly diode array detectors (DAD) that can operate in a wide range of wavelengths, are the detectors most often applied in chromatographic and/or electromigration separations [175]. Isoflavonoids possess two characteristic UV-Vis bands, band I in the 300 to 550 nm range, arising from the B ring, and band II in the 240 to 285 nm range, arising from the A ring. While the band I of isoflavones lies in the 240 – 285 nm range, that of isoflavanone (no C-ring unsaturation) lies in the 270 – 295 nm range; conversely, the band II of isoflavones and isoflavanones lies around 303 – 304 nm [177]. As the UV-Vis spectra of many isoflavones are very similar, the applicability of UV-Vis detectors in identification of isoflavones is very limited, since approximately 700 isoflavones are present in different plant materials [175].

Mass spectrometry (MS) detectors that can detect individual aglycones of isoflavones, their derivatives or glucosides, and their other conjugates are the most effective tools for detailed studies of separated substances and for their identification. In addition to selective analyses, it is possible to apply mass spectrometry for structural analysis. Gas chromatography coupled to MS and electron impact ionization is not widely used in flavonoid analysis owing to the limited volatility of target molecules. Derivatization is needed, making the analysis more time consuming, and the fragmentation patterns of the derivatives are often difficult to interpret. Since the development of atmospheric pressure ionization sources (electrospray ionization (ESI), atmospheric pressure chemical ionization and atmospheric pressure photoionization), liquid chromatography-mass spectrometry (LC-MS) coupling became more efficient and easier to use, making it by far the most popular technique for on-line flavonoid analysis nowadays [178].

ESI, which can be connected to LC or capillary electrophoresis, is the most common technique for ionization of a sample. Very good results were obtained using ESI-quadrupole MS in combination with liquid chromatography after SFE with limit of detections (LODs) for aglycones of 0.2–1.0 fmol and for glucosides of 1.3–3.6 fmol per

injection in negative ionization mode. It was also used for identification of their glucosides or in detection of isoflavones in soybean food samples (LOD for daidzin/genistin were 1.2/1.6 fmol and 1–3 fmol for daidzein, genistein, formononetin, biochanin A, and ononin). Each individual isoflavone can be characterized not only by its molecular ion, but mainly by specific fragmentation products [175]. Fragmentation is controlled by the so-called retro-Diels-Alder (rDA) reaction (by analogy with the Diels-Alder cycloaddition), that involve breaking the C-ring bonds. These fragment ions are the most diagnostic for flavonoid and isoflavonoid identification since they provide information on the number and type of substituents in the A- and B-rings [178]. The aglycone fragment ions can be designated according to the nomenclature proposed by Ma *et al.* [179] (Figure 18/A).

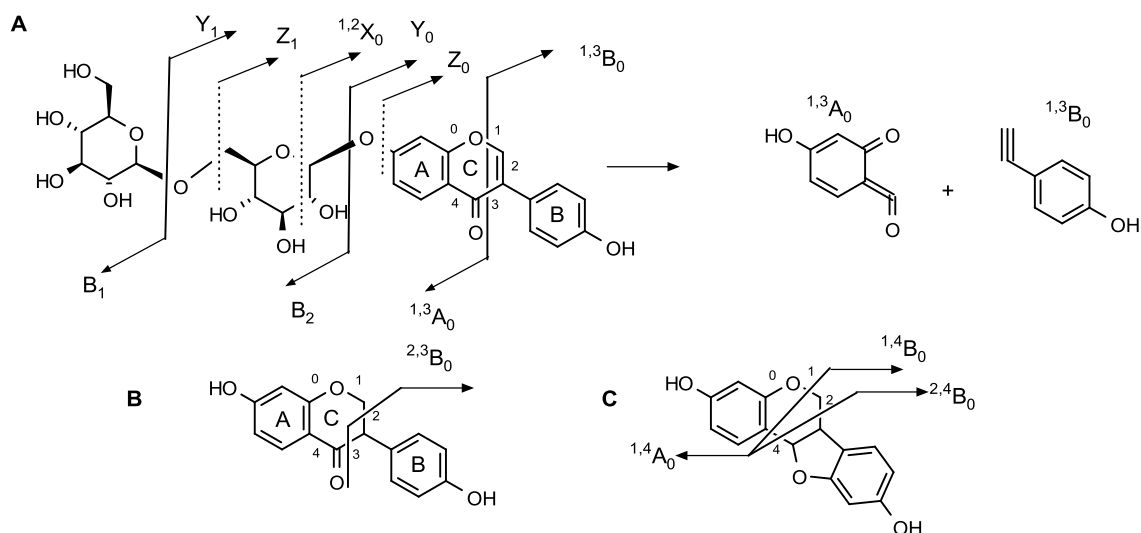


Figure 18: The nomenclature of isoflavonoid fragmentation based on Ma *et al.* and Domon and Castello with the product ions of retro-Diels-Alder fragmentation (A), the specific fragmentation of isoflavanones (B) and pterocarpan (C)

For free aglycones, the $^{i,j}A^+$ and $^{i,j}B^+$ labels refer to the fragments containing intact A- and B-rings, respectively, in which the superscripts *i* and *j* indicate the C-ring bonds that have been broken. For conjugated aglycones, an additional subscript 0 to the right of the letter is used to avoid confusion with the A_i^+ and B_i^+ labels that have been used to designate carbohydrate fragments containing a terminal (non-reducing) sugar unit [178]. The basic rDA fragmentation leads to the cleavage of the C-ring of the isoflavonoid and results in a dien fragment of the A-ring and an alkyne fragment of the B-ring (Figure 18/A). The

characteristic rDA fragment in ESI(+) is the protonated A-ring; the B-ring fragment predominantly remains uncharged and therefore leads to a weaker signal in ESI(+)-MS. The structural information after rDA cleavage results from the distribution of substituents between rings A and B that can easily be estimated from the relationship between the former molecular mass and the mass of the A- ring fragment. However, only the distribution of the number of substituents on both rings is deductible, but no information on the exact position of the substituents in either ring has been obtained yet. A special type of rDA fragmentation occurs for isoflavonoids which are methoxylated in the B-ring. Basically, the same rDA fragments are detected but a specific fragment with 1 amu less than the expected rDA fragment is additionally observed. This second signal results from a charged but not protonated rDA A-ring and based on observations, it is only detectable in the case of *O*-methylation on the B-ring [180]. Regarding isoflavanones the same rDA fragmentation as for isoflavonoids can occur in ESI(+)-MS/MS analysis. However, these molecules can be found in keto and enol form, and stabilizing the equilibrium using derivatizing agents, the enol form proved to be more abundant which can modify the fragmentation behavior of the isoflavanones. Beside the rDA fragmentation reactions, a further cleavage of the C-ring is characteristic for these molecules. In a competitive pathway, the bond between positions 2 and 3 is cleaved, leading to a charged 4-hydroxybenzyl cation fragment of the B-ring (Figure 18/B). This fragment hardly appears in the MS/MS spectra of isoflavones, bearing a double bond between positions 2 and 3. In contrast to the rDA reaction, this fragmentation pathway leads to a dominating charged B-ring product detectable in MS [180]. Pterocarpan, show much more complex fragmentation pathways; MS studies of different deuterated pterocarpan derivatives, as well as of pterocarpan glycosides, points out that these are dominated by various and successive ring openings and/or contractions [185, 186] (Figure 18/C). In addition to the $^{i,j}A^+$ and $^{i,j}B^+$ ions, discussed above, losses of small molecules and/or radicals from the $[M+H]^+$ ion are noted. Losses of 18 u (H_2O), 28 u (CO), 42 u (C_2H_2O) and/or the successive loss of these small groups are commonly observed. These losses are useful for identifying the presence of specific functional groups, i. e. a methoxy group is easily detected by the loss of 15 u (CH_3^\bullet) from the $[M+H]^+$ precursor ion. The loss of a CH_3^\bullet radical appears to be prevalent so that the $[M+H-CH_3]^{+\bullet}$ ion dominates the whole spectrum. This rather uncommon transition from an even-electron to an odd-

electron ion is found to be characteristic for a phenolic methyl ether group. Losses of 56 u (C_4H_8) point to the presence of a prenyl substituent [178]. In the structure analysis of flavonoids, positive ion collision induced dissociation (CID) spectra are most frequently used, whereas negative ion CID spectra are often considered to be more difficult to interpret. The negative ion mode is, however, more sensitive in flavonoid analysis and the fragmentation behavior is different, giving additional and complementary information [178]. In the negative mode, the 1/3 and 0/3 rDA fragmentations are predominant, and the 0/4 fragmentation is also observed sometimes, accompanied by extensive losses of CO, CO₂ and C₃O₂ moieties [187, 188]. In some cases, a direct cleavage of the bond between the B- and C-rings, resulting in an [M-B-ring]⁻ fragment, can be observed. Losses of small neutral molecules, such as CO (-28 u), CO₂ (-44 u), C₂H₂O (-42 u) and the successive loss of these molecules, may also be prominent. Methylated compounds are characterized by the loss of 15 u resulting in an [M-H-CH₃]⁻ radical ion which generally constitutes the base peak [178].

Comparing the fragmentation of isoflavonoids with isomeric flavonoid compounds, isoflavones uniquely can lose two CO units, whereas a similar loss from flavones requires a barely possible aryl shift [184]. The exact mechanism of the double CO loss was investigated using isotope labeled molecules [185]. Abrankó and Szilvássy [186] and Keyume [187] investigated further the ion ratios of the fragmented isomeric or isobaric flavonoids and isoflavonoids helping the differentiation between these phenolic compounds.

Product ions from glycoconjugates are denoted according to the nomenclature introduced by Domon and Costello [188]. Ions containing the aglycone are labeled ^{k,l}X_j, Y_j and Z_j, where j is the number of the interglycosidic bond broken, counting from the aglycone, and the superscripts k and l indicate the cleavages within the carbohydrate rings (Figure 18/A). The glycosidic bond linking the glycan part to the aglycone is numbered 0. O- and C-glycosides can be differentiated by soft ionization techniques with low fragmentation energy, in which glycoside loss from O-glycosides undergo heterolysis of their hemiacetal O-C bonds and give rise to Y_i⁺ ions at low energy. Whereas C-glycosides only produce [M+H]⁺ ions, and intraglycosidic cleavages will happen only on higher energies yielding ^{i,j}X fragments and characteristic ions of water loss in the case of 6-C-glycosides. The sugar type can be easily determined by the characteristic *m/z* values of the A_i, B_i and

C_i fragments arising from hexoses, deoxyhexoses and pentoses, which are not directly observable in the mass spectra but can be computed from the *m/z* differences of the parent ions and corresponding X_i, Y_i and Z_i [177].

Spectroscopic techniques

One of the most immediate applications of circular dichroism (CD) spectroscopy is the determination of the absolute configuration of chiral isoflavonoid molecules, such as isoflavan-4-ols [189], isoflavones [190] and pterocarpanes [168, 196]. CD is also routinely used to study the interaction of many flavonoids with biomolecules, providing valuable information on biomolecule-drug interaction, such as DNA binding, binding to serum albumin and hemoglobin, inhibition of β -amyloid toxicity and fibrillogenesis [177].

One of the main applications of nuclear magnetic resonance (NMR) spectroscopy in flavonoid research is the structural elucidation of novel compounds, although NMR traditionally requires milligram amounts of samples, which is usually challenging to obtain when analyzing novel compounds. ¹H NMR experiments provide valuable information about the number of hydrogens and also their type, by comparison of the recorded chemical shifts with compiled data. This is particularly useful in establishing the aglycone type and the acyl groups attached to it, as well as in identifying the number and the anomeric configuration of the glycoside moieties. ¹³C NMR data is used to complement ¹H NMR data. Definite structural elucidation with the accurate location of the substituents, requires various 2D experiments. ¹H homonuclear 2D experiments such as Correlation spectroscopy (COSY) and total Correlation Spectroscopy (TOCSY) are extremely useful to identify and isolate the ¹H resonances of the individual spin systems and protons of the sugar rings. Heteronuclear Single Quantum Coherence (HSQC) establishes one bond correlations between the protons of a molecule and the carbons to which they are attached. Heteronuclear Multiple Bond Correlation (HMBC) application to flavonoids usually addresses assignment on non-protonated C atoms, from both the aglycones and acyl groups. HMBC can also be used to determine the linkage points of heteroatom-containing groups such as sugar residues and acyl groups. While the above mentioned 2D techniques are useful to establish the connectivities between atoms through bonds, the Nuclear Overhauser Effect (NOE), is effective at connectivities through space. The crosspeaks of 2D NOESY (NOE spectroscopy) spectrum may arise from both intramolecular and intermolecular proton interactions and has been successfully used to

establish rotational conformers and restrictions, establish intermolecular associations and even solve protein-ligand and DNA-ligand structures. Rotating frame Overhauser effect spectroscopy (ROESY) has been used in flavonoid research mainly to establish the stereochemistry of various flavonoids [177].

Analytical methods for the investigation of the isoflavonoid content of *O. spinosa*

While *Ononis radix* has been official in Hungarian Pharmacopoeias since the 5th edition, the described analytical methods are very general even in the newest editions of Hungarian and European Pharmacopoeias. For phytochemical identification thin layer chromatography is prescribed. As only general reference compounds (resorcinol and vanillin) are used for retention factor standardization, the aim of the thin layer chromatography is rather the comparison of fingerprints of the methanolic extract and not the identification of compounds responsible for the pharmacological effect. For tests aiming the determination the quality of the drug, only general methods (loss on drying, total ash content and extractable content) are prescribed.

Table 3: Various isoflavone glucoside derivatives in the extract made of *O. spinosa* roots [6]

	biochanin A	sissotrin	biochanin A GM	genistein	formononetin	ononin	formononetin GM
umol/100g	-	102.1	16.5	12.3	23.0	7.4	294.7
mg/100g	-	29.1	7.4	3.3	6.2	3.2	152.4

Köster *et al.* investigated the isoflavonoid content of *C. arietinum* regarding not only aglycones, but 7-*O*-glucosides and 7-*O*-glucoside 6''-*O*-malonates, as well. They expanded the developed reversed phase HPLC method for the analysis of other plants in the *Leguminosae* family, including *O. spinosa*. Care was taken in these studies to extract the plant material carefully at low temperature with acetone and to avoid long time storage of the extracts at higher temperatures. Quantitative measurements were executed too, in order to define the amounts of biochanin A, biochanin A 7-*O*-glucoside (sissotrin), biochanin A 7-*O*-glucoside 6''-*O*-malonate (biochanin A GM), genistein, formononetin,

formononetin 7-*O*-glucoside (ononin) and formononetin 7-*O*-glucoside 6''-*O*-malonate (formononetin GM). The results show, that formononetin 7-*O*-glucoside 6''-*O*-malonate is the most characteristic molecule of *O. spinosa* roots (Table 3) [6].

Pietta *et al.* published the results of HPLC investigation of *O. spinosa* using reversed-phase C18 column in 1983. They reported the presence of rutin, kaempferol, genistein, formononetin and biochanin A in the 50% ethanolic extract of *O. spinosa* root based only on the consistency of retention time with standard substances (Figure 19). In addition, the quantity of formononetin, genistein and biochanin A were determined using external calibration method (Table 4). The amount of the characterized aglycones definitely not reflected the quantities characteristic to the root because during sample preparation high temperature was used (70°C), which may cause the decomposition of glycosides and glycoside malonates. Moreover, as the completeness of the hydrolyzation was not proved, the results could not interpret the total isoflavonoid content neither [5].

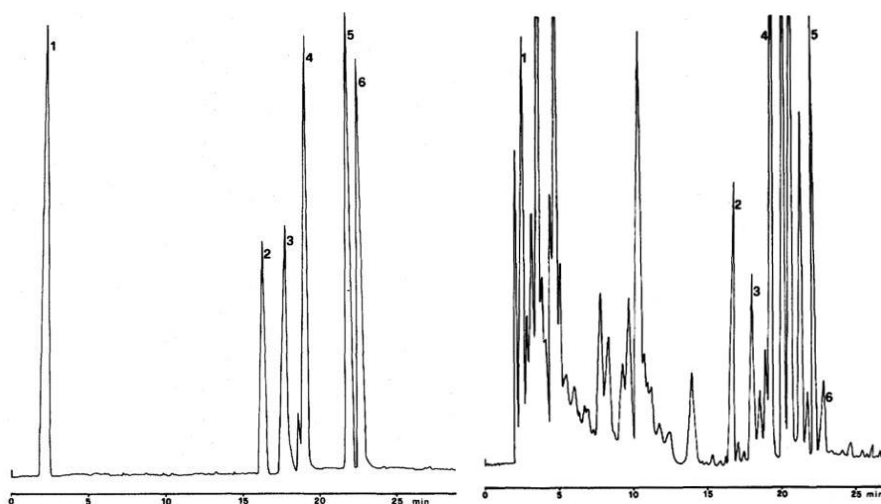


Figure 19: HPLC chromatogram of standards and of *O. spinosa* extract with the identified peaks. 1 = rutin; 2 = genistein; 3 = kaempferol; 4 = formononetin; 5 = benzyl-4-hydroxybenzoate (internal standard); 6 = biochanin A [5]

Seven years later the same research group repeated their experiments, with the application of a diode-array detector. After the same sample preparation method, they used an isocratic method to separate the compounds of *O. spinosa* root based on an eluent system consisting of 2-propanol-tetrahydrofuran-water (28:2:70, v/v/v). For peak identification, formononetin, biochanin A and genistein were used. When the acquired UV spectra were computer normalized, plotted and superimposed, exact coincidence curves were obtained (match factor >990) and consequently, the peaks were assumed to be pure. Quantitative

measurements were implemented for the same compounds and the results showed the same order of magnitude (Table 4) [192].

Benedec *et al.* investigated the isoflavonoid content of *Glycyrrhiza glabra* L., *Glycyrrhiza echinata* L. and *Ononis spinosa* L. using HPLC-MS technique. During sample preparation 80% methanolic extracts were made, then acidic hydrolysis was applied using 2 M HCl.

Table 4: The quantitative results of the isoflavonoid content of *O. spinosa* root extract [5], [192]

<i>O. spinosa</i> samples	genistein (mg/100g)	formononetin (mg/100g)	biochanin A (mg/100g)
Indena [5]	0.8	4.3	0.15
Brisighello [5]	6.6	5.1	0.20
Ulrich [5]	5.3	6.3	0.22
Galke [5]	0.3	3.1	0.06
I [192]	1.7	3.2	0.08
II [192]	2.1	4.7	0.21
III [192]	3.8	5.9	0.30

Table 5: The method of determination and the quantity of various isoflavones before and after hydrolysis [9]

	R _t min	Detection mode	Parent ion	Quantifier ion	isoflavonoid content	
			[M-H] ⁻ m/z	[M-H] ⁻ m/z	mg/100 g drug non-hydr.	hydr.
Daidzin	3.7	SRM	415	253	0.944	-
Genistin	5.5	SRM	431	268, 269	1.173	-
Ononin	8.9	SRM	429	267	175.72	18.939
Daidzein	9.2	SIM	253	283	-	0.819
Glycitein	11.0	SIM	283	283	-	-
Genistein	11.0	SIM	269	269	-	-
Formononetin	14.4	SIM	267	267	9.499	113.622

For the separation of compounds gradient method was used with eluents of 0.1% acetic acid and methanol. Aglycones were detected using Single Ion Monitoring (SIM) in ESI-MS(-) mode, while glucosides were detected with Single Reaction Monitoring. The peaks of the sample were identified by comparison of their retention times with ones of authentic standards and by the m/z value of their pseudo-molecular ion. The quantity of chosen isoflavones were measured using external calibration before and after hydrolysis. The results can be seen in the Table 5. The most characteristic compound of the non-hydrolyzed sample was ononin, while in the hydrolyzed sample, its aglycone, formononetin was the most significant [9]. The deficiency of the method is that no information was obtained about more complex glucosides, like glucoside malonates and that the completeness of the hydrolysis was not checked so that significant amount of glucosides (e. g. ononin) could have left in the sample. It is worth to note, that while the glucoside of genistein could be detected and quantified in the non-hydrolyzed sample, the aglycone, genistein, could not be detected after hydrolysis.

A rapid-resolution HPLC-DAD separation method (separation in less than 1 min) for the determination and identification of genistin, genistein, daidzein, daidzin, glycitin, glycitein, ononin, formononetin, sissotrin and biochanin A in fmol quantities in submicroliter sample volumes was optimized by Klejdus *et al.* on a Zorbax SB C18 column (1.8 μm particle size) at 80 °C. The method was verified using samples of bits of soy and methanolic extracts from *Trifolium pratense*, *Iresine herbstii* and *Ononis spinosa* plants. Formononetin, ononin and pseudobaptigenin glucoside were identified by UV-DAD and ESI-MS in negative ionization mode in the 90% methanolic extract of *O. spinosa* obtained with a Soxhlet apparatus. While the method itself was validated for quantitative aims, too, the isoflavone content of the plant extracts were not quantified and no information was given about the other peaks (Figure 20) [8].

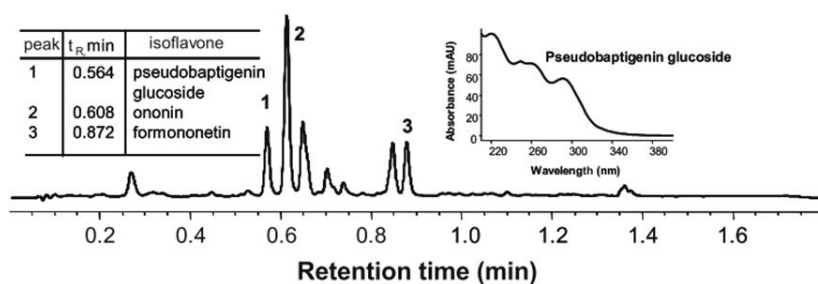


Figure 20: The rapid-resolution HPLC chromatogram of *O. spinosa* root extract [8]

Complete separation of aglycones and glucosides of selected isoflavones (genistin, genistein, daidzin, daidzein, glycitin, glycitein, ononin, sissotrin, formononetin, and biochanin A) was achieved by the same research group in 1.5 min using an UHPLC on different chemically modified stationary phases (C18, cyanopropyl and phenyl). In addition, simultaneous determination of isoflavones together with a group of phenolic acids (gallic, protocatechuic, *p*-hydroxybenzoic, vanillic, caffeic, syringic, *p*-coumaric, ferulic, and sinapic acid) was performed in 1.9 min. Separations were conducted using a gradient elution with a mobile phase consisting of 0.3% aqueous acetic acid and methanol. The developed UHPLC technique on the cyanopropyl column was used for separation of isoflavones and phenolic acids in samples of plant materials (*T. pratense*, *G. max*, *P. sativum* and *O. spinosa*) after acid hydrolysis of the samples and modified Soxhlet extraction. Individual substances were identified by their retention time. In the hydrolyzed extract of *O. spinosa* genistein (G), formononetin (F) and biochanin A (B) were found beside phenolic compounds [175]. However, in the chromatogram it can be clearly observed that the isoflavonoid aglycones are very poorly separated which makes the peak identification cumbersome (Figure 21).

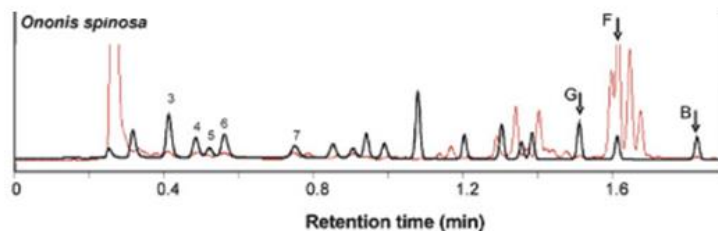


Figure 21: The chromatogram of hydrolyzed *O. spinosa* root extract on cyanopropyl stationary phase [10]

Concluding the results of the analytical methods regarding the isoflavonoid content of *O. spinosa* the following deficiencies can be noticed:

1. The sample preparation was executed at high temperature (with one exception), resulting in the hydrolysis of glucoside malonates, which are the most characteristic compounds of the native plant [6]. On the other hand, the complete hydrolysis was not reached using only heat or 2 M hydrochloric acid [9] (Table 6).

2. The identification of the peaks was based on the similarity of retention times with standard components, which is insufficient in the lack of other evidences. In some cases, the UV spectra were compared with original standards and the molecular masses were checked, but these methods still cannot differentiate isomeric or isobaric compounds with reliability (Table 6).
3. Information about other isoflavonoid compounds, for example isoflavanones and pterocarpanes was not available, as only the compounds were identified which are available as standard substances commercially (Table 6).

Table 6: The summary of analytical methods regarding the isoflavonoid content of *O. spinosa*

	Köster <i>et al.</i> 1983 [6]	Pietta <i>et al.</i> 1983 [5]	Pietta <i>et al.</i> 1990 [192]	Klejdus <i>et al.</i> 2007 [8]	Klejdus <i>et al.</i> 2008 [10]	Benedec <i>et al.</i> 2012 [9]
Sample	cold acetone (no other information)	50% ethanol 70°C 1h	50% ethanol 70°C	90% methanol, Soxhlet	90% methanol, Soxhlet	80% methanol, 60°C
Hydrolysis	-	-	-	-	2 M HCl	2 M HCl -
Purification	-	-	C18 cartridge	0.45µm PTFE membrane filtration		-
Column	LiChrosorb RP 18 (250 x 4 mm, 5 µm)	Waters µBondapak C18 (300 x 3.9 mm)	C8 Aquapore (250 x 4.6 mm, 7 µm)	Zorbax SB-C18 (30 x 2.1 mm, 1.8 µm)	Zorbax SB-CN (50 x 2.1 mm, 1.7 µm)	Zorbax SB-C18 (100 x 3.0 mm, 5 µm)
Eluents	0.8 ml/min gradient 3% acetic acid acetonitril	1.5 ml/min gradient water (pH=2.6 with 10% phosphoric acid) acetonitrile	1 ml/min isocratic 2-propanol - THF - water (28:2:70)	1.4 ml/min gradient 0.2% acetic acid MeOH 80°C	0.7 ml/min gradient 0.3% acetic acid MeOH 60°C	1 ml/min gradient 0.1% acetic acid MeOH
Detection	UV-Vis 261 nm	UV-Vis 263 nm	UV-DAD	UV-DAD ESI-MS(-)	UV-Vis 270 nm	ESI-MS
Identified compounds	genistein, formononetin, ononin, formononetin GM, biochanin A, sissotrin, biochanin A GM	rutin, kaempferol, genistein, formononetin and biochanin A	genistein, formononetin, biochanin A	rothinidin, ononin, formononetin	genistein, formononetin, biochanin A	ononin, formononetin, daidzein, daidzin, genistin hydr. non-hydr.
Quantified compounds (mg/100 g drug)	genistein 3.3 formononetin 6.2 ononin 3.2 sissotrin 29.1 formononetin GM 152.4 biochanin A GM 7.4	genistein 0.3-6.6 formononetin 3.1-6.3 biochanin A 0.06-0.22	genistein 1.7-3.8 formononetin 3.2-5.9 biochanin A 0.08-0.30			ononin 18.9 daidzein 0.8 formono- netin 9.5 genistin 1.2

2. Objectives

The main aim of this work was to characterize the isoflavonoid profile of the *Ononis* species native to Hungary: *Ononis spinosa* L. and *Ononis arvensis* L., since isoflavonoid derivatives possess numerous promising pharmacological effects. Qualitative and quantitative literature data on the isoflavonoid composition of the two *Ononis* species is limited to the compounds available as standard substances and the other isoflavonoid derivatives have not been studied. Although *in vitro* cultures were made from both species, there is no available information about the isoflavonoid content of these samples. Considering the above mentioned, our aims were the following:

1. Explore the isoflavonoid profile of the roots of *O. spinosa* and *O. arvensis* in details and acquire structural information by the means of HPLC-DAD-ESI-MS/MS and UHPLC-DAD-ESI-Orbitrap-MS/MS.
2. For compounds, which could not be identified by solely by mass spectrometry, our objective was to elaborate isolation methods and to characterize them using orthogonal spectroscopic techniques.
3. For the quantitative determination of isoflavonoid aglycones in the herbal drugs and for the determination of the total isoflavonoid content in *O. spinosa*, *O. arvensis* and their *in vitro* hairy root cultures, our aim was to develop and validate a HPLC-DAD method.

3. Materials and methods

3.I. Plant material

O. spinosa root was obtained from Rózsahegyi Ltd. (Erdőkertes, Hungary), Biohorticulture Bio-Berta (Kiskőrös, Hungary) and from Antica Erboristeria Romana Ltd. (Rome, Italy) and was received in a dried and chopped form according to the 9th European Pharmacopoeia. Other root samples were collected from Dunaegyháza (Hungary, 46°50'56.88" N, 18°56'35.57" E) and Hűvösvölgy (Hungary, 47°33'22.88" N, 18°58'33.89" E). *O. arvensis* was collected near Beregújfalu (location: N 48°17'21.1", E 22°48'08.7" – Beregszászi járás, Ukraine) and in the Homoród-valley (Romania, location: N 46°10'29.1", E 25°25'22.5"). The roots and the aerial parts of the plants were separated. The roots were washed to remove soil and the dried roots were ground. The aerial parts were ground without further separation of leaves and stems. *In vitro* hairy root samples of *O. spinosa* and *arvensis* were started in 1989 by Kuzovkina *et al.* [89] using R 1601 plasmid. The integration of the plasmid to the plant DNA was checked by gel electrophoresis after PCR multiplication. The samples were cultivated on B5 liquid medium (with 2% saccharose content for *O. spinosa* and 3% for *O. arvensis*). The samples were harvested 4 weeks after the transplantation and were freeze dried immediately. As the freeze-dried biomasses did not reach the minimal weight of the three parallel samples on their own, five samples were powdered and pooled.

3.II. Solvents and chemicals

HPLC-grade methanol and acetonitrile were obtained from Fisher Scientific (Loughborough, UK). Methanol- d_4 and DMSO- d_6 for NMR measurements were purchased from Sigma-Aldrich (Steinheim, Germany). Purified water prepared by Millipore Milli-Q equipment (Billerica, MA, USA) was used throughout the study. Formononetin, calycosin, naringenin, homoprolin and homopipercolic acid were purchased from Sigma-Aldrich (Steinheim, Germany). Ononin was kindly provided by Professor S. Antus (University of Debrecen, Hungary) and medicarpin and maackiain by Professor J. Hohmann (University of Szeged, Hungary). All other chemicals were of analytical grade.

3.III. Extraction and sample preparation

3.III.1. Analytical samples

General

From the dried and powdered sample 0.5 g was extracted with 2 x 30 ml of aqueous methanol (3:7, v/v) by sonication for 2 x 6 minutes (Braun Labsonic U, Melsungen, Germany). After filtration the solvent was evaporated to dryness under reduced pressure. The residue was redissolved in 2.5 ml of 70% v/v methanol and passed through Supelclean SPE LC-18 column (500 mg, 3 ml; Supelco, Bellefonte, PA, USA). SPE micro columns were activated with 2.5 ml methanol and water before 2.5 ml stock solution was loaded. After air drying the cartridge 1.5 ml methanol was applied to achieve complete elution of isoflavonoids. Prior to HPLC analysis the eluted extract was evaporated to dryness again and redissolved in 2.0 mL 70% v/v methanol and filtered through Minisart RC 15 0.2 µm membrane (Sartorius AG, Goettingen, Germany).

Hydrolyzed sample for the investigation of beta amino acids

For the hydrolyzed sample, 1 ml of the analytical sample was mixed with 1 ml of concentrated ammonia and evaporated to dryness with rotary evaporator set to 60°C. The residue was mixed with 2 ml of purified water and the liquid was passed through the same Minisart filter.

Hydrolyzed sample for the quantitative analysis

- Hydrolysis by hydrochloric acid

0.5 g powdered drug was extracted with 25 ml 70% aqueous methanol three times. The unified extracts were filtered and dried under reduced pressure. Methanol, distilled water and concentrated HCl were added to the dried sample in ratios to obtain 80% methanol and 0.35, 0.4, 0.5, 1.22, 4 and 5 M hydrochloric acid concentration and 25 ml end volume. The samples were boiled under reflux and 1 ml sample was taken out after 10, 30, 50 and 80 minutes. After cooling, the sample was mixed with 5 ml distilled water and applied to SPE LC-18 micro columns activated by 2.5 ml methanol and equilibrated with 2.5 ml water prior. The cartridges were washed with 2.5 ml water to remove the acid content, then isoflavonoid derivatives were eluted using 2.5 ml methanol twice. After filtration on Minisart filter the samples were investigated by HPLC-DAD-ESI-MS/MS.

- Hydrolysis by glucosidase enzyme

0.1000 g was measured from each powdered plant material three times and mixed with 50 µl of methanolic naringenin solution (4.000 mg/ml) then 1.5 ml water was added to the samples and mixed thoroughly. These samples were set aside for 24 hours to activate the indigenous glycosidase enzymes and hydrolyze the glycosides. In the next step, 3.5 ml methanol was added, and the samples were extracted in ultrasonic bath for 25 minutes. After sedimentation the supernatant was collected, and the extraction was repeated twice with 70% methanol. The collected liquid phases were completed to 25.0 ml in volumetric flasks, 2.0 ml was filtered through Minisart RC 15 0.2 µm membrane, before HPLC-DAD and HPLC-DAD-ESI-MS/MS investigation.

3.III.2. Isolation of aglycones

To isolate isoflavonoid aglycones, 50.0 g dried and powdered plant material from Rózsahegyi Ltd. was mixed with 500 ml of water to activate the indigenous glycosidase enzymes of the plant for 24 h. After filtration, the extract was evaporated to dryness. 150 ml acetone was added to the dark brown gum to redissolve the isoflavonoid aglycones and to leave behind the saccharides. The extract was filtered and dried to gain 2 g residual. This was redissolved in HPLC methanol to obtain a solution of 100 mg/ml concentration. For the separation of isoflavonoid aglycones a Hanbon Newstyle NP7000 HPLC system with a Hanbon Newstyle NP3000 UV detector (Hanbon Sci. & Tech. CO. Jiangsu, China) equipped with a Gemini C18 reversed phase column (150 x2 1.2 mm i.d; 5 µm, Phenomenex Inc.; Torrance, CA, USA) was used. Eluents consisted of 0.3% v/v acetic acid (A) and acetonitrile (B). Gradient elution was used with 10 ml/min flow rate and solvent system with 40% B at 0 min to 43% B in 18 min. Six fractions were obtained with this method, which contained pseudobaptigenin (**44**, 1.22 mg), formononetin (**46**, 3.15 mg), onogenin (**41**, 2.87 mg), sativanone (**45**, 2.45 mg), maackiain (**42**, 5.19 mg) and medicarpin (**47**, 5.26 mg), respectively.

3.III.3. Isolation of licoagroside B

20.0 g ground root of *O. arvensis* was extracted with 200 ml of 70% methanol twice using ultrasonic bath at room temperature. After filtration, the extract was dried under reduced pressure. The residue was redissolved in water and 10 ml of acetone was added to remove saccharides. The precipitate was filtered, and the liquid phase was dried. The residue was

redissolved in 10 ml of water and passed through Supelclean SPE LC-18 columns (500 mg, 3 mL; Supelco, Bellefonte, PA, USA). After air drying the cartridges, 3 ml of 50% methanol was used to elute glycosides, then 6 ml pure methanol was applied to achieve complete elution of isoflavonoids. The weights of the first and second eluates were 274 mg and 171 mg, respectively. The 50% methanol fraction was redissolved in 2 ml of water and filtered through 0.22 μm Minisart RC filter before subjected to preparative HPLC. For fractionation, the same preparative HPLC system was used. Eluents consisted of 0.3% v/v acetic acid (A) and methanol (B). Gradient elution was used with a 10 ml/min flow rate and a solvent system using 10% B at 0 min, 40% B in 10 min, 100% B in 15 min and 10% B in 25 min. This method has not been optimized in terms of performance parameters as it only served for isolation purposes. Licoagroside B (**1**) eluted at 11.41 min, the obtained fraction was reinjected for further purification. Finally, 8.9 mg licoagroside B was yielded in high purity

3.III.4. Isolation of but-2-enolide aglycones and calycosin D aglycone

From the powdered roots of *O. arvensis* 30.0 g was mixed with 200 of mL water for 48 h to activate the plant's indigenous glucosidase enzymes. After filtration, the drug was extracted twice with 200 mL of 70% methanol using ultrasonic bath at room temperature. The extract was dried under reduced pressure and redissolved in water. The saccharides were precipitated with the same method as mentioned above. The total weight of the extract was 835 mg and was redissolved in 10 mL of water and filtered through 0.22 μm Minisart RC filter before subjected to the same preparative HPLC system. The chosen chromatographic conditions fulfilled the criteria of isolation but were not optimized in terms of performance parameters. Eluents consisted of 0.3% v/v acetic acid (A) and methanol (B). Gradient elution was used with a 10 ml/min flow rate and solvent system with 50% B at 0 min, 50% B in 10 min, 100% B in 15 min and 50% B in 20 min. Puerol A (**18**) eluted at 8.40 min, while clitorienolactone B (**31**) and calycosine D (**30**) eluted at 12.25 and 13.45 min, respectively. Clitorienolactone B was reinjected for further purification with isocratic 25% acetonitrile as solvent B, and calycosin D with isocratic 35% acetonitrile. The yields were 4.8 mg for puerol A, 3.1 mg for clitorienolactone B and 1.5 mg for calycosin D.

3.III.5. Isolation of but-2-enolide glycosides and calycosin D glycosides

100 g powdered drug was extracted by 400 mL of 70% aqueous methanol twice. After filtration, the liquid phase was dried under reduced pressure at 60°C. The residue was dissolved in water to gain a viscous solution of 500 mg/mL concentration. This sample was purified using a CombiFlash NextGen 300+ (Teledyne ISCO, Lincoln, USA) equipped with a RediSep Rf Gold C18 column (150 g). As eluents methanol (solvent B) and 0.3% acetic acid (solvent A) were used with the following gradient program: 0 min 30% B, 20 min 50% B, 25 min 100% B, 30 min 100% B. The flow was set to 60 ml/min and 16 ml fractions were collected. Fractions 23-27, 38-41 and 49-53 were unified and further purified by the same preparative HPLC system using isocratic 25% acetonitrile as eluent with 10 ml/min flow. Fr 23-27 yielded 15.4 mg calycosin-D 7-*O*-glucoside (compound **2**). From Fr 38-41 puerol A 2'-*O*-glucoside (**6**) was isolated (eluted at 7.2 min, 63.2 mg) along with clitorienolactone B 4'-*O*-glucoside (**7**, eluted at 8.6 min). Clitorienolactone B 4'-*O*-glucoside was further purified on a Luna C18(2) 100 A (5 µm) reversed phase column (150 x 10.00 mm i.d; Phenomenex, Inc; USA) using isocratic 25% acetonitrile and 2 ml/min flow, yielding 2.3 mg. Calycosin-D 6''-*O*-glucoside malonate was isolated from Fr 49-53 eluting at 11.3 min (1.1 mg).

3.III.6. Isolation of homopipercolic acid isoflavonoid glucoside esters

300.0 g dried and powdered plant material from Rózsahegyi Ltd. was extracted with 2 x 3000 ml of 70% methanol in ultrasonic bath for 2 x 25 min. The extract was filtered and evaporated to dryness to obtain a dark brown gum. The residue was redissolved in 200 ml water and divided into 5 ml fractions. Each fraction was mixed with 5 ml of methanol and acetone to precipitate the majority of the saccharides. The supernatant was filtered, and the organic solvents were evaporated at 45 °C. 10 ml portions of the residual dark solution were passed through a weak cation exchanger cartridge (Strata WCX Giga Tube, Phenomenex Inc.; Torrance, CA, USA) in order to enrich the nitrogen-containing compounds. The SPE cartridges were first conditioned by washing with 20 ml methanol and equilibrated with 20 ml water. The loaded cartridges were washed with 40 ml water and 40 ml methanol then eluted with 5% formic acid in methanol. After evaporation to dryness the sample was fractionated by the same preparative HPLC system that was mentioned before. Eluents consisted of 0.3% v/v acetic acid (A) and acetonitrile (B).

Gradient elution was used with 10 ml/min flow rate and solvent system with 20% B at 0 min to 30% B in 20 min. Eight fractions were obtained with this method, out of which Fr 1–2 contained degradation products and minor contaminants. From Fr 3 pseudobaptigenin 7-*O*-glucoside 6''-*O*-piperidine 2-acetate (**12**, 0.6 mg) was obtained as a mixture with another isoflavonoid glucoside derivative. From Fr 4 formononetin 7-*O*-glucoside 6''-*O*-piperidine 2-acetate (**13**, 1.3 mg) was isolated. Onogenin 7-*O*-glucoside 6''-*O*-piperidine 2-acetate (**14**, 1.6 mg) was purified from Fr 5. Fr 6 provided sativanone 7-*O*-glucoside 6''-*O*-piperidine 2-acetate (**17**, 1.5 mg) in high purity. Fr 7 and Fr 8 contained solely the diastereomers of maackiain 3-*O*-glucoside 6''-*O*-piperidine 2-acetate (**20**, 4.5 mg) and medicarpin 3-*O*-glucoside 6''-*O*-piperidine 2-acetate (**23**, 3.7 mg), respectively. For investigation of diastereomers, the two isomers of maackiain 3-*O*-glucoside 6''-*O*-piperidine 2-acetate and medicarpin 3-*O*-glucoside 6''-*O*-piperidine 2-acetate were further purified with the same HPLC equipment. Gradient elution was used with 10 ml/min flow rate and solvent system with 15% B at 0 min to 20% B at 15 min and 20% B at 25 min.

3.IV. Chromatographic conditions

3.IV.1. HPLC-DAD conditions

The isolated isomers of medicarpin 3-*O*-glucoside 6''-*O*-piperidine 2-acetate and their mixture were examined on a Waters 2690 HPLC system with a Waters 996 diode array detector (Waters Corporation, Milford, MA, USA) equipped with a Xselect reversed phase C18 column (150×4.60 mm i.d; 5 μm, Waters Corporation, Milford, MA, USA). Eluents consisted of 0.3% v/v acetic acid (A) and acetonitrile (B). The following gradient program was applied: 0.0 min, 15% B; 20.0 min, 20% B; 30 min, 20% B. Solvent flow rate was 1.0 ml/min and the column temperature was set to 25 °C. 20 μl sample was subjected on the column.

For the quantification of isoflavonoid aglycones, the same HPLC system was used. Eluents consisted of 0.3% v/v acetic acid (A) and acetonitrile (B). The following gradient program was applied: 0.0 min, 35% B; 15 min, 50% B; 18, 20% B, 20 min, 80% B. Solvent flow rate was 1.0 ml/min and the column temperature was set to 25 °C, 20 μl extract was subjected on the column.

3.IV.2. HPLC-DAD-ESI-MS/MS conditions

For chromatographic separation and mass spectrometric analysis of the analytical samples (hydrolyzed by ammonia, hydrochloric acid and glucosidase enzyme) an Agilent 1100 HPLC system (degasser, binary gradient pump, auto-sampler, column thermostat and diode array detector) was used hyphenated with an Agilent 6410 Triple Quad LC/MS system equipped with ESI ion source (Agilent Technologies, Santa Clara, CA, USA). For the screening of *Ononis* extracts HPLC separation was attained on a Zorbax SB-C18 Solvent Saver Plus (3.5 μm) reversed phase column (150 x 3.0mm i.d; Agilent Technologies, Santa Clara, CA, USA). Mobile phase consisted of 0.3% v/v formic acid (A) and methanol (B). The following gradient program was applied: 0.0 min, 29% B; 32.0 min, 80% B; 34 min, 100% B; 37 min, 100% B; 42.0 min, 29% B. Solvent flow rate was 0.4 ml/min and the column temperature was set to 25 °C. The injection volume was 2 μL . Nitrogen was applied as drying gas at the temperature of 350 °C at 9 l/min, the nebulizer pressure was 45 psi. The fragmentor voltage was set between 100 and 135 V and the capillary voltage was 3500 V. Full scan mass spectra were recorded in positive ion mode in the range of m/z 80–1500. For CID the collision energy varied between 10 and 40 eV with fragmentor voltage 135 V. As collision gas, high purity nitrogen was used. Product ion mass spectra were recorded in positive ion mode in the range of m/z 80–600. Fragmentor voltage was set to 80 V and the capillary voltage was 3500 V.

The hydrolyzed sample was analyzed using the same HPLC-MS/MS apparatus equipped with a Zorbax NH_2 normal phase column (150 x 4.6 mm i.d; 5 μm). Mobile phase consisted of 20 mM ammonium formate buffer (pH = 4) (A) and acetonitrile (B). Isocratic mode was applied with 80% B at 1 ml/min flow rate and 25°C. The injection volume was 5 μL . Nitrogen was applied as drying gas at the temperature of 300°C at 6 l/min, the nebulizer pressure was 15 psi. For registering the chromatogram, SIM mode was chosen at m/z 130 (homoproline) and m/z 144 (homopipicolinic acid). For CID the collision energy varied between 10 and 30 eV. As collision gas high purity nitrogen was used. The fragmentor voltage was set to 120 V and the capillary voltage was 4000 V. Product ion mass spectra were recorded in positive ion mode in the range of m/z 50-200.

3.IV.3. UHPLC-DAD-ESI-Orbitrap-MS/MS conditions

For obtaining high resolution mass spectrometric data of the analytical samples a Dionex Ultimate 3000 UHPLC system (3000RS diode array detector, TCC-3000RS column thermostat, HPG-3400RS pump, SRD-3400 solvent rack degasser, WPS-3000TRS autosampler) was used hyphenated with an Orbitrap Q Exactive Focus Mass Spectrometer equipped with electrospray ionization (ESI) (Thermo Fischer Scientific, Waltham, MA, USA). The column and the HPLC method were the same as the ones used with the non-hydrolyzed analytical samples. The ESI source was operated in positive ionization mode and operation parameters were optimized automatically using the built-in software. The working parameters were as follows: spray voltage, 3500 V; capillary temperature 256.25°C; sheath gas (N₂), 47.5°C; auxillary gas (N₂), 11.25 arbitrary units; spare gas (N₂), 2.25 arbitrary units. The resolution of the full scan was of 70.000 and the scanning range was between 120-1000 *m/z* units. The most intense ions detected in full scan spectrum were selected for data-dependent MS/MS scan at a resolving power of 35.000, in the range of 50-1000 *m/z* units. Parent ions were fragmented with normalized collision energy of 10, 30 and 45%.

3.V. Polarimetry and CD conditions

Optical rotations were determined on a Carl Zeiss Polamat A polarimeter with a 1 dm cell and MeOH sample solutions at 25°C. CD spectra of the aglycones (onogenin, sativanone, medicarpin and maackiain) were recorded on a Chirascan CD spectrometer (Applied Photophysics Ltd., Leatherhead, United Kingdom). Quartz cells of 10 and 0.1 mm optical pathlength and an instrument scanning speed of 100 nm/min with 1 s response time were used for measurements. The measurements are the averages of three repetitions between 200 and 300 nm at room temperature. Spectra were baseline-corrected, and the signal contributions of methanol were subtracted.

3.VI. NMR conditions

All NMR experiments were carried out on a 600 MHz Varian DDR NMR spectrometer equipped with a 5 mm inverse-detection gradient (IDPFG) probehead. Standard pulse sequences and processing routines available in VnmrJ 3.2C/Chempack 5.1 were used for structure identifications. The complete resonance assignments were established from direct ¹H-¹³C, long-range ¹H-¹³C, and scalar spin-spin connectivities using 1D ¹H, ¹³C,

^1H - ^1H gCOSY, ^1H - ^1H NOESY, ^1H - ^1H ROESY, ^1H - ^1H TOCSY, ^1H - ^{13}C gHSQCAD ($J = 140$ Hz), ^1H - ^{13}C gHMBCAD ($J = 8$ Hz and 12 Hz) experiments, respectively. The probe temperature was maintained at 298 K and standard 5 mm NMR tubes were used. The ^1H and ^{13}C chemical shifts were referenced to the residual solvent signals.

3.VII.Method validation

Quantification of calycosin D, calycosin, pseudobaptigenin, formononetin, onogenin, sativanone, maackiain and medicarpin in the *O. spinosa* and *O. arvensis* root extracts was performed by the external standard method using HPLC-DAD. The chromatographic conditions are described at section 3.IV.1. The standard substances were isolated from *O. spinosa* (see section 3.III.2) except for formononetin, which was from Sigma-Aldrich. The purity of the isolated compounds was evaluated by HPLC-DAD and it was min. 98% in all cases. Stock solution of the standards was prepared by dissolving the appropriate amounts in methanolic naringenin solution (0.78 $\mu\text{g}/\text{ml}$) made with the same dilution step as the extraction of the samples. Calibration standards were prepared by diluting the stock solutions with the same naringenin solution. In the calibration plots, 10 different concentrations (100.0 , 60.0 , 30.0 , 10.0 , 6.0 , 3.0 , 1.0 , 0.6 , 0.3 and 0.1 $\mu\text{g}/\text{ml}$) were used for each analyte in triplicate. Quality control (QC) samples at high, medium and low concentrations were prepared separately by diluting the stock solutions. All peak areas were standardized to the peak area of the internal standard naringenin. Calibration plot was constructed by plotting standardized peak areas against corresponding concentrations and then linearity range was determined for each calibrant. Slope, intercept and correlation coefficient were determined by least squares polynomial regression analysis. LOD and LOQ parameters were determined at $3/1$ and $10/1$ signal to noise ratios, respectively. The accuracy (deviation from nominal concentration) and precision (relative standard deviation) of this method was assessed by analyzing the QC samples of three levels ($n = 3$).

4. Results

4.I. Qualitative phytochemical results

Based on the literature concerning the phytochemical constituents of *Ononis* species, the presence of isoflavones, isoflavanones and pterocarpanes were presumed in the forms of glucosides, glucoside malonates and aglycones. During our work, 47 components were identified in the extracts of *Ononis* species (Table 7). The majority of these compounds were isoflavonoid derivatives, but beside them, phenolic lactones and a maltol glycoside were found in the samples. In the following, the detailed chromatographic, mass spectrometric and NMR results demonstrate the base of the structural identification.

4.I.1. Chromatographic results

During the chromatography of the analytical samples, pyrrolidine 2-acetate isoflavonoid glucoside esters (**3**, **5**, **8**, **9**, **10**, **15**) eluted first, followed by the piperidine 2-acetate esters (**12**, **13**, **14**, **17**, **20**, **23**). These latter molecules were not separated from glucosides, but the corresponding piperidine 2-acetate esters always eluted firstly. The glucosides were followed by minor 4''-*O*-malonates (**24**, **25**, **28**, **29**), major 6''-*O*-malonates (**11**, **16**, **33**, **35**, **36**, **37**, **38**, **39**) and lastly, aglycones (**30**, **34**, **40-47**) (Figure 22, Figure 23 and Figure 24). Derivatives with methylenedioxy substitution always preceded the methoxy substituted ones. Calycosin and calycosin D derivatives (**2**, **4**, **11**, **16**, **30**, **34**) showed much shorter retention times than the other isoflavones, namely formononetin and pseudobaptigenin. Some peaks showed duplication (for example **20** and **23**). The sensitivity and selectivity of the UV-DAD and ESI-MS(+) detecting methods were very distinct. UV detection was most sensitive to isoflavones with the largest conjugated electron system (Figure 22), while MS detection in positive ionization mode highlighted the easily protonable beta amino acid derivatives (Figure 23). Although most literature sources mention negative ionization mode as the standard method detecting isoflavones, the signal/noise ratio of pterocarpanes were insufficient, so positive ionization mode was used. In the free-range samples, glucoside malonates seemed to be the most characteristic derivatives, while in the *in vitro* samples aglycones were more abundant. The hairy root cultures proved to synthesize much less from the derivatives bearing methylenedioxy substitution, their most important isoflavonoid derivatives contained rather a methoxy group.

Table 7: The identified compounds and their high-resolution MS and MS/MS data

No	Rt	[M+H] ⁺	delta	Protonated formula	Aglycone	MS/MS fragment ions	Identification
	min	m/z	ppm		m/z	m/z	
1	5.08	433.1338	-0.58	C ₁₈ H ₂₅ O ₁₂		145.0493, 127.0390	Licoagroside B *
2	8.95	447.1281	-1.06	C ₂₂ H ₂₃ O ₁₀	285.0753	270.0521, 253.0491, 225.0542, 213.0542, 197.0594	Calycosin-D 7- <i>O</i> -β-D-glucoside *
3	10.07	588.2072	-0.60	C ₂₉ H ₃₄ NO ₁₂	315.0857	287.0912, 274.1284, 177.0545, 163.0383, 130.0861, 70.0658	Onogenin 7- <i>O</i> -β-D-glucoside 6"-pyrrolidine 2-acetate
4	10.29	447.1299	2.97	C ₂₂ H ₂₃ O ₁₀	285.0752	270.0517, 253.0486, 225.0538, 213.0543, 197.0593	Calycosin 7- <i>O</i> -β-D-glucoside
5	10.71	574.2274	-1.55	C ₂₉ H ₃₆ NO ₁₁	301.1064	283.0598, 274.1280, 163.0389, 130.0862, 70.0655	Sativanone 7- <i>O</i> -β-D-glucoside 6"-pyrrolidine 2-acetate
6	11.17	461.1435	-1.57	C ₂₃ H ₂₅ O ₁₀	299.0908	281.0802, 253.0854, 239.0698, 193.0493, 107.0495	Puerol A 2'- <i>O</i> -glucoside *
7	11.82	475.1593	-1.21	C ₂₄ H ₂₇ O ₁₀	313.1069	295.0960, 267.1012, 253.0855, 207.0647, 107.0495	Clitorienolactone B 4'- <i>O</i> -β-D-glucoside *
8	13.07	556.1812	-0.25	C ₂₈ H ₃₀ NO ₁₁	283.0789	274.1284, 70.0650	Pseudobaptigenin 7- <i>O</i> -β-D-glucoside 6"-pyrrolidine 2-acetate
9	13.60	542.2020	0.13	C ₂₈ H ₃₂ NO ₁₀	269.0804	274.1282, 70.0654	Formononetin 7- <i>O</i> -β-D-glucoside 6"-pyrrolidine 2-acetate
10	14.39	558.1968	-0.34	C ₂₈ H ₃₂ NO ₁₁	285.0754	274.1280, 175.0389, 151.0388, 70.0658	Maackiain 3- <i>O</i> -β-D-glucoside 6"-pyrrolidine 2-acetate
11	14.44	533.1295	1.00	C ₂₅ H ₂₅ O ₁₃	285.0753	270.0518, 253.0490, 225.0542, 213.0542, 197.0597	Calycosin-D 7- <i>O</i> -β-D-glucoside malonate *
12	14.50	570.1967	-0.50	C ₂₉ H ₃₂ NO ₁₁	283.0596	288.1434, 84.0814	Pseudobaptigenin 7- <i>O</i> -β-D-glucoside 6"-piperidine 2-acetate *
13	14.87	556.2177	-0.04	C ₂₉ H ₃₄ NO ₁₀	269.0801	288.1436, 144.1017, 84.0814	Formononetin 7- <i>O</i> -β-D-glucoside 6"-piperidine 2-acetate *
14	14.89	602.2231	-0.17	C ₃₀ H ₃₆ NO ₁₂	315.0855	288.1435, 177.0543, 163.0387, 144.1017, 135.0439, 84.0814	Onogenin 7- <i>O</i> -β-D-glucoside 6"-piperidine 2-acetate *
15	15.27	544.2166	-2.06	C ₂₈ H ₃₄ NO ₁₀	271.0961	274.1281, 161.0594, 137.0595, 123.0441, 70.0646	Medicarpin 3- <i>O</i> -β-D-glucoside 6"-pyrrolidine 2-acetate
16	15.39	533.1309	-1.40	C ₂₅ H ₂₅ O ₁₃	285.0753	270.0518, 253.0491, 225.0541, 213.0543, 197.0594,	Calycosin 7- <i>O</i> -β-D-glucoside malonate
17	15.53	588.2434	-0.91	C ₃₀ H ₃₈ NO ₁₁	301.1064	288.1436, 273.1115, 163.0387, 144.1017, 135.0439, 84.0814	Sativanone 7- <i>O</i> -β-D-glucoside 6"-piperidine 2-acetate *
18	15.61	299.0909	-1.67	C ₁₇ H ₁₅ O ₅		281.0804, 253.0805, 239.0699, 193.0493, 107.0495	Puerol A *
19	15.65	445.1124	-1.18	C ₂₂ H ₂₁ O ₁₀	283.0597	253.0491, 225.0543, 197.0595, 169.0647	Pseudobaptigenin 7- <i>O</i> -β-D-glucoside

20	15.95	572.2122	-0.76	C ₂₉ H ₃₄ NO ₁₁	285.0752	288.1436, 175.0387, 151.0388, 144.1017, 84.0814	Maackiain 3- <i>O</i> -β-D-glucoside 6"-piperidine 2-acetate *
21	16.28	431.1345	1.95	C ₂₂ H ₂₃ O ₉	269.0805	254.0570, 237.0543, 226.0622, 213.0907, 118.0415	Formononetin 7- <i>O</i> -β-D-glucoside
22	16.51	477.1382	-1.97	C ₂₃ H ₂₅ O ₁₁	315.0858	297.0753, 287.0909, 257.0805, 229.0857, 178.0623, 163.0388, 147.0439, 135.0440	Onogenin 7- <i>O</i> -β-D-glucoside
23	17.55	558.2326	-1.38	C ₂₉ H ₃₆ NO ₁₀	271.0959	288.1435, 161.0594, 144.1017, 137.0595, 123.0441, 84.0814	Medicarpin 3- <i>O</i> -β-D-glucoside 6"-piperidine 2-acetate *
24	17.33	463.1591	-1.67	C ₂₃ H ₂₇ O ₁₀	301.1065	283.1271, 273.1116, 177.1119, 164.0832, 163.0388, 135.0440	Sativanone 7- <i>O</i> -β-D-glucoside
25	17.59	531.1125	-1.54	C ₂₅ H ₂₃ O ₁₃	283.0596	253.0490, 225.0542	Pseudobaptigenin 7- <i>O</i> -β-D-glucoside 4"-malonate
26	18.14	517.1343	-0.48	C ₂₅ H ₂₅ O ₁₂	269.0804	253.8803	Formononetin 7- <i>O</i> -β-D-glucoside 4"-malonate
27	18.23	447.1272	0.16	C ₂₂ H ₂₃ O ₁₀	285.0751	175.0388, 151.0388, 123.0442	Maackiain 3- <i>O</i> -β-D-glucoside
28	18.31	563.1387	-1.48	C ₂₆ H ₂₇ O ₁₄	315.0858	297.0753, 287.0909, 257.0804, 229.0857, 178.0623, 163.0388, 147.0439, 135.0440	Onogenin 7- <i>O</i> -β-D-glucoside 4"-malonate
29	18.97	549.1600	-0.49	C ₂₆ H ₂₉ O ₁₃	301.1065	273.1117, 177.1119, 163.0388, 135.0440	Sativanone 7- <i>O</i> -β-D-glucoside 4"-malonate
30	19.08	285.0754	1.23	C ₁₆ H ₁₃ O ₅		270.0519, 253.0490, 225.0540, 213.0543, 197.0596, 137.0232	Calycosin-D
31	19.08	313.1066	-2.11	C ₁₈ H ₁₇ O ₅		295.0961, 267.1012, 253.0856, 207.0650, 107.0495	Clitorienolactone B *
32	19.27	433.1487	-1.41	C ₂₂ H ₂₅ O ₉	271.0960	137.0596	Medicarpin 3- <i>O</i> -β-D-glucoside
33	19.68	563.1382	-2.37	C ₂₆ H ₂₇ O ₁₄	315.0855	297.0752, 287.0912, 257.0803, 229.0856, 178.0628, 163.0387, 147.0438, 135.0439	Onogenin 7- <i>O</i> -β-D-glucoside 6"-malonate
34	19.90	285.0752		C ₁₆ H ₁₃ O ₅		270.0519, 253.0490, 225.0542, 213.0543, 197.0592	Calycosin #
35	20.03	531.1132	-0.22	C ₂₅ H ₂₃ O ₁₃	283.0596	253.0491, 225.0543, 197.0594	Pseudobaptigenin 7- <i>O</i> -β-D-glucoside 6"-malonate
36	20.35	549.1595	-1.40	C ₂₆ H ₂₉ O ₁₃	301.1066	283.1001, 273.1110, 177.1144, 164.0832, 163.0471, 135.0455	Sativanone 7- <i>O</i> -β-D-glucoside 6"-malonate
37	20.51	517.1353	2.42	C ₂₅ H ₂₅ O ₁₂	269.0803	254.0569, 237.0541, 213.0906	Formononetin 7- <i>O</i> -β-D-glucoside 6"-malonate
38	20.98	533.1275	-2.75	C ₂₅ H ₂₅ O ₁₃	285.0750	175.0387, 151.0387, 123.0441	Maackiain 3- <i>O</i> -β-D-glucoside 6"-malonate
39	21.77	519.1488	-1.74	C ₂₅ H ₂₇ O ₁₂	271.0959	161.0959, 137.0595, 123.0441	Medicarpin 3- <i>O</i> -β-D-glucoside 6"-malonate
40	23.88	313.0703	-1.17	C ₁₆ H ₁₃ O ₆		298.0469, 283.0598, 281.0440, 268.0362, 255.0647, 240.0413, 212.0465, 162.0310, 151.0388	Cuneatin

41	24.72	315.0858	-1.63	C ₁₇ H ₁₅ O ₆	297.0753, 287.0903, 257.0804, 229.0857, 178.0623, 163.0388, 147.0435, 135.0440	Onogenin *
42	24.81	285.0750	0.88	C ₁₆ H ₁₃ O ₅	175.0388, 151.0388, 123.0442	Maackiain #
43	24.86	299.0916	0.67	C ₁₇ H ₁₅ O ₅	284.0658, 267.0649, 252.0412, 243.1014, 213.0551, 163.0387, 148.0517, 137.0596	2'-methoxy formononetin
44	25.22	283.0596	-1.77	C ₁₆ H ₁₁ O ₅	253.0491, 225.0543, 197.0595, 169, 155, 141, 115	Pseudobaptigenin
45	25.37	301.1061	-3.16	C ₁₇ H ₁₇ O ₅	273.1116, 177.1272, 164.0832, 163.0388, 151.0388, 135.0440, 107.0495	Sativanone *
46	25.65	269.0803	-1.99	C ₁₆ H ₁₃ O ₄	269.0803, 253.0490, 237.0541, 226.0623, 225.0542, 213.0906, 197.0594	Formononetin #
47	25.74	271.0959	1.43	C ₁₆ H ₁₅ O ₄	161.0595, 137.0595, 123.0441	Medicarpin #

*The marked compounds were isolated, and their structures were examined using NMR spectroscopy.

#The retention time and fragmentation patterns of the marked compounds were compared with standard substances. All other components were identified based on HR-MS data.

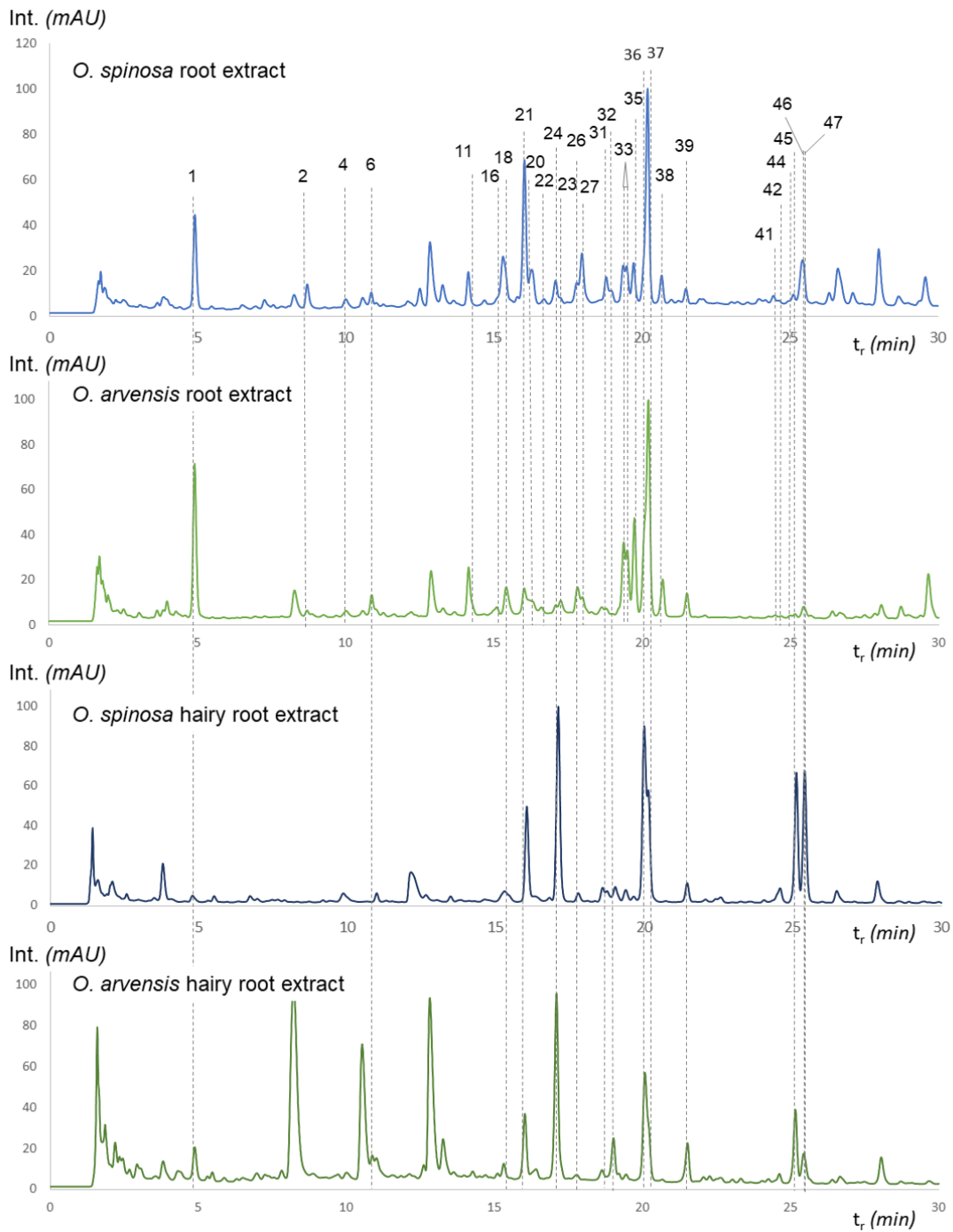


Figure 22: UV chromatograms registrated at 260 nm of the analytical samples made from *O. spinosa* and *O. arvensis* roots and their *in vitro* hairy root cultures

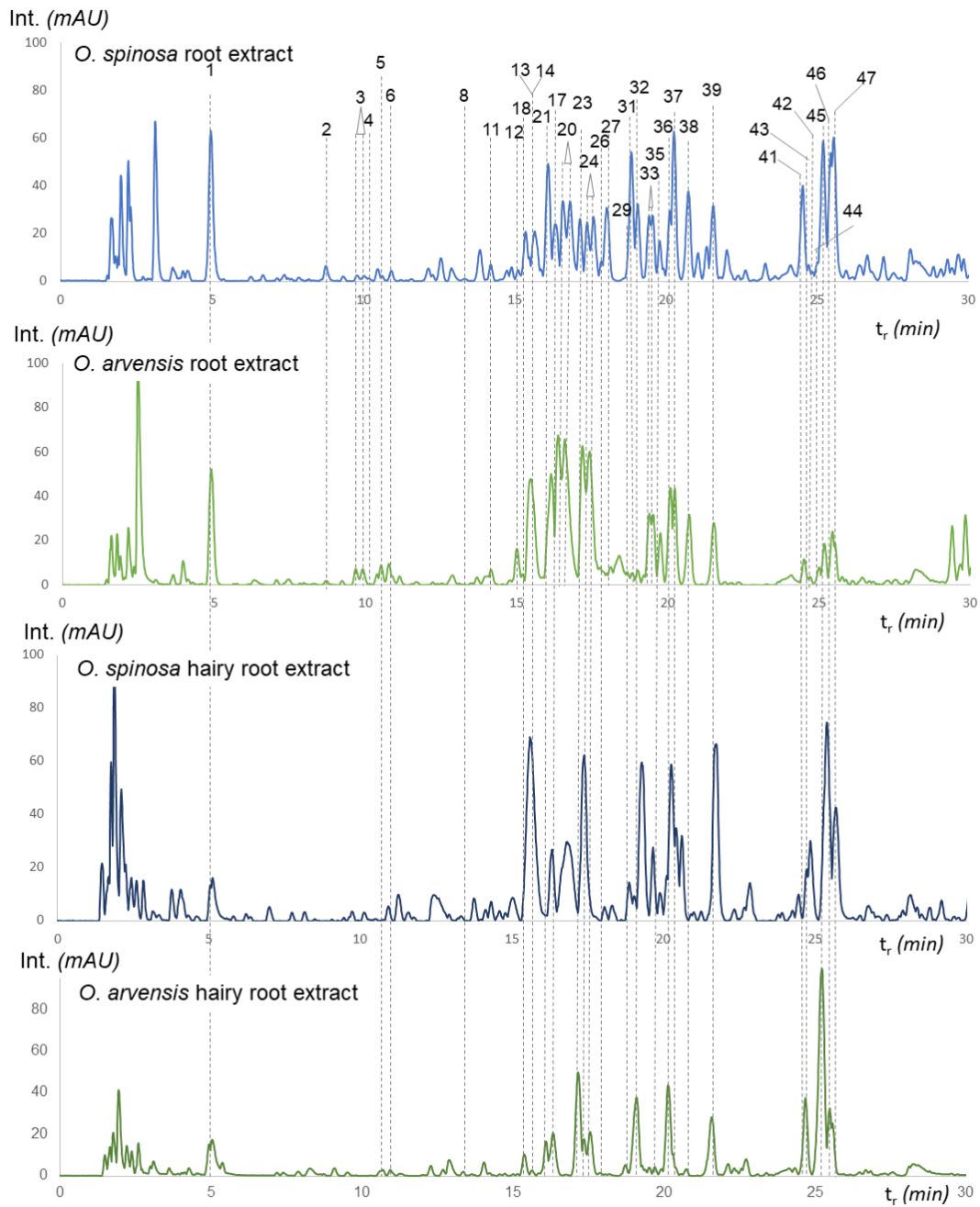


Figure 23: ESI-MS(+) base peak chromatograms of the analytical samples made from *O. spinosa* and *O. arvensis* roots and their *in vitro* hairy root cultures

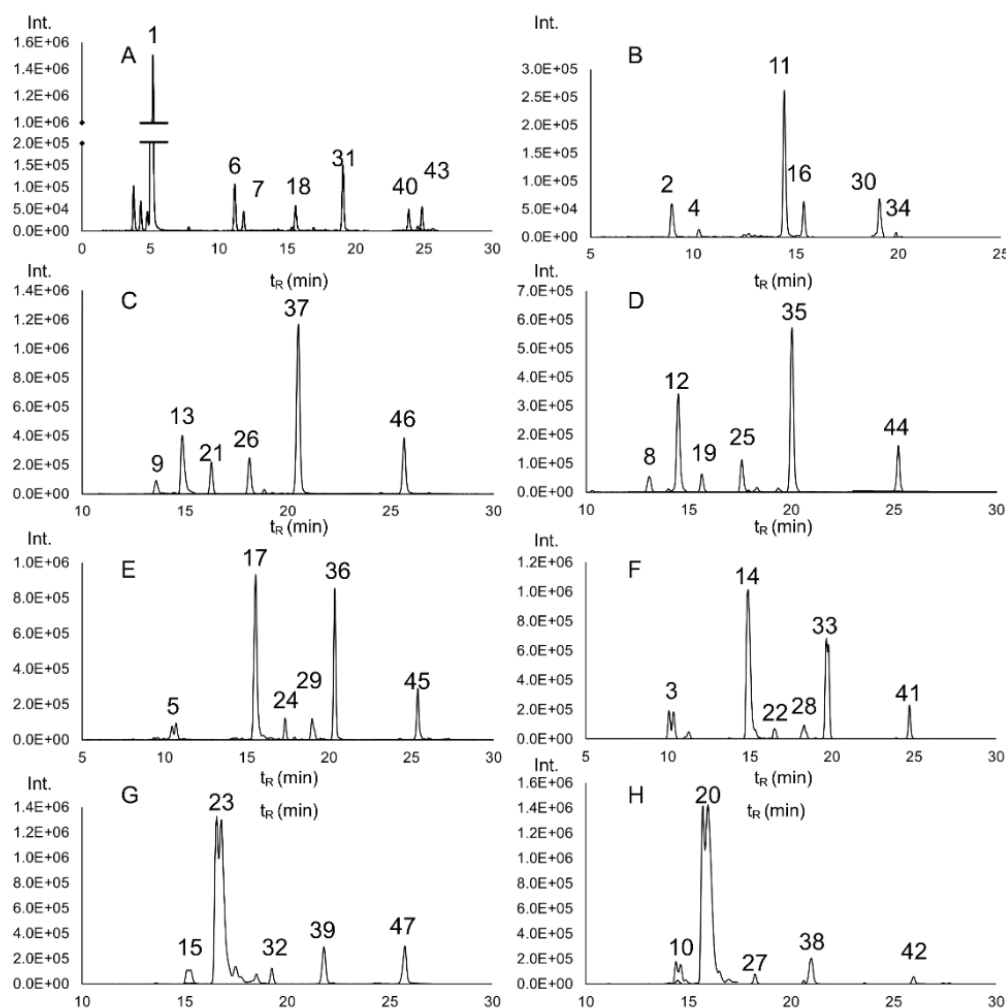


Figure 24: The extracted ion chromatograms of identified compounds with various aglycones from *O. arvensis* root aqueous-methanolic extract. A: licoagroside B (1), puerol derivatives (6, 7, 18, 31), 2'-methoxy isoflavonoids (40, 43) B: calycosin D (2, 11, 30) and calycosin D (4, 16, 34) derivatives C: formononetin derivatives D: pseudobaptigenin derivatives E: sativanone derivatives F: onogenin derivatives G: medicarpin derivatives H: maackiain derivatives

4.I.2. Mass spectrometry results

To obtain high resolution mass spectrometry data about all possible molecule ion or product ion of interest, data independent analysis was used. In addition, to link the fragment ions to their precursor ion, data dependent analysis was applied using ESI(+)-MS/MS. The protonated formulas of the molecular ions and their product ions could be calculated based on the high-resolution mass spectrometric data (see Table 7). In the case

of glucosides and glucoside malonates the neutral loss of 162 and 248 Da could be observed, respectively, and the product ions originating from the aglycone were detected. On the other hand, pyrrolidine and piperidine 2-acetate esters gave rise to protonated product ions containing the esterified glucose moiety or the beta amino acid and the presence of ions originating from the aglycone moiety was much rarer. Pyrrolidine 2-acetate (homoprolin) derivatives had the ions at m/z 274, 130 and 70 in common and piperidine 2-acetate (homopipercolic acid) derivatives the ions at m/z 288, 144 and 84. Dihydroisoflavonoid derivatives showed the most abundant fragmentation profile, while pterocarpan derivatives had only a few characteristic product ions. Components with well-known MS fragmentation and previously reported in the plants (formononetin, pseudobaptigenin, maackiain, medicarpin and their derivatives) could be easily identified solely based on MS. Although, for the identification of new compounds (e.g. sativanone, licoagroside B) or for the differentiation of very similar structural isomers (e.g. calycosin vs. calycosin D, puerol B vs. clitorienolactone B) orthogonal techniques needed to be used.

4.I.3. Detailed structural identification

Structural identification of licoagroside B

As licoagroside B (**1**, Figure 25) was only identified in the hairy root cultures of *Glycyrrhiza glabra* L. till date [193] and even the high-resolution mass spectrometry data could not prove the exact structure, ^1H NMR, ^1H - ^1H COSY, ^1H - ^{13}C HSQC, ^1H - ^{13}C HMBC and ^{13}C NMR experiments were also executed. The ^1H and ^{13}C NMR data of compound **1** can be seen in Table 8.

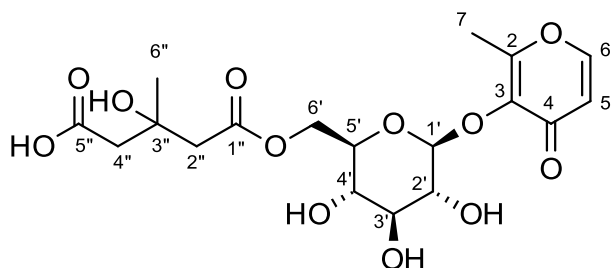


Figure 25: The chemical structure and numbering of licoagroside B (**1**)

Table 8: Complete ^1H and ^{13}C NMR data of licoagroside B (**1**) in methanol- d_4 (δ in ppm, J in Hz)

No.	^1H	^{13}C
2	-	164.6
3	-	143.3
4	-	177.1
5	6.45 (d, $J = 5.0$)	117.4
6	8.00 (d, $J = 5.0$)	157.2
7	2.41 (s)	15.8
1'	4.85 (d, $J = 9.6$)	104.9
2'	3.39 (d, $J = 10.7$)	75.3
3'	3.35 (d, $J = 10.8$)	71.2
4'	3.41 (d, $J = 11.0$)	77.8
5'	3.45 (m)	75.9
6'a	4.20 (dd, $J = 6.0, 6.0$)	64.3
6'b	4.44 (d, $J = 12.0$)	
1''	-	172.3
2''a	2.68 (d, $J = 15.0$)	46.6
2''b	2.62 (d, $J = 15.0$)	
3''	-	70.7
4''a	2.59 (d, $J = 15.0$)	46.6
4''b	2.55 (d, $J = 15.0$)	
5''	-	176.4 (HMBC)
6''	1.33 (s)	27.8

Structural identification of but-2-enolide derivatives

To determine the exact location of substituents on the but-2-enolide skeleton (Figure 25), ^1H NMR, ^1H - ^1H COSY, ^1H - ^1H NOESY, ^1H - ^{13}C HSQC, ^1H - ^{13}C HMBC and ^{13}C NMR experiments were executed (Table 9 and Table 10). Regarding aglycones (compound **18** and **31**), R_1 and R_2 could be a $-\text{H}$ or a $-\text{OCH}_3$ group, while in the case of glucosides (compound **6** and **7**), R_1 and R_2 could be a $-\text{H}$ and a glucose moiety or a $-\text{OCH}_3$ group and a glucose moiety. The position of these groups was located based on the crosspeaks obtained in NOE experiments (Figure 27, 28 and Figure 29).

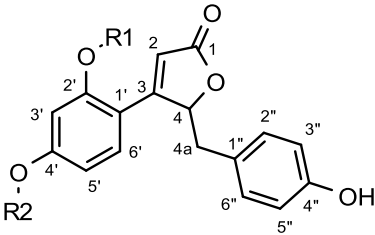
	R_1	R_2	Compound
	H	H	Puerol A
	H	glucose	Puerol A 2'- O -glucoside
	CH_3	H	Puerol B
	CH_3	glucose	Puerol B 2'- O -glucoside
	H	CH_3	Clitorienolactone B
	glucose	CH_3	Clitorienolactone B 4'- O -glucoside

Figure 26: The chemical structure and numbering of but-2-enolide derivatives

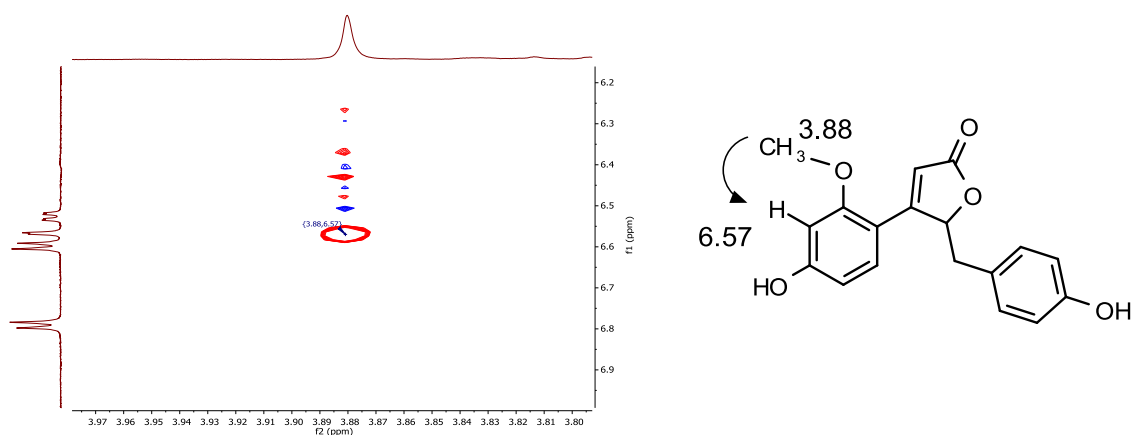


Figure 27: Partial ^1H - ^1H NOESY spectrum of clitorienolactone B (**31**) (600 MHz, methanol- d_4)

Table 9: ^1H and ^{13}C NMR data of puerol A (**18**) and clitorienolactone B (**31**) in methanol- d_4 (δ in ppm, J in Hz)

No.	Puerol A (18)		Clitorienolactone B (31)	
	^1H	^{13}C	^1H	^{13}C
1	-	177.2	-	176.8
2	6.11 (d, $J = 0.8$)	112.4	6.11 (d, $J = 1.4$)	113.66
3	-	168.5	-	167.54
4	5.92 m	88.8	5.90 m	85.5
4a	2.80 (dd, $J = 14.6, 6.0$) 3.25 (dd, $J = 14.6, 3.5$)	39.6	2.79 (dd, $J = 14.6, 5.7$) 3.25 (dd, $J = 14.6, 3.9$)	38.5
1'	-	110.8	-	112.0 (HMBC)
2'	-	163.2	-	163.7
3'	6.42 (d, $J = 2.3$)	104.0	6.57 (d, $J = 2.2$)	100.4
4'	-	160.0	-	161.3
5'	6.43 (d, $J = 8.9, 2.3$)	109.2	6.53 (d, $J = 8.5, 2.2$)	109.4
6'	7.29 (d, $J = 8.9$)	132.2	7.34 (d, $J = 8.5$)	132.4
OCH ₃	-	-	3.94 (s)	55.9
1''	-	127.7	-	127.3
2''	6.85 (d, $J = 8.4$)	131.8	6.79 (d, $J = 8.5$)	131.8
3''	6.61 (d, $J = 8.4$)	115.8	6.60 (d, $J = 8.5$)	115.8
4''	-	157.1	-66	157.3
5''	6.61 (d, $J = 8.4$)	115.8	6.60 (d, $J = 8.5$)	115.8
6''	6.85 (d, $J = 8.4$)	131.8	6.79 (d, $J = 8.5$)	131.8

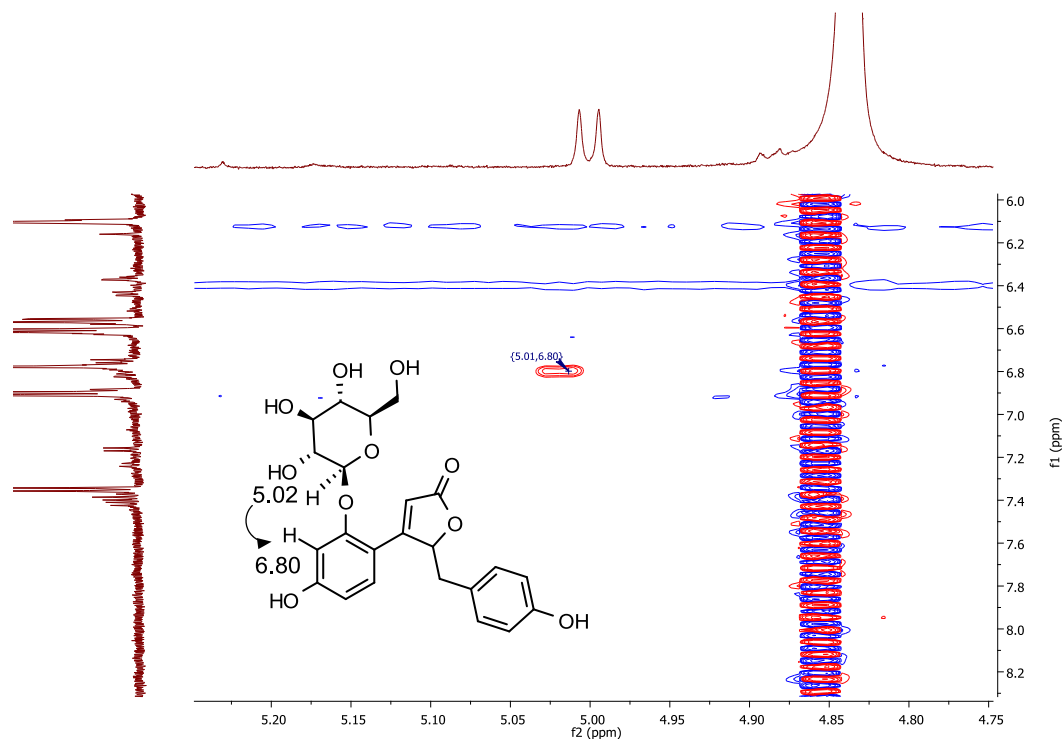


Figure 28: Partial ^1H - ^1H NOESY spectrum of puerol A 2'-*O*-glucoside (**6**) (600 MHz, methanol-*d*₄)

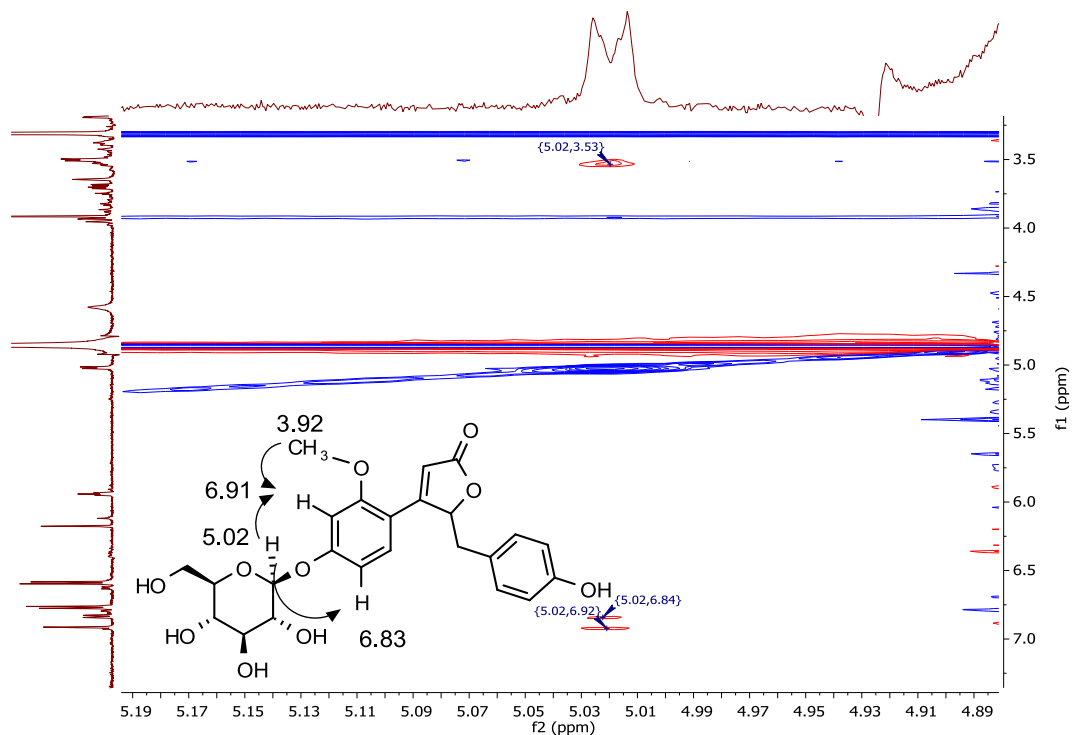


Figure 29: Partial ^1H - ^1H NOESY spectrum of clitorienolactone B 4'-*O*-glucoside (**7**) (600 MHz, methanol-*d*₄)

Table 10: ^1H and ^{13}C NMR data of puerol A 2'-*O*-glucoside (**6**) and clitorienolactone B 4'-*O*-glucoside (**7**) in methanol-*d*4 (δ in ppm, *J* in Hz)

No.	Puerol A 2'- <i>O</i> -glucoside (6)		Clitorienolactone B 4'- <i>O</i> -glucoside (7)	
	^1H	^{13}C	^1H	^{13}C
1	-	177.7	-	n.d.
2	6.12 (d, <i>J</i> = 0.8)	113.5	6.18 (d, <i>J</i> = 0.9)	115.3
3	-	170.4	-	n.d.
4	6.12 m	86.0	5.94 m	85.4
4a	2.78 (dd, <i>J</i> = 14.6, 6.7) 3.20 (dd, <i>J</i> = 14.6, 3.4)	39.1	2.81 (dd, <i>J</i> = 14.6, 5.5) 3.18 (dd, <i>J</i> = 14.6, 3.8)	39.2
1'	-	113.7	-	n.d.
2'	-	164.6	-	n.d.
3'	6.79 (d, <i>J</i> = 2.3)	103.4	6.91 (d, <i>J</i> = 2.0)	102.0
4'	-	159.3	-	n.d.
5'	6.58 (d, <i>J</i> = 8.6, 2.2)	110.1	6.83 (d, <i>J</i> = 8.7, 2.1)	110.0
6'	7.37 (d, <i>J</i> = 8.6)	132.3	7.43 (d, <i>J</i> = 8.4)	132.0
OCH ₃	-	-	3.92 (s)	56.2
1''	-	129.5	-	n.d.
2''	6.92 (d, <i>J</i> = 8.5)	131.6	6.77 (d, <i>J</i> = 8.4)	131.7
3''	6.63 (d, <i>J</i> = 8.5)	115.6	6.59 (d, <i>J</i> = 8.5)	115.7
4''	-	158.2	-	n.d.
5''	6.63 (d, <i>J</i> = 8.5)	115.6	6.59 (d, <i>J</i> = 8.5)	115.7
6''	6.92 (d, <i>J</i> = 8.5)	131.6	6.77 (d, <i>J</i> = 8.4)	131.7
Glu1	5.02 (d, <i>J</i> = 7.3)	101.71	5.02 (d, <i>J</i> = 7.0)	102.0
Glu2	3.45 (m)	78.0	3.50 (m)	78.0
Glu3	3.43 (m)	71.1	3.48 (m)	71.5
Glu4	3.51 (m)	78.2	3.53 (m)	78.5
Glu5	3.48 (m)	74.5	3.51 (m)	74.7
Glu6	3.75 (m)	62.3	3.70 (dd, <i>J</i> = 12.0, 6.4)	62.5
Glu6	3.97 (m)		3.93 (d, <i>J</i> = 12.0)	

^{13}C NMR data for compound **6** and **7** were assigned on the basis of HSQC and HMBC experiments

Structural identification of calycosin derivatives

Calycosin and calycosin D (3'-methoxydaidzein) derivatives did not differ in their UV spectra nor in their MS/MS fragmentation pattern (see Table 7) because of the high structural similarity (Figure 30: The structural difference of calycosin (left) and calycosin

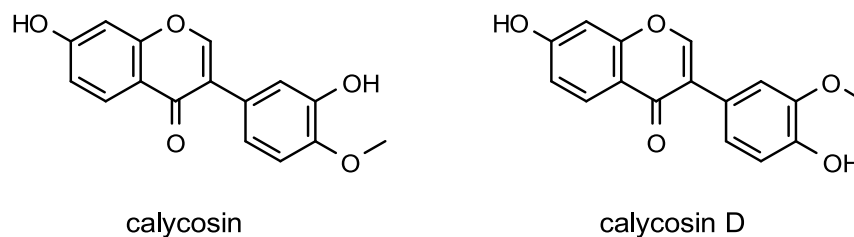


Figure 30: The structural difference of calycosin (left) and calycosin D (or 3'-methoxydaidzein, right)

D (or 3'-methoxydaidzein, right)).

As calycosin aglycon was available as a standard, the two aglycones could be differentiated based on their retention time. However, this method could not be used with glucosides and glucoside malonates, so that ^1H NMR and ^1H - ^1H NOESY experiments were used to identify the isolated compounds **2** and **11** (Figure 31 and Figure 32). Based on the NMR results, they were identified as the glucoside and glucoside malonate of calycosin D. The other two peaks (**4** and **16**) were deduced to be calycosin 7-*O*-glucoside and 7-*O*-glucoside 6''-*O*-malonate.

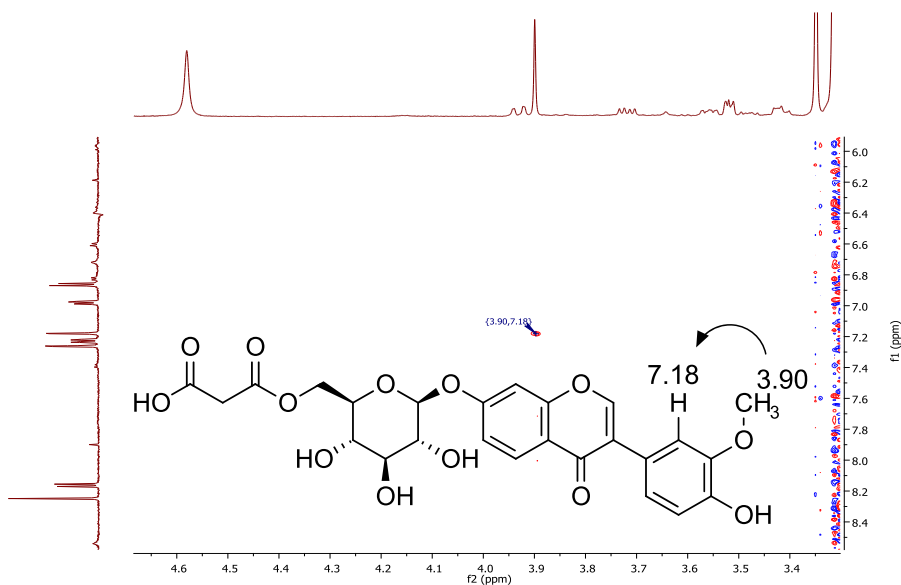


Figure 31: Partial ^1H - ^1H NOESY spectrum of calycosin D 7-*O*-glucoside (**2**) (600 MHz, methanol- d_4)

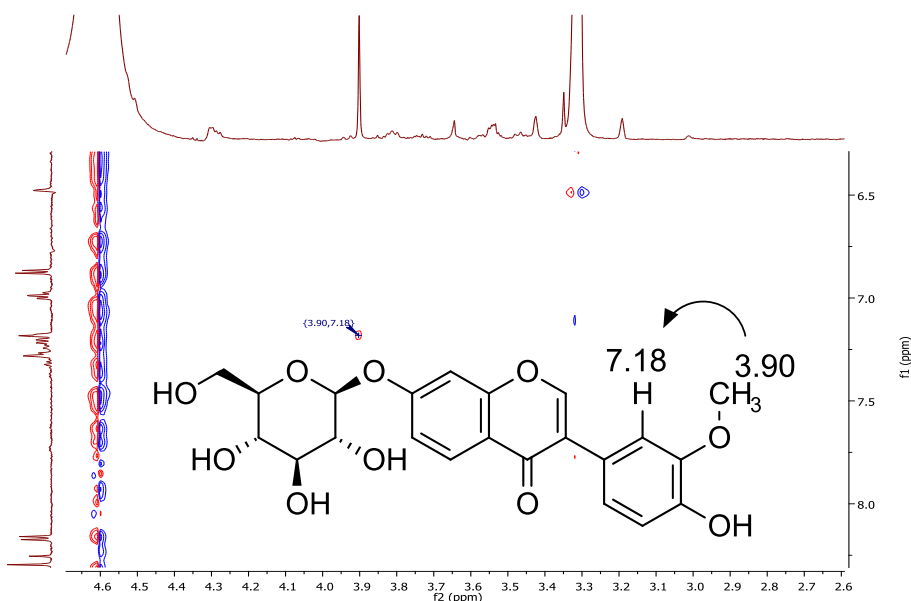


Figure 32: Partial ^1H - ^1H NOESY spectrum of calycosin D 7-*O*-glucoside 6''-*O*-malonate (**11**) (600 MHz, methanol- d_4)

Structural identification of dihydroisoflavonoids

As the onogenin and sativanone derivatives had not been reported before in *O. spinosa*, the isolated compounds were investigated using ^1H NMR, ^1H - ^1H COSY, ^1H - ^1H NOESY, ^1H - ^{13}C HSQC, ^1H - ^{13}C HMBC and ^{13}C NMR experiments (see Table 11). The chirality of the molecules (Figure 33) was investigated by CD spectroscopy, however, their solution did not display any circular dichroism signals, meaning that the two compounds were isolated in a racemic form.

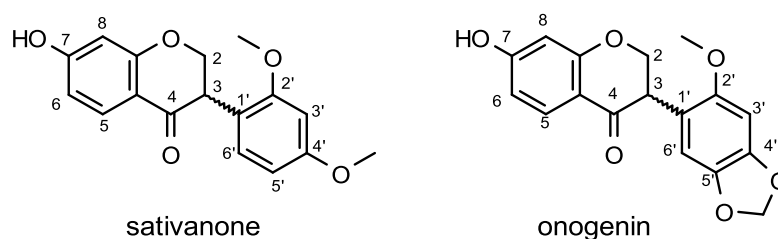


Figure 33: The structure and numbering of sativanone (left) and onogenin (right)

Table 11: ^1H and ^{13}C NMR data of onogenin (**41**) and sativanone (**45**) in methanol- d_4 (δ in ppm, J in Hz)

No.	Onogenin (41)		Sativanone (45)	
	^1H	^{13}C	^1H	^{13}C
2	4.50 – 4.55 (m, 1H) 4.39 – 4.43 (m, 1H)	72.0	4.53 – 4.57 (m, 1H) 4.39 – 4.43 (m, 1H)	72.0
3	4.18 (dd, $J = 11.6, 5.5$ Hz, 1H)	49.2	4.16 (dd, $J = 11.4, 5.4$ Hz, 1H)	49.1
4	-	194.1	-	194.3
4a	-	115.5	-	-
5	7.76 (d, $J = 8.7$ Hz, 1H)	130.3	7.76 (d, $J = 8.7$ Hz, 1H)	130.3
6	6.50 (dd, $J = 8.7, 2.3$ Hz, 1H)	112.5	6.50 (dd, $J = 8.7, 2.3$ Hz, 1H)	112.0
7	-	-	-	-
8	6.32 (d, $J = 2.3$ Hz, 1H)	103.7	6.32 (d, $J = 2.3$ Hz, 1H)	103.7
8a	-	165.7	-	165.7
9	5.89 (d, $J = 1.4$ Hz, 2H)	102.6	3.79 (s, 3H)	55.8
10	3.72 (s, 3H)	57.1	3.76 (s, 3H)	56.0
11	-	-	-	-
12	-	-	-	-
1'	-	117.1	-	-
2'	-	154.3	-	159.8
3'	6.69 (s, 1H)	96.4	6.57 (d, $J = 2.4$ Hz, 1H)	99.9
4'	-	142.8	-	162.2
5'	-	149.3	6.49 (dd, $J = 8.4, 2.4$ Hz, 1H)	106.0
6'	6.61 (s, 1H)	110.9	7.00 (d, $J = 8.4$ Hz, 1H)	131.9

Structural identification of pterocarpan

Although medicarpin and maackiain were known compounds of *Ononis* species (see section 1.I.2.) their stereochemistry was not unequivocal, because plants can synthesize both (+) and (-) medicarpin and maackiain [95]. To determine the absolute configuration of the pterocarpan optical rotatory dispersion and circular dichroism were used. The $[\alpha]_D^{25}$ value of medicarpin and maackiain was -303° and -113° , respectively, showing that in our sample the pterocarpan can be found in the pure form of levorotary (6aR,11aR)-medicarpin (**47**) and (6aR,11aR)-maackiain (**42**) (Figure 34). The minima and maxima of the recorded CD spectra (Figure 35) of medicarpin, $\lambda_{\max} (\Delta\epsilon)$ 208 ($-18.53 \text{ M}^{-1}\cdot\text{cm}^{-1}$), 236 ($-9.67 \text{ M}^{-1}\cdot\text{cm}^{-1}$), 288 ($4.09 \text{ M}^{-1}\cdot\text{cm}^{-1}$) and maackiain 212 ($-4.18 \text{ M}^{-1}\cdot\text{cm}^{-1}$), 240 ($-7.41 \text{ M}^{-1}\cdot\text{cm}^{-1}$); 280 ($0.24 \text{ M}^{-1}\cdot\text{cm}^{-1}$), were in accordance with literature data [168, 199].

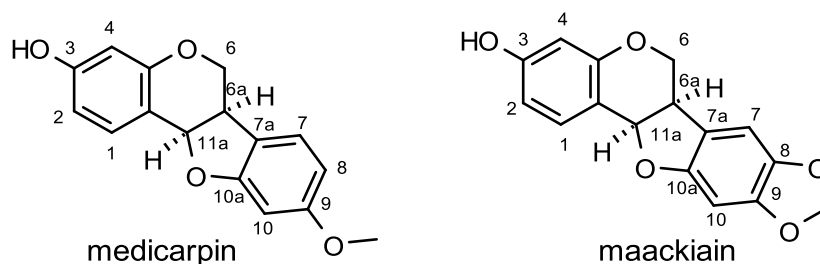


Figure 34: The structure and numbering of (-)-medicarpin (left) and (-)-maackiain (right)

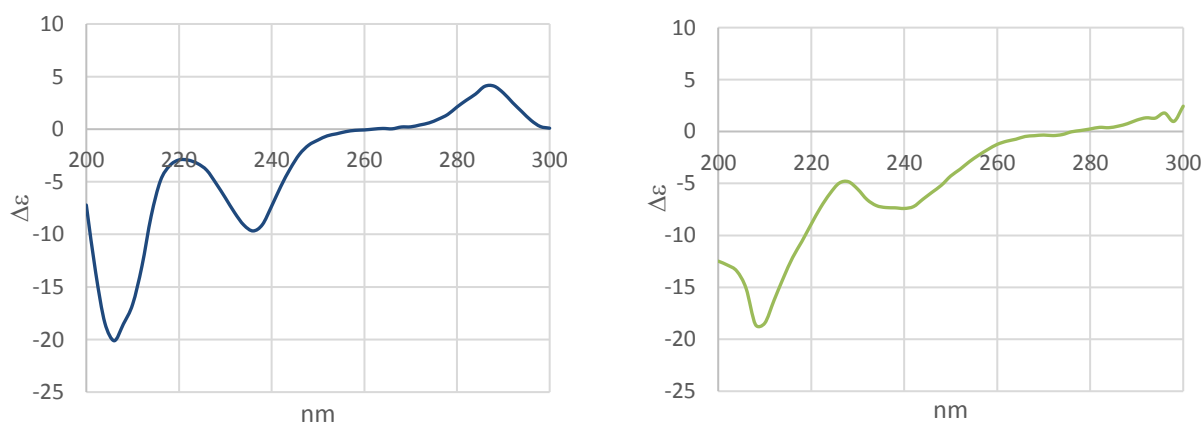


Figure 35: CD spectrum of medicarpin (**47**) (MeOH, pathlength: 0.1 mm $c=1.3165 \text{ mg/ml}$) and maackiain (**42**) (MeOH, pathlength: 0,01 mm $c=0.071 \text{ mg/ml}$)

Structural identification of nitrogen-containing isoflavonoid derivatives

To corroborate the mass spectrometry data of beta amino acid isoflavonoid glucoside esters and to assign the location of the building blocks of the molecules, homopiperidic acid esters were isolated and NMR studies were executed (Table 12, Table 13, Table 14). The most important 2D correlations of medicarpin 3-*O*-glucoside 6''-*O*-piperidine 2-acetate (**23**) are shown in Figure 36.

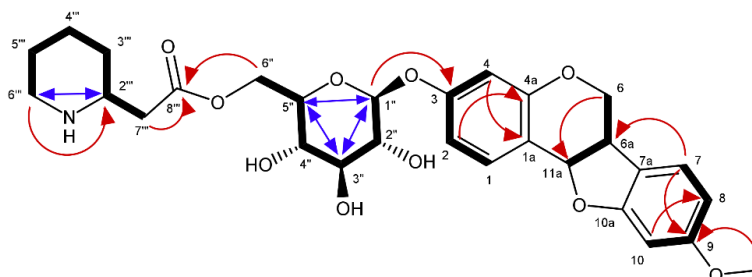


Figure 36: Key 2D correlations of medicarpin glucoside piperidine 2-acetate (**23**) (HMBC – red arrows, TOCSY – bold black lines, NOESY – blue arrows)

The NMR signals showed significant splitting since isomeric pairs were isolated. The members of the pairs in the case of medicarpin and maackiain esters were separated and the first- and second-eluting isomers were subjected to ^1H NMR investigation. It can be clearly seen on the ^1H NMR spectra, that the split signals recorded in the mixture arose from the individual signals of the isolated isomers (Figure 37).

Table 12: ^1H and ^{13}C NMR data of formononetin (**13**) and pseudobaptigenin (**12**) glucoside piperidine 2-acetates in $\text{DMSO-}d_6$ (δ in ppm, J in Hz).

No	Compound 13		Compound 12	
	^1H	^{13}C	^1H	^{13}C
2	8.43/8.44 s	152.5	8.45/8.44 s	153.9
3	-	123.3	-	124.8
4	-	175.1	-	174.6
4a	-	118.9	-	-
5	8.07 d (8.8) 8.06 d (8.9)	127.0	8.06 d (8.8) 8.06 d (8.9)	126.9
6	7.14 dd (8.7, 2.3)	115.4	7.14 dd (8.7, 2.4)	109.3
7	-	161.3	-	161.3
8	7.24/7.22 d (2.3)	103.5	7.23/7.22 d (2.4)	103.3
8a	-	157.1	-	160.8
1'	-	123.8	-	123.6
2'/6'	7.52/7.51 d (8.8)	130.1	7.15 d (2.4)	115.5
3'/5'	7.01 d (8.8)	113.5	-	152.3
4'	-	159.1	-	147.1
5'	-	113.5	7.00 d (7.7)	108.1
6'	-	130.1	7.07/7.06 dd (7.7, 2.4)	122.3
4'- OCH_3	3.79 s	55.1	-	-
4'- OCH_2O -3'	-	-	6.05 s	101.1

1''	5.20 d (5.5) 5.19 d (5.4)	99.4	5.20/5.19 d (5.5)	99.3
2''	3.328 t (8.1)	73.0	3.27 t (8.1)	72.9
3''	3.30 t (9.1)	76.1	3.30 t (9.1)	76.1
4''	3.19/3.18 t (9.1)	69.9	3.15 t (9.1)	69.9
5''	3.76 m	73.8	3.76 m	73.6
6''A	4.10 dd (11.8, 7.3) 4.07 dd (11.8, 7.1)		4.06/4.01 m	
6''B	4.33 dd (11.8, 2.1) 4.32 dd (11.8, 1.9)	63.3	4.30 m	63.2
2'''	2.70/2.65 m	53.1	2.71/2.66 m	53.1
3'''ax	0.96/0.89 m	31.8	0.96 m	31.8
3'''eq	1.50/1.43 m		1.52 m	
4'''ax	1.14 m	24.1	1.15 m	24.1
4'''eq	1.60/1.52 m		1.61m	
5'''ax	1.14 m	25.6	1.15 m	25.6
5'''eq	1.36 m		1.35 m	
6'''ax	2.38/2.31 m	46.0	2.34 m	46.0
6'''eq	2.80/2.75 m		2.83/2.75 m	
7'''	2.29/2.28 m	41.1	2.28m	41.2
8'''	-	171.4	-	171.4

¹³C NMR data for compound **12** and **13** were assigned on the basis of HSQC and HMBC experiments

The two isomers of maackiain were investigated by HPLC-DAD after 1, 5 and 10 days of separation, but no interconversion of isomeric forms was observed (Figure 38). As the pyrrolidine 2-acetate esters were present in minute amounts, their isolation was omitted and thus the structural identification was carried out using indirect methods. In order to release the beta amino acids from their ester forms the extracts were hydrolyzed using ammonia and these samples were spiked with the solution of homoproline and homopiperic acid standards. No difference was observed in the retention times and the fragmentation patterns of the standard substances and compounds present in the hydrolyzed plant extract (see Figure 39).

Table 13: ¹H and ¹³C NMR data of sativanone (**17**) and onogenin (**14**) glucoside piperidine 2-acetates in DMSO-*d*₆ (δ in ppm, *J* in Hz).

Position	Compound 17		Compound 14	
	¹ H	¹³ C	¹ H	¹³ C
2	4.58/4.57 m 4.46 m	70.47	4.59 m 4.45 m	70.36
3	4.21 dd (11.4, 5.4)	46.68	4.25 m	47.23
4	-	190.66	-	190.56
4a	-	115.88	-	115.86
5	7.76 (8.7) 7.76 d (8.9)	128.53	7.76 d (8.7) 7.75 d (8.8)	130.07
6	6.72 dd (8.7, 2.3) 6.72 dd (8.9, 2.5)	110.81	6.74/6.72 dd (8.7, 2.5)	110.83
7	-	162.94	-	162.99
8	6.64 d (2.3) 6.64 d (2.5)	103.45	6.64/6.63 d (2.5)	103.45
8a	-	162.89	-	162.99
1'	-	115.79	-	115.44
2'	-	158.13	-	152.50
3'	6.59 dd (1.3)	98.87	6.82 s	95.77
4'	-	160.09/160.07	-	140.65
5'	6.49/6.48 m	104.99	-	147.24
6'	7.01 d (8.5) 6.99 dd (8.6, 1.3)	130.82/130.64	6.75/6.73 s	109.89
2'-OCH ₃	3.71 s	55.64	3.66/3.65 s	56.65
4'-OCH ₃	3.75 s	55.24	-	-
4'-OCH ₂ O-3'	-	-	5.96/5.95 s	101.11
1''	5.06 d (5.0) 5.05 d (4.9)	99.41	5.06/5.05 d 5.7	99.42
2''	3.27 dd (8.8, 7.8)	73.00	3.28 t 8.1	73.01
3''	3.32 t (8.9)	76.14	3.31 t 9.1	76.14
4''	3.16 t (9.2)	69.89/69.84	3.16 t 9.1	69.96
5''	3.69 m	73.76	3.69 m	73.77
6''A	4.07/4.04 m	63.28	4.07/4.03 m	63.25
6''B	4.35/4.32 m		4.35/4.32 m	
2'''	2.78 m	53.20/53.09	2.73 m	53.29
3'''ax	1.02/0.97 m	31.65	0.96/0.92 m	31.93
3'''eq	1.53 m		1.55/1.48 m	
4'''ax	1.23 m	24.04/24.01	1.22 m	24.21
4'''eq	1.61 m		1.61 m	
5'''ax	1.24 m	25.42	1.21 m	25.69
5'''eq	1.44 m		1.42 m	
6'''ax	2.45 m	45.96	2.43 m	46.15
6'''eq	2.87 m		2.84 m	
7'''	2.32 m	40.98	2.30 m	41.26
8'''	-	171.26/171.23	-	171.37

Table 14: ¹H and ¹³C NMR data of medicarpin (**23**) and maackiain (**20**) glucoside piperidine 2-acetates in DMSO-*d*₆ (δ in ppm, *J* in Hz)

No.	Compound 23		Compound 20	
	¹ H	¹³ C	¹ H	¹³ C
1	7.39/7.38 d (8.7)	131.92	7.37 d (8.7)	131.87
1a	-	114.19	-	114.25
2	6.70 dd (8.7, 2.3)	110.35	6.68 dd (8.7, 2.3)	110.34
3	-	158.23	-	158.23
4	6.54/6.53 d (2.3)	104.02	6.54 d (2.3)	104.01
4a	-	156.18/156.16	-	156.18/156.16
6A	4.28 m	66.03	4.26 m	65.94
6B	3.65 m		3.64 m	
6a	3.65 m	38.84	3.60 m	39.56
7a	-	119.19	-	118.24
7	7.25d (8.5)	125.20	6.98 s	105.37
8	6.45/6.44 d (8.5)	96.34	-	141.12
9	-	160.53	-	147.48
10	6.43/6.42 s	106.11	6.53 s	93.24
10a	-	160.22	-	153.64
11a	5.59 d (7.1)	77.73	5.56 d (7.5)	77.62
9-OCH ₃	3.69 s	55.29		
			5.91 s	
9-OCH ₂ O-8			5.95 s	101.05
1''	4.90/4.89 d (8.5)	99.95	4.89 d (7.7) 4.89 d (7.8)	99.97
2''	3.22 t (8.4)	73.08	3.23 m	73.09
3''	3.29 t (8.9)	76.20	3.29 t (8.9)	76.20
4''	3.15 dd (9.8, 8.7)	69.90/69.85	3.15 m	69.89/69.86
5''	3.60 m	73.65	3.60 m	73.65/73.64
6''A	4.06/4.02 dd (12.0, 6.8)		4.06/4.03 dd (12.0, 6.8)	
6''B	4.33/4.30 dd (12.0, 2.3)	63.21/63.18	4.33/4.30 dd (12.0, 2.4)	63.24/63.23
2'''	2.73 m	53.30/53.21	2.76 m	53.26/53.17
3'''ax	0.99/0.94 m	31.93	1.00/0.96 m	31.75
3'''eq	1.53/1.49 m		1.54/1.50 m	
4'''ax	1.22 m	24.23	1.22 m	24.10
4'''eq	1.64/1.60 m		1.64/1.60 m	
5'''ax	1.20 m	25.69	1.21 m	25.51
5'''eq	1.42 m		1.42 m	
6'''ax	2.42 m	46.15	2.43 m	46.05
6'''eq	2.83 m		2.84 m	
7'''	2.28 m	41.22	2.29 m	41.05
8'''	-	171.40/171.36	-	171.32/171.29

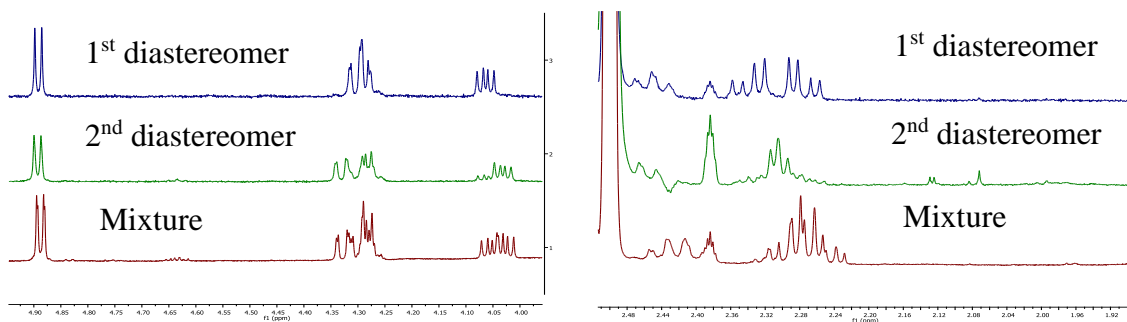


Figure 37: Partial ^1H NMR spectra of isolated isomers and mixture of diastereomers of medicarpin 7-*O*-glucoside 6''-*O*-piperidin-2-acetate (**23**) (600 MHz, $\text{DMSO-}d_6$)

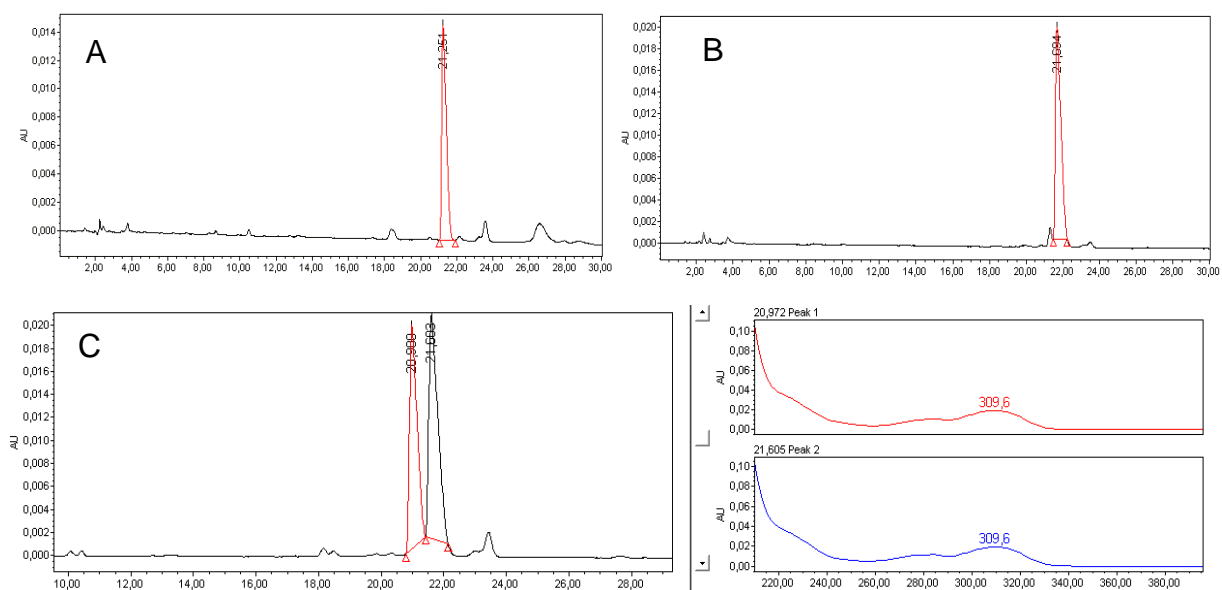


Figure 38: Chromatograms and UV spectra of isolated peaks (A and B) and mixture (C) of maackiain 7-*O*-glucoside 6''-*O*-piperidin-2-acetate **20** after 10 days

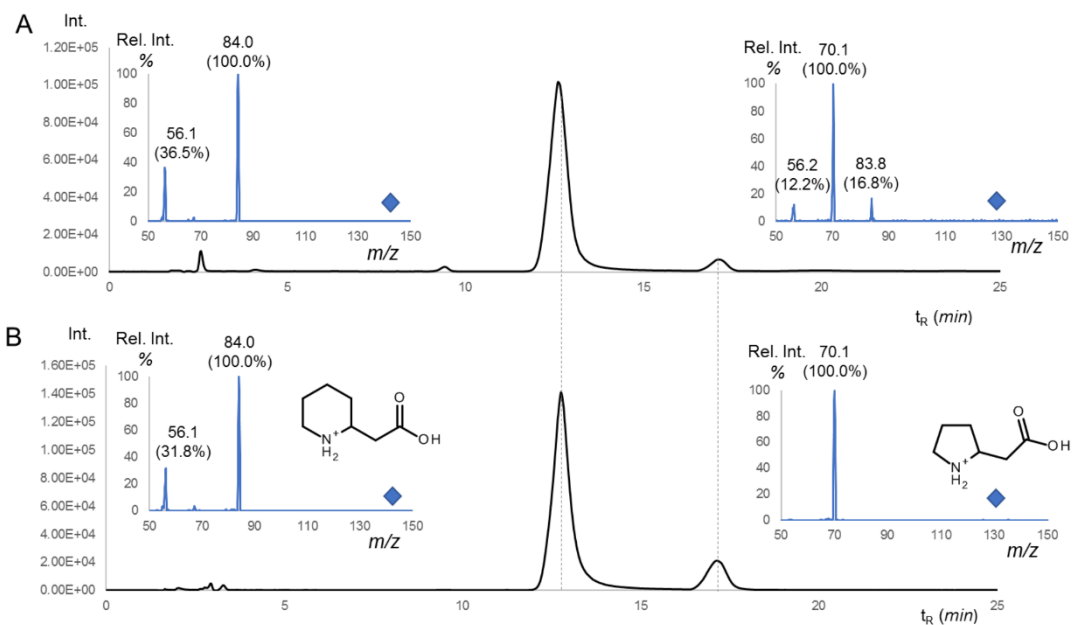


Figure 39: The chromatographic separation and MS spectra of homopiperic acid (12.8 min) and homoproline (17.3 min) in the hydrolyzed sample (A) and spiked with the authentic standards (B)

4.II. Quantitative phytochemical results

4.II.1. Sample preparation

As most literature sources recommend acidic hydrolysis in order to convert isoflavonoid glycosides to aglycones [10], [171], an attempt was made to optimize the hydrolysis time and acid concentration. After the hydrolytic process, the samples were investigated using HPLC-DAD-ESI-MS/MS method, and semi-quantitative results were used to compare the effectiveness of the various hydrolytic methods. The increase of the concentration of hydrochloric acid and time proved to enhance the ratio of aglycones compared to glycosides (see Figure 40).

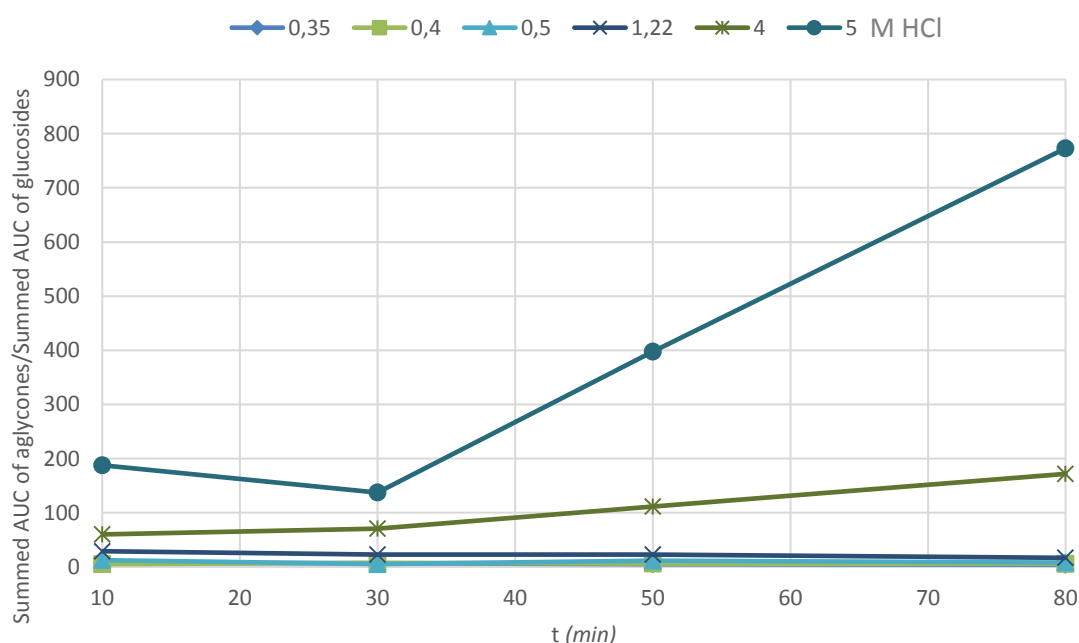


Figure 40: The effect of time and hydrochloric acid concentration on the ratio of summed peak areas of aglycones vs. glucosides

As the 5 M hydrochloric acid resulted to be the most effective, in the following we investigated the amount of each aglycone during the hydrolysis process. As it can be seen in Figure 41, the amount of isoflavones and isoflavanones reached their maximum at 80 min, however the amount of pterocarpanes decreased constantly from the start.

Enzymatic hydrolysis resulted to be much more convenient, as it only cleaved the glycosidic bond and had no effect on the aglycone skeletons. The drastic change in the aglycone vs. glucoside ratio can be observed on the chromatograms of Figure 42. As the

ratio of aglycones showed the same pattern as of the glycosides, it is presumed that no other enzymatic changes were made in the structures.

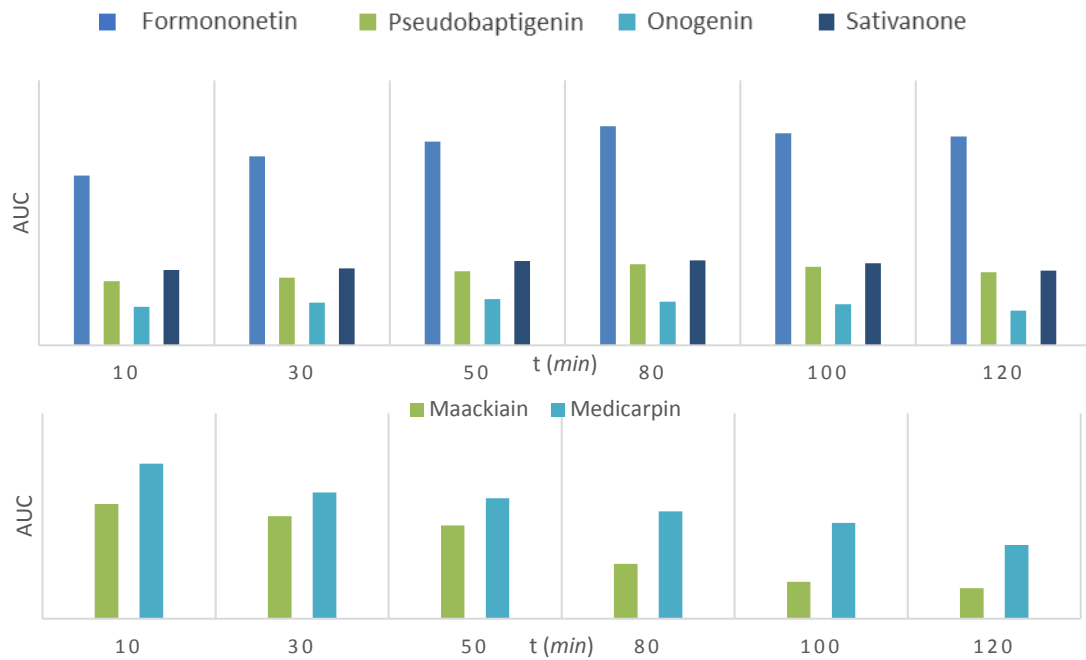


Figure 41: The change in the amount of isoflavone and isoflavanone aglycones (top) and pterocarpan (bottom).

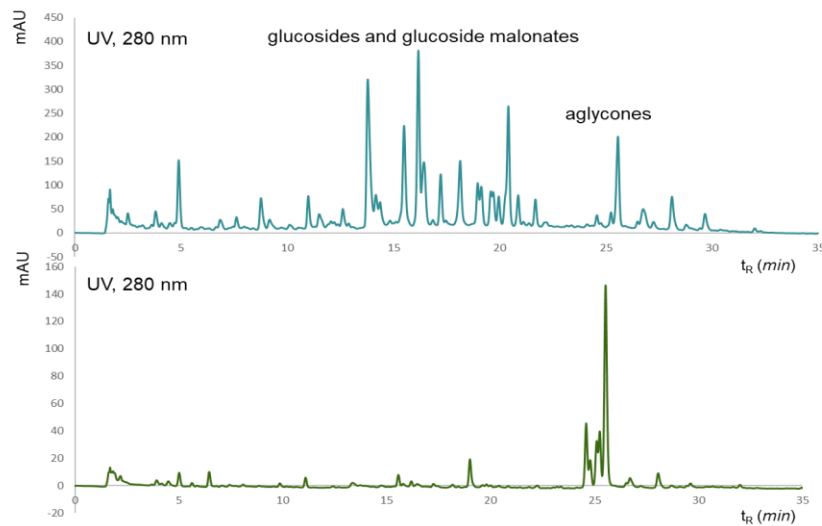


Figure 42: UV chromatogram of the native extract made of *O. spinosa* root (top) and the chromatogram of the sample extracted after 24 h of hydrolysis (bottom).

4.II.2. Method validation

Using optimized conditions, the system enabled baseline separation of 6 target isoflavone aglycones within 14 min. Figure 43 shows chromatograms of a standard mixture and typical hydrolyzed *O. spinosa* root extract under UV detection at wavelength of 270 nm.

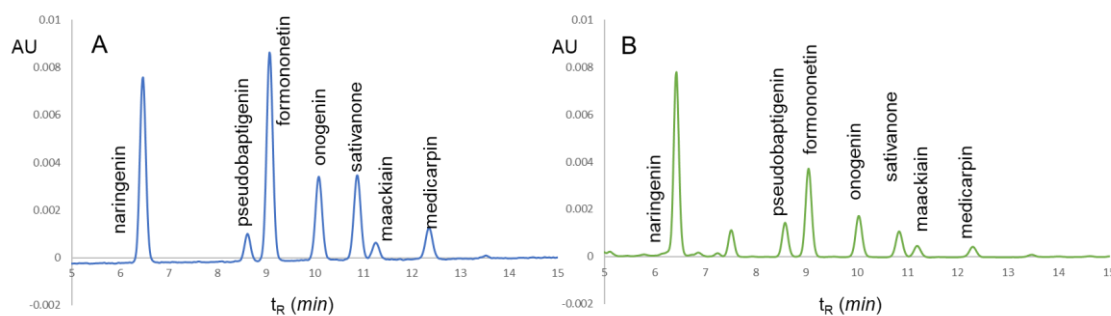


Figure 43: UV chromatograms of the standard mixture (A) and hydrolyzed *O. spinosa* extract (B) registered on 270 nm

The calibration was based on the triplicate analysis of each working solution at 10 concentration levels. The determined linearity ranges can be seen in Table 15 along with the regression equations and the coefficients of determination.

Table 15: Calibrating curves of standard compounds

Name of compound	of linearity range ($\mu\text{g/ml}$) (number of points)	Equation	R^2	LOD ($\mu\text{g/ml}$)	LOQ ($\mu\text{g/ml}$)
Pseudobaptigenin	0.3 – 30.0 (7)	$y = 0.1184x + 0.0268$	1.000	0.1	0.3
Formononetin	0.6 – 100.0 (8)	$y = 0.8967x + 0.3266$	1.000	0.03	0.1
Onogenin	0.3 – 30 (7)	$y = 0.3155x + 0.0219$	1.000	0.03	0.1
Sativanone	0.1 – 30.0 (8)	$y = 0.3328x + 0.0099$	0.999	0.03	0.1
Maackiain	0.3 – 10.0 (6)	$y = 0.1798x + 0.0198$	0.998	0.03	0.1
Medicarpin	0.3 – 10.0 (6)	$y = 0.213x + 0.0246$	0.998	0.03	0.1

The concentrations of the high, medium and low QC samples for each standard can be seen in Table 16 with the intra- and interday accuracy and precision values All results fulfilled the requirements of the FDA and EMEA guidelines of bioanalytical method

validation, as the accuracy and precision values did not exceed $\pm 15\%$, or $\pm 20\%$ in the case of low QC samples at the limit of quantitation.

Table 16: The intra-day precision and accuracy values of the six standards

		Pseudobaptigenin	Formononetin	Onogenin	Sativanone	Maackiain	Medicarpin
High QC ($\mu\text{g/ml}$)		24.5	98.0	24.1	23.9	9.85	10.2
Intra-day	Accuracy (%)	0.8	0.7	0.2	0.8	0.2	0.0
	Precision (%)	2.8	2.3	0.5	0.6	0.1	0.4
Inter-day	Accuracy (%)	-1.4	0.9	0.3	0.7	0.1	0.3
	Precision (%)	0.9	2.4	0.4	0.6	0.5	0.7
Medium QC ($\mu\text{g/ml}$)		2.94	5.88	2.89	0.958	3.69	3.81
Intra-day	Accuracy (%)	10.7	1.0	9.4	-7.4	11.1	10.9
	Precision (%)	0.8	0.6	0.8	1.0	0.6	0.3
Inter-day	Accuracy (%)	11.2	1.1	9.3	-7.1	11.2	10.9
	Precision (%)	0.4	7.4	1.1	0.93	0.5	0.5
Low QC ($\mu\text{g/ml}$)		0.294	0.588	0.289	0.0958	0.37	0.38
Intra-day	Accuracy (%)	-10.3	-17.1	16.5	-6.0	1.1	3.3
	Precision (%)	3.4	0.8	4.8	7.9	5.6	4.2
Inter-day	Accuracy (%)	-20.0	-16.9	11.9	1.3	0.9	0.0
	Precision (%)	5.2	0.9	9.2	15.1	11.9	7.8

4.II.3. Quantitative results

The calculated isoflavonoid concentrations in free-range samples and *in vitro* hairy root cultures of *O. spinosa* and *O. arvensis* can be seen in Table 17. Values are expressed as means of three parallel samples $\pm 95\%$ confidence intervals.

Table 17: The isoflavonoid content of *O. spinosa* and *O. arvensis* samples

	Pseudobaptigenin (g/100g)	Formononetin (g/100g)	Onogenin (g/100g)	Sativanone (g/100g)	Maackiain (g/100g)	Medicarpin (g/100g)	Total (g/100g)
<i>O. spinosa</i>							
Hüvösvölgy	0.33±0.02	0.116±0.006	0.117±0.007	0.078±0.007	0.20±0.01	0.11±0.01	0.95±0.06
Dunaegyháza	0.31±0.04	0.18±0.03	0.13±0.02	0.11±0.01	0.25±0.06	0.24±0.01	1.22±0.18
Commercial 1	0.41±0.04	0.15±0.02	0.25±0.01	0.132±0.007	0.31±0.04	0.21±0.01	1.47±0.14
Commercial 2	0.08±0.04	0.031±0.002	0.091±0.004	0.0693±0.0007	0.133±0.006	0.175±0.004	0.58±0.02
Commercial 3	0.093±0.009	0.028±0.005	0.11±0.01	0.087±0.007	0.15±0.01	0.17±0.01	0.63±0.05
Hairy root	under LOQ	0.43±0.03	0.07±0.01	2.8±0.2	under LOQ	1.37±0.06	4.7±0.3
<i>O. arvensis</i>							
Kárpátalja	0.33±0.021	0.107±0.007	0.201±0.007	0.094±0.007	0.244±0.005	0.138±0.002	1.12±0.05
Udvarhely	0.38±0.01	0.116±0.007	0.106±0.007	0.054±0.002	0.105±0.0065	0.080±0.004	0.84±0.04
Hairy root	under LOQ	0.021±0.002	under LOQ	0.46±0.03	under LOQ	0.39±0.03	0.87±0.06

5. Discussion

5.I. Qualitative phytochemical results

5.I.1. Structural identification of licoagroside B

The m/z value of the pseudo-molecular ion in positive ionization mode of compound **1** (Figure 24) was 433.1338 and its molecular formula calculated on the basis of HR-MS experiments corresponds to $C_{18}H_{24}O_{12}$ (see Table 7). Investigating the fragmentation pattern of this precursor ion, only two fragment ions at m/z 145.0493 ($C_6H_9O_4$) and m/z 127.0390 ($C_6H_7O_3$) could be observed, contrary to the rich fragmentation profile and rDA cleavage of isoflavonoid derivatives [180]. Based on these results, peak **1** was tentatively identified as licoagroside B, the 3-hydroxy-3-methyl-glutarate ester of maltol glucoside. The fragment at m/z 127.0390 could result from the cleavage of the maltol ring together with the anomeric *O* atom,

while the fragment at m/z 145.0493 could be assigned to the hydroxy-methyl-glutaric acid residue (Figure 44). The results of the NMR experiments verified that compound **1** was licoagroside B (Table 8) and the obtained resonances

showed perfect correlation with the ones reported by Li *et al.* [195].

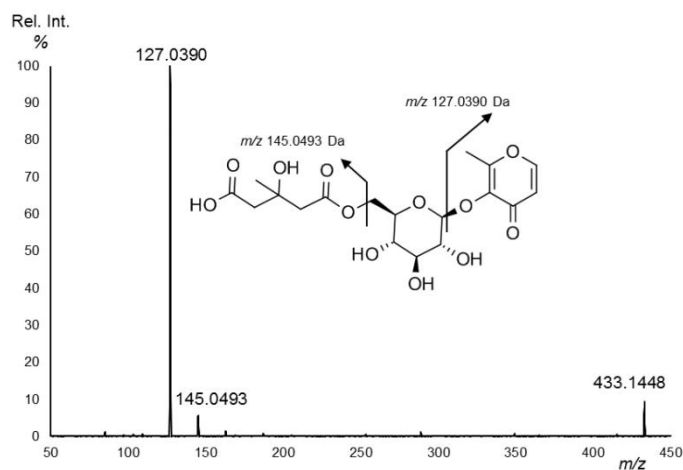
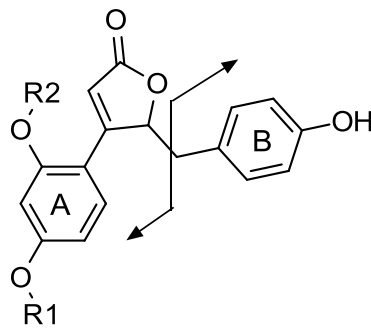


Figure 44: Proposed fragmentation pathway of licoagroside B in positive ionization mode at 10 eV collision energy

5.I.2. Structural identification of but-2-enolides

Peak **18** showed a protonated pseudo-molecular ion at m/z 299.0908 and its fragmentation pattern was identical with that of peak **6** bearing precursor ion at m/z 461.1435 (Figure 24). Based on the protonated molecular formulas ($C_{17}H_{15}O_5$ and $C_{23}H_{25}O_{10}$), these structures were putatively identified as puerol A and its 2'-*O*-glucoside (Table 1). In their

MS/MS spectra two main fragmentation pathways could be observed: the cleavage of the whole molecule to A and B-ring and the neutral loss of small units, as CO and C₂H₂O.



R ₁	R ₂	Compound
H	H	Puerol A
H	glucose	Puerol A 2'-O-glucoside
CH ₃	H	Puerol B
CH ₃	glucose	Puerol B 2'-O-glucoside
H	CH ₃	Clitorienolactone B
glucose	CH ₃	Clitorienolactone B 4'-O-glucoside

Figure 45: The structures of but-2-enolide derivatives and the proposed fragmentation pathway

Between the fragment ions in the spectra of **18** and **31**, a difference of 14 Da could be observed in all cases (Table 7), except for the ion at m/z 107.0495 (C₇H₇O) corresponding to the B-ring. These fragments indicate that a methyl substituent on the A-ring is responsible for the 14 Da shifts of the fragments (Figure 45).

Kirmizgül *et al.* [12] isolated spinonin from *O. spinosa*, which is a monoglycoside and its structure would correspond to puerol A 2''-O-glucoside. Nevertheless, the authors drove to the conclusion, that spinonin contained a 2,3-dihydro-3-oxofurane ring instead of a 2,3-dihydro-2-oxofurane, like the puerol derivatives. Puerol A and its 4'-O-methylated form, puerol B, along with their 2'-O-glucosides were isolated from *O. angustissima* L. by Ghribi *et al* [26], but another O-methylated derivative of puerol A (clitorienolactone B) was isolated from *O. spinosa* by Addotey *et al.* [11]. Puerol B and clitorienolactone differ only in the position of a methyl substitution (Figure 45). In puerol B the methylation occurs at the para OH group of A-ring position, whereas in clitorienolactone B it is in the ortho position. Since the HR-MS/MS investigations alone could not solve the exact location of atoms in the middle ring and the methyl group, peaks **6**, **7**, **18** and **31** were isolated and subjected to NMR experiments in order to clarify the structures. Based on the NMR results (Table 9 and Table 10), the isolated compounds contained a 2,3-dihydro-2-oxofurane ring. The most decisive element was the chemical shift of the carbonyl atoms, as they exhibited chemical shifts at 176.8 and 177.2 ppm,

which are characteristic for unsaturated γ lactones [195], whereas 2,3-dihydro-3-oxofurane rings possess chemical shift above 200 ppm [196]. The glucose moiety of compound **6** joined puerol A through the 2'-OH group, in ortho position (Figure 28). Based on the NOESY spectrum (Figure 28), the methyl group of compound **31** is located in ortho position too, so that this compound was identified as clitorienolactone B. The NOESY spectrum of compound **7** (Figure 29) revealed that the glucose moiety is linked through the 4' OH group, in para position. To the best of our knowledge, this glucoside is characterized for the first time.

5.I.3. Structural identification of isoflavones

Peak **21**, **26**, **37** and **46** (Figure 24) provided $[M+H]^+$ ions at m/z 431.1345 ($C_{22}H_{23}O_9$), 517.1343 ($C_{25}H_{25}O_{12}$), 517.1353 ($C_{25}H_{25}O_{12}$) and 269.0803 ($C_{16}H_{13}O_4$), respectively, but they did not differ in their MS/MS spectra, meaning that they are the derivatives of the same aglycone. The fragmentation of these ions gave rise to m/z 254.0570 ($C_{15}H_{10}O_4$) ion, owing to the radical cleavage of CH_3^{\bullet} and m/z 237.0543 ($C_{15}H_9O_3$), deriving from the loss of a CH_3OH unit, verifying the presence of a methoxy group. The ion at m/z 213.0907 ($C_{14}H_{13}O_2$) is a result of the loss of two CO units which is characteristic for isoflavonoid aglycones [184]. Fragment ion at m/z 118.0415 (C_8H_6O) refers to the ion containing the B-ring resulting from the rDA fragmentation (Figure 18). Although, the intact B-ring with the methoxy group at m/z 133.0648 (C_9H_9O) is barely detectable, the rDA fragment losing the CH_3^{\bullet} radical at m/z 118.0415 is much more intense (Table 7). Regarding this information the aglycone was tentatively identified as formononetin (see Figure 46). The neutral loss of 162.0540 ($C_6H_{10}O_5$) Da of peak **21** corresponded to the loss of a hexose moiety. Taking into account, that isoflavonoids form glycosides with glucose in the vast majority of cases [196], the peak was assigned as formononetin 7-*O*-D-glucoside or ononin (see Figure 47). Peaks **26** and **37** showed the same quasi-molecular ion and fragmentation spectra, and a neutral loss of 248.0550 Da ($C_9H_{12}O_8$), therefore they were attributed as 7-*O*-D-glucoside malonates of formononetin. Based on the significant difference in their quantity and retention times (Figure 24), the firstly eluting minor derivative was tentatively identified as 4''-malonate (**26**) and the later eluting major molecule as 6''-malonate (**37**) (Figure 47) [197].

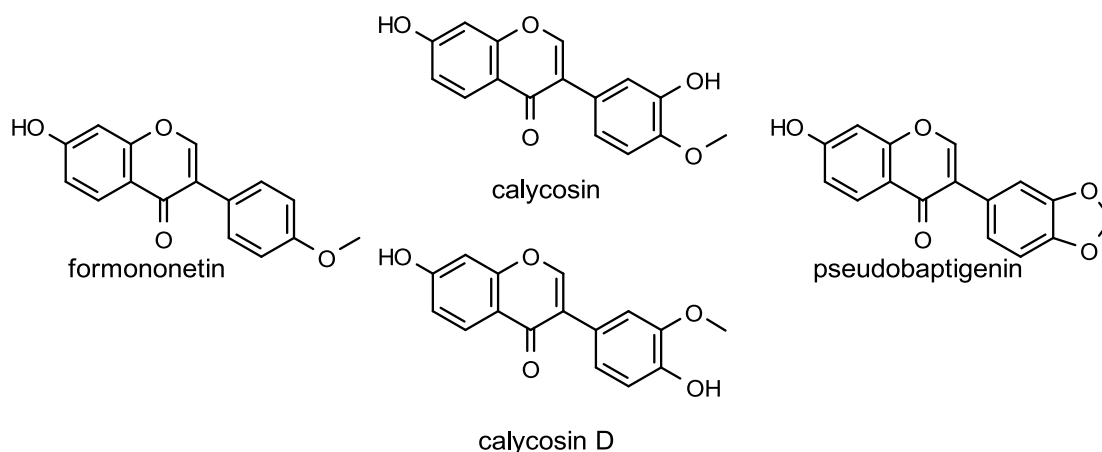
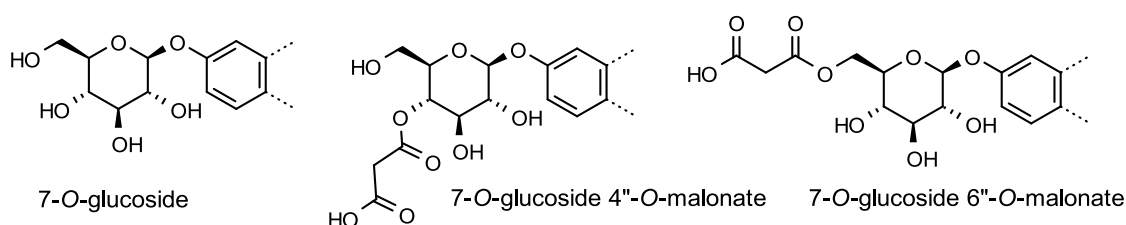


Figure 46: The structures of isoflavone aglycones

Figure 47: The structures of 7-*O*-glucosides, 4''-*O*- and 6''-*O*-malonates

With protonated pseudo-molecular ions at m/z 447.1281 ($C_{22}H_{23}O_{10}$) and 447.1299 ($C_{22}H_{23}O_{10}$), 533.1295 ($C_{25}H_{25}O_{13}$) and 533.1309 ($C_{25}H_{25}O_{13}$), 285.0753 ($C_{16}H_{13}O_5$) and 285.0752 ($C_{16}H_{13}O_5$), two sets of glucosides, glucoside malonates and aglycones were observed, all sharing identical fragmentation pattern. The same neutral losses could be detected as in the case of formononetin, namely the loss of a $CH_3\cdot$ and a CH_3OH , which are a result of a methoxy substitution. These cleavages could be combined with the loss of two CO moieties, resulting in ions at m/z 270.0521 ($C_{15}H_{10}O_5$) $[M+H-CH_3\cdot]^+$, 253.0491 ($C_{15}H_9O_4$) $[M+H-CH_3OH]^+$, 225.0542 ($C_{14}H_9O_3$) $[M+H-CH_3OH-CO]^+$, 213.0542 ($C_{13}H_9O_3$) $[M+H-CH_3OH-CO]^+$, 197.0594 ($C_{13}H_9O_2$) $[M+H-CH_3OH-CO-CO]^+$ (Table 7). The ion at m/z 137.0232 ($C_7H_5O_3$) was presumed to be the rDA fragment containing the A-ring, demonstrating that it could not bear any other substituents but the hydroxy group at C7 (Figure 18). As a result, these molecules were tentatively identified as structural isomers differing only in the position of the hydroxy and methoxy groups of the B-ring. As even the ratios of the fragment ions were not significantly different, the two sets were not distinguishable relying only on mass spectrometry data. Since the firstly

eluting peaks of the pairs were always higher in relative quantity (Figure 24), it was presumed that peaks **2**, **11** and **30** have the same aglycone, and **4**, **16** and **34** another one. The identity of the aglycones was investigated using calycosin as standard substance and its retention time and MS/MS spectrum matched with the later eluting peak (**34**). As Addotey *et al.* isolated calycosin D from *O. spinosa*, which differ only in the position of a methyl group (Figure 30), it was hypothesized, that the major peaks (**4**, **16** and **34**) are the derivatives of this molecule [11]. To verify this hypothesis, the firstly eluting relative major peaks (**2** and **11**) were isolated and investigated by NMR. Based on the NOESY spectra (see Figure 31 and Figure 32), they were the 7-*O*-glucoside and 7-*O*-glucoside 6''-*O*-malonate of calycosin D, so that peaks **4** and **16** were tentatively identified as the 7-*O*-glucoside and 7-*O*-glucoside 6''-*O*-malonate of calycosin, respectively (Figure 46). Peaks **19**, **25** and **35** (Figure 24) had a pseudo-molecular ion at 445.1124 (C₂₂H₂₁O₁₀), 531.1125 (C₂₅H₂₃O₁₃) and 531.1132 (C₂₅H₂₃O₁₃) and each provided the same fragment ions with peak **44** at *m/z* 283.0596 (C₁₆H₁₁O₅). The fragments, which were formed by the loss of a CH₃OH unit from the protonated calycosin ion (*m/z* 253.0491, 225.0543, 197.0595) could be observed with these molecules as well. As the protonated molecular formula of calycosin contains two hydrogens more (C₁₆H₁₃O₅) than the aglycone of these molecules (C₁₆H₁₁O₅) (Table 7), the cause of the same fragment ions is the neutral loss of CH₂O unit instead of a CH₃OH unit. Considering these results, the peaks were tentatively identified as the 7-*O*-D-glucoside (**19**), 4'' and 6''-malonates (**25** and **35**) and the aglycone of pseudobaptigenin (**44**) (Figure 46 Figure 47).

5.I.4. Structural identification of isoflavanones

Peaks **24**, **29**, **36** and **45** (Figure 24) had the quasi-molecular ions at *m/z* 463.1591 (C₂₃H₂₇O₁₀), 549.1600, 549.1595 (C₂₆H₂₉O₁₃) and 301.1061 (C₁₇H₁₇O₅) and their fragmentation pattern significantly differed from those of the isoflavones. Because tandem mass spectrometry experiments alone did not provide satisfactory evidence to identify the aglycone skeleton, the aglycone was isolated from the hydrolyzed plant extract and was unequivocally identified by NMR experiments as sativanone (see page 81). Consequently, the peaks were identified as the 7-*O*-glucoside (**24**), the 4'' and 6''-*O*-glucoside malonates (**29** and **36**) and the aglycone (**45**) of sativanone (Figure 48).

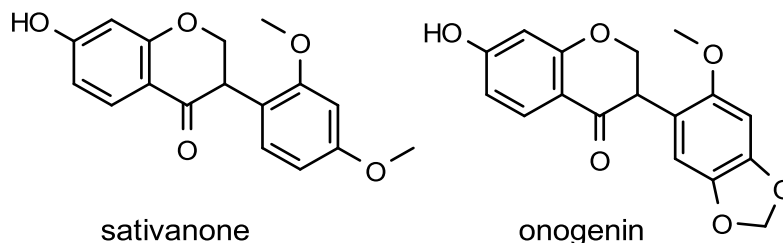


Figure 48: The structure of sativanone (left) and onogenin (right)

Knowing the exact structure of the aglycone, the observed product ions were assigned as follows. All sativanone derivatives produced fragment ions at m/z 283.0965 ($C_{17}H_{15}O_4$) and 273.1119 ($C_{16}H_{17}O_4$), corresponding to the initial ejection of a H_2O or a CO unit. The two intense fragment ions at m/z 163.0388 ($C_9H_7O_3$) and 135.0440 ($C_8H_7O_2$) could be attributed to $[M+H-B-ring]^+$ and $[M+H-B-ring-CO]^+$. As isoflavanones can cleave alongside the bonds 1 and 3 (Figure 18), the product ion at 164.0382 ($C_{10}H_{12}O_2$) could be assigned as $^{1,3}B^{\bullet+}$ (Figure 49). Interestingly, the cleavage of CH_3^{\bullet} groups was not characteristic.

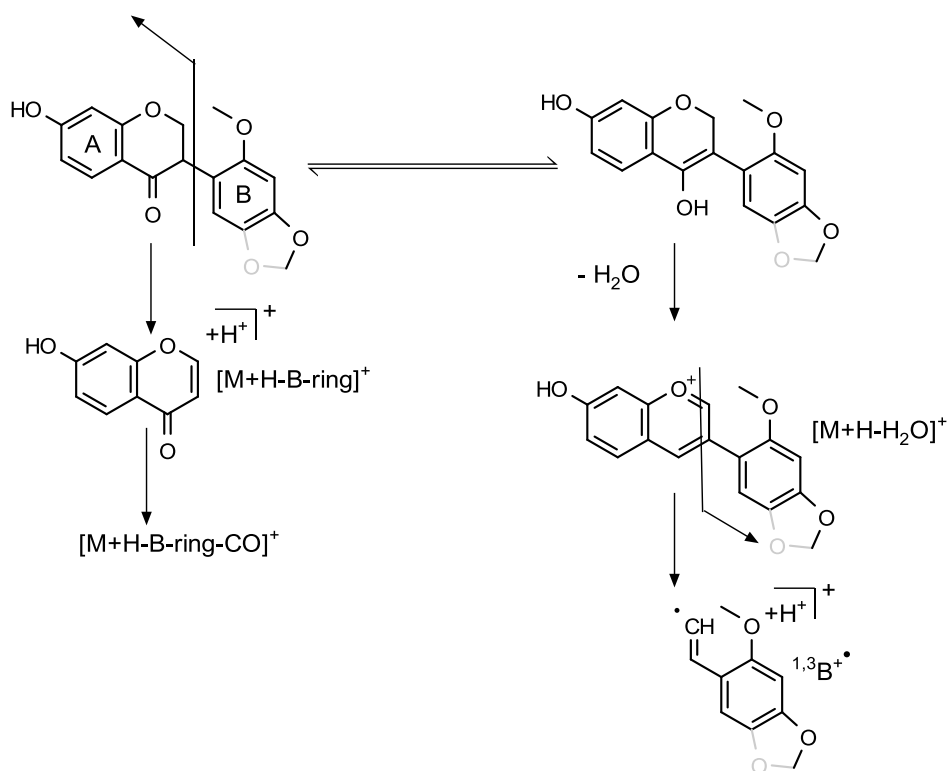


Figure 49: Proposed fragmentation pathway of isoflavanones

The molecular formula of peaks **22**, **28**, **33** and **41** (Figure 24) differed from the corresponding ones of sativanone in that of an extra oxygen and the lack of the two hydrogens which could be a consequence of a methylenedioxy substitution instead of a

methoxy group. The loss of H₂O and CO units could be observed on the MS/MS spectra at m/z 297.0753 (C₁₇H₁₃O₅) and 287.0909 (C₁₆H₁₅O₅). Proving that the substitution patterns of the A-ring of sativanone and the aglycone of these molecules are identical, the same ions at m/z 163.0388 and 135.0440 could be detected. Moreover, as an evidence of the methylenedioxy substituent, ions at m/z 257.0804 (C₁₅H₁₃O₄) [M+H-CO-CH₂O]⁺ and 229.0857 (C₁₄H₁₃O₃) [M+H-2CO-CH₂O]⁺ could be detected (Table 7). There is 14 Da difference between the mass of sativanone and onogenin, which is the result of different B-ring. This difference is only present between product ions at m/z 178.0623 (C₁₀H₁₀O₃) of onogenin and at m/z 164.0382 (C₁₀H₁₂O₂) of sativanone, certifying that these ions containing the B-ring of the molecules (Figure 49). Regarding these aspects, the structures were identified as the 7-*O*-glucoside (**22**), 4'' and 6''-*O*-glucoside malonates (**28** and **33**) and aglycone (**41**) of onogenin (Figure 48) and these results were corroborated by NMR experiments, too (see page 81).

5.I.5. Structural identification of pterocarpan

Peaks **32** and **39** (Figure 24) had a pseudo-molecular ion at m/z 433.1487 (C₂₂H₂₅O₉) and 519.1488 (C₂₅H₂₇O₁₂) and showed a common aglycone fragment at m/z 271.0959 (C₁₆H₁₅O₄) with **47**. Their MS/MS fragments could be detected at m/z 161.0595 (C₁₀H₉O₂), 137.0595 (C₈H₉O₂) and 123.0441 (C₇H₇O₂) (Table 7). These results were in concordance with the fragmentation pattern of the pterocarpan medicarpin 3-*O*-β-D-glucoside (**32**), medicarpin 3-*O*-β-D-glucoside 6''-malonate (**39**) and medicarpin aglycone (**47**) (Figure 34). The rather poor collision induced dissociation might be supported by the rigid structure as well. The ion at m/z 161.0595 is corresponding to the loss of a C₆H₆O₂ ([^{1,4}A]⁺) unit, which can be a consequence of the cleavage of the bonds 1 and 4, whereas the ions at m/z 123.0441 and 137.0595 are the products of the cleavage of bond 2 and 4, resulting [^{2,4}A]⁺ and [^{2,4}B]⁺, respectively (Figure 18). Peaks **27**, **38** and **42** (Figure 24) showed similar fragmentation pattern to those of medicarpin, however a 14 Da difference (+O-2H) could be observed in the case of the quasi-molecular ions and the fragment ions containing the B-ring, namely at m/z 175.0388 (C₁₀H₇O₃) [M+H-C₆H₆O₂]⁺ and 151.0388 (C₈H₇O₃) [^{2,4}B]⁺. Based on this fragmentation pattern and analogy with medicarpin, these ions could be tentatively identified as maackiain 3-*O*-β-D-glucoside (**27**), maackiain 3-*O*-β-D-glucoside 6''-malonate (**38**) and maackiain (**42**)

(Figure 34). As the two molecules differ only in the substitution of the B-ring, the fragment originating from the A-ring is the same at m/z 123.0442 [$^{2,4}A$] $^+$.

5.I.6. Structural identification of 2'-methoxy isoflavones

Peak **43** showed a m/z value for the aglycone, which was not mentioned in *Ononis* species before. The formula calculated from the HR-MS data was $C_{17}H_{14}O_5$ (Table 7), which could refer to known compounds afrormosin, cladrin or 2'-methoxy formononetin (Figure 50).

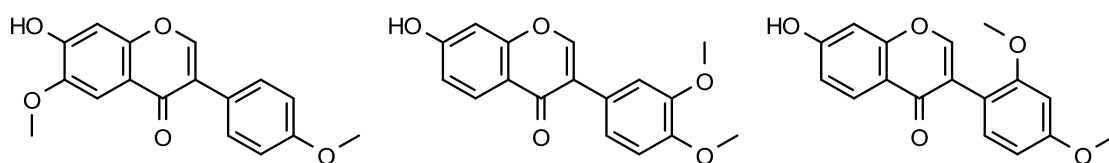


Figure 50: The structure of afrormosin (left), cladrin (middle) and 2'-methoxy formononetin

As a result of collision induced dissociation, ions at m/z 284.0658 ($C_{16}H_{12}O_5$), 267.0649 ($C_{16}H_{11}O_4$), 252.0412 ($C_{15}H_8O_4$) were detected, which could refer to structures $[M+H-CH_3]^+$, $[M+H-CH_3OH]^+$ and $[M+H-CH_3^{\bullet}-CH_3OH]^+$, respectively. These fragments clearly showed that the molecule contained two methoxy groups. The product ion at m/z 243.1014 ($C_{15}H_{15}O_3$) is a result of the ejection of two CO molecules, which is diagnostic for isoflavonoid molecules [184]. The cleavage of the bond between the C-ring and B-ring could provide ions at m/z 163.0387 ($C_9H_7O_3$) $[M+H-B-ring]^+$ and 137.0596 ($C_8H_9O_2$) $[B-ring+H]^+$. Regarding this fragmentation pattern, the A-ring can only bear a hydroxy group, and the two methoxy groups are localized on the B-ring. Further evidence for the position of the substituents is provided by the fragment at m/z 148.0517 ($C_9H_8O_2$), which was presumed to be the rDA product $[^{1,3}B-CH_3]^+$. This fragment corresponds to the $[^{1,3}B-CH_3^{\bullet}]^+$ ion in the MS/MS spectra of formononetin and the mass difference is caused by an extra methoxy substituent (see Figure 51). Since afrormosin has a methoxy and a hydroxy group on the A-ring and a single methoxy substituent on the B-ring, it could be excluded from the list of possible structures (Figure 50). Comparing the MS/MS spectra of cladrin [205, 206] and 2'-methoxy formononetin [200] with our data, the peaks at m/z 163.0, 148.1 and 137.1 could be observed in all cases indicating the double methoxy substitution of the B-ring, however, inspecting fragments in higher m/z regions, our

detected peaks were clearly in agreement with the ones of the 2'-methoxy formononetin. 2'-methoxy formononetin has been isolated from *Dalbergia parviflora* L. [201] and from *Eschscholtzia californica* L. (California poppy) [202], but not from *Ononis* species.

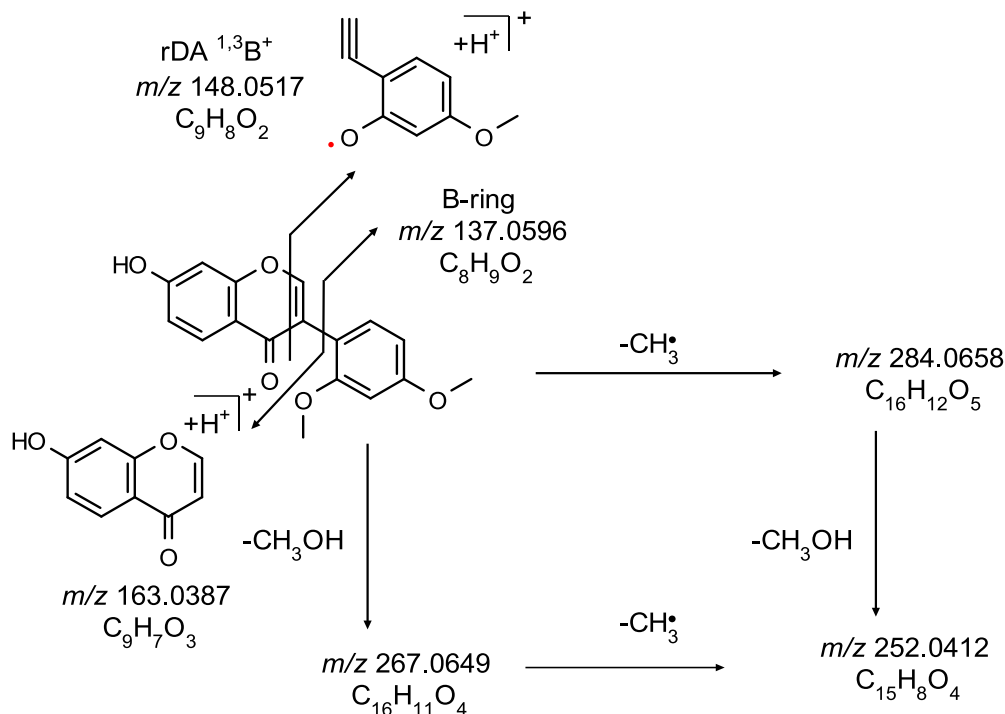


Figure 51: The proposed fragmentation pathway of 2'-methoxy formononetin

The protonated formula calculated based on the exact mass for peak **40** ($C_{17}H_{13}O_6$) (Table 7) suggests that this compound contains an extra oxygen atom and misses two hydrogen atoms compared to 2'-methoxy formononetin. The origin of this difference could be the methoxy – methylenedioxy substitutions of isoflavonoids, just like in the case of formononetin – pseudobaptigenin, sativanone – onogenin, medicarpin – maackiain pairs. The mass difference could be followed through the ions with smaller m/z ratio at 151.0388 ($C_8H_7O_3$) and 162.0310 ($C_9H_6O_3$), which are corresponding the ones of 2'-methoxy formononetin at m/z 137.0596 ($C_8H_9O_2$) and 148.0517 ($C_9H_8O_2$) and were assigned as $[^{1,3}B-CH_3^\bullet]^+$ and $[B\text{-ring}+H]^+$ (Figure 52). Consequently, it can be deduced, that the mass difference arose from the substitution pattern of the B-ring, meaning that beside a methoxy group, an additional methylenedioxy group is localized on it. As a proof of the mutual presence of OCH_3 and OCH_2O substituents, the loss of CH_3^\bullet , CH_3OH and CH_2O units and their combination could be observed on the MS/MS spectrum at m/z 298.0469 ($C_{16}H_{10}O_6$) $[M+H-CH_3^\bullet]^+$, 283.0598 ($C_{16}H_{11}O_5$) $[M+H-CH_2O]^+$, 281.0440 ($C_{16}H_9O_5$)

$[M+H-CH_3OH]^+$, 268.0362 ($C_{15}H_8O_5$) $[M+H-CH_3^*-CH_2O]^+$. Similarly to other isoflavones, the loss of CO units were also detectable at m/z 255.0647 ($C_{15}H_{11}O_4$) $[M+H-CH_2O-CO]^+$, 240.0413 ($C_{14}H_8O_4$) $[M+H-CH_3^*-CH_2O-CO]^+$, 212.0465 ($C_{13}H_8O_3$) $[M+H-CH_3^*-CH_2O-2CO]^+$ (Figure 50). In the literature, only cuneatin fulfills these structural criteria. Cuneatin was described in aerial parts of *Millettia oblata ssp. teitensis* [203], aerial parts of *Retama sphaerocarpa* [204], stem bark of *Dalbergia frutescens* [125], *Eysenhardtia polystachya* [205], aerial parts and roots of *Tephrosia maxima* [206] and most importantly, in *Cicer* species [207]. In his other work [21], Ingham had shown the chemotaxonomic similarity of genus *Ononis* and *Cicer*, and the presence of cuneatin in both genus corroborates this idea.

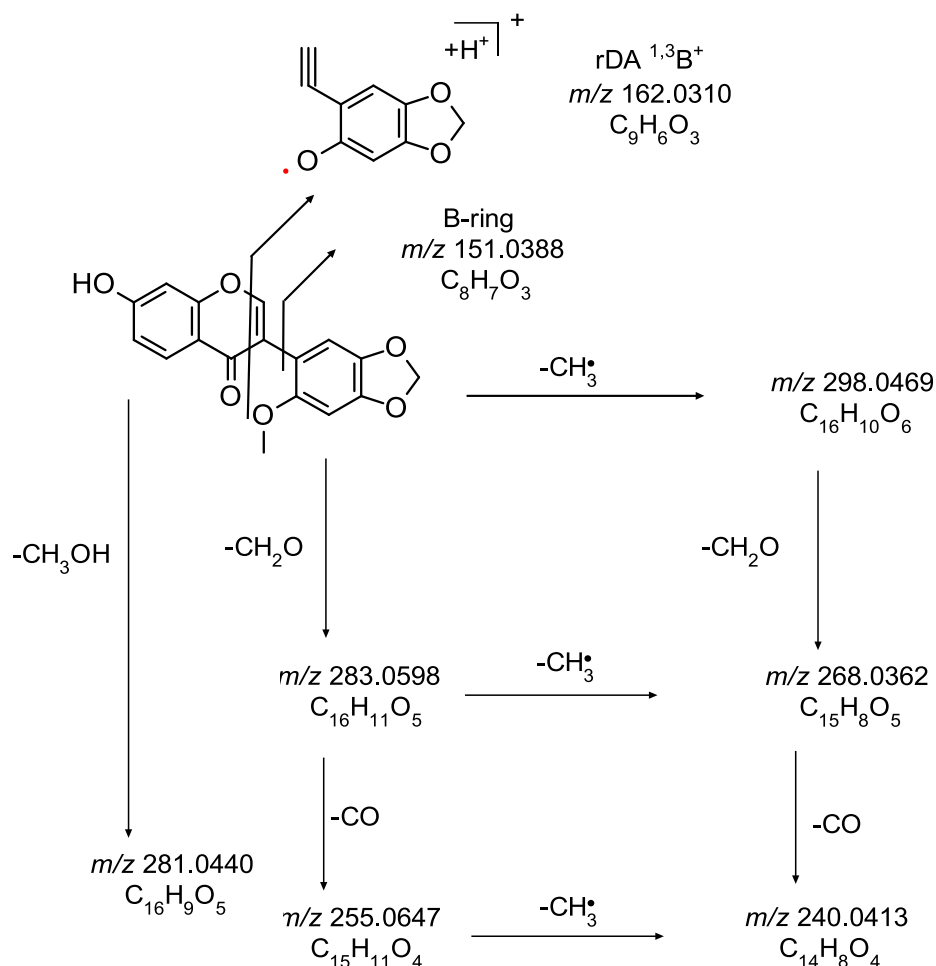


Figure 52: The proposed fragmentation pathway of cuneatin

Other confirmations of the presence of 2'-methoxy formononetin and cuneatin could be acquired from the biosynthesis of isoflavonoids. The final products of the isoflavonoid biosynthesis are medicarpin and maackiain (Figure 14). These phytoalexins with

pterocarpan skeleton possess a methoxy and a methylenedioxy group, respectively. Formononetin serves as the parent compound of medicarpin and through the calycosin-pseudobaptigenin route it could also be considered as the precursor of maackiain. Both formononetin and pseudobaptigenin undergo hydroxylation, converting to 2'-hydroxy formononetin and 2'-hydroxy pseudobaptigenin. These molecules were not detected in our sample, however their 2'-*O*-methylated derivatives, 2'-methoxy formononetin and cuneatin were confirmed. In the following step, the 2'-hydroxy isoflavones are reduced to the dihydro-derivatives: vestitone and sophorol [95]. Their 2'-*O*-methylated derivatives, sativanone and onogenin are representative compound in *Ononis* species, as well as pterocarpan medicarpin and maackiain [61].

5.I.7. Structural identification of nitrogen-containing derivatives

Mass spectrometry

The investigation of the analytical samples by LC-MS revealed characteristic nitrogen-containing compounds (**3**, **5**, **8**, **9**, **10**, **15** and **12**, **13**, **14**, **17**, **20**, **23**) in the total ion chromatogram recorded in positive ionization mode (Figure 24). The even m/z ratio of these peaks indicates the presence of an odd number of nitrogen atoms in the structures. Comparing the total ion chromatogram (TIC) with the UV chromatogram, remarkable intensity differences were observed in the case of the corresponding peaks (see Figure 22 Figure 23). While the peaks of the nitrogen-containing molecules were predominant in the TIC (due to the efficient ionization), the peaks of these compounds could hardly be detected in the UV chromatogram. Compounds **20** and **23** showed however significant splitting on the achiral C18 stationary phase, suggesting diastereomeric compounds. The MS/MS data and the accurate mass measurements (Figure 24) confirmed that the molecules of interest are isoflavonoid derivatives. As isoflavonoids possess high molar absorptivity, the UV chromatogram suggested that these compounds are in minute amount in the extract. All six isoflavonoid skeletons (formononetin, pseudobaptigenin, sativanone, onogenin, medicarpin and maackiain) were present in the form of glucosides bearing a nitrogen-containing moiety. Besides the aglycone and its corresponding fragments, each MS/MS spectrum showed characteristic ions at 288.1452, 144.1025 and 84.0810 or 274.1282, 130.0862 and 70.0652 m/z values, suggesting that all the six compounds share a common structural motif linked to the isoflavonoid glucosides. The

collision induced dissociation cleaves the molecules alongside the glycosidic bond, resulting in the intact aglycone as Y_0^+ and the cleaved fragment composed of the glucose and the nitrogen-containing moiety at m/z 288.1452 ($C_{13}H_{22}NO_6$) or 274.1282 ($C_{12}H_{20}NO_6$). Fragmentation of the isoflavonoid glucoside moiety with a neutral loss results the structure at m/z 144.1025 or 130.0862 and the protonated formula of $C_7H_{13}NO_2$ or $C_6H_{11}NO_2$ which were hypothesized to be the beta amino acid homopipercolic acid (piperidine 2-acetate) and homoproline (pyrrolidine 2-acetate). The cleavage of the heterocyclic ring solely could provide the ion at m/z 84.0814 ($C_5H_{10}N$) or at m/z 70.0650 (C_4H_8N) (Figure 53).

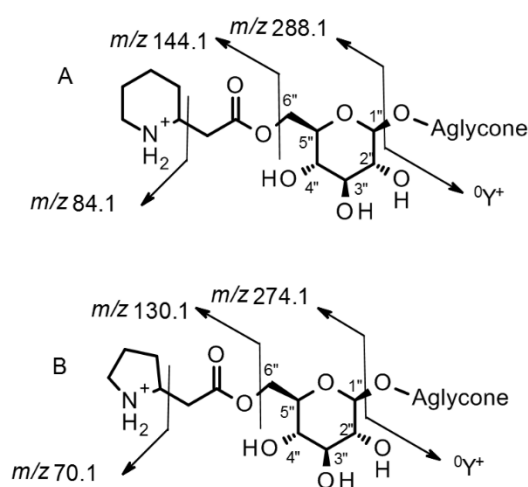


Figure 53: The proposed fragmentation pathway of homopipercolic acid (A) and homoproline (B) isoflavonoid glucoside esters

As these beta amino acid moieties have never been described in higher plants, samples of different origin and vegetational period were subjected for analytical screening to detect the same compounds. These experiments successfully proved the presence of the isoflavonoid glucoside beta amino acid esters, therefore the possibility of sample contamination could be excluded. In order to exclude any further hypothetical structures and to unambiguously identify the new structures, the homopipercolic esters in relatively higher quantities were isolated and NMR experiments were applied (see section 5.I.7.)

NMR studies

The complete structure identification of medicarpin 7-O-glucoside 6''-O-piperidin-2-acetate (**23**) is described herein as an example. In the case of this compound, the MS/MS data suggested the presence of medicarpin aglycone (Table 7). The six aromatic protons at 7.39/7.38 (d $J = 8.7$ 1H), 7.25/7.24 (d $J = 8.2$ Hz 1H), 6.70 (dd $J = 8.7, 2.3$ Hz 1H), 6.54/6.53 (d $J = 2.3$ Hz), 6.45/6.44 (d $J = 8.2$ Hz 1H) and 6.43/6.42 (s 1H) ppm and the characteristic spin system (-O-CH₂-CH-CH) at 4.28 (m 1H), 3.65 (m 2 H) ppm along with the methyl singlet of the -OCH₃ group at 3.69 ppm present in the ¹H NMR spectrum of **23** corroborated by HMBC correlations and literature data [191] confirmed the medicarpin aglycone. The presence of a glucose moiety was also verified by NMR, key HMBC correlations confirmed the glycosidic linkage between the anomeric OH of the glucose and the C3-OH of medicarpin. The careful inspection of the ¹H NMR experiment showed the presence of eleven ¹H resonances in the aliphatic region (δ_{H} 2.83 (m 1H), 2.73 (m 1H), 2.42 (m 1H), 2.28 (m 2H), 1.53/1.49 (m 1H), 1.61/1.58 (m 1H), 1.42 (m 1H), 1.22 (m 1H), 1.20 (m 1H), 0.99/0.94 (m 1H)). The COSY, TOCSY and especially the HMBC spectra with $J = 12$ Hz heteronuclear coupling constant helped to construct the missing building block forming a piperidine ring substituted at C2'''. In the HMBC experiment two crucial correlations were observed for a carbonyl resonance at 171.40/171.36 ppm: intense crosspeaks were detected between the C=O and protons (2.28 ppm) of the side chain and similarly between the C=O and the H6'' (4.06/4.03 ppm) resonance of the glucose moiety (Figure 36). These correlations clearly indicate that the piperidine 2-acetic acid linked to the glucose moiety with an ester bond at the C6'' position. The complete NMR characterization of compound **23** can be found in the Table 14. As the cyclic beta amino acid residue introduces a new stereogenic center, some of the NMR resonances show diastereomeric splitting. The MS/MS fragmentation can also be corroborated by the piperidine 2-acetate moiety. In the case of compound **20**, the NMR data revealed a methylenedioxy group and the lack of the methoxy function in the aglycone skeleton compared to **23**. All ¹H and ¹³C NMR resonances were in agreement with the maackiain aglycone as proposed by the MS experiments (Table 7) thus; compound **20** was identified as maackiain 3-O- β -D-glucoside 6''-O-piperidine 2-acetate. The NMR resonances of the glucose and the piperidine 2-acetate moieties were found to be almost identical for all compounds (**12**, **13**, **14**, **17**, **20**, **23**) confirming the same

structural motif but various aglycones (Table 12 Table 13 Table 14). For compound **13** two sets of aromatic protons and a singlet at 8.44/8.43 ppm indicated isoflavonoid aglycone skeletons. The HMBC spectrum indicated a key correlation between an *O*-methyl resonance (3.79 ppm) and C4' (159.06 ppm) therefore the aglycone was identified as formononetin (Table 12). Compound **12** showed HMBC correlation between the methylenedioxy group (6.05 ppm) and C3' (152.26 ppm) and C4' (147.09 ppm) confirming the isoflavonoid skeleton pseudobaptigenin (Table 12). The NMR characteristics of compound **17** and **14** were similar to **13** and **12** with a subtle difference of an additional methoxy group at C2' and the lack of an aromatic singlet (Table 1). The aglycones of **13** and **12** were identified as sativanone and onogenin, respectively.

Indirect structural analysis

Although, these nitrogen-containing esters ionize extremely well in positive ionization mode, their actual quantity compared to other isoflavonoid derivatives is quite low. The homoproline derivatives are orders of magnitude lower compared to the homopipericolic esters therefore their isolation for NMR experiments was not feasible. In order to verify that the compounds **3**, **5**, **8**, **9**, **10** and **15** are homoproline derivatives, the sample was subjected to hydrolysis to free beta amino acids. This hydrolyzed sample was then spiked with the a standard solution of homopipericolic acid and homoproline in aqueous medium, as they tend to form esters with methanol [208]. The original and the spiked samples were investigated by HPLC-MS/MS. As no differences were observed in retention time and in fragmentation pattern (Figure 39), it could be concluded that the samples factually contain the esters of homopipericolic acid and homoproline.

Stereochemistry

Regarding the aglycones, the two isoflavones, formononetin and pseudobaptigenin contain no chiral atoms. However, the two dihydroisoflavonoids onogenin and sativanone are chiral compounds. Based on the information that the isolated aglycones have no detectable CD spectrum we assumed that our sample contains the derivatives of (*3R,S*)-onogenin and sativanone, in concordance with literature [190]. Pterocarpans contain two chiral centers, however, from the four possible isomers only two, with *cis*-fused benzofuranyl-benzopyran rings can be found in nature [209]. To determine the absolute configuration of the pterocarpans optical rotatory dispersion and circular dichroism were used (see section 1005.I.5.), which proved that they can be found in the form of the

levorotatory enantiomer. Even in the screening chromatographic runs the peaks of medicarpin and maackiain 7-*O*-glucoside 6''-*O*-piperidin-2-acetate (**20** and **23**) showed significant peak splitting on achiral stationary phase. This effect could be observed on all derivatives in the preparative LC chromatogram and was further investigated on various analytical stationary phases (C18, C8, C18 core shell and phenyl-hexyl). The complete separation of the two diastereomers of formononetin, pseudobaptigenin, medicarpin and maackiain derivatives could be achieved on all four columns. However, the four isomers of the racemic onogenin and sativanone could not be baseline separated. Beside the two baseline resolved peaks (originating hypothetically from the diastereomeric splitting due to the racemic nature of the amino acid), a third peak (as a shoulder) can be observed using the core shell C18 column. To investigate the stability of the isomers, the peaks of compound **20** were isolated separately. The isolated compounds were then reinjected after 1, 5 and 10 days. The transformation of the isomers into each other resulting in peak duplication could not be observed (Figure 38). As the NMR signals of all six compounds showed signal duplication, but the stereochemistry of the aglycones are so different, we hypothesized that the source of the phenomenon originated from the common structural motifs. The ¹H NMR spectra of the isolated diastereomers of compound **23** were recorded and it clearly indicates that the duplication of the NMR signals arose from the overlap of the ¹H resonances of the two diastereomers (Figure 37). Examining the chemical shifts and coupling constants of the sugar moiety, the presence of β-D-glucopyranose could be proved in all six molecules. Consequently, the hypothesized source of the diastereomerism is the stereogenic center of the beta amino acid.

5.II. Quantitative phytochemical results

5.II.1. Sample preparation

Because isoflavonoids can be found in *Ononis* species as a very heterogeneous mixture – glucosides, glucoside malonates, beta amino acid derivatives and aglycones – the quantification of all compounds in their native form could not be executed. Moreover, glucoside malonates are very labile derivatives and tend to hydrolyze to glucosides. In order to decrease the complexity of the sample, the hydrolysis of all glucosides to aglycones was aimed. In other sources, acidic hydrolyses with hydrochloric acid was carried out [9], [10], [171], so that we aimed the optimization of a similar method

finetuning the acid concentration and hydrolysis time. Because the acidic hydrolysis digested not only the glycosidic bonds, but the pterocarpan skeletons as well, it was no further used. Based on the work of Boldizsár *et al.* [210], the endogenous glucosidase enzymes of the root was activated with pure distilled water in the dried samples. After 24 hours of enzymatic fermentation, the amount of glucosides and glucoside malonates decreased quantitatively (Figure 42). The samples were extracted after enzymatic hydrolysis using 70% aqueous methanol, three times. In order to correct any possible imperfections and loss during sample extraction, filtration and dilution, naringenin was added at the start of the sample treatment and all results were standardized to the peak of it.

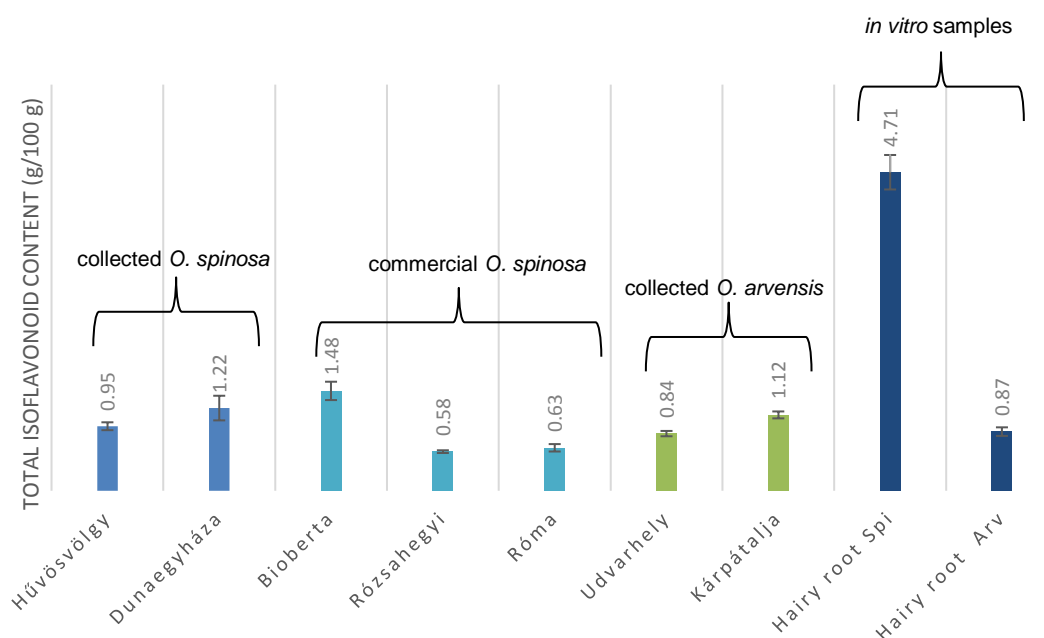


Figure 54: Total isoflavonoid content of *O. spinosa* and *O. arvensis* samples

5.II.2. Quantitative results

Regarding the sum of different isoflavonoid aglycones, the overall content ranged from 0.6 to 4.7 g/100 g with a mean of 0.97 g/100 g (Figure 54) in the free-range samples. Comparing the free-range samples, no significant difference could be observed between the two species ($p_{0.05} = 0.905$). On the other hand, *O. spinosa* hairy root sample showed a significantly higher total isoflavonoid content, than the other samples (one-way ANOVA, Bonferroni *post-hoc* test). Interestingly, the *O. arvensis* hairy root cultures were not so outstandingly rich in isoflavonoids. As the free-range samples had no significant

difference in their total isoflavonoid content, the origin of this phenomenon could not be originated from the genetical variance between the species. One of the possible explanations, is that the Ri plasmid randomly builds into the genetical matter of the plants and in *O. spinosa* it induces the isoflavonoid biosynthesis directly. The other possibility is that the cultures of *O. spinosa* and *O. arvensis* are not equally adapted to the *in vitro* circumstances. The culture of *O. arvensis* is weaker, grows slower and demands higher saccharose concentration in the culture medium (see page 59). The suboptimal circumstances could result in lower isoflavonoid production.

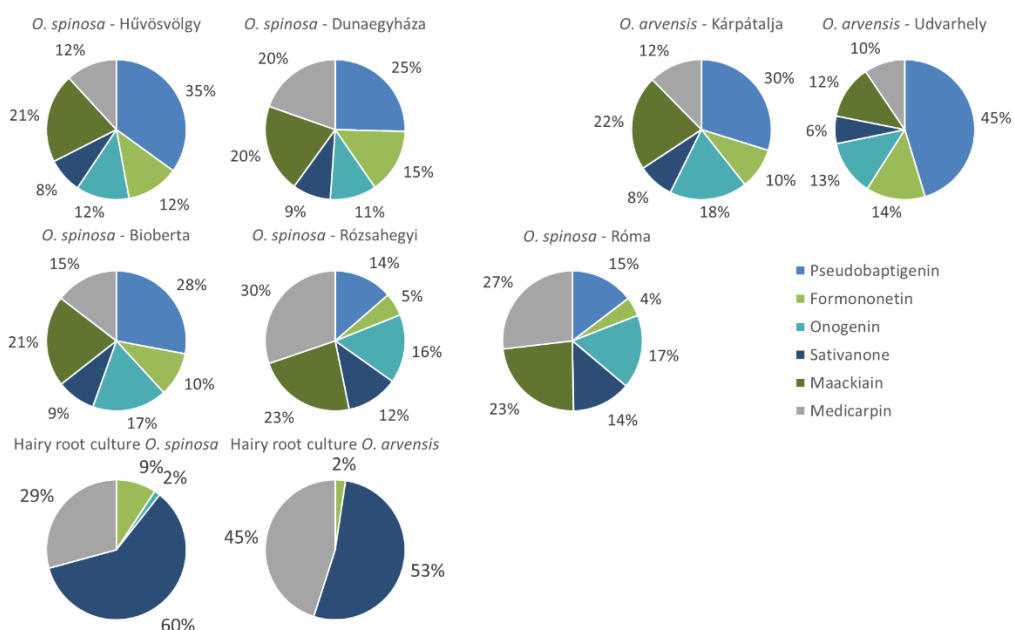


Figure 55: Relative amount of isoflavonoid aglycones in *O. spinosa* and *O. arvensis* samples

Figure 55 shows the relative amount of the different type of aglycones. Whereas earlier formononetin and its derivatives were thought to be the most characteristic compounds of *Ononis* species, it resulted to be only in lower relative quantities in free-range samples. Pseudobaptigenin was present in much higher levels. On the other hand, the detector sensitivity was much lower for pseudobaptigenin, which could mislead the estimation of the quantitative relations of formononetin and pseudobaptigenin. The isoflavanones and pterocarpanes could be found in the free-range samples in a commensurable ratio. Comparing the two species no drastic difference can be observed between the species or places of origin between free-range samples. However, between the free-range samples and *in vitro* cultures, there is an extreme change in the relative isoflavonoid content. The

hairy root cultures produce mainly formononetin, sativanone and medicarpin and the other three derivatives – pseudobaptigenin, onogenin and maackiain – are present only in trace quantities. The common feature of the synthesized molecules in the hairy root cultures that they are all methoxylated, while the missing compounds possess a methylenedioxy ring. Regarding the biosynthesis of the later molecules (see Figure 14), it can be hypothesized, that the function of I3'H or the CYP P450 enzyme closing the methylenedioxy ring is damaged. However, the function of these enzymes is not completely missing, as the molecules of interest can be found, but only in trace quantities.

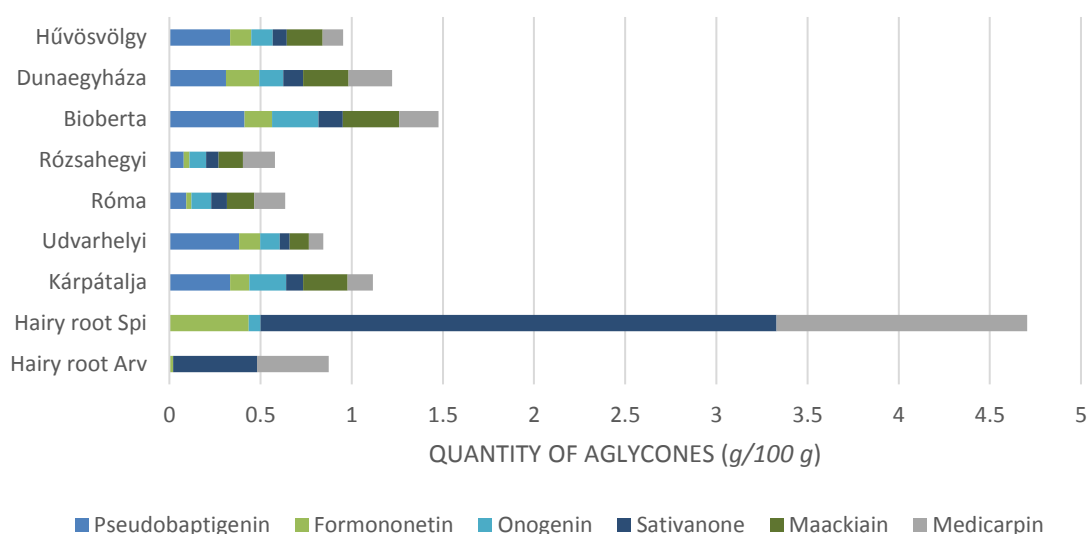


Figure 56: Absolute quantity of isoflavonoid aglycones in *O. spinosa* and *O. arvensis* cultures

One reason of the change in isoflavonoid profile can be genetic transformation which can upregulate the production of methoxylated derivative and suppress the synthesis of the ones with methylenedioxy ring. Another cause can lay in the *in vitro* circumstances. Isoflavonoids are phytoalexins which protects the plant from abiotic and biotic stress. As these stressors (for example UV radiation, heat and drought) do not threat the cultures, they might change their isoflavonoid profile. Moreover, isoflavonoids can be signaling molecules between symbiont *Rhizobium* species [211], and in the lack of these bacteria the plant modifies its set of isoflavonoids.

Investigating the absolute quantity of the aglycones (Figure 56), it can be concluded that the collected samples of *O. spinosa* (from Hűvösvölgy and Dunaegyháza) and the commercial sample (from Bioberta Ltd.) show very similar isoflavonoid content.

Furthermore, the commercial samples from Rózsahegyi Ltd. and from Rome possessed comparable isoflavonoid pattern. The average formononetin content in the free-range samples is 0.10 g/100 g, which shows very good correlation with other values in the literature (Table 6). The *O. spinosa* hairy root contains sativanone and medicarpin in huge quantities compared to the other samples, which makes this *in vitro* culture a promising source of biologically valuable isoflavonoids. Plotting the samples after Principal Component Analysis (Figure 57), the same similarities can be observed. The commercial samples of *O. spinosa* from Rózsahegyi Ltd. and from Rome seem to form a group, but the other free-range *O. spinosa* and *O. arvensis* samples are not distinguishable. Although the two hairy root samples were similar regarding the lack of isoflavonoids with methylenedioxy ring, the huge difference in the absolute quantities of isoflavonoids causes a large distance between the two spots. Because of the low number of the samples, these results are not significant.

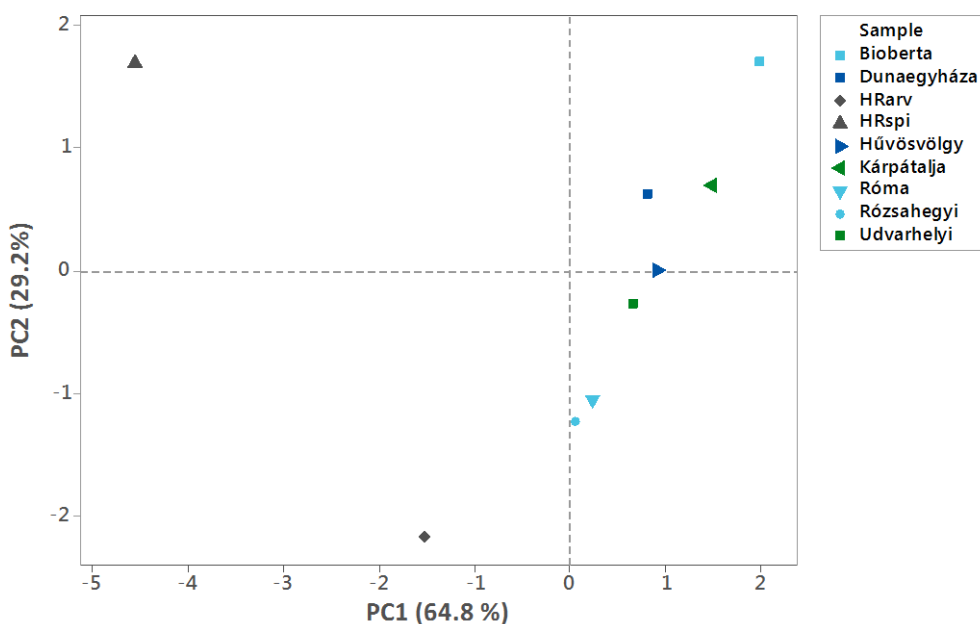


Figure 57: The results of the Principal Component Analysis

6. Conclusions

During the qualitative phytochemical analysis of the root extract made from *O. spinosa* and *arvensis* 47 compounds were identified. These are mostly the glucosides, glucoside malonates and aglycones of isoflavonoids, but some special phenolic lactones – puerol A and clitorienolactone B – and a maltol derivative were described, too. The presence of calycosin, sativanone, onogenin and their derivatives were firstly proved in *O. spinosa*, while in *O. arvensis* pseudobaptigenin, calycosin and sativanone had not been mentioned before. The calycosin content could be established by the biosynthetic pathway of isoflavonoids, as calycosin serves as an intermediate between formononetin and pseudobaptigenin. The presence of 2'-methoxy isoflavones and isoflavanones is justifiable by the biosynthesis, too. Genistein, biochanin A and daidzein had been previously reported in *O. spinosa* root, however, we could not confirm these results. Furthermore, the biosynthetic origin of formononetin is liquiritigenin, while genistein and biochanin A are synthesized from naringenin.

As new isoflavonoid derivatives, beta amino acid esters were characterized for the first time, as well. Homopiperic acid was described before in *Lycopodium* species as an intermediate of the synthesis of *Lycopodium* alkaloids [216, 217], while homoproline was isolated from *Asteraceae* species, as a precursor of pyrrolizidines [208], but their co-occurrence has never been reported in plants and their biosynthetic origin is not known. Their function might be a nitrogen reservoir, or they can protect the plants from insects as toxic amino acid analogues.

The total isoflavonoid content of soy products based on the USDA database is approximately 0.1 - 0.2 g/100 g [214] and the total content of *Trifolium* species varies between 0.6 mg - 1.7 g/100 g [215]. Since free-range and commercially available *Ononis* samples contain an average of 0.97 g/100 g isoflavonoids, their total isoflavonoid content could be considered very high. On the other hand, the isoflavonoid profile of soy and *Ononis* species is very distinct, so deductions about the phytoestrogenic effect of the plants are hard to make. Beside isoflavones, *Ononis* species proved to contain a remarkable amount of isoflavanones and pterocarpanes, which possess convincing biological and pharmacological effects. Moreover, the hairy root cultures of *O. spinosa* could be promising tool to produce methoxylated isoflavones, isoflavanones and pterocarpanes.

7. Summary

The root of *O. spinosa* and *O. arvensis* have been used in ethnomedicine since hundreds of years and the root of *O. spinosa* is official in the European and Hungarian Pharmacopoeia, too. The main use of the herbal remedy is to treat infections and inflammations of the urinary tract and the diuretic effect of *Ononidis radix* is proved *in vivo*, but the responsible phytochemical constituents are poorly defined.

Based on the literature concerning the phytochemical content of *O. spinosa* and *O. arvensis* it can be concluded that they are not characterized in detail. The available literature about other *Ononis* species focused mainly on other phytochemical groups such as essential oil or aromatic alkyl derivatives. Beside the proved diuretic effect, *O. spinosa* extract possesses anti-inflammatory, wound-healing and analgesic effects, based on *in vivo* tests, but the majority of pharmacological information about other *Ononis* species is limited to *in vitro* tests.

During our experimental work, we identified 47 compounds of both *O. spinosa* and *O. arvensis* root extracts, the derivatives of 8 isoflavonoid aglycones, 2 special phenolic lactones and a maltol derivative. In addition, we firstly characterized homopipercolic acid and homoproline esters as special forms of isoflavonoid glucosides. Based on the endogenous glucosidase enzymes of the plant the simplification of the heterogenous glycosidic derivatives was managed. Using the developed and validated quantitative method, the amount of 6 isoflavonoids was determined in the form of aglycones in collected, commercial and *in vitro* cultured samples of *O. spinosa* and *O. arvensis*. Our results confirmed, that these herbal drugs contain significant amount of biologically active isoflavonoid components and *in vitro* cultures can serve as a rich source for their isolation.

8. Összefoglalás

A népgyógyászatban évszázadok óta alkalmazzák a tövises és mezei iglice gyökerét, és a tövises iglice a jelenleg érvényben lévő Európai és Magyar Gyógyszerkönyvekben is hivatalos *Ononidis radix* néven. Az iglicegyökér elsősorban húgyúti fertőzések és gyulladások kezelésében nyer felhasználást, és vizelethajtó hatását állatkísérletekben is igazolták, azonban a hatásért felelős vegyületek nem ismertek. Mivel az *Ononis* fajok legjellemzőbb vegyületei az izoflavonoid származékok, ezért munkánk elsődleges céljaként segítséget szerettünk volna nyújtani a hazai *Ononis* fajok megalapozott fitoterápiás alkalmazásához izoflavonoid profiljuk minőségi és mennyiségi ismeretében. Az *O. spinosa* és *O. arvensis* tartalmi anyagaival foglalkozó irodalmi források igen töredékesnek bizonyultak, és más *Ononis* fajok esetében is sokszor eltérő fitokémiai csoportokra (pl. illóolaj, aromás alkil származékok) helyeződött a hangsúly. A biológiai vizsgálatok során a vizelethajtó hatás mellett sikerült a tövises iglice gyökér gyulladáscsökkentő, fájdalomcsillapító és sebgyógyulást elősegítő hatásait is igazolni állatkísérletekben, azonban a többi *Ononis* fajjal főleg csak *in vitro* vizsgálatokat végeztek.

Kísérletes munkánk során 47 vegyületet azonosítottunk a tövises és mezei iglice gyökeréből készült kivonatban, amelyek 8 izoflavonoid aglikon és 2 speciális lakton származékai, illetve egy maltol származék jelenlétét is igazoltuk. Továbbá elsőként írtuk le a növényekben homopipekolinsav és homoprolin jelenlétét, izoflavonoid glükozid észter formában. A növény saját glükozidáz enzimaktivitását kihasználva a mintaelőkészítés során megvalósítottuk a növényben található változatos glükozid-származékok hidrolízisét aglikonokká. Az általunk fejlesztett validált kvantitatív módszer segítségével 6 izoflavonoid mennyiségét tudtuk jellemezni aglikonok formájában, a szabadban gyűjtött, kereskedelmi és *in vitro* kultúrákban. Eredményeink alapján az iglicegyökér jelentős mennyiséget tartalmaz biológiailag igen értékes izoflavonoidokból, és az *in vitro* kultúrák ígéretes forrást nyújtanak ezen vegyületek kinyeréséhez, akár léptéknövelést is alkalmazva.

9. Bibliography

- [1] Turini FG, Brauchler C, Heubl G, Bräuchler C, and Heubl G. (2010) Phylogenetic relationships and evolution of morphological characters in *Ononis* L. (Fabaceae). *Taxon*, 59: 1077–1090.
- [2] Vogel A. Plant Encyclopaedia: *Ononis spinosa* L. (Spiny Restharrow). https://www.avogel.com/plant-encyclopaedia/ononis_spinosa.php
- [3] NatureGate. Restharrow, *Ononis arvensis*. <http://www.luontoportti.com/suomi/en/kukkakasvit/restharrow>
- [4] Háznagy A, Tóth G, and Tamás J. (1978) Über die Inhaltstoffe des wäßrigen Extraktes von *Ononis spinosa* L. *Arch Pharm (Weinheim)*, 311: 318–323.
- [5] Pietta P, Calatroni A, and Zio C. (1983) High-performance liquid chromatographic analysis of flavonoids from *Ononis spinosa* L. *J Chromatogr A*, 280: 172–175.
- [6] Köster J, Strack D, and Barz W. (1983) High Performance Liquid Chromatographic Separation of Isoflavones and Structural Elucidation of Isoflavone 7-O-glucoside 6''-malonates from *Cicer arietinum*. *Planta Med*, 48: 131–5.
- [7] Blaschek W, Hansel R, Keller K, Reichling J, Rimpler H, and Schneider GE. Hagers Handbuch der Pharmazeutischen Praxis: Drogen L-Z. In: (Eds), Springer, 1997: 263–270.
- [8] Klejdus B, Vacek J, Benešová L, Kopecký J, Lapčík O, and Kubáň V. (2007) Rapid-resolution HPLC with spectrometric detection for the determination and identification of isoflavones in soy preparations and plant extracts. *Anal Bioanal Chem*, 389: 2277–2285.
- [9] Benedec D, Vlase L, Oniga I, Toiu A, Tămaş M, and Tiperciuc B. (2012) Isoflavonoids from *Glycyrrhiza* sp. and *Ononis spinosa*. *Farmacia*, 60: 615–620.
- [10] Klejdus B, Vacek J, Lojková L, Benešová L, and Kubáň V. (2008) Ultrahigh-pressure liquid chromatography of isoflavones and phenolic acids on different stationary phases. *J Chromatogr A*, 1195: 52–59.
- [11] Addotey JN, Lengers I, Jose J, Gampe N, Béni S, Petereit F, and Hensel A. (2018) Isoflavonoids with inhibiting effects on human hyaluronidase-1 and norneolignan clitorienolactone B from *Ononis spinosa* L. root extract. *Fitoterapia*, 130: 169–174.
- [12] Kirmizigül S, Gören N, Yang SW, Cordell GA, and Bozok-Johansson C. (1997)

- Spinonin, a novel glycoside from *Ononis spinosa* subsp. *leiosperma*. *J Nat Prod*, 60: 378–381.
- [13] Rowan MG and Dean PDG. (1972) α -Onocerin and sterol content of twelve species of *Ononis*. *Phytochemistry*, 11: 3263–3265.
- [14] Daruházi ÁE, Szarka S, Héthelyi É, Simándi B, Gyurján I, László M, Szőke É, and Lemberkovics É. (2008) GC-MS Identification and GC-FID Quantitation of Terpenoids in *Ononidis spinosae Radix*. *Chromatographia*, 68: 71–76.
- [15] Shaker K and Dockendorff K. (2004) A new triterpenoid saponin from *Ononis spinosa* and two new flavonoid glycosides from *Ononis vaginalis*. *Zeitschrift fur Naturforsch*, 59b: 124–128.
- [16] Hořojší V and Kocourek J. (1978) Studies of lectins XXXVI. Properties of some lectins prepared by affinity chromatography on O-glycosyl polyacrylamide gels. *Biochim Biophys Acta - Gen Subj*, 538: 299–315.
- [17] Hilp K, Kating H, and Schaden G. (1975) Inhaltsstoffe aus *Ononis spinosa* L., 1. Mitt. Das ätherische Öl der *Radix Ononidis*. *Arch Pharm (Weinheim)*, 308: 429–433.
- [18] Kovalev VN, Borisov MI, and Spiridonov VN. (1976) Phenolic compounds of *Ononis arvensis*. I. *Chem Nat Compd*, 10: 820–821.
- [19] Kovalev VN, Borisov MI, and Spiridonov VN. (1976) Phenolic compounds of *Ononis arvensis*. I. *Chem Nat Compd*, 10: 367–369.
- [20] Kovalev VN, Spiridonov VN, Borisov MI, Kovalev IP, Gordienko VG, and Kolesnikov DD. (1975) Phenolic compounds of *Ononis arvensis*, The structure of onogenin. *Chem Nat Compd*, 11: 367–369.
- [21] Ingham JJJ. (1982) Phytoalexin production by *Ononis* species. *Biochem Syst Ecol*, 10: 233–237.
- [22] Spilková J, Bednář P, and Štroblíková R. (2001) Capillary electrophoretic analysis of hydroxycinnamic acids from *Ononis arvensis* L. *Pharmazie*, 56: 424–425.
- [23] Denes T, Papp N, Marton K, Kaszas A, Felinger A, Varga E, and Boros B. (2015) Polyphenol Content of *Ononis arvensis* L. and *Rhinanthus serotinus* (Schönh. ex Halácsy & Heinr. Braun) Oborny Used in the Transylvanian Ethnomedicine. *Int J Pharmacogn Phytochem*, 30: 2051–7858.
- [24] Sichinava MB, Mcholidze KZ, Churadze M V., Alaniia MD, and Aneli DN. (2014)

- Chemical composition and microstructural peculiarities of overground and underground vegetative organs of field restharrow (*Ononis arvensis* L.). *Georgian Med News*, 88–94.
- [25] Hořojší V, Chaloupecká O, and Kocourek J. (1978) Studies on lectins XLIII. Isolation and characterization of the lectin from restharrow boots (*Ononis hircina* Jacq.). *Biochim Biophys Acta - Gen Subj*, 539: 287–293.
- [26] Ghribi L, Waffo-Téguo P, Cluzet S, Marchal A, Marques J, Mérillon J-MM, and Ben Jannet H. (2015) Isolation and structure elucidation of bioactive compounds from the roots of the Tunisian *Ononis angustissima* L. *Bioorg Med Chem Lett*, 25: 3825–3830.
- [27] Barrero AF, Sanchez JF, Barrón A, Corrales F, and Rodriguez I. (1989) Resorcinol derivatives and other components of *Ononis speciosa*. *Phytochemistry*, 28: 161–164.
- [28] San Feliciano A, Barrero AF, Medarde M, Miguel del Corral JM, and Calle M V. (1983) An isocoumarin and other phenolic components of *Ononis natrix*. *Phytochemistry*, 22: 2031–2033.
- [29] Yerlikaya S, Zengin G, Mollica A, Baloglu MC, Altunoglu YC, and Aktumsek A. (2017) A multidirectional perspective for novel functional products: In vitro pharmacological activities and in silico studies on *Ononis natrix* subsp. *hispanica*. *Front Pharmacol*, 8: 600.
- [30] Barrero AF, Cabrera E, Garcia IR, Rodriguez Garcia I, and Garcia IR. (1998) Pterocarpan from *Ononis viscosa* subsp. *breviflora*. *Phytochemistry*, 48: 187–190.
- [31] Abdel-Kader MS. (2001) Phenolic constituents of *Ononis vaginalis* roots. *Planta Med*, 67: 388–390.
- [32] Abdel-Kader MS. (2010) Preliminary pharmacological study of the pterocarpan macckian and trifolirhizin isolated from the roots of *Ononis vaginalis*. *Pak J Pharm Sci*, 23: 182–187.
- [33] Abdel-Kader MS. (2004) Two isoflavonoid glucoside derivatives from *Ononis serrata* growing in Egypt. *Nat Prod Sci*, 10: 321–324.
- [34] Khouni L, Long C, Haba H, Molinier N, and Benkhaled M. (2014) Anthranilic Acid Derivatives and Other Components from *Ononis pusilla*. *Nat Prod Commun*, 9: 1159–1162.

- [35] Benabderahmane W, Mezrag A, Bouheroum M, Benayache F, and Mosset P. (2014) The chemical investigation of the chloroformic extract of *Ononis angustissima* Lam. Var. species. *Der Pharm Lett*, 6: 88–91.
- [36] Mezrag A, Malafronte N, Bouheroum M, Travaglino C, Russo D, Milella L, Severino L, De Tommasi N, Braca A, and Dal Piaz F. (2017) Phytochemical and antioxidant activity studies on *Ononis angustissima* L. aerial parts: isolation of two new flavonoids. *Nat Prod Res*, 31: 507–514.
- [37] Barrero AF, Herrador MM, Arteaga P, Rodriguez-Garcia I, and Garcia-Moreno M. (1997) Resorcinol derivatives and flavonoids of *Ononis natrix* subspecies *ramosissima*. *J Nat Prod*, 60: 65–68.
- [38] Barrero AF, Sanchez JF, Barrón A, and Rodriguez I. (1989) Specionin and speciosides a and b: New aromatic lactones from *ononis speciosa*. *J Nat Prod*, 52: 1334–1337.
- [39] Youcef M, Chalard P, Figuéredo G, Marchioni E, Benayache F, and Benayache S. (2014) Chemical composition of the essential oil of *Ononis angustissima* (Lam.) Batt. et Trab. *Res J Pharm Biol Chem Sci*, 5: 1307–1310.
- [40] Ghribi L, Nejma A Ben, Besbes M, Harzalla-Skhiri F, Flamini G, and Jannet H Ben. (2016) Chemical Composition, Cytotoxic and Antibacterial Activities of the Essential Oil from the Tunisian *Ononis angustissima* L. (Fabaceae). *J Oleo Sci*, 65: 339–345.
- [41] Elamrani A and Benaissa M. (2010) Chemical composition and antibacterial activity of the essential oil of *ononis natrix* from Morocco. *J Essent Oil-Bearing Plants*, 13: 477–488.
- [42] Erdemgil FZ, Kurkcuoglu M, and Baser KHC. (2002) Composition of the essential oil of *Ononis viscosa* subsp. *breviflora*. *Chem Nat Compd*, 38: 565–567.
- [43] Barrero AF, Sánchez JF, Rodríguez I, and Maqueda M. (1993) Use of alkenylresorcinols from *Ononis Speciosa* as synthetic precursors of compounds with potential biological activity. *J Nat Prod*, 56: 1737–1746.
- [44] Hussain MT, Saeed A, Rama NH, Raza AR, and Bird CW. (2001) Mass Spectrometric Studies of the Principal Dihydroisocoumarins of *Ononis natrix* and Some Related Compounds. *J Chem Soc Pakistan*, 23: 38–41.
- [45] Barrero AF, Sánchez JF, and Rodríguez I. (1982) N- Δ 13-Docosenoylanthranilic

- acid and alkylresorcinols from *Ononis natrix* subsp. *Hispanica*. *Phytochemistry*, 29: 1967–1969.
- [46] Al-Khalil S, Masalmeh A, Abdalla S, Tosa H, and Iinuma M. (1995) N-Arachidylanthranilic Acid, a New Derivative from *Ononis natrix*. *J Nat Prod*, 58: 760–763.
- [47] Yousaf M, Al-Rehaily AJ, Ahmad MS, Mustafa J, Al-Yahya MA, Al-Said MS, Zhao J, and Khan IA. (2015) A 5-alkylresorcinol and three 3,4-dihydroisocoumarins derived from *Ononis natrix*. *Phytochem Lett*, 13: 1–5.
- [48] Rama NH, Saeed A, and Bird CW. (1993) The Synthesis of the Principal Dihydroisocoumarins of *Ononis natrix*. *Liebigs Ann der Chemie*, 1993: 1331–1333.
- [49] Cañedo LM, Miguel del Corral JM, Feliciano AS, del Corral JMM, and San Feliciano A. (1997) 5-Alkylresorcinols from *Ononis natrix*. *Phytochemistry*, 44: 1559–1563.
- [50] Barrero AF, Cabrera E, Rodríguez I, and Fernández-Gallego EM. (1994) Resorcinol derivatives and other components from *Ononis viscosa* subsp. *breviflora*. *Phytochemistry*, 36: 189–194.
- [51] Barrero AF, Sánchez JF, Reyes F, and Rodríguez I. (1991) Resorcinol derivatives from *Ononis viscosa*. *Phytochemistry*, 30: 641–643.
- [52] Barrero AF, Cabrera E, Rodriguez I, Planelles F, Rodríguez I, and Planelles F. (1994) Alkylresorcinols and isocoumarins from *Ononis pubescens*. *Phytochemistry*, 35: 493–498.
- [53] Committee on Herbal Medicinal Products. Assessment report on *Ononis spinosa* L. https://www.ema.europa.eu/documents/herbal-report/final-assessment-report-ononis-spinosa-l-radix_en.pdf 2014
- [54] Süntar İİ, Baldemir A, Coşkun M, Keleş H, and Akkol EK. (2011) Wound healing acceleration effect of endemic *Ononis* species growing in Turkey. *J Ethnopharmacol*, 135: 63–70.
- [55] Bulow W. *Kenntnis der Wirkungen der Radix Ononidis.* , Kaiserlichen Universität, 1891:
- [56] Vollmer H and Hübner K. (1937) Untersuchungen über die diuretische Wirkung der *Folia betulae* an Kaninchen und Mäusen. Vergleich mit anderen Drogen.

- Naunyn Schmiedebergs Arch Exp Pathol Pharmacol, 186: 584–591.
- [57] Vollmer H and Hübner K. (1937) Untersuchungen über die diuretische Wirkung der Fructus juniperi, Radix levistici, Radix ononidis, Folia betulae, Radix liquiritiae und Herba equiseti an Ratten. Naunyn Schmiedebergs Arch Exp Pathol Pharmacol, 186: 592–605.
- [58] Rebuelta M, San Roman L, and Serranillos MG. (1981) Etude de l'effet diuretique de differentes preparations de l'Ononis spinosa L. Plantes Med Phyther, 15: 99–108.
- [59] Bolle P, Faccendini P, and Bello U. (1993) Ononis spinosa L.: pharmacological effect of ethanol extract. Pharmacol reserach, 27: 27–28.
- [60] Yölmaz B, Özbek H, and Çitoğlu G. (2006) Analgesic and hepatotoxic effects of Ononis spinosa L. Phyther Res, 220: 500–503.
- [61] Ergene Öz B, Saltan İşcan G, Küpeli Akkol E, Süntar İ, and Bahadır Acıkara Ö. (2018) Isoflavonoids as wound healing agents from Ononidis Radix. J Ethnopharmacol, 211: 384–393.
- [62] Arnold E, Benz T, Zapp C, and Wink M. (2015) Inhibition of Cytosolic Phospholipase A2 α (cPLA2 α) by Medicinal Plants in Relation to Their Phenolic Content. Molecules, 20: 15033–15048.
- [63] Mahasneh AM and El-Oqlah AA. (1999) Antimicrobial activity of extracts of herbal plants used in the traditional medicine of Jordan. J Ethnopharmacol, 64: 271–276.
- [64] Gülçin SÇ and Nurten A. (2003) Antimicrobial activity of some plants used in folk medicine. J Fac Pharm, 32: 159–163.
- [65] Çoban T, Çitoğlu GS, Sever B, and İşcan M. (2003) Antioxidant Activities of Plants Used in Traditional Medicine in Turkey. Pharm Biol, 41: 608–613.
- [66] Ergene Öz B, Saltan İşcan G, Küpeli Akkol E, Süntar İ, Keleş H, and Bahadır Acıkara Ö. (2017) Wound healing and anti-inflammatory activity of some Ononis taxons. Biomed Pharmacother, 91: 1096–1105.
- [67] Cai Z, Kastell A, Knorr D, and Smetanska I. (2012) Exudation: an expanding technique for continuous production and release of secondary metabolites from plant cell suspension and hairy root cultures. Plant Cell Rep, 31: 461–477.
- [68] Weathers PJ, Towler MJ, and Xu J. (2010) Bench to batch: advances in plant cell

- culture for producing useful products. *Appl Microbiol Biotechnol*, 85: 1339–1351.
- [69] Laoufi H, Benariba N, Adjdir S, and Djaziri R. (2017) In vitro α -amylase and α -glucosidase inhibitory activity of *Ononis angustissima* extracts. *J Appl Pharm Sci*, 7: 191–198.
- [70] Al-Zereini WA. (2017) *Ononis natrix* and *Salvia verbenaca*: Two Jordanian Medicinal Plants with Cytotoxic and Antibacterial Activities. *J Herbs Spices Med Plants*, 23: 18–25.
- [71] Bremner P, Rivera D, Calzado MA, Obón C, Inocencio C, Beckwith C, Fiebich BL, Muñoz E, and Heinrich M. (2009) Assessing medicinal plants from South-Eastern Spain for potential anti-inflammatory effects targeting nuclear factor-Kappa B and other pro-inflammatory mediators. *J Ethnopharmacol*, 124: 295–305.
- [72] Filová A. (2014) Production of secondary metabolites in plant tissue cultures. *Res J os Agric Sci*, 46: 236–245.
- [73] Fedoreyev SA, Kulish NI, Glebko LI, Pokushalova T V., Veselova M. V, Saratikov AS, Vengerovskii AI, and Chuchalin VS. (2004) Maksar: A preparation based on *Amur Maackia*. *Pharm Chem J*, 38: 605–610.
- [74] Łuczkiwicz M and Głód D. (2003) Callus cultures of *Genista* plants—in vitro material producing high amounts of isoflavones of phytoestrogenic activity. *Plant Sci*, 165: 1101–1108.
- [75] Tůmová L. (1996) Effect of an elicitor from *Escherichia coli* on flavonoid production by tissue culture of *Ononis arvensis* L. *Ces a Slov Farm*, 45: 27–30.
- [76] Tůmová L and Bačkovská M. (1998) Effect of chitosan on the production of flavonoids by the culture of *Ononis arvensis* L. in vitro. *Ces a Slov Farm*, 47: 110–114.
- [77] Tůmová L, Poustková J, and Tůma J. (2001) CoCl_2 and NiCl_2 elicitation and flavonoid production in *ononis arvensis* L. culture in vitro. *Ces a Slov Farm*, 51: 159–162.
- [78] Tůmová L and Rusková R. (1998) Effect of CdCl_2 and CuSO_4 on the production of flavonoids by the culture of *Ononis arvensis* L. in vitro. *Ces a Slov Farm*, 47: 261–263.
- [79] Tůmová L, Šnajdrová H, and Tůma J. (1996) Influence of flavonoid production in the culture of *Ononis arvensis* L. in vitro by elicitation with *Aspergillus terreus*.

- Ces a Slov Farm, 45: 305–309.
- [80] Tůmová L, Tůma J, and Dolezal M. (2011) Pyrazinecarboxamides as Potential Elicitors of Flavonolignan and Flavonoid Production in *Silybum marianum* and *Ononis arvensis* Cultures In Vitro. *Molecules*, 16: 9142–9152.
- [81] Tůmová L, Bartáková M, and Zabloudilova J. (2003) Iodoacetic acid as a potential elicitor of increased formation of flavonoids in the culture of *Ononis arvensis* L. in vitro. *Ces a Slov Farm*, 52: 189–192.
- [82] Tůmová L, Brancuzká R, and Tůma J. (2001) The effect of salicylic acid on flavonoid production in *Ononis arvensis* tissue culture. *Ces a Slov Farm*, 52: 327–329.
- [83] Tůmová L and Dusek J. (1995) *Ononis arvensis* L. in vitro - Effects of phenolic substances on the growth of the culture and production of flavonoids. *Ces a Slov Farm*, 44: 206–209.
- [84] Tůmová L and Dusek J. (1994) Verification of the effect of potential growth regulators. *Ces a Slov Farm*, 43: 217–221.
- [85] Tůmová L and Dušek J. (2000) Effect of linoleic acid on the production of secondary metabolites. *Ces a Slov Farm*, 49: 78–81.
- [86] Tůmová L, Gallová K, Tůma J, and Dolejšová J. (2002) Arachidonic acid as elicitor of flavonoid accumulation in. *Ces a Slov Farm*, 52: 299–304.
- [87] Tůmová L and Ostrožlík P. (2002) *Ononis arvensis* in vitro - Abiotická elicítace. *Ces a Slov Farm*, 51: 173–176.
- [88] Tůmová L and Polívková D. (2006) [Effect of AgNO₃ on the production of flavonoids by the culture of *Ononis arvensis* L. in vitro]. 55: 186–8.
- [89] Kuzovkina IN, Al'terman IE, and Karandashov VE. (2004) Genetically Transformed Plant Roots as a Model for Studying Specific Metabolism and Symbiotic Contacts of the Root System. *Biol Bull*, 31: 255–261.
- [90] Veitch NC. (2013) Isoflavonoids of the leguminosae. *Nat Prod Rep*, 30: 988–1027.
- [91] Wink M. (2013) Evolution of secondary metabolites in legumes (Fabaceae). *South African J Bot*, 89: 164–175.
- [92] Boland GM and Donnelly DMX. Isoflavonoids and related compounds. 241–260., 1996:
- [93] Reynaud J, Guilet D, and Terreux R. (2005) Isoflavonoids in non-leguminous

- families: an update. *Nat Prod Commun*, 504–515.
- [94] Wang X. (2011) Structure, function, and engineering of enzymes in isoflavonoid biosynthesis. *Funct Integr Genomics*, 11: 13–22.
- [95] Davies KM and Schwinn KE. *Molecular Biology and Biotechnology of Flavonoid Biosynthesis*. In: Andersen O and Markham K (Eds), *Flavonoids: chemistry, biochemistry and applications*. CRC Press, Boca Raton, 2006: 143–217.
- [96] KEGG PATHWAY: Isoflavonoid biosynthesis - Reference pathway. https://www.genome.jp/kegg-bin/show_pathway?map00943
- [97] Koester J and Barz W. (1984) Malonyl-coenzyme A: Isoflavone 7-O-glucoside-6''-O-malonyltransferase from roots of chick pea (*Cicer arietinum* L.). *Arch Biochem Biophys*, 234: 513–521.
- [98] Chen L, Ou S, Zhou L, Tang H, Xu J, and Guo K. (2017) Formononetin attenuates A β 25-35-induced cytotoxicity in HT22 cells via PI3K/Akt signaling and non-amyloidogenic cleavage of APP. *Neurosci Lett*, 639: 36–42.
- [99] Sun M, Zhou T, Zhou L, Chen Q, Yu Y, Yang H, Zhong K, Zhang X, Xu F, Cai S-Q, Yu A, Zhang H, Xiao R, Xiao D, and Chui D. (2012) Formononetin protects neurons against hypoxia-induced cytotoxicity through upregulation of ADAM10 and sA β PP α . *J Alzheimer's Dis*, 28: 795–808.
- [100] Fei H-X, Zhang Y-B, Liu T, Zhang X-J, and Wu S-L. (2018) Neuroprotective effect of formononetin in ameliorating learning and memory impairment in mouse model of Alzheimer's disease. *Biosci Biotechnol Biochem*, 82: 57–64.
- [101] Li Z, Wang Y, Zeng G, Zheng X, Wang W, Ling Y, Tang H, and Zhang J. (2017) Increased miR-155 and heme oxygenase-1 expression is involved in the protective effects of formononetin in traumatic brain injury in rats. *Am J Transl Res*, 9: 5653–5661.
- [102] Li Z, Zeng G, Zheng X, Wang W, Ling Y, Tang H, and Zhang J. (2018) Neuroprotective effect of formononetin against TBI in rats via suppressing inflammatory reaction in cortical neurons. *Biomed Pharmacother*, 106: 349–354.
- [103] El-Bakoush A and Olajide OA. (2018) Formononetin inhibits neuroinflammation and increases estrogen receptor beta (ERbeta) protein expression in BV2 microglia. *Int Immunopharmacol*, 61: 325–337.
- [104] Jia W-C, Liu G, Zhang C-D, and Zhang S-P. (2014) Formononetin attenuates

- hydrogen peroxide (H₂O₂)-induced apoptosis and NF-kappaB activation in RGC-5 cells. *Eur Rev Med Pharmacol Sci*, 18: 2191–2197.
- [105] Huh J-E, Nam D-W, Baek Y-H, Kang JW, Park D-S, Choi D-Y, and Lee J-D. (2011) Formononetin accelerates wound repair by the regulation of early growth response factor-1 transcription factor through the phosphorylation of the ERK and p38 MAPK pathways. *Int Immunopharmacol*, 11: 46–54.
- [106] Huh J-E, Kwon N-H, Baek Y-H, Lee J-D, Choi D-Y, Jingushi S, Kim K, and Park D-S. (2009) Formononetin promotes early fracture healing through stimulating angiogenesis by up-regulating VEGFR-2/Flk-1 in a rat fracture model. *Int Immunopharmacol*, 9: 1357–1365.
- [107] Auyeung KK-W, Law P-C, and Ko JK-S. (2012) Novel anti-angiogenic effects of formononetin in human colon cancer cells and tumor xenograft. *Oncol Rep*, 28: 2188–2194.
- [108] Wu J, Ke X, Ma N, Wang W, Fu W, Zhang H, Zhao M, Gao X, Hao X, and Zhang Z. (2016) Formononetin, an active compound of *Astragalus membranaceus* (Fisch) Bunge, inhibits hypoxia-induced retinal neovascularization via the HIF-1 α /VEGF signaling pathway. *Drug Des Devel Ther*, Volume 10: 3071–3081.
- [109] Wu J-H, Li Q, Wu M-Y, Guo D-J, Chen H-L, Chen S-L, Seto S-W, Au ALS, Poon CCW, and Leung GPH. (2010) Formononetin, an isoflavone, relaxes rat isolated aorta through endothelium-dependent and endothelium-independent pathways. *J Nutr Biochem*, 21: 613–620.
- [110] Sun T, Liu R, and Cao Y. (2011) Vasorelaxant and antihypertensive effects of formononetin through endothelium-dependent and -independent mechanisms. *Acta Pharmacol Sin*, 32: 1009–1018.
- [111] Sun T, Wang J, Huang L-H, and Cao Y-X. (2013) Antihypertensive effect of formononetin through regulating the expressions of eNOS, 5-HT_{2A/1B} receptors and α 1-adrenoceptors in spontaneously rat arteries. *Eur J Pharmacol*, 699: 241–249.
- [112] Bai F, Makino T, Kono K, Nagatsu A, Ono T, and Mizukami H. (2013) Calycosin and formononetin from astragalus root enhance dimethylarginine dimethylaminohydrolase 2 and nitric oxide synthase expressions in Madin Darby Canine Kidney II cells. *J Nat Med*, 67: 782–789.

- [113] Ha H, Lee HY, Lee J-H, Jung D, Choi J, Song K-Y, Jung HJ, Choi JS, Chang S-I, and Kim C. (2010) Formononetin prevents ovariectomy-induced bone loss in rats. *Arch Pharm Res*, 33: 625–632.
- [114] Tyagi AM, Srivastava K, Singh AK, Kumar A, Changkija B, Pandey R, Lahiri S, Nagar GK, Yadav DK, Maurya R, Trivedi R, and Singh D. (2012) Formononetin reverses established osteopenia in adult ovariectomized rats. *Menopause*, 19: 856–863.
- [115] Mansoori MN, Tyagi AM, Shukla P, Srivastava K, Dev K, Chillara R, Maurya R, and Singh D. (2016) Methoxyisoflavones formononetin and isoformononetin inhibit the differentiation of Th17 cells and B-cell lymphopoiesis to promote osteogenesis in estrogen-deficient bone loss conditions. *Menopause*, 23: 565–576.
- [116] Singh KB, Dixit M, Dev K, Maurya R, and Singh D. (2017) Formononetin, a methoxy isoflavone, enhances bone regeneration in a mouse model of cortical bone defect. *Br J Nutr*, 117: 1511–1522.
- [117] Huh J-E, Seo D-M, Baek Y-H, Choi D-Y, Park D-S, and Lee J-D. (2010) Biphasic positive effect of formononetin on metabolic activity of human normal and osteoarthritic subchondral osteoblasts. *Int Immunopharmacol*, 10: 500–507.
- [118] Gautam AK, Bhargavan B, Tyagi AM, Srivastava K, Yadav DK, Kumar M, Singh A, Mishra JS, Singh AB, Sanyal S, Maurya R, Manickavasagam L, Singh SP, Wahajuddin W, Jain GK, Chattopadhyay N, and Singh D. (2011) Differential effects of formononetin and cladrin on osteoblast function, peak bone mass achievement and bioavailability in rats. *J Nutr Biochem*, 22: 318–327.
- [119] Wang W, Tanaka Y, Han Z, and Higuchi CM. (1995) Proliferative response of mammary glandular tissue to formononetin. *Nutr Cancer*, 23: 131–140.
- [120] Ji Z-N, Zhao WY, Liao GR, Choi RC, Lo CK, Dong TTX, and Tsim KWK. (2006) In vitro estrogenic activity of formononetin by two bioassay systems. *Gynecol Endocrinol*, 22: 578–584.
- [121] Umehara K, Nemoto K, Matsushita A, Terada E, Monthakantirat O, De-Eknamkul W, Miyase T, Warashina T, Degawa M, and Noguchi H. (2009) Flavonoids from the heartwood of the Thai medicinal plant *Dalbergia parviflora* and their effects on estrogenic-responsive human breast cancer cells. *J Nat Prod*, 72: 2163–2168.
- [122] Chen J, Zhang X, Wang Y, Ye Y, and Huang Z. (2016) Formononetin promotes

- proliferation that involves a feedback loop of microRNA-375 and estrogen receptor alpha in estrogen receptor-positive cells. *Mol Carcinog*, 55: 312–319.
- [123] Mu H, Bai Y-H, Wang S-T, Zhu Z-M, and Zhang Y-W. (2009) Research on antioxidant effects and estrogenic effect of formononetin from *Trifolium pratense* (red clover). *Phytomedicine*, 16: 314–319.
- [124] Guo Y-H, Tang F-Y, Wang Y, Huang W-J, Tian J, Lu H-L, Xin M, and Chen J. (2017) Low concentration of formononetin promotes proliferation of estrogen receptor-positive cells through an ERalpha-miR-375-PTEN-ERK1/2-bcl-2 pathway. *Oncotarget*, 8: 100045–100055.
- [125] Khan IA, Very MA, Burandt CL, Goins DK, Mikell JR, Nash TE, Azadegan A, and Walker LA. (2000) Antigiardial activity of isoflavones from *Dalbergia frutescens* bark. *J Nat Prod*, 63: 1414–1416.
- [126] Lauwaet T, Andersen Y, Van de Ven L, Eckmann L, and Gillin FD. (2010) Rapid detachment of *Giardia lamblia* trophozoites as a mechanism of antimicrobial action of the isoflavone formononetin. *J Antimicrob Chemother*, 65: 531–534.
- [127] Choi CW, Choi YH, Cha M-R, Yoo DS, Kim YHS, Yon GH, Hong KS, Kim YHS, and Ryu SY. (2010) Yeast α -glucosidase inhibition by isoflavones from plants of leguminosae as an in vitro alternative to acarbose. *J Agric Food Chem*, 58: 9988–9993.
- [128] Van Bon N, Wang S-L, Nhan NT, Nguyen TH, Dai Nguyen NP, Do Huu N, and Cuong NM. (2018) New records of potent in-vitro antidiabetic properties of *dalbergia tonkinensis* heartwood and the bioactivity-guided isolation of active compounds. *Molecules*, 23: 1589.
- [129] Chen J and Sun L. (2012) Formononetin-induced Apoptosis by Activation of Ras/p38 Mitogen-activated Protein Kinase in Estrogen Receptor-positive Human Breast Cancer Cells. *Horm Metab Res*, 44: 943–948.
- [130] Chen J, Zeng J, Xin M, Huang W, and Chen X. (2011) Formononetin Induces Cell Cycle Arrest of Human Breast Cancer Cells via IGF1/PI3K/Akt Pathways In Vitro and In Vivo. *Horm Metab Res*, 43: 681–686.
- [131] Huang W-J, Bi L-Y, Li Z-Z, Zhang X, and Ye Y. (2013) Formononetin induces the mitochondrial apoptosis pathway in prostate cancer cells via downregulation of the IGF-1/IGF-1R signaling pathway. *Pharm Biol*, 52: 466–470.

- [132] Zhang X, Bi L-Y, Ye Y, and Chen J. (2014) Formononetin induces apoptosis in PC-3 prostate cancer cells through enhancing the Bax/Bcl-2 ratios and regulating the p38/Akt pathway. *Nutr Cancer*, 66: 656–661.
- [133] Yang Y, Zhao Y, Ai X, Cheng B, and Lu S. (2014) Formononetin suppresses the proliferation of human non-small cell lung cancer through induction of cell cycle arrest and apoptosis. *Int J Clin Exp Pathol*, 7: 8453–8461.
- [134] Liu Y, He J, Chen X, Li J, Shen M, Yu W, Yang Y, and Xiao Z. (2014) The Proapoptotic Effect of Formononetin in Human Osteosarcoma Cells: Involvement of Inactivation of ERK and Akt Pathways. *Cell Physiol Biochem*, 34: 637–645.
- [135] Zhang J, Liu L, Wang J, Ren B, Zhang L, and Li W. (2018) Formononetin, an isoflavone from *Astragalus membranaceus* inhibits proliferation and metastasis of ovarian cancer cells. *J Ethnopharmacol*, 221: 91–99.
- [136] Park S, Bazer FW, Lim W, and Song G. (2018) The O-methylated isoflavone, formononetin, inhibits human ovarian cancer cell proliferation by sub G0/G1 cell phase arrest through PI3K/AKT and ERK1/2 inactivation. *J Cell Biochem*,
- [137] Wang A-L, Li Y, Zhao Q, and Fan L-Q. (2018) Formononetin inhibits colon carcinoma cell growth and invasion by microRNA-149-mediated EphB3 downregulation and inhibition of PI3K/AKT and STAT3 signaling pathways. *Mol Med Rep*, 17: 7721–7729.
- [138] Auyeung KK-W and Ko JK-S. (2010) Novel herbal flavonoids promote apoptosis but differentially induce cell cycle arrest in human colon cancer cell. *Invest New Drugs*, 28: 1–13.
- [139] Zhang X, Ni Q, Wang Y, Fan H-W, and Li Y. (2018) Synergistic Anticancer Effects of Formononetin and Temozolomide on Glioma C6 Cells. *Biol Pharm Bull*, 41: 1194–1202.
- [140] Wu Y, Zhang X, Li Z, Yan H, Qin J, and Li T. (2017) Formononetin inhibits human bladder cancer cell proliferation and invasiveness via regulation of miR-21 and PTEN. *Food Funct*, 8: 1061–1066.
- [141] Jin Y, Xu T, Zhao Y, Wang Y, and Cui M. (2014) In vitro and in vivo anti-cancer activity of formononetin on human cervical cancer cell line HeLa. *Tumor Biol*, 35: 2279–2284.
- [142] Kim C, Lee S-G, Yang WM, Arfuso F, Um J-Y, Kumar AP, Bian J, Sethi G, and

- Ahn KS. (2018) Formononetin-induced oxidative stress abrogates the activation of STAT3/5 signaling axis and suppresses the tumor growth in multiple myeloma preclinical model. *Cancer Lett*, 431: 123–141.
- [143] Liu X-J, Li Y-Q, Chen Q-Y, Xiao S-J, and Zeng S-E. (2014) Up-regulating of RASD1 and Apoptosis of DU-145 Human Prostate Cancer Cells Induced by Formononetin in Vitro. *Asian Pacific J Cancer Prev*, 15: 2835–2839.
- [144] Ye Y, Hou R, Chen J, Mo L, Zhang J, Huang Y, and Mo Z. (2012) Formononetin-induced Apoptosis of Human Prostate Cancer Cells Through ERK1/2 Mitogen-activated Protein Kinase Inactivation. *Horm Metab Res*, 44: 263–267.
- [145] Salam NK, Huang THW, Kota BP, Kim MS, Li Y, and Hibbs DE. (2008) Novel PPAR-gamma agonists identified from a natural product library: A virtual screening, induced-fit docking and biological assay study. *Chem Biol Drug Des*, 71: 57–70.
- [146] Matin A, Doddareddy MR, Gavande N, Nammi S, Groundwater PW, Roubin RH, and Hibbs DE. (2013) The discovery of novel isoflavone pan peroxisome proliferator-activated receptor agonists. *Bioorg Med Chem*, 21: 766–778.
- [147] Matin A, Gavande N, Kim MS, Yang NX, Salam NK, Hanrahan JR, Roubin RH, and Hibbs DE. (2009) 7-Hydroxy-benzopyran-4-one derivatives: A novel pharmacophore of peroxisome proliferator-activated receptor α and $-\gamma$ (PPAR α and γ) dual agonists. *J Med Chem*, 52: 6835–6850.
- [148] Promden W, Monthakantirat O, Umehara K, Noguchi H, and De-Eknamkul W. (2014) Structure and antioxidant activity relationships of isoflavonoids from *Dalbergia parviflora*. *Molecules*, 19: 2226–2237.
- [149] Morikawa T, Xu F, Matsuda H, Yoshikawa M, Orikawa TM, Fengming XU, Atsuda HM, Oshikawa MY, Morikawa T, Xu F, Matsuda H, and Yoshikawa M. (2006) Structures of new flavonoids, ercibenins D, E, and F, and NO production inhibitors from *Erycibe expansa* originating in Thailand. *Chem Pharm Bull (Tokyo)*, 54: 1530–1534.
- [150] Fan Y, Wu DZ, Gong YQ, Zhou JY, and Hu ZB. (2003) Effects of calycosin on the impairment of barrier function induced by hypoxia in human umbilical vein endothelial cells. *Eur J Pharmacol*, 481: 33–40.
- [151] Araujo C, Alegrio L V., and Leon LL. (1998) Antileishmanial activity of

- compounds extracted and characterized from *Centrolobium sclerophyllum*. *Phytochemistry*, 49: 751–754.
- [152] ElSohly HN, Joshi AS, and Nimrod AC. (1999) Antigiardial isoflavones from *Machaerium aristulatum*. *Planta Med*, 65: 490.
- [153] Salem MM and Werbovetz KA. (2006) Isoflavonoids and other compounds from *Psoralea argyrea* with antiprotozoal activities. *J Nat Prod*, 69: 43–49.
- [154] Beldjoudi N, Mambu L, Labaïed M, Grellier P, Ramanitrahasimbola D, Rasoanaivo P, Martin MT, and Frappier F. (2003) Flavonoids from *Dalbergia louvelii* and their antiplasmodial activity. *J Nat Prod*, 66: 1447–50.
- [155] Ham SA, Kang ES, Yoo T, Lim HH, Lee WJ, Hwang JS, Paek KS, and Seo HG. (2015) *Dalbergia odorifera* Extract Ameliorates UVB-Induced Wrinkle Formation by Modulating Expression of Extracellular Matrix Proteins. *Drug Dev Res*, 76: 48–56.
- [156] Taniguchi C, Homma M, Takano O, Hirano T, Oka K, Aoyagi Y, Niitsuma T, and Hayashi T. (2000) Pharmacological effects of urinary products obtained after treatment with Saiboku-To, a herbal medicine for bronchial asthma, on type IV allergic reaction. *Planta Med*, 66: 607–611.
- [157] Homma M, Oka K, Niitsuma T, and Itoh H. (1994) A Novel 11 β -Hydroxysteroid Dehydrogenase Inhibitor Contained in Saiboku-To, a Herbal Remedy for Steroid-dependent Bronchial Asthma. *J Pharm Pharmacol*, 46: 305–309.
- [158] Liu Z-L, Tanaka S, Horigome H, Hirano T, and Oka K. (2002) Induction of apoptosis in human lung fibroblasts and peripheral lymphocytes in vitro by Shosaiko-to derived phenolic metabolites. *Biol Pharm Bull*, 25: 37–41.
- [159] Trivedi R, Maurya R, and Mishra DP. (2014) Medicarpin, a legume phytoalexin sensitizes myeloid leukemia cells to TRAIL-induced apoptosis through the induction of DR5 and activation of the ROS-JNK-CHOP pathway. *Cell Death Dis*, 5: e1465–e1465.
- [160] Gatouillat G, Magid AA, Bertin E, El btaouri H, Morjani H, Lavaud C, and Madoulet C. (2015) Medicarpin and millepurpan, two flavonoids isolated from *Medicago sativa*, induce apoptosis and overcome multidrug resistance in leukemia P388 cells. *Phytomedicine*, 22: 1186–1194.
- [161] Maurya R, Yadav DK, Singh G, Bhargavan B, Narayana Murthy PSS, Sahai M,

- and Singh MM. (2009) Osteogenic activity of constituents from *Butea monosperma*. *Bioorg Med Chem Lett*, 19: 610–613.
- [162] Bhargavan B, Singh D, Gautam AK, Mishra JS, Kumar A, Goel A, Dixit M, Pandey R, Manickavasagam L, Dwivedi SD, Chakravarti B, Jain GK, Ramachandran R, Maurya R, Trivedi A, Chattopadhyay N, and Sanyal S. (2012) Medicarpin, a legume phytoalexin, stimulates osteoblast differentiation and promotes peak bone mass achievement in rats: evidence for estrogen receptor β -mediated osteogenic action of medicarpin. *J Nutr Biochem*, 23: 27–38.
- [163] Tyagi AM, Gautam AK, Kumar A, Srivastava K, Bhargavan B, Trivedi R, Saravanan S, Yadav DK, Singh N, Pollet C, Brazier M, Mentaverri R, Maurya R, Chattopadhyay N, Goel A, and Singh D. (2010) Medicarpin inhibits osteoclastogenesis and has nonestrogenic bone conserving effect in ovariectomized mice. *Mol Cell Endocrinol*, 325: 101–109.
- [164] Goel A, Kumar A, Hemberger Y, Raghuvanshi A, Jeet R, Tiwari G, Knauer M, Kureel J, Singh AK, Gautam A, Trivedi R, Singh D, and Bringmann G. (2012) Synthesis, optical resolution, absolute configuration, and osteogenic activity of cis-pterocarpan. *Org Biomol Chem*, 10: 9583–9592.
- [165] Delserone LM, Matthews DE, and VanEtten HD. (1992) Differential toxicity of enantiomers of maackiain and pisatin to phytopathogenic fungi. *Phytochemistry*, 31: 3813–3819.
- [166] Mizuguchi H, Nariai Y, Kato S, Nakano T, Kanayama T, Kashiwada Y, Nemoto H, Kawazoe K, Takaishi Y, Kitamura Y, Takeda N, and Fukui H. (2015) Maackiain is a novel antiallergic compound that suppresses transcriptional upregulation of the histamine H1 receptor and interleukin-4 genes. *Pharmacol Res Perspect*, 3:
- [167] Nariai Y, Mizuguchi H, Ogasawara T, Nagai H, Sasaki Y, Okamoto Y, Yoshimura Y, Kitamura Y, Nemoto H, Takeda N, and Fukui H. (2015) Disruption of Heat Shock Protein 90 (Hsp90)-Protein Kinase C δ (PKC δ) Interaction by (–)-Maackiain Suppresses Histamine H 1 Receptor Gene Transcription in HeLa Cells. *J Biol Chem*, 290: 27393–27402.
- [168] Ryu YB, Curtis-Long MJ, Kim JH, Jeong SH, Yang MS, Lee KW, Lee WS, and Park KH. (2008) Pterocarpan and flavanones from *Sophora flavescens* displaying

- potent neuraminidase inhibition. *Bioorg Med Chem Lett*, 18: 6046–6049.
- [169] Lee HW, Ryu HW, Kang M-GG, Park D, Oh S-RR, and Kim H. (2016) Potent selective monoamine oxidase B inhibition by maackiain, a pterocarpan from the roots of *Sophora flavescens*. *Bioorg Med Chem Lett*, 26: 4714–4719.
- [170] de Rijke E, Out P, Niessen WMA, Ariese F, Gooijer C, and Brinkman UAT. (2006) Analytical separation and detection methods for flavonoids. *J Chromatogr A*, 1112: 31–63.
- [171] Csupor D, Bognár J, Karsai J, and Hohmann J. (2010) Method development and optimization for isoflavone quantification in dry soy extract containing products. *Planta Med*, 76: P537.
- [172] de Rijke E, Zafra-Gómez A, Ariese F, Brinkman UAT, and Gooijer C. (2001) Determination of isoflavone glucoside malonates in *Trifolium pratense* L. (red clover) extracts: quantification and stability studies. *J Chromatogr A*, 932: 55–64.
- [173] Vacek J, Klejdus B, Lojková L, and Kubáň V. (2008) Current trends in isolation, separation, determination and identification of isoflavones: a review. *J Sep Sci*, 31: 2054–2067.
- [174] Klejdus B, Lojková L, Lapčík O, Koblovská R, Moravcová J, and Kubáň V. (2005) Supercritical fluid extraction of isoflavones from biological samples with ultra-fast high-performance liquid chromatography/mass spectrometry. *J Sep Sci*, 28: 1334–1346.
- [175] Vacek J and Klejdus B. (2008) Current trends in isolation, separation, determination and identification of isoflavones: a review. *J Sep Sci*, 2054–2067.
- [176] Klejdus B, Mikelová R, Petřlová J, Potěšil D, Adam V, Stiborová M, Hodek P, Vacek J, Kizek R, and Kubáň V. (2005) Determination of isoflavones in soy bits by fast column high-performance liquid chromatography coupled with UV–visible diode-array detection. *J Chromatogr A*, 1084: 71–79.
- [177] Pinheiro P and Justino G. Structural analysis of flavonoids and related compounds—a review of spectroscopic applications. In: Dr. Venketeshwer R (Eds), *Phytochemicals - A Global Perspective of Their Role in Nutrition and Health*. InTech, 2012: 33–56.
- [178] Cuyckens F and Claeys M. (2004) Mass spectrometry in the structural analysis of flavonoids. *J Mass Spectrom*, 39: 1–15.

- [179] Ma YL, Li QM, Van den Heuvel H, and Claeys M. (1997) Characterization of flavone and flavonol aglycones by collision-induced dissociation tandem mass spectrometry. *Rapid Commun Mass Spectrom*, 11: 1357–1364.
- [180] Maul R, Schebb NH, and Kulling SE. (2008) Application of LC and GC hyphenated with mass spectrometry as tool for characterization of unknown derivatives of isoflavonoids. *Anal Bioanal Chem*, 391: 239–250.
- [181] Tóth E, Dinya Z, and Antus S. (2000) Mass spectrometric studies of the pterocarpan skeleton. *Rapid Commun Mass Spectrom*, 14: 2367–2372.
- [182] Zhang L, Xu L, Xiao S-S, Liao Q-F, Li Q, Liang J, Chen X-H, and Bi K-S. (2007) Characterization of flavonoids in the extract of *Sophora flavescens* Ait. by high-performance liquid chromatography coupled with diode-array detector and electrospray ionization mass spectrometry. *J Pharm Biomed Anal*, 44: 1019–1028.
- [183] March RE, Miao X-S, Metcalfe CD, Stobiecki M, and Marczak L. (2004) A fragmentation study of an isoflavone glycoside, genistein-7-O-glucoside, using electrospray quadrupole time-of-flight mass spectrometry at high mass resolution. *Int J Mass Spectrom*, 232: 171–183.
- [184] Kuhn F, Oehme M, Romero F, Abou-Mansour E, and Tabacchi R. (2003) Differentiation of isomeric flavone/isoflavone aglycones by MS² ion trap mass spectrometry and a double neutral loss of CO. *Rapid Commun Mass Spectrom*, 17: 1941–1949.
- [185] Nakata R, Yoshinaga N, Teraishi M, Okumoto Y, Huffaker A, Schmelz EA, and Mori N. (2018) A fragmentation study of isoflavones by IT-TOF-MS using biosynthesized isotopes. *Biosci Biotechnol Biochem*, 82: 1309–1315.
- [186] Abrankó L and Szilvássy B. (2015) Mass spectrometric profiling of flavonoid glycoconjugates possessing isomeric aglycones. *J Mass Spectrom*, 50: 71–80.
- [187] Ablajan K. (2011) A study of characteristic fragmentation of isoflavonoids by using negative ion ESI-MSⁿ. *J Mass Spectrom*, 46: 77–84.
- [188] Domon B and Costello CE. (1988) A systematic nomenclature for carbohydrate fragmentations in FAB-MS/MS spectra of glycoconjugates. *Glycoconj J*, 5: 397–409.
- [189] Kim M, Won D, and Han J. (2010) Absolute configuration determination of isoflavan-4-ol stereoisomers. *Bioorg Med Chem Lett*, 20: 4337–4341.

- [190] Yi J, Du G, Yang Y, Li Y, Li Y, and Guo F. (2016) Chiral discrimination of natural isoflavanones using (R)- and (S)-BINOL as the NMR chiral solvating agents. *Tetrahedron Asymmetry*, 27: 1153–1159.
- [191] Feng Z-GG, Bai W-J, and Pettus TRRR. (2015) Unified Total Syntheses of (–)-Medicarpin, (–)-Sophoracarpin A, and (±)-Kushecarpin A with Some Structural Revisions. *Angew Chemie Int Ed*, 54: 1864–1867.
- [192] Pietta P, Mauri P, Manera E, and Ceva P. (1990) Determination of isoflavones from *Ononis spinosa* L. extracts by high-performance liquid chromatography with ultraviolet diode-array detection. *J Chromatogr A*, 513: 397–400.
- [193] Li W, Koike K, Asada Y, Hirotani M, Rui H, Yoshikawa T, and Nikaido T. (2002) Flavonoids from *Glycyrrhiza pallidiflora* hairy root cultures. *Phytochemistry*, 60: 351–355.
- [194] Rueda DC, De Mieri M, Hering S, and Hamburger M. (2014) HPLC-based activity profiling for GABAA receptor modulators in *Adenocarpus cincinnatus*. *J Nat Prod*, 77: 640–649.
- [195] Li W, Asada Y, and Yoshikawa T. (2000) Flavonoid constituents from *Glycyrrhiza glabra* hairy root cultures. *Phytochemistry*, 55: 447–456.
- [196] Farag MA, Huhman D V., Lei Z, and Sumner LW. (2007) Metabolic profiling and systematic identification of flavonoids and isoflavonoids in roots and cell suspension cultures of *Medicago truncatula* using HPLC-UV-ESI-MS and GC-MS. *Phytochemistry*, 68: 342–354.
- [197] de Rijke E, de Kanter F, Ariese F, Brinkman UAT, and Gooijer C. (2004) Liquid chromatography coupled to nuclear magnetic resonance spectroscopy for the identification of isoflavone glucoside malonates in *T. pratense* L. leaves. *J Sep Sci*, 27: 1061–1070.
- [198] Rashid M, Singh SK, Malik MY, Jahan S, Chaturvedi S, Taneja I, Raju KS, Naseem Z, Gayen JR, and Wahajuddin M. (2018) Development and validation of UPLC-MS/MS assay for quantification of cladrin: Absolute bioavailability and dose proportionality study in rats. *J Pharm Biomed Anal*, 152: 289–297.
- [199] Manickavasagam L, Gupta S, Mishra S, Maurya R, Chattopadhyay N, and Jain GK. (2011) LC-MS/MS method for simultaneous analysis of cladrin and equol in rat plasma and its application in pharmacokinetics study of cladrin. *Med Chem*

- Res, 20: 1566–1572.
- [200] PubChem. 3-(2,4-Dimethoxyphenyl)-7-hydroxychromen-4-one | C17H14O5 - PubChem.
<https://pubchem.ncbi.nlm.nih.gov/compound/5781145#section=General-MS>
- [201] Umehara K, Monthakantirat O, Matsushita A, Terada E, Miyase T, De-Eknamkul W, and Noguchi H. (2010) Estrogenic activities of flavonoids in Thai medicinal plant *Dalbergia parviflora*. *Planta Med*, 76: P241.
- [202] Jain L, Tripathi M, Pandey VB, and Rücker G. (1996) Flavonoids from *Eschscholtzia Californica*. *Phytochemistry*, 41: 661–662.
- [203] Deyou T, Marco M, Heydenreich M, Pan F, Gruhonjic A, Fitzpatrick PA, Koch A, Derese S, Pelletier J, Rissanen K, Yenesew A, Erdélyi M, Yuan F, Gao L, Han F, Marks IS, Kang JS, Jones BT, Landmark KJ, Cleland AJ, and Taton TA. (2017) Isoflavones and Rotenoids from the Leaves of *Millettia oblata* ssp. *teitensis*. *J Nat Prod*, 80: 1–2.
- [204] Louaar S, Akkal S, Laouer H, and Guilet D. (2007) Flavonoids of *Retama sphaerocarpa* leaves and their antimicrobial activities. *Chem Nat Compd*, 43: 616–617.
- [205] Alvarez L, Rios MY, Esquivel C, Chávez MI, Delgado G, Aguilar MI, Villarreal ML, and Navarro V. (1998) Cytotoxic Isoflavans from *Eysenhardtia polystachya*. *J Nat Prod*, 61: 767–770.
- [206] Rao EV, Murthy MSR, and Ward RS. (1984) Nine isoflavones from *Tephrosia maxima*. *Phytochemistry*, 23: 1493–1501.
- [207] Ingham JL. (1981) Isolation and identification of *Cicer* isoflavonoids. *Biochem Syst Ecol*, 9: 125–128.
- [208] Paßreiter CM. (1992) Co-occurrence of 2-pyrrolidineacetic acid with the pyrrolizidines tussilaginic acid and isotussilaginic acid and their 1-epimers in *Arnica* species and *Tussilago farfara*. *Phytochemistry*, 31: 4135–4137.
- [209] Tőkés AL, Litkei G, Gulácsi K, Antus S, Baitz-Gács E, Szántay C, and Darkó LL. (1999) Absolute configuration and total synthesis of (-)-cabenegrin A-I. *Tetrahedron*, 55: 9283–9296.
- [210] Boldizsár I, Füzfai Z, and Molnár-Perl I. (2013) Characterization of the endogenous enzymatic hydrolyses of *Petroselinum crispum* glycosides:

- Determined by chromatography upon their sugar and flavonoid products. *J Chromatogr A*, 1293: 100–106.
- [211] Ye H, Gemperline E, Venkateshwaran M, Chen R, Delaux P-MM, Howes-Podoll M, Ané J-M, and Li L. (2013) MALDI mass spectrometry-assisted molecular imaging of metabolites during nitrogen fixation in the *Medicago truncatula*-*Sinorhizobium meliloti* symbiosis. *Plant J*, 75: 130–145.
- [212] Marshall WD, Nguyen TT, MacLean DB, and Spenser ID. (1975) Biosynthesis of Lycopodine . The Question of the Intermediacy of Piperidine-2-acetic Acid. *Can J Chem*, 53: 41–50.
- [213] Nilsu T, Thorroad S, Ruchirawat S, and Thasana N. (2016) Squarrosine A and Pyrrolhuperzine A, New Lycopodium Alkaloids from Thai and Philippine *Huperzia squarrosa*. *Planta Med*, 82: 1046–1050.
- [214] Bhagwat S, Haytowitz DB, and Holden JM. USDA Database for the Isoflavone Content of Selected Foods, Release 2.0. https://www.ars.usda.gov/ARUserFiles/80400525/Data/isoflav/Isoflav_R2.pdf 2008
- [215] Wu Q, Wang M, and Simon JE. (2003) Determination of isoflavones in red clover and related species by high-performance liquid chromatography combined with ultraviolet and mass spectrometric detection. *J Chromatogr A*, 1016: 195–209.

10. List of own publications

Regarding the topic of the thesis:

Gampe N, Darcsi A, Lohner S, Béni S, Kursinszki L. (2016) Characterization and identification of isoflavonoid glycosides in the root of Spiny restharrow (*Ononis spinosa* L.) by HPLC-QTOF-MS, HPLC-MS/MS and NMR. J Pharmaceut Biomed, 123: 74-81.

Gampe N, Darcsi A, Kursinszki L, Béni S. (2018) Separation and characterization of homopipelic acid isoflavonoid ester derivatives isolated from *Ononis spinosa* L. root. J Chrom B, 1091: 21-28

Gampe N, Darcsi A, Nagyné Nedves A, Boldizsár I, Kursinszki L, Béni S. (2018) Phytochemical analysis of *Ononis arvensis* L. by liquid chromatography coupled with mass spectrometry. J Mass Spec

Other publications:

Addotey JN, Lengers I, Jose J, Gampe N, Béni S, Petereit F, Hensel A: Isoflavonoids with inhibiting effects on human hyaluronidase-1 and norneolignan clitorienolactone B from *Ononis spinosa* L. root extract. Fitoterapia, 130:169-174

11. Acknowledgement

On the first page of this work, the name of only one author can be written, but this doctoral thesis could only be born with the contribution of many helping hands.

Firstly, I would like to express my gratitude to my supervisors, Dr. Szabolcs Béni and Dr. László Kursinszki for their faith and trust which accompanied my doctoral work. I am very thankful that they had already had trust in me, before I had trust in myself. Furthermore, I would like to thank the huge amount of time and work they have paid to my professional development.

I am grateful to Dr. András Darcsi for his patience and endurance that he showed during the analysis of my challenging samples.

I would like to thank Dr. Imre Boldizsár, Dr. Szilvia Lohner, Dr. Anikó Nemes and Zsófia Zámbo, as beyond their technical help they always supported me with professional advises, too

I really appreciate the work of Dr. Eszter Riethmüller, who restlessly weeded out the mistakes and typos from this thesis and who always provided a helping hand in serious and not-so-serious questions.

The process of isolating an herbal compound is like manufacturing the finest artisan product, in which Tamás Czeglédi and Andrea Nagyné Nedves provided essential help. I am grateful that I could count on them even in the most boring and nerve-racking tasks. But what is more important, I am grateful for their friendship.

I would like to express my thank to Prof. Éva Szőke for the biotechnological samples and for Kati Koller Béláné, who cared them whole-heartedly.

I could not define the direct work of the following colleagues in this thesis, but I am very grateful for Anita Zempléni-Tóth, Dr. Ida Fejős, Annamária Mészáros, Rita Könye, Dr. Anna Bucsy-Sólyomváry, Rita Péntes, Petra Malcsiner, Dániel Vesztergombi. Their friendship and company helped me through deadlocks, impelled me to endurance and proved an atmosphere which was good to join from day to day. I truly appreciate the work of all other colleagues of the Department who supported my studies and research.

Finally, I would like to express my warmest gratitude to my partner and family for the safe, supporting and upholding heartland they have provided.



Characterization and identification of isoflavonoid glycosides in the root of Spiny restharrow (*Ononis spinosa* L.) by HPLC-QTOF-MS, HPLC-MS/MS and NMR



Nóra Gampe^a, András Darcsi^a, Szilvia Lohner^b, Szabolcs Béni^{a,*}, László Kursinszki^{a,*}

^a Semmelweis University, Department of Pharmacognosy, Üllői út 26, H-1085 Budapest, Hungary

^b National Institute of Pharmacy and Nutrition, Zrínyi u. 3, H-1051 Budapest, Hungary

ARTICLE INFO

Article history:

Received 22 December 2015

Received in revised form 26 January 2016

Accepted 27 January 2016

Available online 2 February 2016

Keywords:

Isoflavone

Pterocarpin

Dihydroisoflavone

Structural analysis

MS fragmentation pattern

ABSTRACT

Restharrow root has been used in traditional medicine for thousands of years; however, the active ingredients responsible for the diuretic effect are still unknown. Previous studies have proved that the root extract contains isoflavonoids, however only few derivatives were identified, mostly relying on retention times or UV data. The aim of our work was to perform a detailed structural characterization of the complete isoflavonoid profile in the aqueous-methanolic extract of *Ononis spinosa* root by high-performance liquid chromatography coupled with electrospray ionization accurate-mass quadrupole time-of-flight and tandem mass spectrometry in positive ionization mode (HPLC-ESI-QTOF-MS, HPLC-ESI-MS/MS) and nuclear magnetic resonance spectroscopy (NMR). On the basis of the accurate masses and fragmentation patterns isoflavones (formononetin, calycosin and pseudobaptigenin) and pterocarpan (maackiain and medicarpin) were identified. Two further dihydroisoflavone aglycones, namely onogenin and sativanone and a unique glucoside were isolated and their structures were elucidated by NMR experiments. Calycosin, onogenin and sativanone were detected in this plant for the first time. In contrast to previous works, the presence of biochanin A could not be confirmed, however its regioisomer calycosin and its derivatives were identified. Similarly, neither tectorigenin derivatives could be detected, however the isobar compound sativanone and its various glucosides were elucidated. The presence of genistein and daidzein could not be confirmed in the extract. Fragmentation pathways for onogenin and sativanone are presented. In the aqueous-methanolic extract 9 glucosides, 6 minor and 8 major glucoside malonates, 4 glucoside acetates and 7 aglycones were found. In total, 34 compounds were successfully identified.

© 2016 Elsevier B.V. All rights reserved.

1. Introduction

Ononis spinosa L. is a member of the Fabaceae family, and widely spread in Europe and in the Mediterranean region [1]. It is known for thousands of years that spiny restharrow root possesses diuretic effect and the drug is official in many pharmacopoeias. Nowadays several spiny restharrow root products are on the market: it is available in the form of single herbal substance products, in herbal teas or liquid extracts combined with other diuretic herbs. Preparations from spiny restharrow root are conventionally used as infusions for the stimulation of diuresis, to treat inflammatory conditions of the lower urinary tract and as a remedy for kidney disorders such as gravels and small stones [2]. These indications were con-

firmed by animal studies but no clinical trials have been done yet. Although the herb is used since ancient times, there is no evidence for the active compound of the root responsible for the diuretic effect. Recent *in vivo* experiments certified that the root extract not only increases the excreted urinary volume but holds antioxidant, analgesic, antimicrobial and anti-inflammatory features [3]. That could serve as an explanation why *Ononis* species are used for gout, rheumatic complaints and externally for skin disorders and wound healing as folk remedies in Turkey [4].

Phytosterols, phenolic acids, essential oil and a specific triterpene, α -onocerin, beside isoflavonoids and their glucosides are the major constituents in restharrow root [2] (Fig. 1). Isoflavonoids are phytoestrogens due to their structural similarity to estradiol and possess antioxidant activity. Moreover, isoflavonoids can play an important role in the prevention and treatment of hormone-dependent cancers, osteoporosis, cardiovascular diseases and diseases of civilization like metabolic syndrome or

* Corresponding authors.

E-mail addresses: beni.szabolcs@pharma.semmelweis-univ.hu (S. Béni), kursinszki.laszlo@pharma.semmelweis-univ.hu (L. Kursinszki).

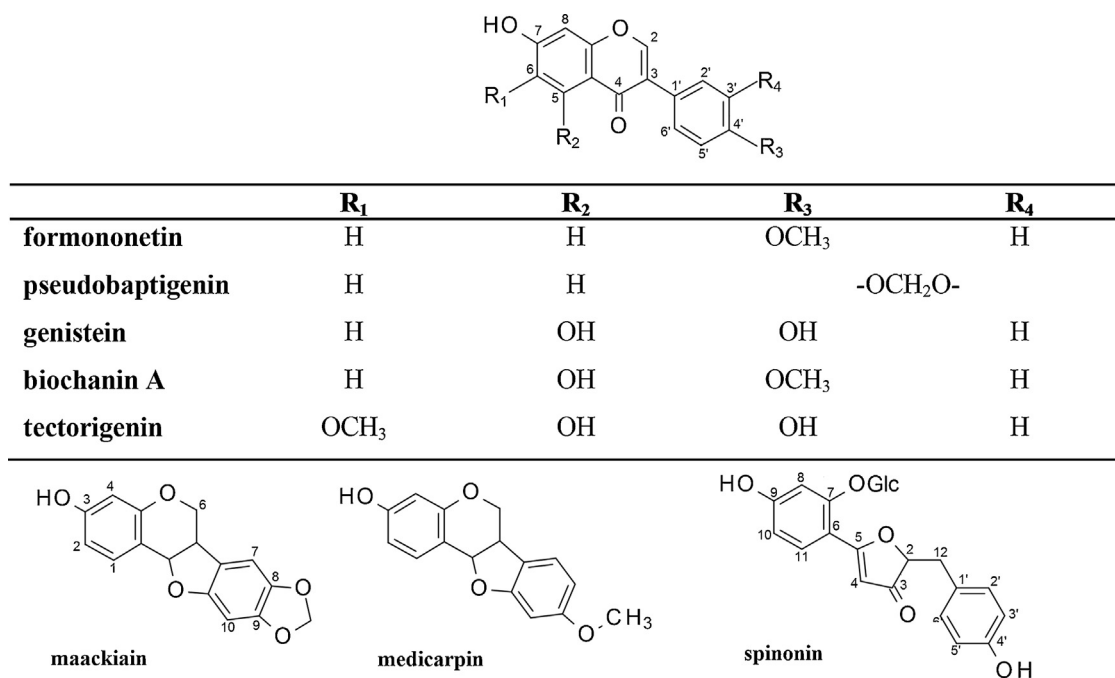


Fig. 1. The structures of the known isoflavonoids along with spinonin in the extract of restharrow root.

polycystic ovary syndrome [5]. As a consequence, plants with high isoflavonoid content (such as soy or red clover) are under thorough investigations. Interestingly, during the traditional use of *O. spinosa* none of the above mentioned effects was observed, therefore we aimed at analyzing the isoflavonoids in restharrow root.

To date, the following isoflavonoids were described in restharrow root: formononetin, ononin (formononetin 7-*O*-glucoside), pseudobaptigenin glucoside, genistein, biochanin A 7-*O*-glucoside 6"-*O*-malonate, formononetin 7-*O*-glucoside 6"-*O*-malonate, 2,3-dihydro-ononin, tectoridin (tectorigenin 7-*O*-glucoside), trifolirhizin (maackiain 7-*O*-glucoside) and medicarpin 7-*O*-glucoside [2] (see Fig. 1).

High performance liquid chromatography is the fundamental technique for separating flavonoids and isoflavonoids. Because isocratic elution is usually insufficient to separate compounds with subtle differences, an optimized gradient elution is preferred for the separation [6].

From an analytical point of view, one of the most powerful tools is mass spectrometry since it provides high sensitivity, opportunities of coupling with liquid chromatography and the possibility of tandem mass spectrometry. Single stage MS joined with UV detector is seldom employed for full structural characterization, but if standards or reference data are available it is efficient for confirming or identifying target isoflavonoids. Tandem mass spectrometry grants various utilization modes which can be remarkably helpful in the investigation of flavonoid derivatives. The highest sensitivity can be reached by negative ionization mode, on the other hand, positive ionization mode yields a more complete fragmentation profile of the structurally similar aglycones [7]. With the application of Q-TOF hybrid instruments an accurate mass determination can be performed. As a result, the molecular formula of the investigated substance can be calculated and isobar molecules and molecule fragments can be differentiated.

In the structural elucidation of unknown molecules the application of various NMR techniques is inevitable. This technique is essential to distinguish positional isomers of flavonoids and isoflavonoids with a complete assignment of the aglycone skeleton. On the other hand, NMR requires considerably large amounts

of substances, therefore preparative sample isolation has to be performed.

Previous studies on the isoflavonoids in the spiny restharrow root confirmed the presence of the major representatives, however their structural identification strongly relied on UV data [8–13]. In addition, high temperature was applied during the extraction precluding the analysis of the glucosides and glucoside malonates [11,13]. Until now, no efforts have been made to systematically identify the isoflavonoid profile of *O. spinosa*. Therefore, the aim of this study is to provide detailed structural information on the isoflavonoid profile of the aqueous-methanolic extract of *O. spinosa* root by HPLC-ESI-MS/MS, HPLC-ESI-QTOF-MS in positive ionization mode and NMR.

2. Experimental

Formononetin and calycosin were purchased from Sigma-Aldrich (Steinheim, Germany). Ononin was kindly provided by Professor S. Antus (University of Debrecen, Hungary), medicarpin and maackiain by Professor J. Hohmann (University of Szeged, Hungary). Standard solutions of ononin, formononetin and calycosin were prepared at 1 mg/mL concentration in 70% v/v methanol. Standard solutions of medicarpin and maackiain were prepared at 300 µg/mL concentration in a mixture of methanol and DMSO (9:1, v/v). HPLC-grade methanol and DMSO were obtained from Sigma Aldrich (Steinheim, Germany). CD₃OD (99.8 atom% D) for NMR were purchased from Sigma-Aldrich (Steinheim, Germany). Purified water prepared by Millipore Milli-Q equipment (Billerica, MA, USA) was used throughout the study. All other chemicals were of analytical reagent grade.

2.1. Sample preparation

2.1.1. Analytical sample

O. spinosa L. (*Fabaceae*) root was obtained from Biohorticulture Bio-Berta (Kiskörös, Hungary) and was received in a dried and chopped form according to the 8th European Pharmacopoeia. Voucher specimens were deposited in the Department of Pharma-

cognosy, Semmelweis University, Budapest with voucher number 141016-On06.

From the dried and powdered sample 0.5 g was extracted with 2×30 mL of aqueous methanol (3:7, v/v) by sonication for 2×6 min (Braun Labsonic U, Melsungen, Germany). After filtration the solvent was evaporated to dryness under reduced pressure (Büchi Rotavapor R-200, Flawil, Switzerland). The residue was redissolved in 2.5 mL of 70% v/v methanol and passed through Supelclean SPE LC-18 column (500 mg, 3 mL; Supelco, Bellefonte, PA, USA). SPE micro columns were activated with 2.5 mL methanol and water before 2.5 mL stock solution was loaded. After air drying the cartridge 1.5 mL methanol was applied to achieve complete elution of isoflavonoids. Prior to HPLC analysis the eluted extract was evaporated to dryness again and redissolved in 2.0 mL 70% v/v methanol and filtered through Minisart RC 15 0.2 μ m membrane (Sartorius AG, Goettingen, Germany).

2.1.2. Extraction and isolation of aglycones

The same plant material was used for preparative samples. 10.0 g dried and powdered plant material was hydrolyzed and extracted with the mixture of 400 mL acetone and 40 mL of 25% v/v hydrochloric acid for 60 min on its boiling point with reflux. After filtration, the extract was diluted with 800 mL purified water and was partitioned with petroleum ether and ethyl-acetate. The ethyl-acetate phase was evaporated to dryness under reduced pressure and the residue was dissolved in methanol and filtered, since the extract contains considerable amount of saccharide. The methanolic phase was evaporated again in order to concentrate the extract and the residue was redissolved in 5.0 mL methanol and filtered through Minisart RC 15 0.2 μ m membrane (Sartorius AG, Göttingen, Germany). The solution was fractionated by a Waters 2690 HPLC system with a Waters 996 diode array detector (Waters Corporation, Milford, MA, USA) equipped with a Luna C18(2) 100 A (5 μ m) reversed phase column (150 \times 10.00 mm i.d.; Phenomenex, Inc; USA). Eluents consisted of 0.3% v/v acetic acid (A) and methanol (B). The following gradient program was applied: 0.0 min, 10% B; 30.0 min, 100% B; 34 min, 100% B. Solvent flow rate was 4.0 mL/min and the column temperature was set to 30 °C, 100 μ L extract was subjected on the column. The fraction containing the aglycones of interest was collected and evaporated to dryness, finally redissolved in methanol. This solution was injected again to the same column using isocratic elution. The mobile phase consisted of 27% acetonitrile and 73% of the aqueous solvent. Altogether seven fractions were collected of which Fr2 was determined as formononetin (2.11 mg), Fr4 as onogenin (2.08 mg) and Fr6 as sativanone (2.54 mg).

2.1.3. Extraction and isolation of glucosides

20.0 g dried and powdered plant material was extracted with 2×200 mL of 70% methanol in ultrasonic bath for 2×25 min. The extract was filtered and evaporated to 100 mL. Four SPE micro columns (500 mg, 3 mL; Supelco, Bellefonte, PA, USA) were activated with 2×2.5 mL methanol and 2×2.5 mL water. 3×2.5 mL of the extract were applied on each cartridge, then washed with 2.5 mL water and the glucosides were eluted with 2.5 mL of 50% v/v methanol. These fractions were pooled and evaporated to dryness, redissolved in 1.5 mL of 50% v/v methanol and filtered before partitioned by HPLC. The same equipment was used for separation as mentioned in 2.1.2. and 100 μ L was injected. Mobile phases consisted of methanol (B) and 0.3% v/v acetic acid (A). Linear gradient elution was applied from 30% B up to 38% B from start to 12.0 min, 70% B from 12.1 min to 22.0 min. Flow rate was 4.0 mL/min, column temperature was 30 °C. Fr3 was determined as spinonin (11.80 mg).

2.2. HPLC-DAD-ESI-MS/MS conditions

For chromatographic separation and mass spectral analysis an Agilent 1100 HPLC system (degasser, binary gradient pump, autosampler, column thermostat and diode array detector) was used hyphenated with an Agilent 6410 Triple Quad LC/MS system equipped with ESI ion source (Agilent Technologies, Santa Clara, CA, USA).

HPLC separation was attained on a Zorbax SB-C18 Solvent Saver Plus (3.5 μ m) reversed phase column (150 \times 3.0 mm i.d.; Agilent Technologies, Santa Clara, CA, USA). Mobile phase consisted of 0.3% v/v formic acid (A) and methanol (B). The following gradient program was applied: 0.0 min, 29% B; 32.0 min, 80% B; 34 min, 100% B; 37 min, 100% B; 42.0 min, 29% B. Solvent flow rate was 0.4 mL/min and the column temperature was set to 25 °C. The injection volume was 2 μ L. Nitrogen was applied as drying gas at the temperature of 350 °C at 9 L/min, the nebulizer pressure was 45 psi. Full scan mass spectra were recorded in positive ion mode in the range of m/z 80–1500.

For collision induced dissociation (CID) the collision energy varied between 10 and 60 eV. As collision gas high purity nitrogen was used. The fragmentor voltage was set to 80 V and the capillary voltage was 3500 V. Product ion mass spectra were recorded in positive ion mode in the range of m/z 80–600.

2.3. HPLC-DAD-ESI-QTOF conditions

For exact mass determination an Agilent 1200 Series HPLC system was used hyphenated with an UV-vis diode array detector (DAD) and with an Agilent 6520 Time of Flight Mass spectrometer (Agilent Technologies, Santa Clara, CA, USA) equipped with an ESI ion source (dual electro-spray) operated in positive ionization mode. HPLC separation was attained on a Zorbax SB-C18 Solvent Saver Plus (3.5 μ m) reversed phase column (150 \times 3.0 mm i.d.; Agilent Technologies, Santa Clara, CA, USA). Mobile phase consisted of 0.3% v/v formic acid (A) and methanol (B). The following gradient program was applied: 0.0 min, 29% B; 32.0 min, 80% B; 34 min, 100% B; 37 min, 100% B; 42.0 min, 29% B. Solvent flow rate was 0.4 mL/min and the column temperature was set to 25 °C. The injection volume was 2 μ L and 30% of the eluent was allowed to flow into the mass spectrometer by solvent splitting. Nitrogen was applied as drying gas at the temperature of 325 °C at 5 L/min, the nebulizer pressure was 30 psi. Full scan mass spectra were recorded in positive ion mode in the range of m/z 80–1200.

For collision induced dissociation (CID) the collision energy varied between 10 and 60 eV. As collision gas high purity nitrogen was used. The fragmentor voltage was set to 175 V and the capillary voltage was 3500 V. Product ion mass spectra were recorded in positive ion mode in the range of m/z 25–700.

2.4. NMR conditions

All NMR experiments were carried out on a 600 MHz Varian DDR NMR spectrometer equipped with a 5 mm inverse-detection gradient (IDPFG) probehead. Standard pulse sequences and processing routines available in Vnmrj 3.2C/Chempack 5.1 were used for structure identifications. The complete resonance assignments were established from direct ^1H - ^{13}C , long-range ^1H - ^{13}C , and scalar spin-spin connectivities using 1D ^1H , ^{13}C , ^1H - ^1H gCOSY, ^1H - ^1H NOESY, ^1H - ^{13}C gHSQCAD ($J = 140$ Hz), ^1H - ^{13}C gHMBCAD ($J = 8$ Hz) experiments, respectively. The probe temperature was maintained at 298 K and standard 5 mm NMR tubes were used. The ^1H chemical shifts were referenced to the applied NMR solvent CD_3OD (δ (CD_2HOD) = 3.310 ppm) and ^{13}C chemical shifts were referenced to 49.00 ppm.

3. Result and discussion

Considering the literature data a liquid chromatographic method was developed to separate the isoflavonoids in the extract of restharrow root. The obtained chromatogram can be seen in Fig. 2. According to their hydrophobicity, firstly glucosides, followed by the glucoside malonates and glucoside acetates eluted, finally the aglycones reached the detector. In contrary to previous works, in the methanolic-aqueous extract of *O. spinosa* two sets of glucoside malonates could be detected. According to the experiments of de Rijke et al. the major and later eluting ones were identified as 7-*O*- β -D-glucoside 6''-*O*-malonates while the minor ones eluting earlier as 7-*O*- β -D-glucoside 4''-*O*-malonates, respectively [14]. The elution order of glucosides and their 4''-*O*-malonate derivatives follows the same pattern, ie: calycosin, pseudobaptigenin, formononetin, onogenin and sativanone. The major glucoside malonates and aglycones showed a different order which could be originated from the gradient elution. To screen for isoflavonoid derivatives in *O. spinosa* root extract, sample was investigated in full scan mode. For the identification of isoflavonoids, the total ion chromatogram was compared to the one registered by UV as the former was rather complex solely. Under the employed conditions protonated molecular ions, monomer and dimer sodium adducts were observable. Ion source fragmentation occurred frequently; therefore information on the aglycones could be gained as well. Altogether 34 compounds (labeled as peak 1, 2 etc. according to elution order) were identified as isoflavonoid derivatives (see Table 1). For complete structure identifications MS/MS scan mode was chosen. In the characterization of aglycone isomers and the elucidation of fragmentation pathways product ion analysis provided invaluable help.

3.1. Isoflavones

In the case of isoflavone aglycones two characteristic fragmentation pathways can be distinguished: the retrocyclization of the C-ring, or the gradual degradation of the molecule. The most common retrocyclization is the retro Diels-Alder (rDA) reaction in which the molecule cleaves alongside the bonds 1 and 3 creating two product ions containing intact A and B-rings. Both fragments can be protonated, but the $^{1,3}A^+$ fragment could be observed more frequently. Fragmentation nomenclature according to Ma et al. [15] can be seen in Fig. 3. The other fragmentation pathway, the gradual degradation of the molecule occurs by the loss of CO, CH₃ and CH₄O. The loss of two CO moieties with the expansion of the C-ring is diagnostic for isoflavonoids [16]. Only methoxylated molecules can lose a CH₃ radical, which leads to a product ion with even electrons. In the extract, three isoflavones and their derivatives were found. The fragmentation properties of formononetin standard were studied first in positive ESI-MS and ESI-MS/MS experiments, to provide entry points in structure elucidation of isoflavonoids. MS data obtained was in accordance with other literature sources [16,17]. Formononetin provided protonated molecular ion [M+H]⁺ at *m/z* 269 and yielded main fragments at *m/z* 254, 237, 226, 213, 136, 118, respectively. The fragmentation pathway, in which the gradual degradation of the molecule occurs by the loss of CO, CH₃ and CH₄O units can be seen in the product ion spectrum of formononetin: *m/z* 254 [M+H-CH₃]⁺, *m/z* 237 [M+H-CH₄O]⁺, *m/z* 226 [M+H-CH₃-CO]⁺, *m/z* 213 [M+H-CO-CO]⁺. Regarding retro Diels Alder reaction *m/z* 137 [$^{1,3}A$]⁺ and *m/z* 118 [$^{1,3}B-CH_3$]⁺ could be easily assigned to the appropriate fragments, however beside *m/z* 137 (13.15%), *m/z* 136 (15.18%) can be observed at 43 eV collision energy. In the case of an odd *m/z* value for the pseudo molecular ion, the loss of the CH₃ radical yields product ion with even *m/z* value. However, the origin of the *m/z* 136 fragment can not be explained as A-ring of formononetin is not methylated. Maul et al. [17] experienced the same

phenomenon, namely a fragment, 1 Da less than the expected rDA fragment, was additionally observed and explained this with the formation of charged but not protonated rDA A-ring. It is found, that this mechanism occurs only in the case of isoflavonoids *O*-methylated on the B-ring, such as formononetin or biochanin A.

In the extract of *O. spinosa* root we managed to determine five formononetin derivatives. They differed in the mass of pseudo molecular ion but possessed identical collision-induced dissociation patterns. Peak 9 provided [M+H]⁺ ion at *m/z* 431 and was identified as ononin also confirmed by authentic standard. Peak 13 and 21 both were tentatively identified as formononetin *O*-glycoside malonates since they showed identical product ion spectrum and [M+H]⁺ at *m/z* 517, although there was a more than 2 min difference in their retention time. Peak 25 was identified as formononetin *O*-glycoside-acetate as it exhibited an [M+H]⁺ ion at *m/z* 473 and CID resulted in [M+H-204]⁺ at *m/z* 269 related to the neutral loss of an acetyl-glycoside residue. The retention time is also in accordance with the structure as glucoside acetate elutes between glucoside malonates and the aglycone. Peak 33 possessed the same spectrum as the standard so it was confirmed to be formononetin aglycone.

Compound 1, 2, 4 and 7 were derivatives with [M+H]⁺ at *m/z* 285 in full scan mode. Among the known compounds of *O. spinosa* reported in the literature, biochanin A and maackiain both possess 284 Da molecular weights (Fig. 1). However, these aglycones could be excluded. Maackiain has a rigid, apolar pterocarpan core structure which contradicts early elution and the product ion spectrum of its authentic standard differed from the observed ones. Biochanin A possesses a hydroxyl group in C5 position, capable of hydrogen bonding with the oxo group, resulting in a significant increase in its retention time [18]. Moreover, since biochanin A is dihydroxylated on A-ring, it gives a $^{1,3}A^+$ rDA fragment at *m/z* 153 which could not be observed. On the other hand, a fragment ion at *m/z* 137 appears indicating an aglycone with a single OH group on A-ring (Fig. 4). Based on these information, the presence of calycosin is much more corroborated by experimental facts, therefore the presence of biochanin A can be excluded. Supporting that the investigated molecules are the glucosidic derivatives of calycosin, their spectra were compared with that of the authentic standard and literature data as well, and they were in good agreement. In addition, calycosin is the link between formononetin and pseudobaptigenin in the biosynthesis of isoflavonoids [19]. Peaks 1, 2, 4 and 7 exhibited product ions *m/z* 285 [Y₀+H]⁺, 270 [Y₀+H-CH₃]⁺, 253 [Y₀+H-CH₄O]⁺, 225 [Y₀+H-CH₄O-CO]⁺, 214 [Y₀+H-CH₃-2CO]⁺, 197 [Y₀+H-CH₄O-2CO]⁺ and 137 [$^{1,3}A$]⁺ (Table 1). Peaks 1 and 2 were identified as calycosin glycosides as calycosin 7-*O*-glucoside is more polar than 3'-*O*-glucoside [20]. Most isoflavonoid glucosides bear a sugar moiety at the C-7 position, however, as calycosin has two hydroxyl groups it is possible that in a less significant amount of C-3' glucosides are also biosynthesized. Peaks 4 and 7 were determined as calycosin glucoside malonate isomers. Calycosin and its derivatives have not been found in *O. spinosa* till date. Peak 8, 12, 19, 24 and 31 showed aglycone fragment at *m/z* 283 and possessed similar fragmentation pattern as calycosin (Table 1). Based on the 2 Da difference and the similarity of fragmentation patterns these compounds were identified as pseudobaptigenin glucoside, pseudobaptigenin glucoside malonate isomers, pseudobaptigenin glucoside acetate and pseudobaptigenin aglycone, respectively (Fig. 1). The fragmentation pathway of pseudobaptigenin has not been described yet. However, comparing the structures of calycosin and pseudobaptigenin high similarity can be seen since calycosin is the precursor of the latter. While on the B-ring of calycosin a methoxy and a hydroxyl group are located, pseudobaptigenin possesses a methylenedioxy group at the same position (see Figs. 1 and 4). Following the cleavage of a CH₄O and a CH₂O unit for calycosin and pseudobaptigenin,

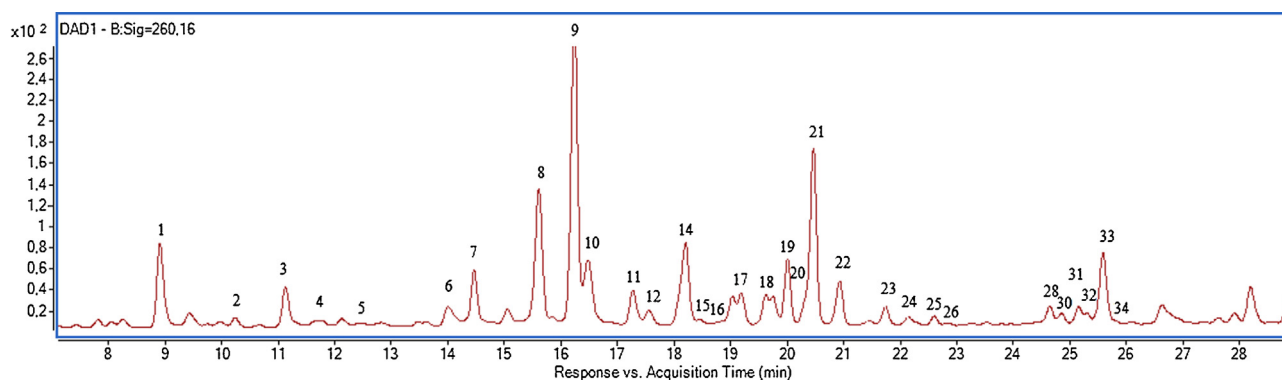


Fig. 2. UV-DAD chromatogram of the aqueous-methanolic extract of spiny restharrow root on a Zorbax SB-C18 Solvent Saver Plus column.

Table 1

The observed and calculated exact masses along with the characteristic product ions of the identified compounds.

No.	R _t	[M+H] ⁺ m/z	M _t observed Da	M _t calculated Da	Error ppm	Aglycon m/z	Fragments	Name
1	8.93	447	446.1224	446.1213	2.47	285	270, 253, 225, 214, 197, 137	Calycosin 7-O-β-D-glucoside
2	10.18	447	446.1210	446.1213	-0.67	285		Calycosin 3'-O-β-D-glucoside
4	11.64	533	532.1221	532.1217	0.75	285		Calycosin 7-O-β-D-glucoside 4''-O-malonate
7	14.53	533	532.1228	532.1217	2.07	285		Calycosin 7-O-β-D-glucoside 6''-O-malonate
3	11.18	461	460.1370	460.1369	0.22	299	281, 253, 239, 193, 107	Spinonin
5	12.69	547	546.1373	546.1373	0.00	299		Spinonin 4''-O-malonate
6	14.09	547	546.1375	546.1373	0.37	299		Spinonin 6''-O-malonate
29	24.86	299	298.0842	298.0841	0.34	299		Spinonin aglycone
8	15.65	445	444.1068	444.1056	2.70	283	253, 225, 197, 183, 169, 141, 115	Pseudobaptigenin 7-O-β-D-glucoside
12	17.62	531	530.1062	530.1060	0.38	283		Pseudobaptigenin 7-O-β-D-glucoside 4''-O-malonate
19	20.09	531	530.1063	530.1060	0.57	283		Pseudobaptigenin 7-O-β-D-glucoside 6''-O-malonate
24	22.22	487	486.1166	486.1162	0.82	283		Pseudobaptigenin 7-O-β-D-glucoside 6''-O-acetate
31	25.27	283	282.0530	282.0528	0.71	283		Pseudobaptigenin
9	16.26	431	430.1264	430.1264	0.00	269	254, 237, 226, 213, 197, 136, 118	Formononetin 7-O-β-D-glucoside
13	18.14	517	516.1269	516.1268	0.19	269		Formononetin 7-O-β-D-glucoside 4''-O-malonate
21	20.55	517	516.1280	516.1268	2.33	269		Formononetin 7-O-β-D-glucoside 6''-O-malonate
25	22.69	473	472.1368	472.1369	-0.21	269		Formononetin 7-O-β-D-glucoside 6''-O-acetate
33	25.78	269	268.0737	268.0736	0.37	269		Formononetin
10	16.54	477	476.1325	476.1332	-1.47	315	297, 287, 257, 229, 177, 163, 147, 135	Onogenin 7-O-β-D-glucoside
15	18.34	563	562.1324	562.1323	0.18	315		Onogenin 7-O-β-D-glucoside 4''-O-malonate
18	19.69	563	562.1328	562.1323	0.89	315		Onogenin 7-O-β-D-glucoside 6''-O-malonate
28	24.60	315	314.0794	314.0790	1.27	315		Onogenin
11	17.35	463	462.1533	462.1526	1.51	301	283, 273, 213, 163, 151, 135, 121, 107	Sativanone 7-O-β-D-glucoside
16	18.98	549	548.1532	548.1530	0.36	301		Sativanone 7-O-β-D-glucoside 4''-O-malonate
20	20.26	549	548.1538	548.1530	1.46	301		Sativanone 7-O-β-D-glucoside 6''-O-malonate
26	22.84	505	504.1630	504.1632	-0.40	301		Sativanone 7-O-β-D-glucoside 6''-O-acetate
32	25.37	301	300.0998	300.0998	1.33	301		Sativanone
14	18.25	447	446.1215	446.1213	0.45	285	175, 165, 151, 147, 135, 123	Maackiain 3-O-β-D-glucoside
22	21.00	533	532.1219	532.1217	0.38	285		Maackiain 3-O-β-D-glucoside 6''-O-malonate
30	24.93	285	284.0686	284.0685	0.35	285		Maackiain
17	19.25	433	432.1423	432.1420	0.69	271	161, 147, 137, 123, 109	Medicarpin 3-O-β-D-glucoside
23	21.81	519	518.1425	518.1424	0.19	271		Medicarpin 3-O-β-D-glucoside 6''-O-malonate
27	24.46	475	474.1524	474.1526	-0.42	271		Medicarpin 3-O-β-D-glucoside 6''-O-acetate
34	25.84	271	270.0895	270.0892	1.11	271		Medicarpin

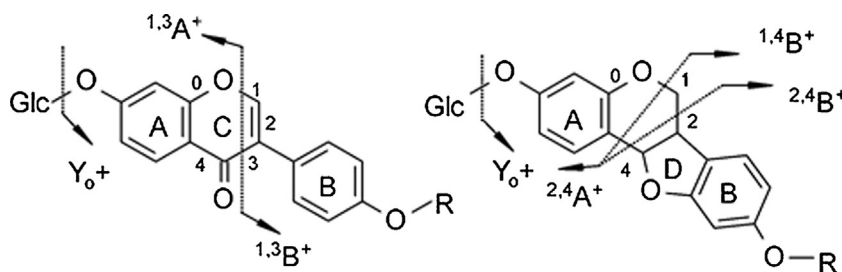


Fig. 3. Proposed fragmentation pathways of isoflavones and pterocarpan.

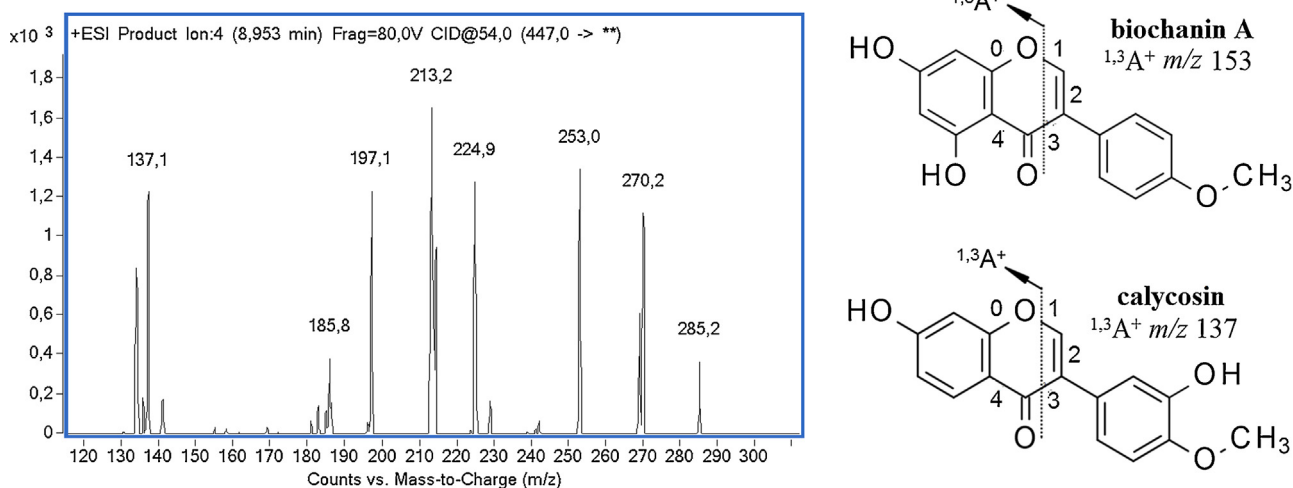


Fig. 4. ESI-MS/MS spectra of compound 1 and the rDA fragmentation of biochanin A and calycosin.

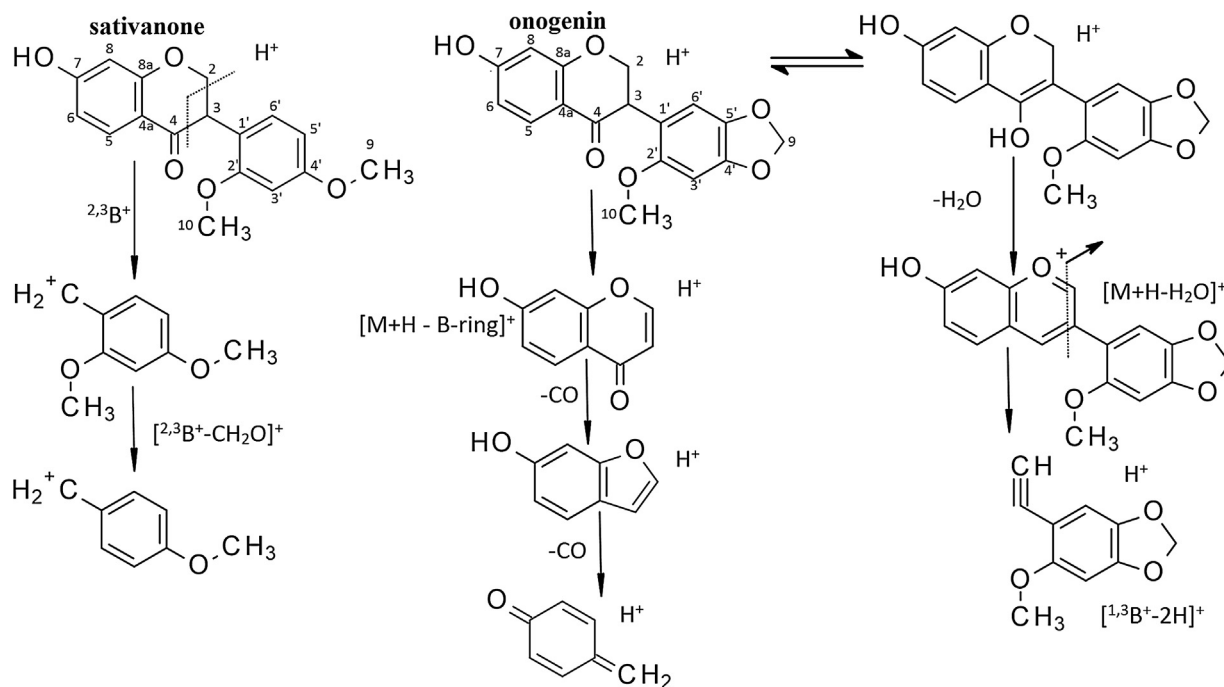


Fig. 5. The proposed fragmentation pathways of sativanone and onogenin.

respectively, the degradation pathways of the two molecules show considerable similarity. The lack of the m/z 270 product ion in the MS/MS spectrum of pseudobaptigenin is also diagnostic since no methyl loss can occur in the case of pseudobaptigenin (see Table 1). Other characteristic fragments detected for pseudobaptigenin are m/z 183, m/z 169 and m/z 141.

3.2. Pterocarpan

Peak 14, 22 and with the same m/z 285 were determined as monoglucoside and glucoside malonate of maackiain; while peak 30 was identified as the free aglycone (Fig. 1). Observed fragments can be assigned based on the pathway suggested by Zhang et al. [21] as m/z 285 $[M+H]^+$, m/z 175 $[M+H-C_6H_6O_2]^+$, m/z 151 $[2,4B]^+$, m/z 123 $[2,4B-CO]^+$ (Fig. 3). These results were confirmed with authentic standard as well.

In the determination of peaks 17, 23, 27 and 34 the same analogy could be used. According to the retention times and the molecular mass of the aglycone these compounds were identified as medicarpin glucoside, medicarpin glucoside malonate and medicarpin (Fig. 1). The fragmentation pattern of medicarpin was deduced from that of maackiain due to high structural similarity. Both medicarpin glucoside and the aglycone followed directly the corresponding peaks of maackiain glucoside and maackiain. Maackiain and medicarpin are both pterocarpan derivatives differing in the substitution of B-ring. Maackiain possesses a methylenedioxy substituent while medicarpin has a single methoxy group. This 14 Da mass difference between the two compounds can be observed by pairing their product ions as well. In the spectrum of medicarpin derivatives product ions could be determined as follows: m/z 271 $[Y_0+H]^+$, m/z 161 $[Y_0+H-C_6H_6O_2]^+$, m/z 137 $[2,4B]^+$, m/z 109 $[2,4B-CO]^+$ while fragment ion of m/z 123 could be found in the case of both maackiain and medicarpin, so that it was identified as $[2,4A]^+$ (Table 1). The

Table 2¹H- and ¹³C NMR data of onogenin, sativanone and spinonin.

No.	Onogenin		Sativanone		Spinonin	
	¹ H	¹³ C	¹ H	¹³ C	¹ H	¹³ C
2	4.50–4.55 (m, 1H) 4.39–4.43 (m, 1H)	72.0	4.53–4.57 (m, 1H) 4.39–4.43 (m, 1H)	72.0	6.11–6.09 (m, 1H)	86.3
3	4.18 (dd, <i>J</i> = 11.6, 5.5 Hz, 1H)	49.2	4.16 (dd, <i>J</i> = 11.4, 5.4 Hz, 1H)	49.1	–	176.5
4	–	194.1	–	194.3	6.11 (d, <i>J</i> = 1.5 Hz, 1H)	113.7
4a	–	115.5	–	–	–	–
5	7.76 (d, <i>J</i> = 8.7 Hz, 1H)	130.3	7.76 (d, <i>J</i> = 8.7 Hz, 1H)	130.3	–	169.0
6	6.50 (dd, <i>J</i> = 8.7, 2.3 Hz, 1H)	112.5	6.50 (dd, <i>J</i> = 8.7, 2.3 Hz, 1H)	112.0	–	112.8
7	–	–	–	–	–	158.3
8	6.32 (d, <i>J</i> = 2.3 Hz, 1H)	103.7	6.32 (d, <i>J</i> = 2.3 Hz, 1H)	103.7	6.80 (d, <i>J</i> = 2.3 Hz, 1H)	103.7
8a	–	165.7	–	165.7	–	–
9	5.89 (d, <i>J</i> = 1.4 Hz, 2H)	102.6	3.79 (s, 3H)	55.8	–	163.5
10	3.72 (s, 3H)	57.1	3.76 (s, 3H)	56.0	6.58 (dd, <i>J</i> = 8.6, 2.3 Hz, 1H)	111.4
11	–	–	–	–	7.37 (d, <i>J</i> = 8.6 Hz, 1H)	132.6
12	–	–	–	–	3.20 (dd, <i>J</i> = 14.8, 3.6 Hz, 1H)	39.4
					2.78 (dd, <i>J</i> = 14.7, 6.6 Hz, 1H)	
1'	–	117.1	–	–	–	128.0
2'	–	154.3	–	159.8	6.92 (d, <i>J</i> = 8.4 Hz, 2H)	131.9
3'	6.69 (s, 1H)	96.4	6.57 (d, <i>J</i> = 2.4 Hz, 1H)	99.9	6.63 (d, <i>J</i> = 8.4 Hz, 2H)	115.8
4'	–	142.8	–	162.2	–	157.3
5'	–	149.3	6.49 (dd, <i>J</i> = 8.4, 2.4 Hz, 1H)	106.0	–	–
6'	6.61 (s, 1H)	110.9	7.00 (d, <i>J</i> = 8.4 Hz, 1H)	131.9	–	–
1''	–	–	–	–	5.02 (d, <i>J</i> = 7.3 Hz, 1H)	102.0
2''	–	–	–	–	3.47–3.5 (m, 1H)	74.7
3''	–	–	–	–	3.44–3.47 (m, 1H)	78.3
4''	–	–	–	–	3.42–3.45 (m, 1H)	71.3
5''	–	–	–	–	3.49–3.52 (m, 1H)	78.5
6''	–	–	–	–	3.97 (dd, <i>J</i> = 12.1, 2.3 Hz, 1H)	62.6
					3.73–3.77 (m, 1H)	

same product ions could be observed in the spectrum of medicarpin standard.

3.3. Dihydroisoflavones

In the plant extract two aglycones were observed with exact molecular masses and predicted formulas which had not been mentioned in the literature of *O. spinosa* before. Since their CID spectra differed significantly from that of isoflavones and pterocarpans, tandem mass spectrometry experiments alone did not provide satisfactory evidence to identify the aglycon skeleton. From the hydrolyzed plant extract the aglycones were isolated and were unequivocally identified by NMR experiments as sativanone and onogenin (Fig. 5). The complete resonance assignments can be seen in Table 2.

Investigating the tandem mass spectra of isoflavones some common features can be observed. Both molecules tend to lose one CO moiety and H₂O. However, sativanone and onogenin are methoxylated derivatives, the cleavage of a CH₃ radical or CH₃O moiety can not be seen. Opposed to isoflavones, these dihydroisoflavans do not yield rDA fragments from the intact molecule. Sativanone and onogenin are identical considering the A and C-ring and differ only in the substitution of the B-ring alike medicarpin and maackiain. The fragments with *m/z* 163, 135, 107 are present in the spectra of both dihydroisoflavones so it was concluded that these fragments originated from corresponding parts of the aglycons. Regarding this, the product ions were assigned as [M+H-B-ring]⁺, [M+H-B-ring-CO]⁺, [M+H-B-ring-2CO]⁺, respectively (Fig. 5). There is 14 Da difference between the mass of the two molecules, which is the result of different B-ring. This difference is present between product ion *m/z* 177 of onogenin and *m/z* 163 of sativanone, too. Consequently, these fragments were assigned as [^{1,3}B-2H]⁺ (Fig. 5). There could be perceived some differences between the fragmentation pathways of the two dihydroisoflavones. Firstly, product ions *m/z* 257 [M+H-CH₂O-CO]⁺ and *m/z* 229 [M+H-CH₂O-2CO]⁺ were only present in the MS/MS spectrum of onogenin, while these could not be found

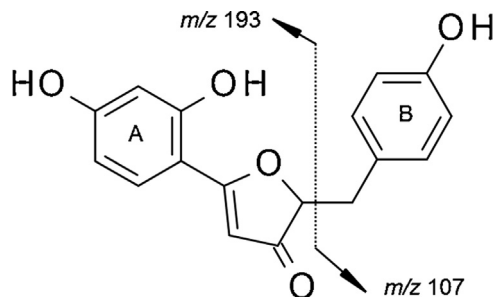


Fig. 6. The proposed fragmentation of spinonin aglycone.

in the product ion spectrum of sativanone (Table 1). On the other hand, only sativanone yields product ions *m/z* 151 [^{2,3}B-CH₂O]⁺ and *m/z* 121 [^{2,3}B-CH₂O]⁺ (Fig. 5). Based on these facts, peaks 11, 16, 20, 26 and 32 were identified as the glucoside, glucoside malonates, glucoside acetate and the aglycone of sativanone, respectively. Peaks 10, 15, 18 and 28 showed [M+H]⁺ ions at *m/z* 477, 563, 563 and 315, so they were identified as the glucoside, two glucoside malonates and aglycone of onogenin. None of these derivatives were mentioned before in this plant.

3.4. Spinonin

This molecule with a unique aglycone skeleton was firstly mentioned by Kirmizigül et al. [22] (Fig. 1). As its fragmentation pattern was not available in literature and its molecular formula can refer to several isoflavonoids, NMR experiments had to be performed to characterize it unambiguously (Table 2). The following product ions with the characteristic losses were proposed: *m/z* 299 [M+H]⁺, *m/z* 281 [M+H-H₂O]⁺, *m/z* 253 [M+H-H₂O-CO]⁺, *m/z* 239 [M+H-H₂O-C₂H₂O]⁺ (Table 1). In addition, the aglycone can cleave between C2 and C12 to yield product ions *m/z* 193 and *m/z* 107 (Fig. 6). In the extract of *O. spinosa* beside the glucoside two glucoside malonates and the aglycone were present.

4. Conclusions

HPLC-ESI-MS/MS and HPLC-ESI-QTOF-MS analysis in positive ionization mode is a very promising tool for aglycone analysis of isoflavonoids. The MS fragmentations described in this study was successfully applied for the differentiation of structural isomers as biochanin A, calycosin and maackiain; and verify the presence of homologous derivatives as calycosin and pseudobaptigenin or medicarpin and maackiain. On the other hand, in the investigation of new compounds with unknown fragmentation routes and in the exact characterization of aglycon structures NMR must be used.

The presence of formononetin, pseudobaptigenin, medicarpin and maackiain derivatives was confirmed. However, biochanin A, genistein and daidzein, mentioned in earlier works, were not found in the extract. Calycosin, sativanone and onogenin was described for the first time in this plant. Moreover, 4"-O glucoside malonates of pseudobaptigenin, formononetin, calycosin and spinonin beside 6"-O ones were characterized. Fragmentation patterns of medicarpin, pseudobaptigenin, onogenin and sativanone were proposed for the first time.

Acknowledgments

The financial support from OTKA PD 109373 is highly appreciated. Sz. Beni thanks the Hungarian Academy of Sciences for the financial support under the János Bolyai Research Scholarship. The authors gratefully acknowledge the support of Waters Kft. Hungary for providing access to the HPLC system.

References

- [1] ESCOP Monographs: The Scientific Foundation for Herbal Medicinal Products, Thieme, 2003.
- [2] Assessment report on *Ononis spinosa* L., <http://www.ema.europa.eu/docs/en_GB/document_library/Herbal_-_HMPC_assessment_report/2013/08/WC500148188.pdf>.
- [3] P. Bolle, P. Faccendini, U. Bello, *Ononis spinosa* L. pharmacological effect of ethanol extract, *Pharmacol. Res.* 27 (1993) 27–28.
- [4] B. Yilmaz, H. Özbek, G. Çitoğlu, Analgesic and hepatotoxic effects of *Ononis spinosa* L, *Phyther. Res.* 220 (2006) 500–503, <http://dx.doi.org/10.1002/ptr>.
- [5] H. Wiseman, Isoflavonoids and human health, in: O.M. Andersen, K.R. Markham (Eds.), *Flavonoids Chem. Biochem. Appl.*, CRC Press, Boca Raton, 2006, pp. 371–396.
- [6] Pedro F. Pinheiro, Gonçalo C. Justino, (2012). Structural Analysis of Flavonoids and Related Compounds—A Review of Spectroscopic Applications, *Phytochemicals—A Global Perspective of Their Role in Nutrition and Health*, Dr Venketeshwer Rao ISBN: 978-953-51-0296-0, InTech, Available from: <<http://www.intechopen.com/books/phytochemicals-a-global-perspective-of-their-role-in-nutrition-and-health/structural-analysis-of-flavonoids-and-related-compounds-a-review-of-spectroscopic-applications>>.
- [7] L. Abrankó, B. Szilvássy, Mass spectrometric profiling of flavonoid glycoconjugates possessing isomeric aglycones, *J. Mass Spectrom.* (2015) 71–80, <http://dx.doi.org/10.1002/jms.3474>.
- [8] A. Háznagy, G. Tóth, J. Tamás, Über die Inhaltsstoffe des wóürigen Extraktes von *Ononis spinosa* L, *Arch. Pharm.* (Weinheim) 311 (1978) 318–323, <http://dx.doi.org/10.1002/ardp.19783110408>.
- [9] P. Pietta, P. Mauri, E. Manera, P. Ceva, Determination of isoflavones from *Ononis spinosa* L. extracts by high-performance liquid chromatography with ultraviolet diode-array detection, *J. Chromatogr. A* 513 (1990) 397–400, [http://dx.doi.org/10.1016/S0021-9673\(01\)89464-4](http://dx.doi.org/10.1016/S0021-9673(01)89464-4).
- [10] P. Pietta, A. Calatroni, C. Zio, High-performance liquid chromatographic analysis of flavonoids from *Ononis spinosa* L., *J. Chromatogr. A* 280 (1983) 172–175, [http://dx.doi.org/10.1016/S0021-9673\(00\)91555-3](http://dx.doi.org/10.1016/S0021-9673(00)91555-3).
- [11] J. Köster, D. Strack, W. Barz, High performance liquid chromatographic separation of isoflavones and structural elucidation of isoflavone 7-O-glucoside 6"-malonates from *Cicer arietinum*, *Planta Med.* 48 (1983) 131–135, <http://dx.doi.org/10.1055/s-2007-969907>.
- [12] D. Benedec, L. Vlase, I. Oniga, A. Toiu, M. Tãmaş, B. Tiperciuc, Isoflavonoids from *Glycyrrhiza* sp. and *Ononis spinosa*, *Farmacia* 60 (2012) 615–620.
- [13] B. Klejduš, J. Vacek, L. Benešová, Rapid-resolution HPLC with spectrometric detection for the determination and identification of isoflavones in soy preparations and plant extracts, *Anal. Bioanal. Chem.* (2007) 2277–2285, <http://dx.doi.org/10.1007/s00216-007-1606-3>.
- [14] E. de Rijke, F. de Kanter, U.A.T. Ariese, C. Gooijer, Liquid chromatography coupled to nuclear magnetic resonance spectroscopy for the identification of isoflavone glucoside malonates in *T. pratense* L. leaves, *J. Sep. Sci.* 27 (2004) 1061–1070, <http://dx.doi.org/10.1002/jssc.200401844>.
- [15] Y.L. Ma, Q.M. Li, H. Van den Heuvel, M. Claeys, Characterization of flavone and flavonol aglycones by collision-induced dissociation tandem mass spectrometry, *Rapid Commun. Mass Spectrom.* 11 (1997) 1357–1364, [http://dx.doi.org/10.1002/\(SICI\)1097-0231\(199708\)11:12<1357::AID-RCM983>3.0.CO;2-9](http://dx.doi.org/10.1002/(SICI)1097-0231(199708)11:12<1357::AID-RCM983>3.0.CO;2-9).
- [16] F. Kuhn, M. Oehme, F. Romero, E. Abou-Mansour, R. Tabacchi, Differentiation of isomeric flavone/isoflavone aglycones by MS2 ion trap mass spectrometry and a double neutral loss of CO, *Rapid Commun. Mass Spectrom.* 17 (2003) 1941–1949, <http://dx.doi.org/10.1002/rcm.1138>.
- [17] R. Maul, N.H. Schebb, S.E. Kulling, Application of LC and GC hyphenated with mass spectrometry as tool for characterization of unknown derivatives of isoflavonoids, *Anal. Bioanal. Chem.* 391 (2008) 239–250, <http://dx.doi.org/10.1007/s00216-008-1884-4>.
- [18] B. Klejduš, D. Vitamvášová-Štěrbová, V. Kubáň, Identification of isoflavone conjugates in red clover (*Trifolium pratense*) by liquid chromatography-mass spectrometry after two-dimensional solid-phase, *Anal. Chim. Acta.* 450 (2001) 81–97.
- [19] K.M. Davies, K.E. Schwinn, in: O. Andersen, K. Markham (Eds.), *Molecular Biology and Biotechnology of Flavonoid Biosynthesis*, *Flavonoids Chem. Biochem. Appl.*, Boca Raton, 2006, pp. 143–217.
- [20] X.-H. Liu, L.-G. Zhao, J. Liang, L. Guo, Y.-L. Yang, F. Hu, et al., Component analysis and structure identification of active substances for anti-gastric ulcer effects in *Radix Astragali* by liquid chromatography and tandem mass spectrometry, *J. Chromatogr. B. Analyt. Technol. Biomed. Life Sci.* 960 (2014) 43–51, <http://dx.doi.org/10.1016/j.jchromb.2014.04.020>.
- [21] L. Zhang, L. Xu, S.-S. Xiao, Q.-F. Liao, Q. Li, J. Liang, et al., Characterization of flavonoids in the extract of *Sophora flavescens* Ait. by high-performance liquid chromatography coupled with diode-array detector and electrospray ionization mass spectrometry, *J. Pharm. Biomed. Anal.* 44 (2007) 1019–1028, <http://dx.doi.org/10.1016/j.jpba.2007.04.019>.
- [22] S. Kirmizigül, N. Gören, S.W. Yang, G.A. Cordell, C. Bozok-Johansson, Spinonin, a novel glycoside from *Ononis spinosa* subsp. *leiosperma*, *J. Nat. Prod.* 60 (1997) 378–381.



Separation and characterization of homopipecolic acid isoflavonoid ester derivatives isolated from *Ononis spinosa* L. root



Nóra Gampe, András Darcsi, László Kursinszki, Szabolcs Béni*

Semmelweis University, Department of Pharmacognosy, Üllői út 26, H-1085 Budapest, Hungary

ARTICLE INFO

Keywords:

Ononis spinosa L.
Leguminosae
Isoflavonoid
Homopipecolic acid
Piperidin-2-yl-acetic acid
HPLC-MS/MS
NMR

ABSTRACT

Spiny restharrow root (*Ononis spinosa* L.) and its preparations are mainly used for the treatment of urinary infections or bladder stones in numerous countries. Spiny restharrow root is rich in isoflavonoids (formononetin, calycosin and pseudobaptigenin), pterocarpan (medicarpin and maackiain) and dihydroisoflavonoids (onogenin and sativanone), which metabolites are present as glucosides, glucoside malonates, glucoside acetates and free aglycones in the root. The in-depth analysis of tandem mass spectrometric (MS) and high-resolution MS (HR-MS) data revealed the presence of nitrogen-containing compounds in the root extracts. An ion-exchange-based purification and a preparative-scale reversed phase chromatographic isolation procedure was developed for the characterization of these new natural products. For the unambiguous identification of the isolated compounds NMR experiments were carried out. The thorough characterization confirmed the presence of six piperidin-2-yl-acetic acid (homopipecolic acid) esters of isoflavonoid glucosides. This is the first report of homopipecolic acid esters isolated from higher plants.

1. Introduction

The *Ononis* genus includes 75 species, out of which *Ononis spinosa* L. (Fabaceae) is native to the semi-arid grasslands and pastures of Europe, Western Asia and Northern Africa. Spiny restharrow is a perennial subshrub with pink papilionaceous flowers and straight thorns [1]. The dried root of the plant can be found in the 9th European Pharmacopoeia as *Ononidis radix*. The drug and its preparations are used mainly for the treatment of urinary infections or bladder stones [2]. Its diuretic and flushing-out effect were established by *in vivo* studies [3]. However, clinical studies have not been done to confirm the effectiveness in humans.

Several studies aimed to elucidate the chemical composition of Spiny restharrow root. Firstly, Háznagy et al. investigated the essential oil components of the root, and Daruházi et al. described its phytosterol profile [4,5]. In our view, the most promising bioactive secondary metabolites in *Ononidis radix* are the isoflavonoids. Attempts were made to characterize the isoflavonoid content of the plant material [6–8], however the used methods relied mainly on their chromatographic behavior and UV spectra. In our previous work, we have provided the most complete isoflavonoid profile of the aqueous-methanolic extract of the root supported by detailed structural studies. As a result, isoflavonoids (formononetin, calycosin and pseudobaptigenin), pterocarpan (medicarpin and maackiain) and dihydroisoflavonoids

(onogenin and sativanone) were found in the forms of glucosides, glucoside malonates, glucoside acetates and aglycones [9]. The thorough mass spectrometric investigation of the extract in positive ionization mode revealed nitrogen-containing derivatives of the isoflavonoids mentioned above. Previous studies confirmed the presence of anthranilic acid derivatives in the aerial parts of *Ononis* species [10], however the high-resolution mass spectrometry experiments and product ion spectra excluded these structures. Although nitrogen-containing pterocarpan derivatives were reported before [11], the spectroscopic data of these structures were not in agreement with our results, so the isolated compounds must have a different structure. In order to identify the structures of these derivatives, the combination of mass spectrometric and NMR data of the isolated compounds were used. Herein we report the unambiguous identification of six previously undescribed isoflavonoid derivatives from the aqueous-methanolic extract of spiny restharrow root.

2. Material and methods

2.1. General and plant material

HPLC-grade methanol and acetonitrile were obtained from Fisher Scientific (Loughborough, UK). DMSO- d_6 , for NMR measurements was purchased from Sigma-Aldrich (Steinheim, Germany). Purified water

* Corresponding author at: Budapest H-1085, Üllői út 26, Hungary.
E-mail address: beni.szabolcs@pharma.semmelweis-univ.hu (S. Béni).

prepared by Millipore Milli-Q equipment (Billerica, MA, USA) was used throughout the study. All other chemicals were of analytical grade.

Ononis spinosa L. (Leguminosae) root was obtained from Rózsahegyi Ltd. (Erdőkertes, Hungary) and was received in a dried and chopped form according to the 8th European Pharmacopoeia. Other root samples were collected from Dunaegyháza (Hungary, 46°50'56.88" N, 18°56'35.57" E) and Hűvösvölgy (Hungary, 47°33'22.88" N, 18°58'33.89" E) and were identified by Dr. Imre Boldizsár from the Department of Plant Anatomy, Eötvös Loránd University. Voucher specimens were deposited in the Department of Pharmacognosy, Semmelweis University, Budapest with voucher number 141016-On06, 160725-On01 and 150710-On03, respectively.

2.2. Sample preparation of analytical samples

From the dried and powdered sample of all three plant material extracts were made using the same method as described in our previous work [9].

2.3. Extraction and isolation of the isoflavonoid derivatives

300.0 g dried and powdered plant material from Rózsahegyi Ltd. was extracted with 2 × 3000 mL of 70% methanol in ultrasonic bath for 2 × 25 min. The extract was filtered and evaporated to dryness to obtain a dark brown gum. The residue was redissolved in 200 mL water and divided into 5 mL fractions. Each fraction was mixed with 5 mL of methanol and acetone to precipitate the majority of the saccharides. The supernatant was filtered and the organic solvents were evaporated at 45 °C. 10 mL portions of the residual dark solution were passed through a weak cation exchanger cartridge (Strata WCX Giga Tube, Phenomenex Inc.; Torrance, CA, USA) in order to enrich the nitrogen-containing compounds. The SPE cartridges were first conditioned by washing with 20 mL methanol and equilibrated with 20 mL water. The loaded cartridges were washed with 40 mL water and 40 mL methanol then eluted with 5% formic acid in methanol. After evaporation to dryness the sample was fractionated by a Hanbon Newstyle NP7000 HPLC system with a Hanbon Newstyle NP3000 UV detector (Hanbon Sci. & Tech. CO. Jiangsu, China) equipped with a Gemini C18 reversed phase column (150 × 21.2 mm i.d.; 5 μm, Phenomenex Inc.; Torrance, CA, USA). Eluents consisted of 0.3% v/v acetic acid (A) and acetonitrile (B). Gradient elution was used with 10 mL/min flow rate and solvent system with 20% B at 0 min to 30% B in 20 min. Eight fractions were obtained with this method, out of which Fr 1–2 contained degradation products and minor contaminants. From Fr 3 compound 2 (0.6 mg) was obtained as a mixture with another isoflavonoid glucoside derivative. From Fr 4 compound 1 (1.3 mg) was isolated. Compound 4 (1.6 mg) was purified from Fr 5. Fr 6 provided compound 3 (1.5 mg) in high purity. Fr 7 and Fr 8 contained solely the diastereomers of compound 6 (4.5 mg) and compound 5 (3.7 mg), respectively. For investigation of diastereomers, the two isomers of compound 5 and 6 was further purified with the same HPLC equipment. Gradient elution was used with 10 mL/min flow rate and solvent system with 15% B at 0 min to 20% B at 15 min and 20% B at 25 min. The isolated isomers of compound 5 were investigated by NMR experiments and diastereomers of compound 6 were kept at 35 °C and their stability were examined after 1 day, 5 days and 10 days of isolation.

2.4. HPLC-DAD conditions

The isolated isomers of compound 6 and their mixture were examined on a Waters 2690 HPLC system with a Waters 996 diode array detector (Waters Corporation, Milford, MA, USA) equipped with a Xselect reversed phase C18 column (150 × 4.60 mm i.d.; 5 μm, Waters Corporation, Milford, MA, USA). Eluents consisted of 0.3% v/v acetic acid (A) and acetonitrile (B). The following gradient program was applied: 0.0 min, 15% B; 20.0 min, 20% B; 30 min, 20% B. Solvent flow

rate was 1.0 mL/min and the column temperature was set to 25 °C.

2.5. HPLC-DAD-ESI-MS/MS conditions

For chromatographic separation and mass spectrometric analysis an Agilent 1100 HPLC system (degasser, binary gradient pump, auto-sampler, column thermostat and diode array detector) was used hyphenated with an Agilent 6410 Triple Quad LC/MS system equipped with ESI ion source (Agilent Technologies, Santa Clara, CA, USA). For the screening of *Ononis* extracts HPLC separation was attained on a Zorbax SB-C18 Solvent Saver Plus (3.5 μm) reversed phase column (150 × 3.0 mm i.d.; Agilent Technologies, Santa Clara, CA, USA). Mobile phase consisted of 0.3% v/v formic acid (A) and methanol (B). The following gradient program was applied: 0.0 min, 29% B; 32.0 min, 80% B; 34 min, 100% B; 37 min, 100% B; 42.0 min, 29% B. Solvent flow rate was 0.4 mL/min and the column temperature was set to 25 °C. The injection volume was 2 μL. For the separation of diastereomers of nitrogen-containing isoflavonoid glucoside esters the same column was tested beside a Phenomenex Luna C-8 column (300 × 4.6 mm i.d.; 5 μm), a Kinetex C-18 core shell column (100 × 2.1 mm i.d.; 2.6 μm; both Phenomenex Inc.; Torrance, CA, USA) and a Waters XSelect CSH Phenyl-Hexyl column (100 × 2.1 mm i.d.; 2.5 μm; Waters Corporation, Milford, MA, USA). The eluents were 0.1% TFA in water (A) and acetonitrile (B). The injection volume was 1 μL from the eluted fraction gained from the WCX cartridges and the temperature was set to 25 °C. Applying the Zorbax C-18 column, isocratic 25% B was used with 0.4 mL/min flow rate. On the XSelect Phenyl-Hexyl column isocratic 20% B was used with 0.1 mL/min flow rate, while isocratic 25% B was used with 1 mL/min flow rate on the C-8 column. The separation using the Kinetex column required an isocratic method using 20% B with a 0.2 mL/min flow rate. Nitrogen was applied as drying gas at the temperature of 350 °C at 9 L/min, the nebulizer pressure was 45 psi. The fragmentor voltage was set between 100 and 135 V and the capillary voltage was 3500 V. Full scan mass spectra were recorded in positive ion mode in the range of m/z 80–1500. For collision induced dissociation (CID) the collision energy varied between 10 and 40 eV with fragmentor voltage 135 V. As collision gas, high purity nitrogen was used. Product ion mass spectra were recorded in positive ion mode in the range of m/z 80–600.

2.6. HPLC-DAD-ESI-QTOF conditions

For exact mass determination, an Agilent 1200 Series HPLC system was used hyphenated with an UV–vis diode array detector and with an Agilent 6520 Time of Flight Mass spectrometer (Agilent Technologies, Santa Clara, CA, USA) equipped with an ESI ion source (dual electrospray) operated in positive ionization mode. HPLC separation was attained on a Zorbax SB-C18 Solvent Saver Plus (3.5 μm) reversed phase column. The same eluents and gradient program were used as on the Agilent 1100 HPLC system. Solvent flow rate was 0.4 mL/min and the column temperature was set to 25 °C. The injection volume was 2 μL and 30% of the eluent was allowed to flow into the mass spectrometer by solvent splitting. Nitrogen was applied as drying gas at the temperature of 325 °C at 5 L/min, the nebulizer pressure was 30 psi. Full scan mass spectra were recorded in positive ion mode in the range of m/z 80–1200. For collision induced dissociation (CID), the collision energy varied between 20 and 40 eV. As collision gas, high purity nitrogen was used. The fragmentor voltage was set to 175 V and the capillary voltage was 3500 V. Product ion mass spectra were recorded in positive ion mode in the range of m/z 25–700.

2.7. NMR conditions

All NMR experiments were carried out on a 600 MHz Varian DDR NMR spectrometer equipped with a 5 mm inverse-detection gradient (IDPF) probehead. Standard pulse sequences and processing routines

available in VnmrJ 3.2C/Chempack 5.1 were used for structure identifications. The complete resonance assignments were established from direct ^1H - ^{13}C , long-range ^1H - ^{13}C , and scalar spin-spin connectivities using 1D ^1H , ^{13}C , ^1H - ^{13}C gCOSY, ^1H - ^1H NOESY, ^1H - ^1H ROESY (mixing time 300 ms), ^1H - ^1H TOCSY (mixing time 150 ms), ^1H - ^{13}C gHSQCAD ($J = 140$ Hz), ^1H - ^{13}C gHMBCAD ($J = 8$ Hz and 12 Hz) experiments, respectively. The probe temperature was maintained at 298 K and standard 5 mm NMR tubes were used. The ^1H and ^{13}C chemical shifts were referenced to the residual solvent signal $\delta_{\text{H}} = 2.500$ ppm and $\delta_{\text{C}} = 39.52$ ppm, respectively.

2.8. Investigation of optical rotation power and circular dichroism

To isolate isoflavonoid aglycones, 50.0 g dried and powdered plant material from Rózsáhegyi Ltd. was mixed with 500 mL of water to activate the indigenous glycosidase enzymes of the plant for 24 h. After filtration, the extract was evaporated to dryness. 150 mL acetone was added to the dark brown gum to redissolve the isoflavonoid aglycones and to leave behind the saccharides. The extract was filtered and dried to gain 2 g residual. This was redissolved in HPLC methanol to obtain a solution of 100 mg/mL concentration. For the separation of isoflavonoid aglycones the same preparative HPLC system was used. Eluents consisted of 0.3% v/v acetic acid (A) and acetonitrile (B). Gradient elution was used with 10 mL/min flow rate and solvent system with 40% B at 0 min to 43% B in 18 min. Six fractions were obtained with this method, which contained pseudobaptigenin (1.22 mg), formononetin (3.15 mg), onongenin (2.87 mg), sativanone (2.45 mg), maackiain (5.19 mg) and medicarpin (5.26 mg), respectively. The aglycones were redissolved in HPLC methanol to further experiments. Optical rotations were determined on a Carl Zeiss Polamat A polarimeter with a 1 dm cell and MeOH sample solutions at 25 °C. CD spectra of the aglycones were recorded on a Chirascan CD spectrometer (Applied Photophysics Ltd., Leatherhead, United Kingdom). Quartz cells of 10 and 0.1 mm optical path length and an instrument scanning

speed of 100 nm/min with 1 s response time were used for measurements. The measurements are the averages of three repetitions between 200 and 300 nm at room temperature. Spectra were baseline-corrected and the signal contributions of methanol were subtracted.

3. Results and discussion

3.1. LC-MS/MS analysis

The investigation of the analytical samples by LC-MS revealed characteristic nitrogen-containing compounds (1–6) in the total ion chromatogram recorded in positive ionization mode (Fig. 1). The even m/z ratio of these peaks indicates the presence of an odd number of nitrogen atoms in the structures. Comparing the total ion chromatogram (TIC) with the UV chromatogram, remarkable intensity differences were observed in the case of the corresponding peaks (Fig. 1). While the peaks of the nitrogen-containing molecules were predominant in the TIC (due to the efficient ionization), these compounds could hardly be detected in the UV chromatogram. Compounds 5 and 6 showed however significant splitting on the achiral C18 stationary phase, suggesting diastereomeric compounds. The tandem mass spectrometric (MS/MS) data and the accurate mass measurements (Table 1) compared with our previous study confirmed that the molecules of interest are isoflavonoid derivatives [9]. As isoflavonoids possess high molar absorptivity, the UV chromatogram suggested that these compounds are in minute amount in the extract. All six isoflavonoid skeleton (formononetin, pseudobaptigenin, sativanone, onongenin, medicarpin and maackiain) were present in the form of glucosides bearing a nitrogen-containing moiety. Besides the aglycone and its corresponding fragments, each MS/MS spectrum showed characteristic ions at 288.1452, 144.1025 and 84.0810 m/z values, respectively (Fig. 2), suggesting that all the six compounds share a common structural motif linked to the isoflavonoid glucosides. The collision induced dissociation cleaves the molecules alongside the glycosidic bond, resulting in the

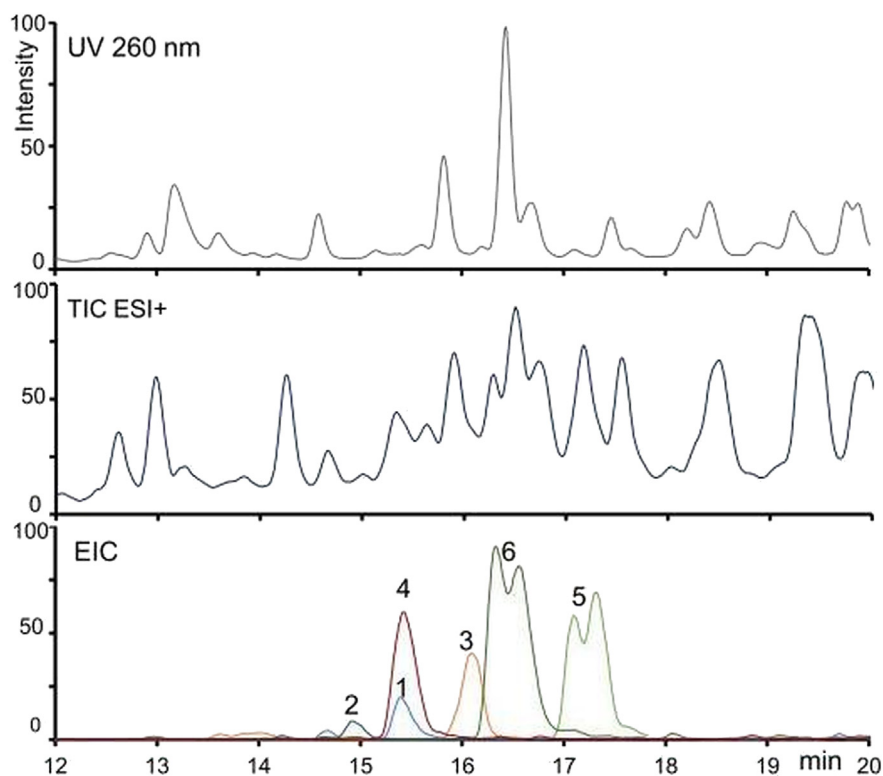


Fig. 1. The extract ion chromatograms of the compounds of interest (EIC, bottom), total ion chromatogram (TIC, middle) along with the UV chromatogram detected at 260 nm (top).

Table 1
Accurate masses and MS/MS data of the six new isoflavonoid derivatives.

No.	R _t min	[M + H] ⁺ m/z	Calc. exact mass for [M + H] ⁺ m/z	Formula	Error ppm	Aglycone ^a m/z	Fragments of the aglycone ^a m/z	N-containing fragments ^b m/z	Name of the compound
1	15.7	556.2183	556.2177	C ₂₉ H ₃₃ NO ₁₀	1.1	269	254, 237	288.1452, 144.1025, 84.0810	Formononetin 7-O-β-D-glucoside 6"-O-piperidin-2-ylacetate
2	15.2	570.1971	570.1970	C ₂₉ H ₃₁ NO ₁₁	0.2	283	270, 253		Pseudobaptigenin 7-O-β-D-glucoside 6"-O-piperidin-2-ylacetate
3	16.4	588.2446	588.2439	C ₃₀ H ₃₇ NO ₁₁	1.2	301	273, 163, 135		Sativanone 7-O-β-D-glucoside 6"-O-piperidin-2-ylacetate
4	15.7	602.2240	602.2232	C ₃₀ H ₃₅ NO ₁₂	1.3	315	287, 163, 135		Onogenin 7-O-β-D-glucoside 6"-O-piperidin-2-ylacetate
5	17.4	558.2353	558.2334	C ₂₉ H ₃₅ NO ₁₀	3.4	271	161, 137, 123		Medicarpin 3-O-β-D-glucoside 6"-O-piperidin-2-ylacetate
6	16.6	572.2149	572.2126	C ₂₉ H ₃₃ NO ₁₁	4.0	285	175, 151, 123		Maackiain 3-O-β-D-glucoside 6"-O-piperidin-2-ylacetate

^a From QQQ-MS/MS experiments.

^b For all compounds.

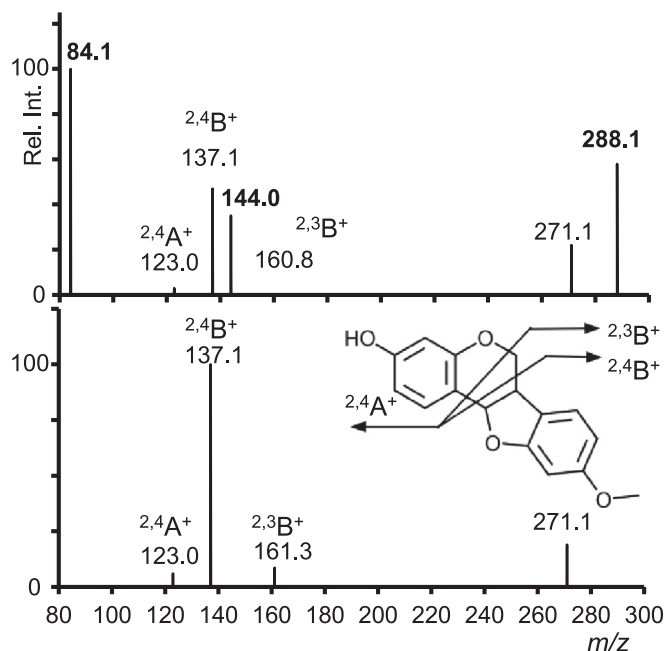


Fig. 2. Partial product ion spectrum of medicarpin 7-O-β-D-glucoside (bottom) and that of medicarpin 7-O-β-D-glucoside-derivative, labeled as compound 5 (top). The *m/z* values in bold face correspond to the nitrogen-containing fragments.

intact aglycone as Y_0^+ and the cleaved fragment composed of the glucose and the nitrogen-containing moiety at *m/z* 288.1452 (Fig. 3). Fragmentation of the isoflavonoid glucoside moiety with a neutral loss results the unknown structure at 144.1025 *m/z* and the protonated formula of $C_7H_{13}NO_2$. This formula may correspond to the common natural compound stachydrine (also known as proline betaine). As this compound can be found in various plants exposed to drought-stress [12], it would be a plausible explanation for its presence in spiny restharrow root, as well. Moreover, the co-localization of isoflavonoid glucosides and stachydrine in plant tissues has already been proven by Ye et al. (2013) [13]. The tandem mass spectrometric results could also support the presence of stachydrine, as the characteristic base peak at 84 *m/z* in the QQQ-MS/MS spectrum (Fig. 2) may also originate from this moiety [14]. Wood et al. described the MS/MS behavior of stachydrine and showed that a rearrangement fragmentation process resulting in the loss of C_3H_6 followed by loss of water provides the characteristic fragment at 84 *m/z* with a protonated molecular ion formula of C_4H_6NO [15]. Based on the HRMS experiments the protonated fragment ion at 84.0810 *m/z* value in our samples possesses a formula of $C_5H_{10}N$, which could exclude the possibility of stachydrine, but could arise from monosubstituted piperidine derivatives (e.g. homopipercolic acid) [16,17], however the occurrence of these derivatives in the plant kingdom is rather rare. As the piperidin-2-ylacetate moiety has never been described in higher plants, samples of different origin and vegetational period were subjected for analytical screening to detect the same compounds. These experiments successfully proved the presence of the isoflavonoid homopipercolinic glucosides, therefore the possibility of sample contamination could be excluded. In order to exclude any further hypothetical structures and to unambiguously identify the unknown structure, NMR experiments were applied.

3.2. NMR experiments

All the six compounds were isolated and subjected to NMR experiments. The complete structure identification of compound 5 is described herein as an example. In the case of compound 5 the MS/MS data suggested the presence of medicarpin aglycone (see Table 2). The

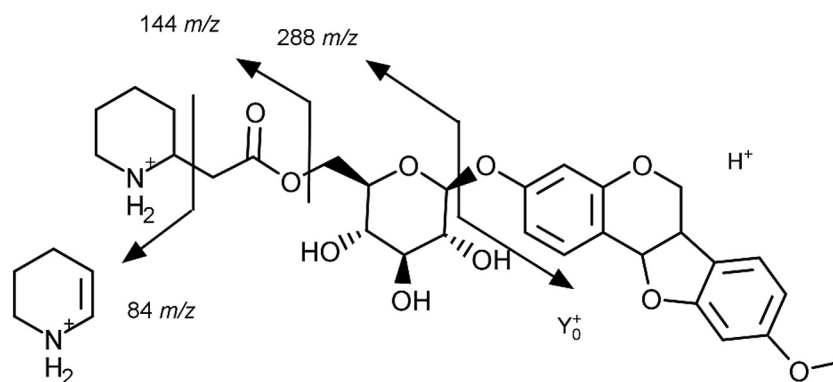


Fig. 3. The fragmentation pattern of the piperidin-2-ylacetate esters illustrated on the example of compound 5.

Table 2

^1H and ^{13}C NMR data of medicarpin (5) and maackiain (6) glucoside piperidin-2-ylacetates in $\text{DMSO-}d_6$ (δ in ppm, J in Hz).

No.	Compound 5		Compound 6	
	^1H	^{13}C	^1H	^{13}C
1	7.39/7.38 d (8.7)	131.92	7.37 d (8.7)	131.87
1a	–	114.19	–	114.25
2	6.69 dd (8.7, 2.3)	110.35	6.68 dd (8.7, 2.3)	110.34
3	–	158.23	–	158.23
4	6.54/6.53 d (2.3)	104.02	6.53 d (2.3)	104.01
4a	–	156.18/ 156.16	–	156.18/ 156.16
6A	4.28 m	66.03	4.27 m	65.94
6B	3.65 m	–	3.66 m	–
6a	3.65 m	38.84	3.61 m	39.56
7a	–	119.19	–	118.24
7	7.25 d (8.5)	125.20	6.98 s	105.37
8	6.45 d (8.5)	96.34	–	141.12
9	–	160.53	–	147.48
10	6.42 dd (8.5, 2.3)	106.11	6.52 s	93.24
10a	–	160.22	–	153.64
11a	5.59 d (7.1)	77.73	5.56 d (7.5)	77.62
9-OCH ₃	3.69 s	55.29	–	–
9-OCH ₂ O-8	–	–	5.90 s 5.94 s	101.05
1''	4.90/4.89 d (8.5)	99.95	4.89 d (7.7) 4.89 d (7.8)	99.97
2''	3.22 t (8.4)	73.08	3.23 m	73.09
3''	3.29 t (8.9)	76.20	3.29 t (8.9)	76.20
4''	3.15 dd (9.8, 8.7)	69.90/69.85	3.15 m	69.89/69.86
5''	3.60 m	73.65	3.60 m	73.65/73.64
6''A	4.06/4.02 dd (12.0, 6.8)	63.21/63.18	4.07/4.04 dd (12.0, 6.8)	63.24/63.23
6''B	4.33/4.30 dd (12.0, 2.3)	–	4.33/4.30 dd (12.0, 2.4)	–
2'''	2.73 m	53.30/53.21	2.78 m	53.26/53.17
3'''ax	0.99/0.94 m	31.93	1.00/0.96 m	31.75
3'''eq	1.53/1.49 m	–	1.56/1.52 m	–
4'''ax	1.22 m	24.23	1.22 m	24.10
4'''eq	1.64/1.60 m	–	1.64/1.60 m	–
5'''ax	1.20 m	25.69	1.21 m	25.51
5'''eq	1.42 m	–	1.44 m	–
6'''ax	2.42 m	46.15	2.46 m	46.05
6'''eq	2.83 m	–	2.87 m	–
7'''	2.28 m	41.22	2.29 m	41.05
8'''	–	171.40/ 171.36	–	171.32/ 171.29

six aromatic protons at 7.39/7.38 (d $J = 8.7$ 1H), 7.25 (d $J = 8.5$ Hz 1H), 6.69 (dd $J = 8.7, 2.3$ Hz 1H), 6.54/6.53 (d $J = 2.3$ Hz), 6.45 (d $J = 8.5$ Hz 1H) and 6.42 (dd $J = 8.5, 2.3$ Hz 1H) ppm and the characteristic spin system (-O-CH₂-CH-CH) at 4.28 (m 1H), 3.65 (m 2H) ppm along with the methyl singlet of the -OCH₃ group at 3.69 ppm present in the ^1H NMR spectrum of 5 corroborated by HMBC correlations and literature data [18] confirmed the medicarpin aglycone. The presence of a glucose moiety was also verified by NMR, key HMBC correlations confirmed the glycosidic linkage between the anomeric OH of the glucose and the C3-OH of medicarpin. The careful inspection of the ^1H NMR experiment showed the presence of eleven ^1H resonances in the aliphatic region (δ_{H} 2.83 (m 1H), 2.73 (m 1H), 2.42 (m 1H), 2.28 (m 2H), 1.53/1.49 (m 1H), 1.64/1.60 (m 1H), 1.42 (m 1H), 1.22 (m 1H), 1.20 (m 1H), 0.99/0.94 (m 1H)). The COSY, TOCSY and especially the HMBC spectra with $J = 12$ Hz heteronuclear coupling constant helped to construct the missing building block forming a piperidine ring substituted at C2''. In the HMBC experiment two crucial correlations were observed for a carbonyl resonance at 171.40/171.36 ppm: intense crosspeaks were detected between the C=O and protons (2.28 ppm) of the side chain and similarly between the C=O and the H6'' (4.06/4.03 ppm) resonance of the glucose moiety (Fig. 4). These correlations clearly indicate that the piperidin-2-yl-acetic acid linked to the glucose moiety with an ester bond at the C6'' position. The complete NMR characterization of compound 5 can be found in Table 2. As the cyclic beta amino acid residue introduces a new stereogenic center, some of the NMR resonances show diastereomeric splitting. The MS/MS fragmentation can also be corroborated by the piperidin-2-ylacetate moiety. As indicated in Fig. 3., the loss of the entire beta amino acid residue refers to the fragment 144 m/z , while the cleavage of the acetic acid side chain provides the protonated fragments 1,2,3,4-tetrahydropyridine at 84 m/z . In the case of compound 6 the NMR data revealed a methylenedioxy group and the lack of the methoxy function in the aglycone skeleton compared to 5. All ^1H and ^{13}C NMR resonances were in agreement with the maackiain aglycone as proposed by the MS experiments (Fig. 5) thus; compound 6 was identified as maackiain 3-O- β -D-glucoside-6''-O-piperidin-2-ylacetate. The NMR resonances of the glucose and the piperidin-2-ylacetate moieties were found to be almost identical for all compounds (1–6) confirming the same structural motif but various aglycones (Tables 2–4). For compound 1 two sets of aromatic protons and a singlet at 8.44/8.43 ppm indicated isoflavonoid aglycone skeletons. The HMBC spectrum indicated a key correlation between an O-methyl resonance (3.79 ppm) and C4' (159.06 ppm) therefore the aglycone was identified as formononetin (Table 3). Compound 2 showed HMBC correlation between the methylenedioxy group (6.05 ppm) and C3' (152.26 ppm) and C4' (147.09 ppm) confirming the isoflavonoid skeleton pseudobaptigenin (Fig. 5). The complete NMR resonance assignment can be found in Table 3. The NMR characteristics of compound 3 and 4 were similar to 1 and 2 with a subtle difference of an additional methoxy group at C2' and the lack of

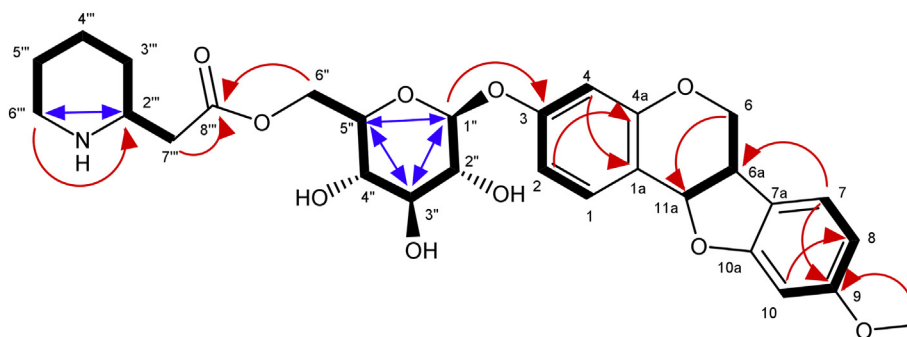


Fig. 4. Key HMBC (curved arrows), COSY (bold lines) and ROESY (straight arrows) correlations for compound 5.

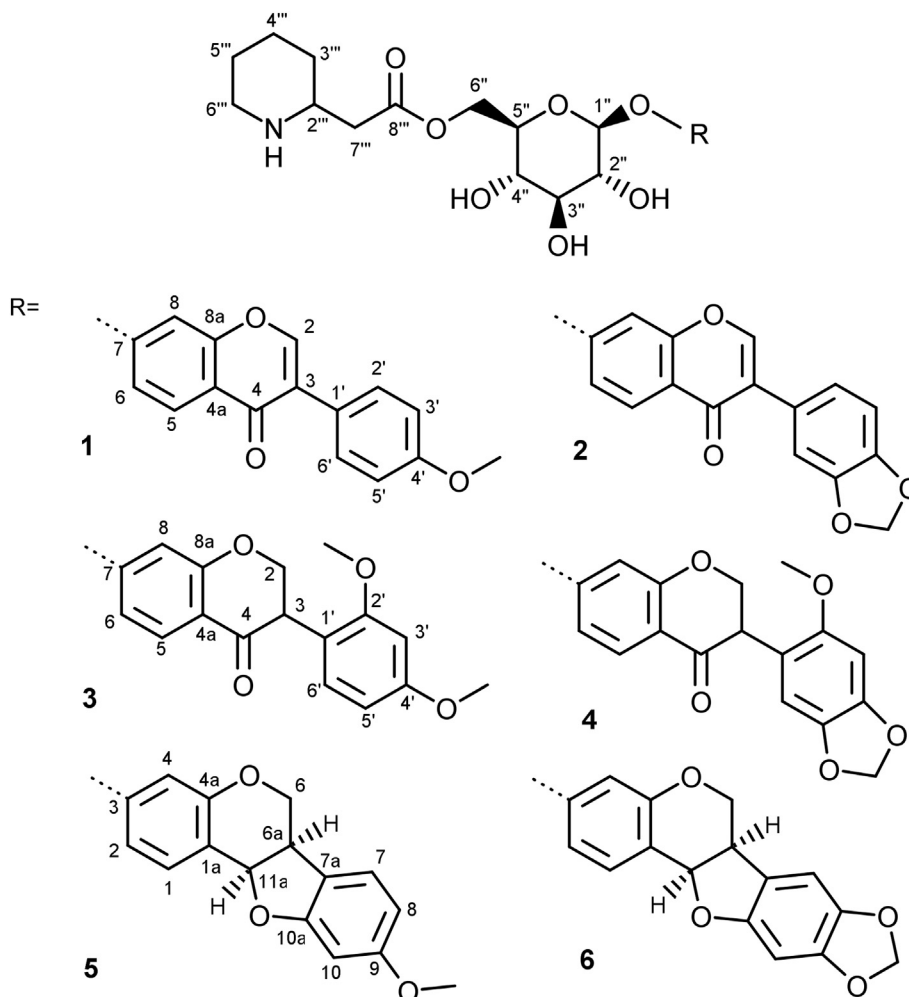


Fig. 5. The structures and numbering of isoflavonoid glucoside 6''-O-piperidin-2-ylacetates 1–6.

an aromatic singlet (Table 4). The aglycones of 3 and 4 were identified as sativanone and onogenin, respectively (Fig. 5).

3.3. Stereochemistry

Regarding the aglycones, the two isoflavones, formononetin and pseudobaptigenin contain no chiral atoms. However, the two dihydroisoflavonoids onogenin and sativanone are chiral compounds. Based on the information that the isolated aglycones have no detectable CD spectrum we assumed that our sample contains the derivatives of (3*R*,5*S*)-onogenin and sativanone, in concordance with literature [19]. Pterocarpans contain two chiral centers, however, from the four

possible isomers only two, with *cis*-fused benzofuranyl-benzopyran rings can be found in nature (Tökés et al., 1999) [20]. In the ROESY experiment of compound 6 intense crosspeaks were detected between the H6a (3.60 ppm) and H11a (5.56 ppm) verifying the *cis* configuration of the aglycone maackiain. To determine the absolute configuration of the pterocarpans optical rotatory dispersion and circular dichroism were used. The $[\alpha]_D^{25}$ value of medicarpin and maackiain was -303° and -113° , respectively, showing that in our sample the pterocarpans can be found in the pure form of (6*aR*,11*aR*)-medicarpin and (6*aR*,11*aR*)-maackiain. The minima and maxima of the recorded CD spectra (medicarpin, λ_{\max} ($\Delta\epsilon$) 208 ($-18.53 \text{ M}^{-1}\cdot\text{cm}^{-1}$), 236 ($-9.67 \text{ M}^{-1}\cdot\text{cm}^{-1}$), 288 ($4.09 \text{ M}^{-1}\cdot\text{cm}^{-1}$); maackiain 212

Table 3

¹H and ¹³C NMR data of formononetin (1) and pseudobaptigenin (2) glucoside piperidin-2-ylacetates in DMSO-*d*₆ (δ in ppm, *J* in Hz).

Position	Compound 1		Compound 2	
	¹ H	¹³ C	¹ H	¹³ C
2	8.43/8.44 s	152.5	8.45/8.44 s	153.9
3	–	123.3	–	124.8
4	–	175.1	–	174.6
4a	–	118.9	–	–
5	8.07 d (8.8) 8.06 d (8.9)	127.0	8.06 d (8.8) 8.06 d (8.9)	126.9
6	7.14 dd (8.8, 2.3)	115.4	7.14 dd (8.8, 2.4)	109.3
7	–	161.3	–	161.3
8	7.24/7.22 d (2.3)	103.5	7.23/7.22 d (2.4)	103.3
8a	–	157.1	–	160.8
1'	–	123.8	–	123.6
2'/6'	7.52/7.51 d (8.8)	130.1	7.15 d (2.4)	115.5
3'/5'	7.01 d (8.8)	113.5	–	152.3
4'	–	159.1	–	147.1
5'	–	113.5	7.00 d (7.7)	108.1
6'	–	130.1	7.07/7.06 dd (7.7, 2.4)	122.3
4'-OCH ₃	3.79 s	55.1	6.06 s	101.1
4'-OCH ₂ O-3'				
1''	5.20 d (7.5) 5.19 d (7.4)	99.4	5.21/5.20 d (5.5)	99.3
2''	3.28 t (8.1)	73.0	3.23 t (8.1)	72.9
3''	3.30 t (9.1)	76.1	3.30 t (9.1)	76.1
4''	3.19/3.18 t (9.1)	69.9	3.15 t (9.1)	69.9
5''	3.76 m	73.8	3.76 m	73.6
6''A	4.10 dd (11.8, 7.3) 4.07 dd (11.8, 7.1)	63.3	4.06/4.01 m	63.2
6''B	4.33 dd (11.8, 2.1) 4.32 dd (11.8, 1.9)		4.30 m	
2'''	2.70/2.65 m	53.1	2.70/2.66 m	53.1
3'''ax	0.96/0.89 m	31.8	0.96 m	31.8
3'''eq	1.50/1.43 m		1.52 m	
4'''ax	1.14 m	24.1	1.15 m	24.1
4'''eq	1.60/1.52 m		1.61 m	
5'''ax	1.14 m	25.6	1.15 m	25.6
5'''eq	1.36 m		1.35 m	
6'''ax	2.38/2.31 m	46.0	2.34 m	46.0
6'''eq	2.80/2.75 m		2.83/2.75 m	
7'''	2.29/2.28 m	41.1	2.28 m	41.2
8'''	–	171.4	–	171.4

¹³C NMR data for Compound 1 and 2 were assigned on the basis of HSQC and HMBC experiments.

($-4.18 \text{ M}^{-1} \cdot \text{cm}^{-1}$), 240 ($-7.41 \text{ M}^{-1} \cdot \text{cm}^{-1}$); 280 ($0.24 \text{ M}^{-1} \cdot \text{cm}^{-1}$)) were in accordance with literature data [21,22] (Figs. S58 and S59). Even in the screening chromatographic runs the peaks of compound 5 and 6 showed significant peak splitting on achiral stationary phase. This effect could be observed on all derivatives in the preparative LC chromatogram and was further investigated on various analytical stationary phases (C-18, C-8, C-18 core shell and phenyl-hexyl). The complete separation of the two diastereomers of formononetin, pseudobaptigenin, medicarpin and maackiain derivatives could be achieved on all four columns (Figs. S60–S67). However, the four isomers of the racemic onogenin and sativanone could not be baseline separated. Beside the two baseline resolved peaks (originating hypothetically from the diastereomeric splitting due to the racemic nature of the amino acid), a third peak (as a shoulder) can be observed using the core shell C18 column (Fig. S67). To investigate the stability of the isomers, the peaks of compound 6 were isolated separately. The isolated compounds were then reinjected after 1, 5 and 10 days. The transformation of the isomers into each other resulting in peak duplication could not be observed (Figs. S56 and S57). As the NMR signals of all six compounds showed signal duplication, but the stereochemistry of the aglycones are so different, we hypothesized that the source of the phenomenon originated from the common structural motifs. The ¹H NMR spectra of the isolated diastereomers of compound 5 were recorded and it clearly

Table 4

¹H and ¹³C NMR data of sativanone (3) and onogenin (4) glucoside piperidin-2-ylacetates in DMSO-*d*₆ (δ in ppm, *J* in Hz).

Position	Compound 3		Compound 4	
	¹ H	¹³ C	¹ H	¹³ C
2	4.59/4.57 m 4.46 m	70.47	4.59 m 4.45 m	70.36
3	4.21 dd (11.4, 5.4)	46.68	4.25 m	47.23
4	–	190.66	–	190.56
4a	–	115.88	–	115.86
5	7.76 d (8.8) 7.75 d (8.8)	128.53	7.76 d (8.7) 7.75 d (8.7)	130.07
6	6.72 dd (8.8, 2.4)	110.81	6.73/6.72 dd (8.7, 2.5)	110.83
7	–	162.94	–	162.99
8	6.64 d (2.4)	103.45	6.64/6.63 d (2.5)	103.45
8a	–	162.89	–	162.99
1'	–	115.79	–	115.44
2'	–	158.13	–	152.50
3'	6.58 d (1.3)	98.87	6.82 s	95.77
4'	–	160.09/ 160.07	–	140.65
5'	6.49/6.48 m	104.99	–	147.24
6'	7.01/6.99 d (8.6)	130.82/ 130.64	6.74/6.72 s	109.89
2'-OCH ₃	3.71/3.70 s	55.64	3.66/3.65 s	56.65
4'-OCH ₃	3.75 s	55.24	–	–
4'-OCH ₂ O-3'				
1''	5.06 d (7.5) 5.05 d (6.5)	99.41	5.06 d (7.0) 5.05 d (6.7)	99.42
2''	3.27 t (8.8)	73.00	3.28 t (8.1)	73.01
3''	3.32 t (8.9)	76.14	3.31 t (9.1)	76.14
4''	3.16 t (9.2)	69.89/69.84	3.16 t (9.1)	69.96
5''	3.69 m	73.76	3.69 m	73.77
6''A	4.07/4.04 m	63.28	4.07/4.03 m	63.25
6''B	4.35/4.32 m		4.35/4.32 m	
2'''	2.78 m	53.20/53.09	2.73 m	53.29
3'''ax	1.02/0.97 m	31.65	0.96/0.92 m	31.93
3'''eq	1.53 m		1.55/1.48 m	
4'''ax	1.23 m	24.04/24.01	1.22 m	24.21
4'''eq	1.61 m		1.61 m	
5'''ax	1.24 m	25.42	1.21 m	25.69
5'''eq	1.44 m		1.42 m	
6'''ax	2.45 m	45.96	2.43 m	46.15
6'''eq	2.87 m		2.84 m	
7'''	2.32 m	40.98	2.30 m	41.26
8'''	–	171.26/ 171.23	–	171.37

indicates that the duplication of the NMR signals arose from the overlap of the ¹H resonances of the two diastereomers (Figs. S33–S37). Examining the chemical shifts and coupling constants of the sugar moiety, the presence of β -D-glucopyranose could be proved in all six molecules. Consequently, the hypothesized source of the diastereomerism is the stereogenic center of the beta amino acid.

4. Conclusions

A preparative method was developed and applied to separate, isolate and characterize six unknown isoflavonoid glucoside homopiperidic esters using the combination of ion exchange purification and preparative reversed phase chromatographic isolation. The unexpected structures were characterized by the means of HR-MS/MS, NMR and CD spectroscopy. The presence of the beta amino acid homopiperidic acid is firstly published in higher plants. Although the botanical function of these compounds is unclear, their presence of homopiperidic acid in the form of isoflavonoid esters can serve as chemotaxonomic marker in the Fabaceae family.

Acknowledgement

The financial supports from NKFIH PD109373 and from ÚNKP-16-4 New National Excellence Program of the Ministry of Human Capacities are highly appreciated. The authors would like to express their gratitude to Dr. Szilvia Lohner and Dr. Zsuzsanna Urbancsok to access the HR-MS instrument and to Dr. Anikó Nemes and Miss Zsófia Zámbo for their help of optical rotation power and circular dichroism experiments. The technical assistance of Andrea Nedves and Tamás Czeglédi is acknowledged.

Appendix A. Supplementary data

Supplementary data to this article can be found online at <https://doi.org/10.1016/j.jchromb.2018.05.023>.

References

- [1] M. Wichtl (Ed.), *Herbal Drugs and Phytopharmaceuticals: A Handbook for Practice on a Scientific Basis*, 3rd ed., CRC Press, Boca Raton, 2004.
- [2] J. Gruenwald, T. Brendler, C. Wyble, M. Hamid, J. Nathan, J.C. Potter, K. Rodgers, A.M. Phayre (Eds.), *Physician's Desk Reference for Herbal Medicines*, 3rd ed., Medical Economics Company, Inc., Montvale, 2000, [http://dx.doi.org/10.1016/S0737-0806\(99\)80323-2](http://dx.doi.org/10.1016/S0737-0806(99)80323-2).
- [3] P. Bolle, P. Faccendini, U. Bello, *Ononis spinosa* L.: pharmacological effect of ethanol extract, *Pharmacol. Res.* 27 (1993) 27–28.
- [4] A. Háznagy, G. Tóth, J. Tamás, Über die Inhaltstoffe des wäßrigen Extraktes von *Ononis spinosa* L. *Arch. Pharm. (Weinheim)* 311 (1978) 318–323, <http://dx.doi.org/10.1002/ardp.19783110408>.
- [5] Á.E. Daruházi, S. Szarka, É. Héthelyi, B. Simándi, I. Gyurján, M. László, É. Szőke, É. Lemberkovics, GC-MS identification and GC-FID quantitation of Terpenoids in *Ononis spinosa* Radix, *Chromatographia* 68 (2008) 71–76, <http://dx.doi.org/10.1365/s10337-008-0679-2>.
- [6] P. Pietta, A. Calatroni, C. Zio, High-performance liquid chromatographic analysis of flavonoids from *Ononis spinosa* L, *J. Chromatogr. A* 280 (1983) 172–175, [http://dx.doi.org/10.1016/S0021-9673\(00\)91555-3](http://dx.doi.org/10.1016/S0021-9673(00)91555-3).
- [7] P. Pietta, P. Mauri, E. Manera, P. Ceva, Determination of isoflavones from *Ononis spinosa* L. Extracts by high-performance liquid chromatography with ultraviolet diode-array detection, *J. Chromatogr. A* 513 (1990) 397–400, [http://dx.doi.org/10.1016/S0021-9673\(01\)89464-4](http://dx.doi.org/10.1016/S0021-9673(01)89464-4).
- [8] B. Klejduš, J. Vacek, L. Lojtková, L. Benesová, V. Kubán, Ultrahigh-pressure liquid chromatography of isoflavones and phenolic acids on different stationary phases, *J. Chromatogr. A* 1195 (2008) 52–59, <http://dx.doi.org/10.1016/j.chroma.2008.04.069>.
- [9] N. Gampe, A. Darcsi, S. Lohner, S. Béni, L. Kursinszki, Characterization and identification of isoflavonoid glycosides in the root of spiny restharrow (*Ononis spinosa* L.) by HPLC-QTOF-MS, HPLC-MS/MS and NMR, *J. Pharm. Biomed. Anal.* 123 (2016) 74–81, <http://dx.doi.org/10.1016/j.jpba.2016.01.058>.
- [10] L. Khouni, C. Long, H. Haba, N. Molinier, M. Benkhaled, Anthranilic acid derivatives and other components from *Ononis pusilla*, *Nat. Prod. Commun.* 9 (2014) 1159–1162.
- [11] X.N. Li, Z.Q. Lu, S. Qin, H.X. Yan, M. Yang, S.H. Guan, X. Liu, H.M. Hua, L.J. Wu, D.A. Guo, Tonkinensines A and B, two novel alkaloids from *Sophora tonkinensis*, *Tetrahedron Lett.* 49 (2008) 3797–3801, <http://dx.doi.org/10.1016/j.tetlet.2008.04.003>.
- [12] B.P. Naidu, L.G. Paleg, G.P. Jones, Nitrogenous compatible solutes in drought-stressed *Medicago* spp. *Phytochemistry* 31 (1992) 1195–1197, [http://dx.doi.org/10.1016/0031-9422\(92\)80259-H](http://dx.doi.org/10.1016/0031-9422(92)80259-H).
- [13] H. Ye, E. Gemperline, M. Venkateshwaran, R. Chen, P.-M.M. Delaux, M. Howes-Podoll, J.-M.M. Ané, L. Li, MALDI mass spectrometry-assisted molecular imaging of metabolites during nitrogen fixation in the *Medicago truncatula-Sinorhizobium meliloti* symbiosis, *Plant J.* 75 (2013) 130–145, <http://dx.doi.org/10.1111/tpj.12191>.
- [14] L. Servillo, A. Giovane, R. Casale, M.L. Balestrieri, D. Cautela, M. Paolucci, F. Siano, M.G. Volpe, D. Castaldo, Betaines and related ammonium compounds in chestnut (*Castanea sativa* mill.), *Food Chem.* 196 (2016) 1301–1309, <http://dx.doi.org/10.1016/j.foodchem.2015.10.070>.
- [15] K.V. Wood, C.C. Bonham, D. Miles, A.P. Rothwell, G. Peel, B.C. Wood, D. Rhodes, Characterization of betaines using electrospray MS/MS, *Phytochemistry* 59 (2002) 759–765, [http://dx.doi.org/10.1016/S0031-9422\(02\)00049-3](http://dx.doi.org/10.1016/S0031-9422(02)00049-3).
- [16] T. Nilus, S. Thorrold, S. Ruchirawat, N. Thasana, Squarrosine A and Pyrrolhuperzine A, new Lycopodium alkaloids from Thai and Philippine *Huperzia squarrosa*, *Planta Med.* 82 (2016) 1046–1050, <http://dx.doi.org/10.1055/s-0042-106904>.
- [17] L. Kursinszki, É. Szőke, HPLC-ESI-MS/MS of brain neurotransmitter modulator lobeline and related piperidine alkaloids in *Lobelia inflata* L, *J. Mass Spectrom.* 50 (2015) 727–733, <http://dx.doi.org/10.1002/jms.3581>.
- [18] Z.-G. Feng, W.-J. Bai, T.R.R. Pettus, Unified total syntheses of (–)-Medicarpin, (–)-Sophoracarpin A, and (±)-Kushcarpin A with some structural revisions, *Angew. Chem. Int. Ed.* 54 (2015) 1864–1867, <http://dx.doi.org/10.1002/anie.201408910>.
- [19] J. Yi, G. Du, Y. Yang, Y. Li, Y. Li, F. Guo, Chiral discrimination of natural isoflavanones using (R)- and (S)-BINOL as the NMR chiral solvating agents, *Tetrahedron Asymmetry* 27 (2016) 1153–1159, <http://dx.doi.org/10.1016/j.tetasy.2016.09.002>.
- [20] A.L. Tokés, G. Litkei, K. Gulácsi, S. Antus, E. Baitz-Gács, C. Szántay, L.L. Darkó, Absolute configuration and total synthesis of (–)-cabenegrin A-I, *Tetrahedron* 55 (1999) 9283–9296, [http://dx.doi.org/10.1016/S0040-4020\(99\)00490-1](http://dx.doi.org/10.1016/S0040-4020(99)00490-1).
- [21] A. Goel, A. Kumar, Y. Hemberger, A. Raghuvanshi, R. Jeet, G. Tiwari, M. Knauer, J. Kureel, A.K. Singh, A. Gautam, R. Trivedi, D. Singh, G. Bringmann, Synthesis, optical resolution, absolute configuration, and osteogenic activity of cis-pterocarpan, *Org. Biomol. Chem.* 10 (2012) 9583–9592, <http://dx.doi.org/10.1039/c2ob25722j>.
- [22] D.C. Rueda, M. De Mieri, S. Hering, M. Hamburger, HPLC-based activity profiling for GABAA receptor modulators in *Adenocarpus cincinnatus*, *J. Nat. Prod.* 77 (2014) 640–649, <http://dx.doi.org/10.1021/np500016z>.

RESEARCH ARTICLE

Phytochemical analysis of *Ononis arvensis* L. by liquid chromatography coupled with mass spectrometry

Nóra Gampe¹  | András Darcsi¹ | Andrea Nagyné Nedves¹ | Imre Boldizsár² | László Kursinszki¹ | Szabolcs Béni¹ 

¹Department of Pharmacognosy, Semmelweis University, Budapest, Hungary

²Department of Plant Anatomy, Eötvös Lóránd University, Budapest, Hungary

Correspondence

László Kursinszki and Szabolcs Béni, Semmelweis University, Department of Pharmacognosy, Üllői út 26, Budapest 1085, Hungary.

Email: kursinszki.laszlo@pharma.semmelweis-univ.hu; beni.szabolcs@pharma.semmelweis-univ.hu

Funding information

János Bolyai Research Scholarship; EFOP-3.6.3-VEKOP-16-2017-00009; Bolyai+ÚNKP-18-4-SE-121 New National Excellence Program; ÚNKP-18-3-III-SE-30 New National Excellence Program; National Research, Development and Innovation Office, Grant/Award Number: VEKOP-2.3.3-15-2017-00020

Abstract

Ononis arvensis L. can be found overall in Europe and is used to treat infections of the urinary tract and skin diseases in ethnopharmacology. Flavonoids, hydroxycinnamic acids, oxycoumarin, scopoletin and scopolin, phytosterols, lectins, and some selected isoflavonoids were identified in *O. arvensis* till date; however, there is a lack of the detailed investigation of the isoflavonoid profile of the plant. With the application of high-resolution tandem mass spectrometry, the fragmentation patterns of isoflavonoid derivatives found in *O. arvensis* roots and aerial parts were investigated and discussed. Isoflavonoid glucosides, glucoside malonates, aglycones, and beta amino acid derivatives were characterized, among which homoproline isoflavonoid glucoside esters were described for the first time. Besides the known isoflavonoid aglycones described earlier in other *Ononis* species, two 2'-methoxy isoflavonoid derivatives were detected. The presence of licoagroside B was verified, and its structure was also corroborated by NMR experiments. Altogether, the high-resolution fragmentation pattern of 47 isoflavonoids and glycosides is presented, and their relative quantity in the roots and the aerial parts can be evaluated. Based on this information, the chemotaxonomic relation of *Ononis* species and the biosynthesis of their compounds could be comprehended to a greater depth.

KEYWORDS

fragmentation, HPLC-ESI-MS/MS, isoflavonoid, *Ononis*, UHPLC-ESI-Orbitrap-MS/MS

1 | INTRODUCTION

The members of the *Ononis* genus, which belongs to the family Leguminosae, are natively distributed in Europe, Central Asia, and North Africa. *Ononis arvensis* L. is a perennial shrub preferring humid fields and meadows overall in Europe. The 50 to 100 cm-high erect stem is covered by trichomes. It has elliptical leaves and pink flowers.¹ The synonym names are *Ononis hircina* Jacq. and *Ononis spinosa subsp. hircina* (Jacq.) Gams. In the Renaissance, it was used in the treatment of epilepsy,² but its most widespread use is to treat infections of the urinary tract and for skin diseases.³ In ethnomedicinal reports, the decoction of the aerial part has been applied to liver and stomach disorders in the human and veterinary medicine, as well.^{4,5}

In the aerial parts, flavonoids and hydroxycinnamic acids were characterized and determined quantitatively using UHPLC-ESI-Q-TOF-MS.⁵ Sichinava et al. isolated oxycoumarins, scopoletin and scopolin from the plant.⁶ The distribution of phytosterols and triterpene onocerin was investigated in the aerial parts and the roots of *O. arvensis* by GLC-MS.⁷ Only a limited number of papers can be found dealing with the chemical composition of the roots. Horoejsi et al. isolated and characterized the lectins of *O. arvensis* root.⁸ The isoflavonoid glucoside ononin and the dihydroisoflavonoid onogenin were isolated from the roots, and the structure of onogenin was elucidated by NMR spectroscopy⁹; however, there is a lack of the detailed investigation of the isoflavonoid profile of the plant.

For screening numerous isoflavonoid derivatives, liquid chromatography coupled with tandem mass spectrometry is the most powerful tool regarding its selectivity and sensitivity. With the application of tandem mass spectrometry, the fragmentation patterns of isoflavonoid derivatives can be examined and compared. As isoflavonoids can be found in the form of glucosides, glucoside malonates, aglycones¹⁰ and beta amino acid glucoside esters,¹¹ the similarity of their product ion spectra can be used to classify the derivatives with the same aglycone. In some cases, mass spectrometry on its own is not sufficient for the complete structural elucidation, so the application of NMR techniques is inevitable. To obtain the necessary amount of pure compound for NMR experiments, the most repeatable and reliable way is to use preparative HPLC.

Previous studies on the composition of *O. arvensis* aerial parts and root dealt in depth only with selected compounds, and the structural analysis and characterization of other derivatives were missed. Therefore, the aim of this study is to systematically identify the isoflavonoid profile of the aqueous-methanolic extract of *O. arvensis* aerial parts and root by HPLC-ESI-MS/MS, UHPLC-ESI-FTMS/MS in positive ionization mode in conjunction with NMR.

2 | EXPERIMENTAL

2.1 | General and plant material

HPLC-grade methanol was obtained from Fisher Scientific (Loughborough, UK). Methanol- d_4 , for NMR measurements, was purchased from Sigma-Aldrich (Steinheim, Germany). Purified water prepared by Millipore Milli-Q equipment (Billerica, MA, USA) was used throughout the study. Calycosin, homoprolin, and homopipecolic acid were purchased from Sigma-Aldrich (Steinheim, Germany). All other chemicals were of analytical grade. *O. arvensis* was collected near Beregúfalu (location: N 48°17'21.1", E 22°48'08.7"—Beregzászi járás, Ukraine, July 2017). Voucher specimens were deposited in the Department of Pharmacognosy, Semmelweis University, Budapest with voucher number 170727-OnArv02. The roots and the aerial parts of the plant were separated. The roots were washed to remove soil, and the dried roots were ground. The aerial parts were ground without further separation of leaves and stems.

2.2 | Preparation of analytical sample

From the ground plant material, 0.500 g was mixed with 30 mL of 70% aqueous methanol and extracted in ultrasonic bath for 10 minutes on 25°C. After filtration, the sample was dried under vacuum with rotary evaporator (60°C, Heidolph Instruments, Laborata 4000, Schwabach, Germany). The resulting residue was redissolved in 2 mL of 70% aqueous methanol and filtered through 0.22 μ m PTFE filter (Nantong FilterBio Membrane Co., Ltd; Nantong City, Jiangsu P. R China). For the hydrolyzed sample, 1 mL of the analytical sample was mixed with 1 mL of concentrated ammonia and evaporated to dryness with rotary evaporator set to 60°C. The residue was mixed with 2 mL of purified water, and the liquid was passed through the same PTFE filter.

2.3 | HPLC-ESI-MS/MS conditions

For chromatographic separation and mass spectral analysis, an Agilent 1100 HPLC system (degasser, binary gradient pump, autosampler, column thermostat, and diode array detector) was used hyphenated with an Agilent 6410 Triple Quad LC/MS system equipped with ESI ion source (Agilent Technologies, Santa Clara, CA, USA). The HPLC separation of the root and aerial part extracts was attained on a Zorbax SB-C18 Solvent Saver Plus (3.5 μ m) reversed phase column (150 \times 3.0 mm i.d; Agilent Technologies, Santa Clara, CA, USA). Mobile phase consisted of 0.3% v/v formic acid (A) and methanol (B). The following gradient program was applied: 0.0 minutes, 29% B; 32.0 minutes, 80% B; 34 minutes, 100% B; 37 minutes, 100% B; 42.0 minutes, 29% B. Solvent flow rate was 0.4 mL/min, and the column temperature was set to 25°C. The injection volume was 2 μ L. Nitrogen was applied as drying gas at the temperature of 350°C at 9 L/min; the nebulizer pressure was 45 psi. Full scan mass spectra were recorded in positive ionization mode in the range of m/z 80 to 1500. For collision induced dissociation (CID), the collision energy varied between 10 and 40 eV. As collision gas, high purity nitrogen was used. The fragmentor voltage was set to 80 V, and the capillary voltage was 3500 V. Product ion mass spectra were recorded in positive ionization mode in the range of m/z 50 to 600.

The hydrolyzed sample was analyzed using the same HPLC-MS/MS apparatus equipped with a Zorbax NH₂ normal phase column (150 \times 4.6 mm i.d; 5 μ m). Mobile phase consisted of 20 mM ammonium formate buffer (pH = 4) (A) and acetonitrile (B). Isocratic mode was applied with 80% B at 1 mL/min flow rate and at 25°C. The injection volume was 5 μ L. Nitrogen was applied as drying gas at the temperature of 300°C at 6 L/min; the nebulizer pressure was 15 psi. For registering the chromatogram, selective ion monitoring mode was chosen at m/z 130 (homoprolin) and m/z 144 (homopipecolic acid). For CID, the collision energy varied between 10 and 30 eV. As collision gas high purity nitrogen was used. The fragmentor voltage was set to 120 V, and the capillary voltage was 4000 V. Product ion mass spectra were recorded in positive ion mode in the range of m/z 50 to 200.

2.4 | UPLC-ESI-Orbitrap-MS/MS conditions

For obtaining high resolution mass spectrometric data of the root and aerial part extracts, a Dionex Ultimate 3000 UHPLC system (3000RS diode array detector, TCC-3000RS column thermostat, HPG-3400RS pump, SRD-3400 solvent rack degasser, WPS-3000TRS autosampler) was used hyphenated with a Orbitrap Q Exactive Focus Mass Spectrometer equipped with electrospray ionization (Thermo Fischer Scientific, Waltham, MA, USA). The column and the HPLC method were the same as the ones used with the non-hydrolyzed analytical samples. The electrospray ionization source was operated in positive ionization mode, and operation parameters were optimized automatically using the built-in software. The working parameters were as follows: spray voltage, 3500 V; capillary temperature 256.25°C; sheath gas (N₂), 47.5°C; auxiliary gas (N₂), 11.25 arbitrary units; spare gas (N₂), and 2.25 arbitrary units. The resolution of the full scan was of 70 000, and the scanning range was between 120 and 1000 m/z units.

The most intense ions detected in full scan spectrum were selected for data-dependent MS/MS scan at a resolving power of 35 000, in the range of 50 to 1000 m/z units. Parent ions were fragmented with normalized collision energy of 10%, 30%, and 45%.

2.5 | NMR conditions

All NMR experiments were carried out on a 600 MHz Varian DDR NMR spectrometer equipped with a 5 mm inverse-detection gradient (IDPFG) probehead. Standard pulse sequences and processing routines available in VnmrJ 3.2C/Chempack 5.1 were used for structure identifications. The complete resonance assignments were established from direct ^1H - ^{13}C , long-range ^1H - ^{13}C , and scalar spin-spin connectivities using 1D ^1H , ^{13}C , ^1H - ^1H gCOSY, ^1H - ^1H NOESY, ^1H - ^1H ROESY, ^1H - ^1H TOCSY, ^1H - ^{13}C gHSQCAD ($J = 140$ Hz), and ^1H - ^{13}C gHMBCAD ($J = 8$ Hz and 12 Hz) experiments, respectively. The probe temperature was maintained at 298 K, and standard 5 mm NMR tubes were used. The ^1H and ^{13}C chemical shifts were referenced to the residual solvent signal $\delta_{\text{H}} = 3.310$ ppm and $\delta_{\text{C}} = 49.00$ ppm, respectively.

2.6 | Isolation of licoagroside B

Using ultrasonic bath on room temperature, 20.0 g ground root was extracted with 200 mL of 70% methanol twice. After filtration, the extract was dried under reduced pressure. The residue was redissolved in water, and 10 mL of acetone was added to remove saccharides. The precipitate was filtered, and the liquid phase was dried. The residue was redissolved in 10 mL of water and passed through Supelclean SPE LC-18 columns (500 mg, 3 mL; Supelco, Bellefonte, PA, USA). After air drying the cartridges, 3 mL of 50% methanol was used to elute glycosides, then 6 mL pure methanol was applied to achieve complete elution of isoflavonoids. The weights of the first and second eluates were 274 and 171 mg, respectively. The 50% methanol fraction was redissolved in 2 mL of water and filtered through 0.22 μm PTFE filter before subjected to preparative HPLC. For fractionation, a Hanbon Newstyle NP7000 HPLC system with a Hanbon Newstyle NP3000 UV detector (Hanbon Sci. & Tech. CO. Jiangsu, China) equipped with a Gemini C18 reversed phase column (150 \times 21.2 mm i.d.; 5 μm , Phenomenex Inc; Torrance, CA, USA) was used. Eluents consisted of 0.3% v/v acetic acid (A) and methanol (B). Gradient elution was used with a 10 mL/min flow rate and a solvent system using 10% B at 0 minutes, 40% B in 10 minutes, 100% B in 15 minutes, and 10% B in 25 minutes. This method has not been optimized in terms of performance parameters as it only served for isolation purposes. Licoagroside B eluted at 11.41 minutes, the obtained fraction was reinjected for further purification. Finally, 8.9-mg licoagroside B was yielded in high purity

2.7 | Isolation of but-2-enolide aglycones

From the same plant material, 30.0 g was mixed with 200 mL water for 48 hours to activate the plant's indigenous glucosidase enzymes. After filtration, the drug was extracted twice with 200 mL of 70%

methanol using ultrasonic bath at room temperature. The extract was dried under reduced pressure and redissolved in water. The saccharides were precipitated with the same method as mentioned above. The total weight of the extract was 835 mg and was redissolved in 10 mL of water and filtered through 0.22 μm PTFE filter before subjected to the same preparative HPLC system. The chosen chromatographic conditions fulfilled the criteria of isolation but were not optimized in terms of performance parameters. Eluents consisted of 0.3% v/v acetic acid (A) and methanol (B). Gradient elution was used with a 10 mL/min flow rate and solvent system with 50% B at 0 minutes, 50% B in 10 minutes, 100% B in 15 minutes, and 50% B in 20 minutes. Puerol A eluted at 8.40 minutes, while clitorienolactone B eluted at 12.25 minutes. Clitorienolactone B was reinjected for further purification with isocratic 25% acetonitrile as solvent B. The yields were 4.8 mg for puerol A and 3.1 mg for clitorienolactone B, respectively.

2.8 | Isolation of but-2-enolide glycosides and calycosin D glycosides

100 gram powdered drug was extracted by 400 mL of 70% aqueous methanol twice. After filtration, the liquid phase was dried under reduced pressure at 60°C. The residue was dissolved in water to gain a viscous solution of 500 mg/mL concentration. This sample was purified using a CombiFlash NextGen 300+ (Teledyne ISCO, Lincoln, USA) equipped with a RediSep Rf Gold C18 column (150 g). As eluents, methanol (solvent B) and 0.3% acetic acid (solvent A) were used with the following gradient program: 0 minutes 30% B, 20 minutes 50% B, 25 minutes 100% B, and 30 minutes 100% B. The flow was set to 60 mL/min and 16 mL fractions were collected. Fractions 23 to 27, 38 to 41, and 49 to 53 were unified and further purified by the same preparative HPLC system using isocratic 25% acetonitrile as eluent with 10 mL/min flow. Fractions 23 to 27 yielded 15.4 mg calycosin D glucoside. From fractions 38 to 41, puerol A 2'-O-glucoside was isolated (eluted at 7.2 minutes, 63.2 mg) along with clitorienolactone B 4'-O-glucoside (eluted at 8.6 minutes). Clitorienolactone B 4'-O-glucoside was further purified on a Luna C18(2) 100 A (5 μm) reversed phase column (150 \times 10.00 mm i.d.; Phenomenex, Inc; USA) using isocratic 25% acetonitrile and 2 mL/min flow, yielding 2.3 mg. Calycosin D 6''-O-glucoside malonate was isolated from fractions 49 to 53 eluting at 11.3 min (1.1 mg).

3 | RESULTS AND DISCUSSION

In the aqueous-methanolic extract of *O. arvensis* aerial parts and roots altogether, 47 compounds were described (Figure 1). Isoflavonoids, dihydroisoflavonoids, and pterocarpanes were characterized in the form of glucosides, glucoside malonates, aglycones, and esters of homopiepicolic acid besides several new compounds. Moreover, the glucosides of some special phenolic compounds with their aglycones (puerol A and clitorienolactone B) and a maltol glucoside derivative (licoagroside B) were also identified in the samples (see Table 1). In the case of nitrogen containing compounds, diastereomeric splitting could be observed depending on the type of the aglycone and the

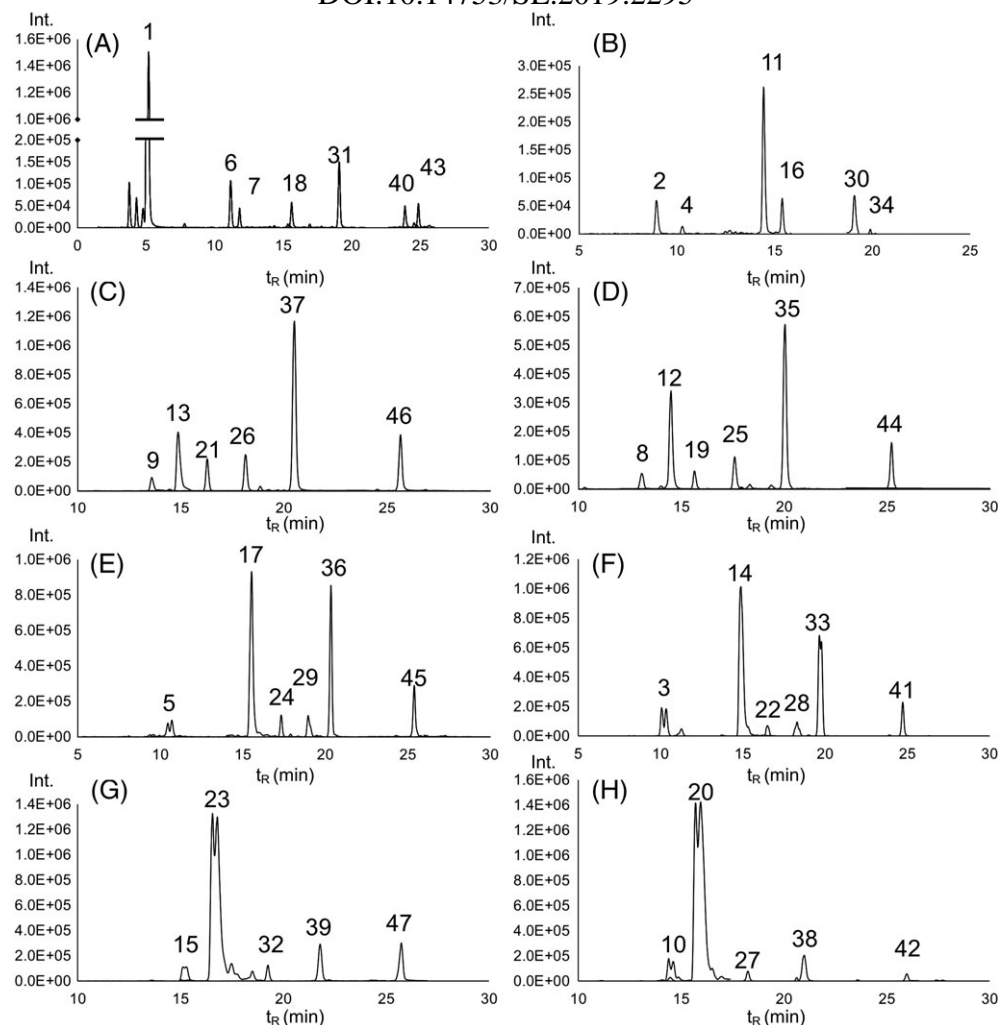


FIGURE 1 The extracted ion chromatograms of the described compounds with various aglycones from *O. arvensis* root aqueous-methanolic extract. A, Licoagroside B (1–433.1338), puerol derivatives (6–461.1435, 7–475.1593, 18–299.0909, 31–313.1066), 2'-methoxy isoflavonoids (39–313.0703, 42–299.0916); B, Calycosin D derivatives (2–447.1281, 11–533.1295, 30–285.0754) and calycosin derivatives (4–447.1299, 16–533.1309, 34–285.0752); C, Formononetin derivatives (9–542.2020, 13–556.2177, 21–431.1345, 26–517.1343, 36–517.1353, 45–269.0803); D, Pseudobaptigenin derivatives (8–556.1812, 12–570.1967, 19–445.1124, 25–531.1125, 35–531.1132, 44–283.0596); E, Sativanone derivatives (5–574.2274, 17–588.2234, 24–463.1591, 29–549.1600, 36–549.1595, 45–301.1061); F, Onogenin derivatives (3–588.2072, 14–602.2231, 22–477.1382, 28–563.1387, 33–563.1382, 41–315.0858); G, Medicarpin derivatives (15–544.2166, 23–558.2326, 32–433.1487, 39–519.1488, 47–271.0989); H, Maackiain derivatives (10–558.1968, 20–572.2122, 27–447.1272, 38–533.1275, 42–285.0750)

retention time (Figure 1). Comparing the metabolic profile of the aerial parts and the roots, a significant difference emerges between the amounts of dihydroisoflavonoid compounds (onogenin and sativanone). These derivatives could be found in the aerial parts only in trace quantities, while they were quite abundant in the root extracts, indicating a divergence in biosynthesis (Table 1).

3.1 | Identification of licoagroside B

The m/z value of the pseudo-molecular ion in positive ionization mode of compound 1 (Figure 1A) was 433.1338, and its molecular formula calculated on the basis of HR-MS experiments corresponds to $C_{18}H_{24}O_{12}$ (see Table 1). Investigating the fragmentation pattern of this precursor ion, only two fragment ions at m/z 145.0493

($C_6H_9O_4$) and m/z 127.0390 ($C_6H_7O_3$) could be observed, contrary to the rich fragmentation profile and retro Diels-Alder (rDA) cleavage of isoflavonoid derivatives.¹² Based on these results, peak 1 was tentatively identified as licoagroside B, the 3-hydroxy-3-methyl-glutarate ester of maltol glucoside. The fragment at m/z 127.0390 could result from the cleavage of the maltol ring together with the anomeric O atom, while the fragment at m/z 145.0493 could be assigned to the hydroxy-methyl-glutaric acid residue (Figure 2). The results of the NMR experiments verified that compound 1 was licoagroside B (Table S1), and the obtained resonances showed perfect correlation with the ones reported by Li et al.¹³ Licoagroside B was only identified in the hairy root cultures of *Glycyrrhiza glabra* L. till date. However, licoagroside B is present in high quantity in *O. arvensis*, showing that this compound is a characteristic metabolite of *Ononis* species.

TABLE 1 The identified compounds and their high-resolution MS and MS/MS data of *O. arvensis* root and aerial parts

No	Rt min	[M + H] ⁺ m/z	Delta ppm	Protonated Formula	Aglycone m/z	MS/MS Fragment Ions (Protonated Formula) m/z	Identification	Roots	Aerial Parts
1	5.08	433.1338	-0.58	C ₁₈ H ₂₅ O ₁₂	285.0753	145.0493 (C ₉ H ₉ O ₄), 127.0390 (C ₆ H ₇ O ₃)	Licoagroside B	+	+
2	8.95	447.1281	-1.06	C ₂₂ H ₂₃ O ₁₀	285.0753	270.0521 (C ₁₅ H ₁₀ O ₅), 253.0491 (C ₁₅ H ₉ O ₄), 225.0542 (C ₁₄ H ₉ O ₃), 213.0542 (C ₁₃ H ₉ O ₃), 197.0594 (C ₁₃ H ₉ O ₂)	Calycosin D 7-O-β-D-glucoside	+	+
3	10.07	588.2072	-0.60	C ₂₉ H ₃₄ NO ₁₂	315.0857	287.0912 (C ₁₆ H ₁₅ O ₅), 274.1284 (C ₁₂ H ₂₀ NO ₆), 177.0545 (C ₁₀ H ₉ O ₃), 163.0387 (C ₉ H ₇ O ₂), 130.0861 (C ₆ H ₁₂ NO ₂), 70.0658 (C ₄ H ₈ N)	Onogenin 7-O-β-D-glucoside 6''-pyrrolidine 2-acetate	+	-
4	10.29	447.1299	2.97	C ₂₂ H ₂₃ O ₁₀	285.0752	270.0517 (C ₁₅ H ₁₀ O ₅), 253.0486 (C ₁₅ H ₉ O ₄), 225.0538 (C ₁₄ H ₉ O ₃), 213.0543 (C ₁₃ H ₉ O ₃), 197.0593 (C ₁₃ H ₉ O ₂)	Calycosin 7-O-β-D-glucoside	+	+
5	10.71	574.2274	-1.55	C ₂₉ H ₃₆ NO ₁₁	301.1064	283.0598 (C ₁₄ H ₁₁ O ₅), 274.1280 (C ₁₂ H ₂₀ NO ₆), 163.0389 (C ₉ H ₇ O ₃), 130.0862 (C ₆ H ₁₂ NO ₂), 70.0655 (C ₄ H ₈ N)	Sativanone 7-O-β-D-glucoside 6''-pyrrolidine 2-acetate	+	-
6	11.17	461.1435	-1.57	C ₂₃ H ₂₅ O ₁₀	299.0908	281.0802 (C ₁₇ H ₁₃ O ₄), 253.0854 (C ₁₆ H ₁₃ O ₃), 239.0698 (C ₁₅ H ₁₁ O ₃), 193.0493 (C ₁₀ H ₉ O ₄), 107.0495 (C ₇ H ₇ O)	Puerol A 2'-O-glucoside	+	+
7	11.82	475.1593	-1.21	C ₂₄ H ₂₇ O ₁₀	313.1069	295.0960 (C ₁₈ H ₁₅ O ₄), 267.1012 (C ₁₇ H ₁₅ O ₃), 253.0855 (C ₁₆ H ₁₃ O ₃), 207.0647 (C ₁₁ H ₁₁ O ₄), 107.0495 (C ₇ H ₇ O)	Clitorienolactone B 4'-O-β-D-glucoside	+	+
8	13.07	556.1812	-0.25	C ₂₈ H ₃₀ NO ₁₁	283.0789	274.1284 (C ₁₂ H ₂₀ NO ₆), 70.0650 (C ₄ H ₈ N)	Pseudobaptigenin 7-O-β-D-glucoside 6''-pyrrolidine 2-acetate	+	+
9	13.60	542.2020	0.13	C ₂₈ H ₃₂ NO ₁₀	269.0804	274.1282 (C ₁₂ H ₂₀ NO ₆), 70.0654 (C ₄ H ₈ N)	Formononetin 7-O-β-D-glucoside 6''-pyrrolidine 2-acetate	+	+
10	14.39	558.1968	-0.335	C ₂₈ H ₃₂ NO ₁₁	285.0754	274.1280 (C ₁₂ H ₂₀ NO ₆), 175.0389 (C ₁₀ H ₇ O ₃), 151.0388 (C ₈ H ₇ O ₃), 70.0658 (C ₄ H ₈ N)	Maackiain 3-O-β-D-glucoside 6''-pyrrolidine 2-acetate	+	+
11	14.44	533.1295	1.00	C ₂₅ H ₂₅ O ₁₃	285.0753	270.0518 (C ₁₅ H ₁₀ O ₅), 253.0490 (C ₁₅ H ₉ O ₄), 225.0542 (C ₁₄ H ₉ O ₃), 213.0542 (C ₁₃ H ₉ O ₃), 197.0597 (C ₁₃ H ₉ O ₂)	Calycosin D 7-O-β-D-glucoside malonate	+	+
12	14.50	570.1967	-0.504	C ₂₉ H ₃₂ NO ₁₁	283.0596	288.1434 (C ₁₃ H ₂₂ NO ₆), 84.0814 (C ₅ H ₁₀ N)	Pseudobaptigenin 7-O-β-D-glucoside 6''-piperidine 2-acetate	+	+
13	14.87	556.2177	-0.04	C ₂₉ H ₃₄ NO ₁₀	269.0801	288.1436 (C ₁₃ H ₂₂ NO ₆), 144.1017 (C ₇ H ₁₄ NO ₂), 84.0814 (C ₅ H ₁₀ N)	Formononetin 7-O-β-D-glucoside 6''-piperidine 2-acetate	+	+
14	14.89	602.2231	-0.17	C ₃₀ H ₃₆ NO ₁₂	315.0855	288.1435 (C ₁₃ H ₂₂ NO ₆), 177.0543 (C ₁₀ H ₉ O ₃), 163.0387 (C ₉ H ₇ O ₃), 144.1017 (C ₇ H ₁₄ NO ₂), 135.0439 (C ₈ H ₇ O ₂), 84.0814 (C ₅ H ₁₀ N)	Onogenin 7-O-β-D-glucoside 6''-piperidine 2-acetate	+	-
15	15.27	544.2166	-2.063	C ₂₈ H ₃₄ NO ₁₀	271.0961	274.1281 (C ₁₂ H ₂₀ NO ₆), 161.0594 (C ₁₀ H ₉ O ₂), 137.0595 (C ₈ H ₇ O ₂), 123.0441 (C ₇ H ₇ O ₂), 70.0646 (C ₄ H ₈ N)	Medicarpin 3-O-β-D-glucoside 6''-pyrrolidine 2-acetate	+	+
16	15.39	533.1309	-1.40	C ₂₅ H ₂₅ O ₁₃	285.0753	270.0518 (C ₁₅ H ₁₀ O ₅), 253.0491 (C ₁₅ H ₉ O ₄), 225.0541 (C ₁₄ H ₉ O ₃), 213.0543 (C ₁₃ H ₉ O ₃), 197.0594 (C ₁₃ H ₉ O ₂)	Calycosin 7-O-β-D-glucoside malonate	+	+
17	15.53	588.2434	-0.91	C ₃₀ H ₃₈ NO ₁₁	301.1064	288.1436 (C ₁₃ H ₂₂ NO ₆), 273.1115 (C ₁₆ H ₁₇ O ₄), 163.0387 (C ₉ H ₇ O ₃), 144.1017 (C ₇ H ₁₄ NO ₂), 135.0439 (C ₈ H ₇ O ₂), 84.0814 (C ₅ H ₁₀ N)	Sativanone 7-O-β-D-glucoside 6''-piperidine 2-acetate	+	-
18	15.61	299.0909	-1.67	C ₁₇ H ₁₅ O ₅	281.0804 (C ₁₇ H ₁₃ O ₄), 253.0805 (C ₁₆ H ₁₃ O ₃), 239.0699 (C ₁₅ H ₁₁ O ₃), 193.0493 (C ₁₀ H ₉ O ₄), 107.0495 (C ₇ H ₇ O)		Puerol A	+	+
19	15.65	445.1124	-1.18	C ₂₂ H ₂₁ O ₁₀	283.0597	253.0491 (C ₁₅ H ₉ O ₄), 225.0543 (C ₁₄ H ₉ O ₃), 197.0595 (C ₁₃ H ₉ O ₂), 169.0647 (C ₁₂ H ₉ O)	Pseudobaptigenin 7-O-β-D-glucoside	+	+
20	15.95	572.2122	-0.76	C ₂₉ H ₃₄ NO ₁₁	285.0752	288.1436 (C ₁₃ H ₂₂ NO ₆), 175.0387 (C ₁₀ H ₇ O ₃), 151.0388 (C ₈ H ₇ O ₃), 144.1017 (C ₇ H ₁₄ NO ₂), 84.0814 (C ₅ H ₁₀ N)	Maackiain 3-O-β-D-glucoside 6''-piperidine 2-acetate	+	+

(Continues)

TABLE 1 (Continued)

No	Rt min	[M + H] ⁺ m/z	Delta ppm	Protonated Formula	Aglycone m/z	MS/MS Fragment Ions (Protonated Formula) m/z	Identification	Roots	Aerial Parts
21	16.28	431.1345	1.95	C ₂₂ H ₂₃ O ₉	269.0805	254.0570 (C ₁₅ H ₁₀ O ₄), 237.0543 (C ₁₅ H ₉ O ₃), 226.0622 (C ₁₄ H ₁₀ O ₃), 213.0907 (C ₁₄ H ₁₃ O ₂), 118.0415 (C ₈ H ₆ O)	Formononetin 7-O-β-D-glucoside	+	+
22	16.51	477.1382	-1.97	C ₂₃ H ₂₅ O ₁₁	315.0858	297.0753 (C ₁₇ H ₁₅ O ₅), 287.0909 (C ₁₆ H ₁₅ O ₅), 257.0805 (C ₁₅ H ₁₃ O ₄), 229.0857 (C ₁₄ H ₁₃ O ₃), 178.0623 (C ₁₀ H ₁₀ O ₃), 163.0388 (C ₉ H ₇ O ₃), 147.0439 (C ₉ H ₇ O ₂), 135.0440 (C ₈ H ₇ O ₂)	Onogenin 7-O-β-D-glucoside	+	-
23	16.55	558.2326	-1.384	C ₂₉ H ₃₆ NO ₁₀	271.0959	288.1435 (C ₁₃ H ₂₂ NO ₆), 161.0594 (C ₁₀ H ₉ O ₂), 144.1017 (C ₇ H ₁₄ NO ₂), 137.0595 (C ₈ H ₉ O ₂), 123.0441 (C ₇ H ₇ O ₂), 84.0814 (C ₅ H ₁₀ N)	Medicarpin 3-O-β-D-glucoside 6''-piperidine 2-acetate	+	+
24	17.33	463.1591	-1.67	C ₂₃ H ₂₇ O ₁₀	301.1065	283. (C ₁₆ H ₁₁ O ₅), 273.1116 (C ₁₆ H ₁₇ O ₄), 177.1119 (C ₈ H ₁₇ O ₄), 163.0388 (C ₉ H ₇ O ₂), 135.0440 (C ₈ H ₇ O ₂)	Sativanone 7-O-β-D-glucoside	+	-
25	17.59	531.1125	-1.54	C ₂₅ H ₂₃ O ₁₃	283.0596	253.0490 (C ₁₅ H ₉ O ₄), 225.0542 (C ₁₄ H ₉ O ₃)	Pseudobaptigenin 7-O-β-D-glucoside 4''-malonate	+	+
26	18.14	517.1343	-0.48	C ₂₅ H ₂₅ O ₁₂	269.0804	253.0483 (C ₁₅ H ₉ O ₄)	Formononetin 7-O-β-D-glucoside 4''-malonate	+	+
27	18.23	447.1272	0.16	C ₂₂ H ₂₃ O ₁₀	285.0751	175.0388 (C ₁₀ H ₇ O ₃), 151.0388 (C ₈ H ₇ O ₃), 123.0442 (C ₇ H ₇ O ₂)	Maackiain 3-O-β-D-glucoside	+	+
28	18.31	563.1387	-1.48	C ₂₈ H ₂₇ O ₁₄	315.0858	297.0753 (C ₁₇ H ₁₅ O ₅), 287.0909 (C ₁₆ H ₁₅ O ₅), 257.0804 (C ₁₅ H ₁₃ O ₄), 229.0857 (C ₁₄ H ₁₃ O ₃), 178.0623 (C ₁₀ H ₁₀ O ₃), 163.0388 (C ₉ H ₇ O ₃), 147.0439 (C ₉ H ₇ O ₂), 135.0440 (C ₈ H ₇ O ₂)	Onogenin 7-O-β-D-glucoside 4''-malonate	+	-
29	18.97	549.1600	-0.49	C ₂₈ H ₂₉ O ₁₃	301.1065	273.1117 (C ₁₆ H ₁₇ O ₄), 177.1119 (C ₈ H ₁₇ O ₄), 163.0388 (C ₉ H ₇ O ₃), 135.0440 (C ₈ H ₇ O ₂)	Sativanone 7-O-β-D-glucoside 4''-malonate	+	-
30	19.08	285.0754	1.23	C ₁₆ H ₁₃ O ₅	270.0519 (C ₁₅ H ₁₀ O ₅), 253.0490 (C ₁₅ H ₉ O ₄), 225.0540 (C ₁₄ H ₉ O ₃), 213.0543 (C ₁₃ H ₉ O ₃), 197.0596 (C ₁₃ H ₉ O ₂), 137.0232 (C ₇ H ₅ O ₃)	Calycosin D	+	+	
31	19.08	313.1066	-2.11	C ₁₈ H ₁₇ O ₅	295.0961 (C ₁₈ H ₁₅ O ₄), 267.1012 (C ₁₇ H ₁₅ O ₃), 253.0856 (C ₁₆ H ₁₃ O ₃), 207.0650 (C ₁₁ H ₁₁ O ₄), 107.0495 (C ₇ H ₇ O)	Clitorienolactone B	+	+	
32	19.27	433.1487	-1.41	C ₂₂ H ₂₅ O ₉	271.0960	137.0596 (C ₈ H ₉ O ₂)	Medicarpin 3-O-β-D-glucoside	+	+
33	19.68	563.1382	-2.37	C ₂₈ H ₂₇ O ₁₄	315.0855	297.0752 (C ₁₇ H ₁₅ O ₅), 287.0912 (C ₁₆ H ₁₅ O ₅), 257.0803 (C ₁₅ H ₁₃ O ₄), 229.0856 (C ₁₄ H ₁₃ O ₃), 178.0628 (C ₁₀ H ₁₀ O ₃), 163.0387 (C ₉ H ₇ O ₃), 147.0438 (C ₉ H ₇ O ₂), 135.0439 (C ₈ H ₇ O ₂)	Onogenin 7-O-β-D-glucoside 6''-malonate	+	-
34	19.90	285.0752		C ₁₆ H ₁₃ O ₅	270.0519 (C ₁₅ H ₁₀ O ₅), 253.0490 (C ₁₅ H ₉ O ₄), 225.0542 (C ₁₄ H ₉ O ₃), 213.0543 (C ₁₃ H ₉ O ₃), 197.0592 (C ₁₃ H ₉ O ₂)	Calycosin			
35	20.03	531.1132	-0.22	C ₂₅ H ₂₃ O ₁₃	283.0596	253.0491 (C ₁₅ H ₉ O ₄), 225.0543 (C ₁₄ H ₉ O ₃), 197.0594 (C ₁₃ H ₉ O ₂)	Pseudobaptigenin 7-O-β-D-glucoside 6''-malonate	+	+
36	20.35	549.1595	-1.40	C ₂₈ H ₂₉ O ₁₃	301.1066	283.1001 (C ₁₆ H ₁₁ O ₅), 273.1110 (C ₁₆ H ₁₇ O ₄), 177.1144 (C ₈ H ₁₇ O ₄), 163.0471 (C ₉ H ₇ O ₃), 135.0455 (C ₈ H ₇ O ₂)	Sativanone 7-O-β-D-glucoside 6''-malonate	+	-
37	20.51	517.1353	2.42	C ₂₅ H ₂₅ O ₁₂	269.0803	254.0569 (C ₁₈ H ₁₀ O ₄), 237.0541 (C ₁₅ H ₉ O ₃), 213.0906 (C ₁₄ H ₁₃ O ₂)	Formononetin 7-O-β-D-glucoside 6''-malonate	+	+
38	20.98	533.1275	-2.75	C ₂₅ H ₂₅ O ₁₃	285.0750	175.0387 (C ₁₀ H ₇ O ₃), 151.0387 (C ₈ H ₇ O ₃), 123.0441 (C ₇ H ₇ O ₂)	Maackiain 3-O-β-D-glucoside 6''-malonate	+	+
39	21.77	519.1488	-1.74	C ₂₅ H ₂₇ O ₁₂	271.0959	161.0959 (C ₁₀ H ₉ O ₂), 137.0595 (C ₈ H ₉ O ₂), 123.0441 (C ₇ H ₇ O ₂)	Medicarpin 3-O-β-D-glucoside 6''-malonate	+	+

(Continues)

TABLE 1 (Continued)

Rt No	[M + H] ⁺ m/z	Delta ppm	Protonated Formula	Aglycone m/z	MS/MS Fragment Ions (Protonated Formula) m/z	Identification	Roots	Aerial Parts
40	23.88	313.0703	-1.17	C ₁₆ H ₁₃ O ₆	298.0469 (C ₁₆ H ₁₀ O ₆), 283.0598 (C ₁₆ H ₁₁ O ₅), 281.0440 (C ₁₆ H ₉ O ₅), 268.0362 (C ₁₅ H ₉ O ₅), 255.0647 (C ₁₅ H ₁₁ O ₄), 240.0413 (C ₁₄ H ₈ O ₄), 212.0465 (C ₁₃ H ₈ O ₃), 162.0310 (C ₉ H ₆ O ₃), 151.0388 (C ₈ H ₇ O ₃)	Cuneatin	+	+
41	24.72	315.0858	-1.63	C ₁₇ H ₁₅ O ₆	297.0753 (C ₁₇ H ₁₃ O ₅), 287.0903 (C ₁₆ H ₁₅ O ₅), 257.0804 (C ₁₅ H ₁₃ O ₄), 229.0857 (C ₁₄ H ₁₃ O ₃), 178.0623 (C ₁₀ H ₁₀ O ₃), 163.0388 (C ₉ H ₇ O ₃), 147.0435 (C ₉ H ₇ O ₂), 135.0440 (C ₈ H ₇ O ₂)	Onogenin	+	-
42	24.81	285.0750	0.88	C ₁₆ H ₁₃ O ₅	175.0388 (C ₁₀ H ₇ O ₃), 151.0388 (C ₈ H ₇ O ₃), 123.0442 (C ₇ H ₇ O ₂)	Maackiain	+	+
43	24.86	299.0916	0.67	C ₁₇ H ₁₅ O ₅	284.0658 (C ₁₆ H ₁₂ O ₅), 267.0649 (C ₁₆ H ₁₁ O ₄), 252.0412 (C ₁₅ H ₈ O ₄), 243.1014 (C ₁₅ H ₁₅ O ₃), 213.0551 (C ₁₃ H ₉ O ₃), 163.0387 (C ₉ H ₇ O ₃), 148.0517 (C ₉ H ₈ O ₂), 137.0596 (C ₈ H ₉ O ₂)	2'-methoxy formononetin	+	+
44	25.22	283.0596	-1.77	C ₁₆ H ₁₁ O ₅	253.0491 (C ₁₅ H ₉ O ₄), 225.0543 (C ₁₄ H ₉ O ₃), 197.0595 (C ₁₃ H ₉ O ₂)	Pseudobaptigenin	+	+
45	25.37	301.1061	-3.16	C ₁₇ H ₁₇ O ₅	273.1116 (C ₁₆ H ₁₇ O ₄), 177.1272 (C ₈ H ₁₇ O ₃), 163.0388 (C ₉ H ₇ O ₃), 151.0388 (C ₈ H ₇ O ₃), 135.0440 (C ₈ H ₇ O ₂), 107.0495 (C ₇ H ₇ O)	Sativanone	+	-
46	25.65	269.0803	-1.99	C ₁₆ H ₁₃ O ₄	253.0490 (C ₁₅ H ₉ O ₄), 237.0541 (C ₁₅ H ₉ O ₃), 226.0623 (C ₁₄ H ₁₀ O ₃), 225.0542 (C ₁₄ H ₉ O ₃), 213.0906 (C ₁₄ H ₁₃ O ₂), 197.0594 (C ₁₃ H ₉ O ₂)	Formononetin	+	+
47	25.74	271.0959	1.43	C ₁₆ H ₁₅ O ₄	161.0595 (C ₁₀ H ₉ O ₂), 137.0595 (C ₈ H ₉ O ₂), 123.0441 (C ₇ H ₇ O ₂)	Medicarpin	+	+

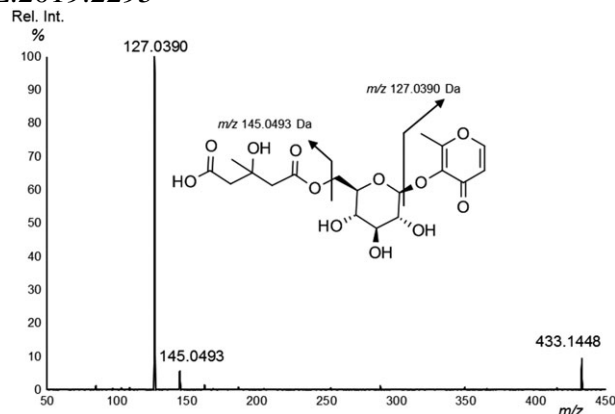


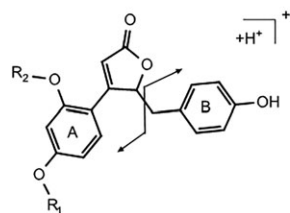
FIGURE 2 Proposed fragmentation profile of licoagroside B in positive ionization mode at 10 eV collision energy

3.2 | Identification of but-2-enolides

Peak 18 showed a protonated pseudo-molecular ion at m/z 299.0908, and its fragmentation pattern was identical with that of peak 6 bearing precursor ion at m/z 461.1435 (Figure 1A). Based on the protonated molecular formulas (C₁₇H₁₅O₅ and C₂₃H₂₅O₁₀), these structures were putatively identified as puerol A and its 2'-O-glucoside (Table 1). In their MS/MS spectra, two main fragmentation pathways could be observed: the cleavage of the whole molecule to A and B-ring and the neutral loss of small units, as CO and C₂H₂O.

Applying the same fragmentation pattern described above, 7 and 31 (Figure 1A) were assigned as the methylated derivative of puerol A and its O-glucoside, respectively. Between the fragment ions in the spectra of 18 and 31, a difference of 14 Da could be observed in all cases (Table 1), except for the ion at m/z 107.0495 (C₇H₇O) corresponding to the B-ring (Figure 3). These fragments indicate that a methyl substituent on the A-ring is responsible for the 14 Da shifts of the fragments (Figure 3).

The nomenclature and structural identification of puerol derivatives are rather tangled in previous interpretations; naming and structures are briefly discussed below and summarized in Figure S8. Firstly, Kinjo et al. isolated pueroside A and B in 1985 and identified them as diglycosides of a ζ -lactone.¹⁴ Shirataki et al. isolated sophoraside A (monoglycoside) and two aglycones, puerol A, and its 4'-O-methylated form, puerol B, possessing the same ζ -lactone structure,¹⁵ and Barrero et al. identified specionin and its glucoside speciozide A with ζ -lactone structure in *O. speciosa*.¹⁶ In their later work, Nohara et al.¹⁷ described that pueroside A and B and sophoraside A were actually γ -lactones, in contrary to previous works. Kirmizgöl et al.¹⁸ isolated spinonin from *O. spinosa*, which is a monoglycoside and its structure would correspond to puerol A 2'-O-glucoside. Nevertheless, the authors drove to the conclusion that spinonin contained a 2,3-dihydro-3-oxofurane ring instead of a 2,3-dihydro-2-oxofurane, like the puerol derivatives. Puerol A and its 4'-O-methylated form, puerol B, along with their 2'-O-glucosides were isolated from *O. angustissima* L. by Ghribi et al.¹⁹ but another O-methylated derivative of puerol A (clitorienolactone B) was isolated from *O. spinosa* by Addotey et al.²⁰ (See Figure S8). Puerol B and clitorienolactone differ only in the position of a methyl substitution. In puerol B, the methylation occurs at



R ₁	R ₂	Compound
H	H	Puerol A
H	glucose	Puerol A 2''-O-glucoside
CH ₃	H	Puerol B
CH ₃	glucose	Puerol B 2''-O-glucoside
H	CH ₃	Clitorienolactone B
glucose	CH ₃	Clitorienolactone B 4'-O-glucoside

FIGURE 3

The structure of puerol derivatives

the *para* OH group of A-ring position, whereas in clitorienolactone B it is in the *ortho* position. Since the HR-MS/MS investigations alone could not solve the exact location of atoms in the middle ring and the methyl group, peaks **6**, **7**, **18**, and **31** were isolated and subjected to NMR experiments in order to clarify the structures. Based on the NMR results, the isolated compounds contained a 2,3-dihydro-2-oxofurane ring. The most decisive element was the chemical shift of the carbonyl atoms, as they exhibited chemical shifts at 176.8 and 177.2 ppm which are characteristic for unsaturated γ -lactones,²¹ whereas 2,3-dihydro-3-oxofurane rings possess chemical shift above 200 ppm.²² The glucose moiety of compound **6** joined puerol A through the 2'-OH group, in *ortho* position. Based on the NOESY spectrum, the methyl group of compound **31** is located in *ortho* position, too, so that this compound was identified as clitorienolactone B. The NOESY spectrum of compound **7** revealed that the glucose moiety is linked through the 4' OH group, in *para* position. To the best of our knowledge, this glucoside is characterized for the first time.

3.3 | Identification of isoflavonoids

Peak **21**, **26**, **37**, and **46** (Figure 1C) provided $[M + H]^+$ ions at m/z 431.1345 (C₂₂H₂₃O₉), 517.1343 (C₂₅H₂₅O₁₂), 517.1353 (C₂₅H₂₅O₁₂), and 269.0803 (C₁₆H₁₃O₄), respectively, but they did not differ in their MS/MS spectra, meaning that they are the derivatives of the same aglycone. The fragmentation of these ions gave rise to m/z 254.0570 (C₁₅H₁₀O₄) ion, owing to the radical cleavage of CH₃[•] and m/z 237.0543 (C₁₅H₉O₃), deriving from the loss of a CH₃OH unit, verifying the presence of a methoxy group. The ion at m/z 213.0907 (C₁₄H₁₃O₂) is a result of the loss of two CO units which is characteristic for isoflavonoid aglycones.²³ Fragment ion at m/z 118.0415 (C₈H₆O) refers to the ion containing the B-ring resulting from the rDA fragmentation (Figure 4A). Although, the intact B-ring with the methoxy group at m/z 133.0648 (C₉H₇O) is barely detectable, the rDA fragment losing the CH₃[•] radical at m/z 118.0415 is much more intense (Table 1). Regarding this information, the aglycone was tentatively identified as formononetin. The neutral loss of 162.0540 (C₆H₁₀O₅) Da of peak **21**

corresponded to the loss of a hexose moiety. Taking into account, that isoflavonoids form glycosides with glucose in the vast majority of cases,²⁴ the peak was assigned as formononetin 7-O- β -D-glucoside or ononin. Peaks **26** and **37** showed the same quasi-molecular ion and fragmentation spectra, and a neutral loss of 248.0550 Da (C₉H₁₂O₈); therefore, they were attributed as 7-O- β -D-glucoside malonates of formononetin. Based on the significant difference in their quantity and retention times (Figure 1C), the firstly eluting minor derivative was tentatively identified as 4''-malonate (**26**) and the later eluting major molecule as 6''-malonate (**37**).²⁵

With protonated pseudo-molecular ions at m/z 447.1281 (C₂₂H₂₃O₁₀) and 447.1299 (C₂₂H₂₃O₁₀), 533.1295 (C₂₅H₂₅O₁₃) and 533.1309 (C₂₅H₂₅O₁₃), 285.0753 (C₁₆H₁₃O₅) and 285.0752 (C₁₆H₁₃O₅), two sets of glucosides, glucoside malonates and aglycones were observed, all sharing identical fragmentation pattern. The same neutral losses could be detected as in the case of formononetin, namely the loss of a CH₃[•] and a CH₃OH, which are a result of a methoxy substitution. These cleavages could be combined with the loss of two CO moieties, resulting in ions at m/z 270.0521 (C₁₅H₁₀O₅) $[M + H - CH_3]^+$, 253.0491 (C₁₅H₉O₄) $[M + H - CH_3OH]^+$, 225.0542 (C₁₄H₉O₃) $[M + H - CH_3OH - CO]^+$, 213.0542 (C₁₃H₉O₃) $[M + H - CH_4OH - CO - CO]^+$, 197.0594 (C₁₃H₉O₂) $[M + H - CH_3OH - CO - CO]^+$ (Table 1). The ion at m/z 137.0232 (C₇H₅O₃) was presumed to be the rDA fragment containing the A-ring, demonstrating that it could not bear any other substituents but the hydroxy group at C7 (Figure 4A). As a result, these molecules were tentatively identified as structural isomers differing only in the position of the hydroxy and methoxy groups of the B-ring. As even the ratios of the fragment ions were not significantly different, the two sets were not distinguishable relying only on mass spectrometry data. Since the firstly eluting peaks of the pairs were always higher in relative quantity (see Figure 1), it was presumed that peaks **2**, **11**, and **30** have the same aglycone, and **4**, **16**, and **34** another one. The identity of the aglycones was investigated using calycosin as standard substance and its retention time and MS/MS spectrum matched with the later eluting peak (**34**). As Addotey et al. isolated calycosin D from *O. spinosa*,²⁰ which differ only in the position of a methyl group (see Figure 7), it

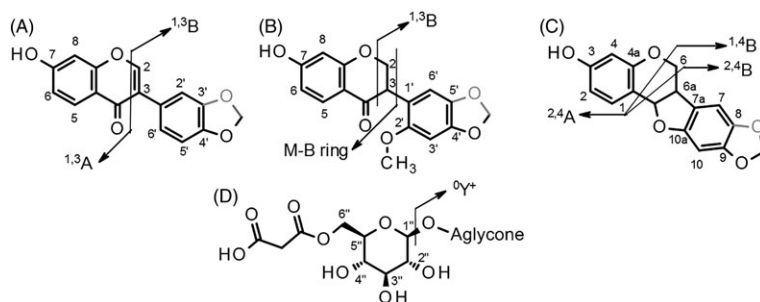


FIGURE 4 Schematic structures and main proposed fragmentation patterns of *Ononis* isoflavonoids (A), pterocarpans (B), dihydroisoflavonoids (C) and their glycosides (D)

DOI:10.14753/SE.2019.2295

was hypothesized that the major peaks (**4**, **16**, and **34**) are the derivatives of this molecule. To verify this hypothesis, the firstly eluting relative larger peaks (**2** and **11**) were isolated and investigated by NMR. Based on the NOESY spectra, they were the 7-O-glucoside and 7-O-glucoside 6''-O-malonate of calycosin D, so that peaks **4** and **16** were tentatively identified as the 7-O-glucoside and 7-O-glucoside 6''-O-malonate of calycosin, respectively. Peaks **19**, **25**, and **35** (Figure 1D) had a pseudo-molecular ion at 445.1124 (C₂₂H₂₁O₁₀), 531.1125 (C₂₅H₂₃O₁₃) and 531.1132 (C₂₅H₂₃O₁₃) and each provided the same fragment ions with peak **44** at *m/z* 283.0596 (C₁₆H₁₁O₅). The fragments, which were formed by the loss of a CH₃OH unit from the protonated calycosin ion (*m/z* 253.0491, 225.0543, 197.0595), could be observed with these molecules as well. As the protonated molecular formula of calycosin contains two hydrogens more (C₁₆H₁₃O₅) than the aglycone of these molecules (C₁₆H₁₁O₅) (Table 1), the cause of the same fragment ions is the neutral loss of CH₂O unit instead of a CH₃OH unit. Considering these results, the peaks were tentatively identified as the 7-O-β-D-glucoside (**19**), 4'' and 6''-malonates (**25** and **35**), and the aglycone of pseudobaptigenin (**44**) (Figure 7).

3.4 | Identification of pterocarpan

Peaks **32** and **39** (Figure 1G) had a pseudo-molecular ion at *m/z* 433.1487 (C₂₂H₂₅O₉) and 519.1488 (C₂₅H₂₇O₁₂) and showed a common aglycone fragment at *m/z* 271.0959 (C₁₆H₁₅O₄) with **47**. Their MS/MS fragments could be detected at *m/z* 161.0595 (C₁₀H₉O₂), 137.0595 (C₈H₉O₂), and 123.0441 (C₇H₇O₂) (Table 1). These results were in concordance with the fragmentation pattern of the pterocarpan medicarpin 3-O-β-D-glucoside (**32**), medicarpin 3-O-β-D-glucoside 6''-malonate (**39**), and medicarpin aglycone (**47**) (Figure 7). The ion at *m/z* 161.0595 is corresponding to the loss of a C₆H₆O₂ ([^{1,4}A]⁺) unit, which can be a consequence of the cleavage of the bonds 1 and 4, whereas the ions at *m/z* 123.0441 and 137.0595 are the products of the cleavage of bond 2 and 4, resulting [^{2,4}A]⁺ and [^{2,4}B]⁺, respectively (Figure 4C). Peaks **27**, **38**, and **42** (Figure 1H) showed similar fragmentation pattern to those of medicarpin; however, a 14-Da difference (+O-2H) could be observed in the case of the quasi-molecular ions and the fragment ions containing the B-ring, namely at *m/z* 175.0388 (C₁₀H₇O₃) [M + H- C₆H₆O₂]⁺ and 151.0388 (C₈H₇O₃) [^{2,4}B]⁺. Based on this fragmentation pattern and analogy with medicarpin, these ions could be tentatively identified as maackiain 3-O-β-D-glucoside (**27**), maackiain 3-O-β-D-glucoside 6''-malonate (**38**), and maackiain (**42**) (Figure 7). As the two molecules differ only in the substitution of the B-ring, the fragment originating from the A-ring is the same at *m/z* 123.0442 [^{2,4}A]⁺.

3.5 | Identification of dihydroisoflavonoids

Peak **24**, **29**, **36**, and **45** (Figure 1E) had the quasi-molecular ions at *m/z* 463.1591 (C₂₃H₂₇O₁₀), 549.1600, 549.1595 (C₂₆H₂₉O₁₃), and 301.1061 (C₁₇H₁₇O₅), and their fragmentation pattern significantly differed from those of the isoflavones. The MS/MS of these ions produced *m/z* 283.0965 (C₁₇H₁₅O₄) and 273.1119 (C₁₆H₁₇O₄) ions,

corresponding to the initial ejection of a H₂O or a CO unit (Table 1). The two intense fragment ions at *m/z* 163.0388 (C₉H₇O₃) and 135.0440 (C₈H₇O₂) could be attributed to [M + H-B-ring]⁺ and [M + H-B-ring-CO]⁺ (Figure 4B). This typical fragmentation pattern was in agreement with our previous results¹⁰; consequently, the peaks were tentatively identified as the 7-O-glucoside (**24**), the 4'' and 6''-O-glucoside malonates (**29** and **36**), and the aglycone (**45**) of sativanone (Figure 7). The molecular formula of peaks **22**, **28**, **33**, and **41** (Figure 1F) differed from the corresponding ones of sativanone in that of an extra oxygen and the lack of the two hydrogens which could be a consequence of a methylenedioxy substitution instead of a methoxy group. The loss of H₂O and CO units could be observed on the MS/MS spectra at *m/z* 297.0753 (C₁₇H₁₃O₅) and 287.0909 (C₁₆H₁₅O₅). Proving that the substitution patterns of the A-ring of sativanone and the aglycone of these molecules are identical, the same ions at *m/z* 163.0388 and 135.0440 could be detected. Moreover, as an evidence of the methylenedioxy substituent, ions at *m/z* 257.0804 (C₁₅H₁₃O₄) [M + H-CO-CH₂O]⁺ and 229.0857 (C₁₄H₁₃O₃) [M + H-2CO-CH₂O]⁺ could be detected (Table 1). Regarding these aspects, the structures were putatively identified as the 7-O-glucoside (**22**), 4'' and 6''-O-glucoside malonates (**28** and **33**), and aglycone (**41**) of onogenin (Figure 7).

3.6 | Identification of the rare 2'-methoxy isoflavonoids

All the former discussed isoflavonoids, dihydroisoflavonoids, and pterocarpan were already known for *O. spinosa*¹⁰; however, peak **43** showed a *m/z* value for the aglycone which was not mentioned in *Ononis* species before. The formula calculated from the HR-MS data was C₁₇H₁₄O₅ (Table 1), which could refer to known compounds afrormosin, cladrin, or 2'-methoxy formononetin. As a result of CID, ions at *m/z* 284.0658 (C₁₆H₁₂O₅), 267.0649 (C₁₆H₁₁O₄), and 252.0412 (C₁₅H₈O₄) were detected, which could refer to structures [M + H-CH₃•]⁺, [M + H-CH₃OH]⁺, and [M + H-CH₃•-CH₃OH]⁺, respectively. These fragments clearly showed that the molecule contained two methoxy groups. The product ion at *m/z* 243.1014 (C₁₅H₁₅O₃) is a result of the ejection of two CO molecules, which is diagnostic to isoflavonoid molecules.¹² The cleavage of the bond between the C-ring and B-ring could provide ions at *m/z* 163.0387 (C₉H₇O₃) [M + H-B-ring]⁺ and 137.0596 (C₈H₉O₂) [B-ring+H]⁺. Regarding this fragmentation pattern, the A-ring can only bear a hydroxy group, and the two methoxy groups are localized on the B-ring. Further evidence for the position of the substituents is provided by the fragment at *m/z* 148.0517 (C₉H₈O₂), which was presumed to be the rDA product [^{1,3}B-CH₃•]⁺. This fragment corresponds to the [^{1,3}B-CH₃•]⁺ ion in the MS/MS spectra of formononetin, and the mass difference is caused by an extra methoxy substituent. Since afrormosin has a methoxy and a hydroxy group on the A-ring and a single methoxy substituent on the B-ring, it could be excluded from the list of possible structures (Figure 5). Comparing the MS/MS spectra of cladrin^{26,27} and 2'-methoxy formononetin²⁸ with our data, the peaks at *m/z* 163.0, 148.1, and 137.1 could be observed in all cases indicating the double methoxy substitution of the B-ring; however,

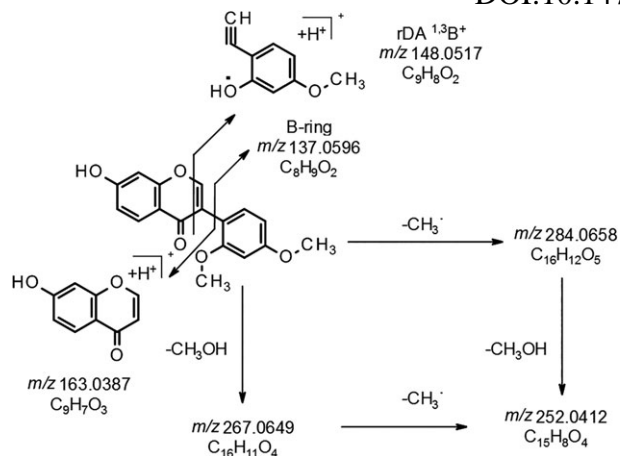


FIGURE 5 Proposed fragmentation pathway of 2'-methoxy formononetin

inspecting fragments in higher m/z regions, our detected peaks were clearly in agreement with the ones of the 2'-methoxy formononetin. 2'-Methoxy formononetin has been isolated from *Dalbergia parviflora* L.²⁹ and from *Eschscholtzia californica* L. (California poppy),³⁰ but not from *Ononis* species. The protonated formula calculated based on the exact mass for peak 40 ($C_{17}H_{13}O_6$) (Table 1) suggests that this compound contains an extra oxygen atom and misses two hydrogen atoms compared with 2'-methoxy formononetin. The origin of this difference could be the methoxy-methylenedioxy substitutions of isoflavonoids, just like in the case of formononetin-pseudobaptigenin, sativanone-onogenin, and medicarpin-maackiain pairs. The mass difference could be followed through the ions with smaller m/z ratio at 151.0388 ($C_8H_7O_3$) and 162.0310 ($C_9H_6O_3$), which are corresponding to the ones of 2'-methoxy formononetin at m/z 137.0596 ($C_8H_9O_2$) and 148.0517 ($C_9H_8O_2$) and were assigned as $[^{1,3}B-CH_3]^+$ and $[B\text{-ring}+H]^+$ (Figure 6). Consequently, it can be deduced that the mass difference arose from the substitution pattern of the B-ring, meaning

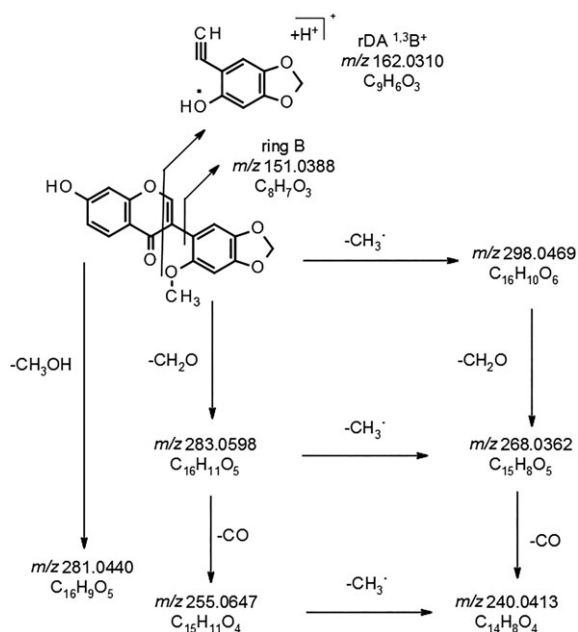


FIGURE 6 Proposed fragmentation pathway of cuneatin

that beside a methoxy group an additional methylenedioxy group is localized on it. As a proof of the mutual presence of OCH_3 and OCH_2O substituents, the loss of CH_3^\bullet , CH_3OH , and CH_2O units and their combination could be observed on the MS/MS spectrum at m/z 298.0469 ($C_{16}H_{10}O_6$) $[M + H-CH_3]^+$, 283.0598 ($C_{16}H_{11}O_5$) $[M + H-CH_2O]^+$, 281.0440 ($C_{16}H_9O_5$) $[M + H-CH_3OH]^+$, and 268.0362 ($C_{15}H_6O_5$) $[M + H-CH_3^\bullet-CH_2O]^+$. Similarly to other isoflavones, the loss of CO units was also detectable at m/z 255.0647 ($C_{15}H_{11}O_4$) $[M + H-CH_2O-CO]^+$, 240.0413 ($C_{14}H_8O_4$) $[M + H-CH_3^\bullet-CH_2O-CO]^+$, and 212.0465 ($C_{13}H_8O_3$) $[M + H-CH_3^\bullet-CH_2O-2CO]^+$ (Table 1). In the literature, only cuneatin fulfills these structural criteria. Cuneatin was described in aerial parts of *Milletia oblata* ssp. *teitensis*,³¹ aerial parts of *Retama sphaerocarpa*,³² stem bark of *Dalbergia frutescens*,³³ *Eysenhardtia polystachya*,³⁴ aerial parts and roots of *Tephrosia maxima*³⁵ and most importantly, in *Cicer* species.³⁶ In his other work,³⁷ Ingham had shown the chemotaxonomic similarity of genus *Ononis* and *Cicer*, and the presence of cuneatin in both genus corroborates this idea.

Other confirmations of the presence of 2'-methoxy formononetin and cuneatin could be acquired from the biosynthesis of isoflavonoids. The final products of the isoflavonoid biosynthesis are medicarpin and maackiain (Figure 7). These phytoalexins with pterocarpan skeleton possess a methoxy and a methylenedioxy group, respectively. Formononetin serves as the parent compound of medicarpin, and through the calycosin-pseudobaptigenin route it could also be considered as the precursor of maackiain. Both formononetin and pseudobaptigenin undergo hydroxylation, converting to 2'-hydroxy formononetin and 2'-hydroxy pseudobaptigenin. These molecules were not detected in our sample; however, their 2'-O-methylated derivatives, 2'-methoxy formononetin, and cuneatin were confirmed. In the following step, the 2'-hydroxy isoflavones are reduced to the dihydro-derivatives: vestitone and sophorol.³⁸ Their 2'-O-methylated derivatives, sativanone and onogenin, are representative compound in *Ononis* species, as well as the pterocarpan medicarpin and maackiain.³⁹

3.7 | Identification of beta amino acid derivatives

The most intense peaks in the chromatogram in positive ionization mode were 12, 13, 14, 17, 20, and 23 (Figure 1). Based on our previous work,¹¹ these compounds were identified as homopipecolic acid esters of isoflavonoid glucosides. These molecules are analogous structures to glucoside malonates, but instead of a malonic acid, the beta amino acid homopipecolic acid is involved in the esterification. However, their fragmentation differs rather from the glucoside malonates, where solely the $^{\text{O}}Y^+$ ion and its fragments emerge and the glucose moiety along with the malonic acid cleave as a neutral fragment (Figure 4D). In the case of homopipecolic esters, the beta amino acid protonates relatively easily due to the secondary amine function enabling the detection of the fragments containing the glycosidic part as well (Table 1). These nitrogen-containing product ions were common for all six isoflavonoid derivatives, whereas the exact mass of the $^{\text{O}}Y^+$ ion and its smaller fractions promoted the identification of the aglycone. The whole homopipecolic acid isoflavonoid

DOI:10.14753/SE.2019.2295

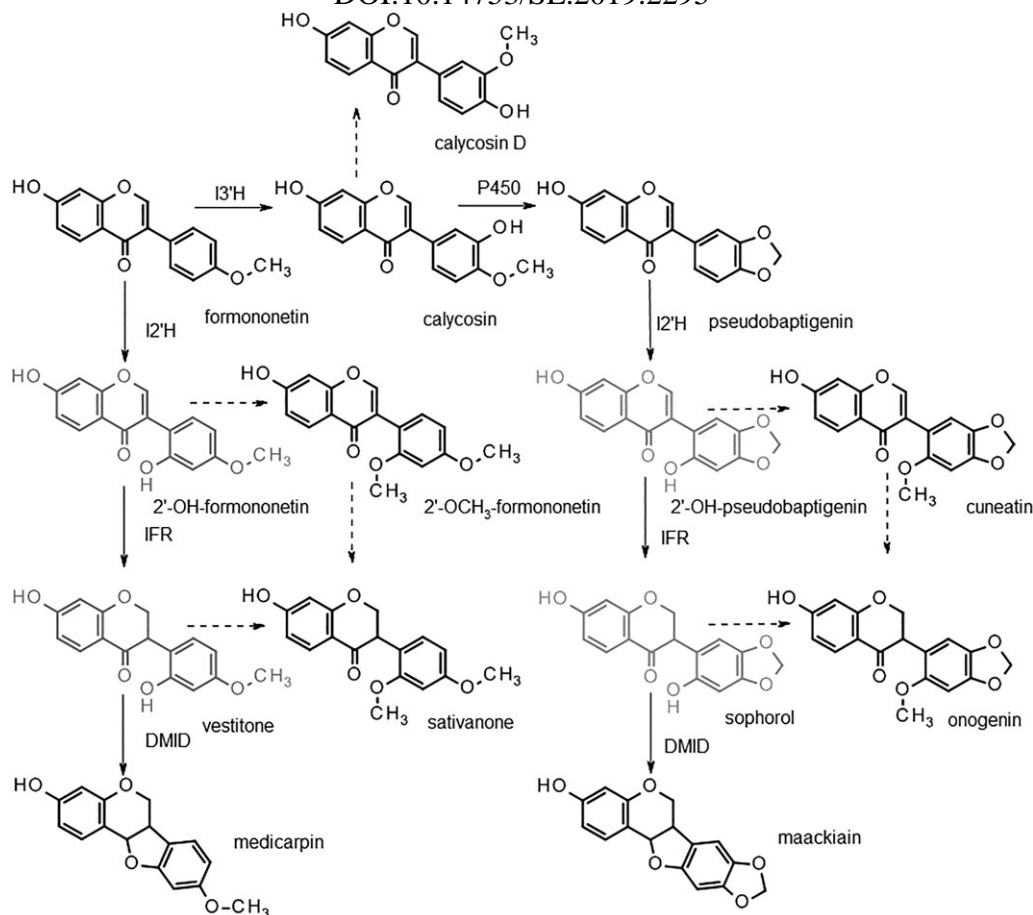


FIGURE 7 Biosynthesis of isoflavonoid and pterocarpans (based on the work of Davies and Schwinn, 2006). Grey: Compounds not detected. Dashed arrows: Unknown enzymatic steps

glucoside ester could cleave alongside the glycosidic bond, resulting in the intact protonated aglycone or the homopiperolic glucoside ester with a truncated glucose moiety at m/z 288.1435 ($C_{13}H_{22}NO_6$). As a protonated fragment at m/z 144.1017 ($C_7H_{14}NO_2$), the beta amino acid unit dissociates from the molecule. The cleavage of the heterocyclic ring solely could provide the ion at m/z 84.0814 ($C_5H_{10}N$) (Figure 8A). Interestingly, an analogous fragmentation pattern could be observed for compounds 3, 5, 8, 9, 10, and 15. The HR-MS/MS data suggested that these compounds contained the same isoflavonoid aglycones mentioned before; however, the complete formula is short of a CH_2 unit (Table 1). Investigating the MS/MS spectra, fragment ions at m/z 274.1284 ($C_{12}H_{20}NO_6$), 130.0862 ($C_6H_{12}NO_2$), and 70.0658 (C_4H_8N) were detected, indicating that the CH_2 difference arose from the heterocyclic ring (Figure 8B). As a homologue of homopiperolic acid, the pyrrolidine ring containing beta amino acid homoproline was presumed.

Although, these nitrogen-containing esters ionize extremely well in positive mode, their actual quantity compared with other isoflavonoid derivatives is quite low. The homoproline derivatives are orders of magnitude lower compared with the homopiperolic esters; therefore, their isolation for NMR experiments was not feasible. In order to verify that the compounds 3, 5, 8, 9, 10, and 15 are homoproline derivatives, the sample was subjected to hydrolysis to free beta amino acids. This hydrolyzed sample was then spiked with the a standard solution of homopiperolic acid and homoproline in

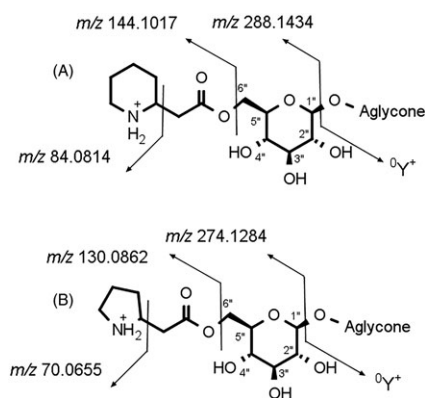


FIGURE 8 The proposed fragmentation pathways of homopiperolic acid (A) and homoproline esters (B)

aqueous medium, as they tend to form esters with methanol.⁴⁰ The original and the spiked samples were investigated by HPLC-MS/MS. As no differences were observed in retention time and in fragmentation pattern (Figure 9), it could be concluded that the samples actually contained the esters of homopiperolic acid and homoproline. Homopiperolic acid was described before in *Lycopodium* species as an intermediate of the synthesis of *Lycopodium* alkaloids,^{41,42} while homoproline was isolated from *Asteraceae* species, as a precursor of pyrrolizidines,⁴⁰ but their co-occurrence has never been reported in plants and their biosynthetic origin is not known.

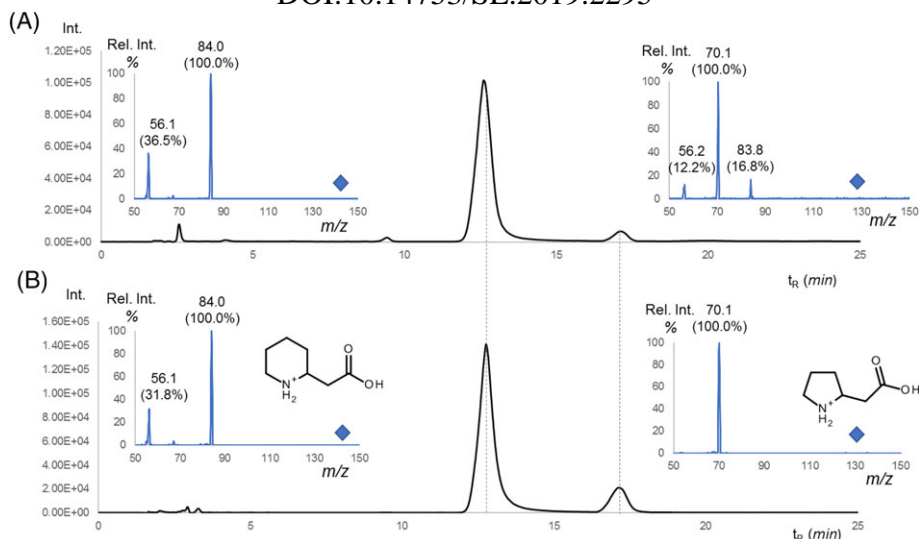


FIGURE 9 Chromatographic separation of homopipercolic acid (12.8 min) and homopropiline (17.2 min) along with their product ion spectra in hydrolyzed plant sample (A) and hydrolyzed plant sample spiked with homopipercolic acid and homopropiline standards (B)

ACKNOWLEDGEMENT

The financial support from the Bolyai fellowship for S. B. and I. B. and the support of EFOP-3.6.3-VEKOP-16-2017-00009 for N. G. are gratefully acknowledged. This work was supported by the ÚNKP-18-3-III-SE-30 New National Excellence Program of the Ministry of Human Capacities, by the Bolyai+ ÚNKP-18-4-SE-121 New National Excellence Program of the Ministry of Human Capacities, and by the National Research, Development and Innovation Office (project: VEKOP-2.3.3-15-2017-00020).

ORCID

Nóra Gampe  <https://orcid.org/0000-0001-7208-9372>

Szabolcs Béni  <https://orcid.org/0000-0001-7056-6825>

REFERENCES

- Dénes T, Bartha SG, Kerényi M, et al. Histological and antimicrobial study of *Ononis arvensis* L. *Acta Biol Hung*. 2017;68(3):321-333.
- Adams M, Schneider SV, Kluge M, Kessler M, Hamburger M. Epilepsy in the renaissance: a survey of remedies from 16th and 17th century German herbals. *J Ethnopharmacol*. 2012;143(1):1-13.
- Süntar İİ, Baldemir A, Coşkun M, Keleş H, Akkol EK. Wound healing acceleration effect of endemic *Ononis* species growing in Turkey. *J Ethnopharmacol*. Apr. 2011;135(1):63-70.
- Verma N, Khosa RL. Hepatoprotective effect of *Zanthoxylum armatum* DC. In: Rasooli I, ed. *Bioactive Compounds in Phytomedicine*. InTech; 2012.
- Dénes T, Papp N, Márton K, et al. Polyphenol content of *Ononis arvensis* L. and *Rhinanthus serotinus* (Schönh. Ex Halácsy & Heinr. Braun) Oborny used in the Transylvanian Ethnomedicine. *Int J Pharmacogn Phytochem*. 2015;30(1):2051-7858.
- Sichinava MB, Mcheldize KZ, Churadze MV, Alaniia MD, Aneli DN. Chemical composition and microstructural peculiarities of overground and underground vegetative organs of field restharrow (*Ononis arvensis* L.). *Georgian Med News*. 2014;231:88.
- Rowan MG, Dean PDG. α -Onocerin and sterol content of twelve species of *Ononis*. *Phytochemistry*. 1972;11(11):3263-3265.
- Hořejší V, Kocourek J. Studies of lectins XXXVI. Properties of some lectins prepared by affinity chromatography on O-glycosyl polyacrylamide gels. *Biochim Biophys Acta - Gen Subj*. 1978;538(2):299-315.
- Kovalev VN, Borisov MI, Spiridonov VN. Phenolic compounds of *Ononis arvensis*. I. *Chem Nat Compd*. 1976;10(6):367-369.
- Gampe N, Darcsi A, Lohner S, Béni S, Kursinszki L. Characterization and identification of isoflavonoid glycosides in the root of spiny restharrow (*Ononis spinosa* L.) by HPLC-QTOF-MS, HPLC-MS/MS and NMR. *J Pharm Biomed Anal*. 2016;123:74-81.
- Gampe N, Darcsi A, Kursinszki L, Béni S. Separation and characterization of homopipercolic acid isoflavonoid ester derivatives isolated from *Ononis spinosa* L. root. *J Chromatogr B Anal Technol Biomed Life Sci*. 2018;1091:21.
- Nakata R, Yoshinaga N, Teraishi M, et al. A fragmentation study of isoflavones by IT-TOF-MS using biosynthesized isotopes. *Biosci Biotechnol Biochem*. 2018;82:1309.
- Li W, Asada Y, Yoshikawa T. Flavonoid constituents from *Glycyrrhiza glabra* hairy root cultures. *Phytochemistry*. 2000;55(5):447-456.
- ei Kinjo J, ichi Furusawa J, Nohara T. Two novel aromatic glycosides, pueroside-a and -B, from puerariae radix. *Tetrahedron Lett*. 1985;26(49):6101-6102.
- Shirataki Y, Tagaya Y, Yokoe I, Komatsu M, Sophoroside A. A new aromatic glycoside from the roots of *Sophora japonica*. *Chem Pharm Bull*. 1987;35(4):1637-1640.
- Barrero AF, Sanchez JF, Barron A, Rodriguez I. Specionin and speciosides a and b: new aromatic lactones from *Ononis speciosa*. *J Nat Prod*. 1989;52(6):1334-1337.
- Nohara T, Kinjo J, Furusawa J, et al. But-2-enolides from *Pueraria lobata* and revised structures of puerosides A, B and sophoroside A. *Phytochemistry*. 1993;33(5):1207-1210.
- Kirmizigül S, Gören N, Yang SW, Cordell GA, Bozok-Johansson C. Spinonin, a novel glycoside from *Ononis spinosa* subsp. *leiosperma*. *J Nat Prod*. 1997;60(4):378-381.
- Ghribi L, Waffo-Téguo P, Cluzet S, et al. Isolation and structure elucidation of bioactive compounds from the roots of the Tunisian *Ononis angustissima* L. *Bioorg Med Chem Lett*. 2015;25(18):3825-3830.
- Addotey JN, Lengers I, Jose J, et al. Isoflavonoids with inhibiting effects on human hyaluronidase-1 and norneolignan clitorienolactone B from *Ononis spinosa* L. root extract. *Fitoterapia*. 2018;130:169-174.

DOI:10.14753/SE.2019.2295

21. Eidman KF, MacDougall BS. Synthesis of loliolide, actinidiolide, dihydroactinidiolide, and aeginetolide via cerium enolate chemistry. *J Org Chem*. 2006;71(25):9513-9516.
22. Chimichi S, Boccalini M, Cosimelli B, Dall'Acqua F, Viola G. New 5-(2-ethenylsubstituted)-3(2H)-furanones with in vitro antiproliferative activity. *Tetrahedron*. 2003;59(28):5215-5223.
23. Kuhn F, Oehme M, Romero F, Abou-Mansour E, Tabacchi R. Differentiation of isomeric flavone/isoflavone aglycones by MS2 ion trap mass spectrometry and a double neutral loss of CO. *Rapid Commun Mass Spectrom*. 2003;17(17):1941-1949.
24. Farag MA, Huhman DV, Lei Z, Sumner LW. Metabolic profiling and systematic identification of flavonoids and isoflavonoids in roots and cell suspension cultures of *Medicago truncatula* using HPLC-UV-ESI-MS and GC-MS. *Phytochemistry*. 2007;68(3):342-354.
25. de Rijke E, de Kanter F, Ariese F, Brinkman UAT, Gooijer C. Liquid chromatography coupled to nuclear magnetic resonance spectroscopy for the identification of isoflavone glucoside malonates in *T. pratense* L. leaves. *J Sep Sci*. 2004;27(13):1061-1070.
26. Rashid M, Singh SK, Malik MY, et al. Development and validation of UPLC-MS/MS assay for quantification of cladrin: absolute bioavailability and dose proportionality study in rats. *J Pharm Biomed Anal*. 2018;152:289-297.
27. Manickavasagam L, Gupta S, Mishra S, Maurya R, Chattopadhyay N, Jain GK. LC-MS/MS method for simultaneous analysis of cladrin and equol in rat plasma and its application in pharmacokinetics study of cladrin. *Med Chem Res*. 2011;20(9):1566-1572.
28. PubChem, 3-(2,4-Dimethoxyphenyl)-7-hydroxychromen-4-one| C17H14O5 - PubChem. [Online].
29. Umehara K, Monthakantirat O, Matsushita A, et al. Estrogenic activities of flavonoids in Thai medicinal plant *Dalbergia parviflora*. *Planta Med*. 2010;76(12):P241.
30. Jain L, Tripathi M, Pandey VB, Rücker G. Flavonoids from *Eschscholtzia Californica*. *Phytochemistry*. 1996;41(2):661-662.
31. Deyou T, Marco M, Heydenreich M, et al. Isoflavones and Rotenoids from the leaves of *Millettia oblata* ssp. *teitensis*. *J Nat Prod*. 2017;80(7):1-2.
32. Louaar S, Akkal S, Laouer H, Guilet D. Flavonoids of *Retama sphaerocarpa* leaves and their antimicrobial activities. *Chem Nat Compd*. 2007;43(5):616-617.
33. Khan IA, Avery MA, Burandt CL, et al. Antigiardial activity of isoflavones from *Dalbergia frutescens* bark. *J Nat Prod*. 2000;63(10):1414-1416.
34. Alvarez L, Rios MY, Esquivel C, et al. Cytotoxic Isoflavans from *Eysenhardtia polystachya*. *J Nat Prod*. 1998;61(6):767-770.
35. Rao EV, Murthy MSR, Ward RS. Nine isoflavones from *Tephrosia maxima*. *Phytochemistry*. 1984;23(7):1493-1501.
36. Ingham JL. Isolation and identification of *Cicer* isoflavonoids. *Biochem Syst Ecol*. 1981;9(2-3):125-128.
37. Ingham JL. Phytoalexin production by *Ononis* species. *Biochem Syst Ecol*. 1982;10(3):233-237.
38. Davies KM, Schwinn KE. Molecular Biology and Biotechnology of Flavonoid Biosynthesis. In: Andersen O, Markham K, eds. *Flavonoids: chemistry, biochemistry and applications*. Boca Raton: CRC Press; 2006.
39. Ergene Öz B, Saltan İşcan G, Küpeli Akkol E, Süntar İ, Bahadır Acıkara Ö. Isoflavonoids as wound healing agents from *Ononidis Radix*. *J Ethnopharmacol*. 2018;211:384.
40. Paßreiter CM. Co-occurrence of 2-pyrrolidineacetic acid with the pyrrolizidines tussilaginic acid and isotussilaginic acid and their 1-epimers in *Arnica* species and *Tussilago farfara*. *Phytochemistry*. 1992;31(12):4135-4137.
41. Marshall WD, Nguyen TT, MacLean DB, Spenser ID. Biosynthesis of Lycopodine. The question of the intermediacy of Piperidine-2-acetic acid. *Can J Chem*. 1975;53(1):41-50.
42. Nilsu T, Thorrood S, Ruchirawat S, Thasana N, Squarrosine A, Pyrrolhuperzine A. New Lycopodium alkaloids from Thai and Philippine *Huperzia squarrosa*. *Planta Med*. 2016;82(11-12):1046-1050.

SUPPORTING INFORMATION

Additional supporting information may be found online in the Supporting Information section at the end of the article.

How to cite this article: Gampe N, Darcsi A, Nagyné Nedves A, Boldizsár I, Kursinszki L, Béni S. Phytochemical analysis of *Ononis arvensis* L. by liquid chromatography coupled with mass spectrometry. *J Mass Spectrom*. 2019;54:121-133. <https://doi.org/10.1002/jms.4308>